

**A MULTIDISCIPLINARY APPROACH
TO THE IDENTIFICATION AND EVALUATION
OF NOVEL CONCEPTS FOR DEEPLY BURIED
HARDENED TARGET DEFEAT**

A Thesis
Presented to
the Academic Faculty

by

Ewell Caleb Branscome

In Partial Fulfillment
of the Requirements for the Degree
Doctor of Philosophy

School of Aerospace Engineering
Georgia Institute of Technology
December 2006

Copyright © 2006 by Ewell Caleb Branscome

**A MULTIDISCIPLINARY APPROACH
TO THE IDENTIFICATION AND EVALUATION
OF NOVEL CONCEPTS FOR DEEPLY BURIED
HARDENED TARGET DEFEAT**

Approved by:

Dr. Dimitri N. Mavris, Advisor
School of Aerospace Engineering
Georgia Institute of Technology

Dr. Daniel P. Schrage
School of Aerospace Engineering
Georgia Institute of Technology

Dr. C. K. Chris Wang
School of Mechanical Engineering
Georgia Institute of Technology

Dr. Robert Sierakowski
School of Aerospace Engineering
Georgia Institute of Technology

Mr. Eugene L. Fleeman
School of Aerospace Engineering
Georgia Institute of Technology

Date Approved: March 7, 2006

*To my wife,
Jessica,
for her loving support.*

ACKNOWLEDGEMENTS

Before mentioning the individuals whose support enabled me to complete this effort, I would like to acknowledge those who enabled me to begin it in the first place. Curtis and Anne Branscome, my parents, have supported and encouraged all my academic endeavors over the years. Joe Onstott and Brian Nakasone, managers at Rocketdyne, approved my educational leave of absence from Boeing to pursue graduate studies. Dr. Dimitri Mavris, my advisor, grew the Aerospace Systems Design Lab into an outstanding organization staffed with outstanding individuals – and was generous enough to allow me to work among them. All of these people enabled me to start upon the path to a Ph.D.

Thanks to the following individuals who have gone out of their way to help me complete the journey...

Professor Dimitri Mavris, Director of the Aerospace Systems Design Lab, Georgia

Institute of Technology: his remarkable insight into the needs of the Aerospace decision making community and leadership in providing innovative solutions has driven the remarkable success of the Aerospace Systems Design Lab. As a result of his efforts, over a hundred students a year have the opportunity to pursue their graduate studies through the lab.

Mr. Gene Fleeman of the Aerospace Systems Design Lab, Georgia Institute of

Technology, for: his editorial input; program management advice; and contribution of his broad knowledge of tactical and strategic weapon systems.

Dr. Chris Wang of the School of Mechanical Engineering, Georgia Institute of Technology, for: general advice and constructive criticism on all things nuclear.

Dr. Bryce Roth, formerly of the Aerospace Systems Design Lab, Georgia Institute of Technology. Bryce is one of those individuals -- organized, good-natured, imaginative, technically capable, and with a gift for clarity in thought and writing -- from whose participation any project or effort invariably benefits.

Dr. Bruce Schnitzler of the Department of Energy, Idaho National Laboratory, Advanced Test Reactor (ATR) Facility, who provided much useful information regarding ATR operational characteristics as well as isotope production capabilities and past activities at ATR.

Dr. Charles Alexander of the Department of Energy, Oak Ridge National Laboratory, High Flux Isotope Reactor (HFIR) Facility, who provided information regarding HFIR operational characteristics and capabilities.

Dr. Frank Tarallo of Theragenics Corporation, for his estimates regarding Plasma Separation Process enrichment costs for isotopes of ytterbium and hafnium.

Last but not least – my good friends Captain John H. Alderman IV, Dennis Graham Schalles, Adam Tyler Broughton, and my fellow ASDL graduate students, who provided fellowship and support along the way.

TABLE OF CONTENTS

ACKNOWLEDGEMENTS	iv
LIST OF TABLES	x
LIST OF FIGURES	xiv
LIST OF SYMBOLS, ABBREVIATIONS, AND ACRONYMS.....	xx
Symbols	xx
Abbreviations & Acronyms.....	xxv
GLOSSARY OF TERMINOLOGY.....	xxxiii
SUMMARY	liv
INTRODUCTION.....	1
Motivation	1
Problem Statement.....	3
Approach.....	4
Identifying need.....	7
Defining the problem.....	7
Analyzing system/requirements.....	8
Generating feasible alternatives.....	11
Assessing robustness of alternative.....	21
Assessing potentially enabling technologies for alternative.....	23
Research Questions, Contributions, and Tasks.....	26
Research contributions.....	27
Research tasks.....	28
BACKGROUND	31
Hard Targets.....	31
Hard target taxonomy	31
Deeply Buried Hardened Targets	34
Historical Capabilities for Air-Delivery of Munitions (and other payloads).....	38
Payload capabilities of assorted aircraft	38
Concepts for munition carriage/separation.....	41
Historically demonstrated unitary payload separation capability.....	45
Alternatives Considered for Defeat of a Hard Target	52
“Finesse” alternatives	52

Isolation through closure of known surface openings and communications utilities disruption by bombardment.....	53
Radiological, Biological, and Chemical alternatives.....	54
HPM, EMP, and other RF DE options	55
Robotic options.....	56
Information system attack.....	59
Squash warheads.....	60
Long rod penetrators.....	65
Shaped charges	93
Alternative rock removal/displacement technologies.....	109
Thermal subterrenes.....	114
Selected Concept: Radioisotope Powered Thermal Penetrator.....	121
System components	121
Concept of operation.....	124
Advantages of RIPTP concept.....	127
Performance concerns.....	127
Safety concerns.....	128
THERMAL PENETRATOR PRIOR WORK.....	129
Morphological Categories of Published Thermal Penetrator Literature	129
Prior Thermal Penetrator Application Categories	132
New Areas of Engineering Analysis as Compared to Prior Thermal Subterrene Literature	133
MULTIDISCIPLINARY ANALYSIS IMPLEMENTATION	134
RIPTP Radioisotope Production Assumptions.....	134
Implications of assumptions	138
Possible Reactor Facilities for Production of Radioisotope Considered	143
High Flux Isotope Reactor.....	144
Advanced Test Reactor.....	144
Commercial Pressurized Water Reactor	145
Hypothetical new reactor.....	145
Moth-balled isotope production reactors.....	146
Calculation of Radioisotope Production – Bateman Equations.....	146
Calculation of Radioisotope Thermal Power	147
Calculation of RIPTP Internal Volume	147
Calculation of Reactor Neutron Economy	148
Calculation of Number of RIPTPs Produced	150
Calculation of Rough Order of Magnitude Radioisotope Costs	150
Determining Penetration Rate and Surface Temperature as a Function of Power	152
Model used for preliminary analysis	153
Close contact melting analytical solutions: Stoke’s Problem with melting	155
Parametric Rock Viscosity	162
Estimation of Thermal Penetrator Internal Temperatures	165

Radiative equilibrium temperature	167
Thermal Equilibrium in an Insulating Medium:	170
MCNP Radiation and HOTSPOT Radioisotope Exposure Calculations	171
BENCHMARKING	172
Feasibility Investigation	172
Characteristics determining suitability of a radioisotope	173
Screening of radioisotopes to power a RIPTP	174
RIPTP RHS baseline-radioisotope selection	179
RIPTP baseline performance analysis results	184
Heat source inventory concept for baseline radioisotope	193
Feasibility conclusions	195
Safety Investigation	196
Background	196
Literature research and observations	198
Enumeration of safety concerns	207
Prioritization of safety concerns	212
Intact penetrator case radiation calculations	226
Bulk fragmentation	233
Explosive dispersal	236
Safety conclusions	243
EXAMPLE PARAMETRIC EXERCISES OF MULTIDISCIPLINARY CODE FOR ROBUSTNESS AND ENABLING TECHNOLOGY	
ANALYSIS	245
System Space Parameterization and Experimental Design	249
Reduction of Results	254
Penetration rate	254
Maximum mission depth	255
Total penetrator mass	257
Penetrator radius	258
External wall surface temperature	259
Thermal power	260
Feasibility of Penetrating Eighty Meters of Granite with Baseline Tm₂O₃ RIPTP in Less than Twenty-Four Hours	261
Baseline feasibility assessment	261
Baseline uncertain variable distribution definitions	262
Identification of system variables most important to penetration variability	267
Discussion of possible technologies to effect changes in identified variables	271
Performance variability given best settings for power density	274
CONCLUSIONS AND RECOMMENDATIONS	277

APPENDIX A – ISOTOPES EVALUATED.....	283
APPENDIX B – PROPERTIES OF GRANITE VS. TEMPERATURE	294
APPENDIX C – THERMAL CONDUCTIVITY OF REPRESENTATIVE PENETRATOR MATERIALS.....	299
APPENDIX D – RADIOISOTOPE PRODUCTION BACKGROUND	302
APPENDIX E – ISOTOPE ENRICHMENT TECHNOLOGIES.....	305
APPENDIX F – SOME NOTES ON THE FEASIBLE DESIGN SPACE ASSESSMENT PROPOSED IN TIF	309
APPENDIX G – NOTES ON FISSILE IMPLEMENTATION.....	315
Fissile Powered Thermal Penetrator – Motivation	316
Challenges with Implementation	317
Functional Requirements	318
Achievement of Compact Size Required for Aerial Delivery.....	319
Options Considered for Implementation	319
Fissile vs. Radioisotope Implementations.....	321
Ideal thermal penetrator	321
Radioisotope powered penetrator	322
Fission powered penetrator.....	323
REFERENCES.....	327
VITA.....	355

LIST OF TABLES

Table 1:	Approximate aircraft system capabilities.....	40
Table 2:	A selection of large unitary payloads separated mid-air.....	51
Table 3:	Hard target defeat concepts and their limitations	64
Table 4:	Penetration equation variables	66
Table 5:	Penetration equation assumptions.....	76
Table 6:	Optimistic estimate of penetration for BLU-113 and MOP for 400 MPa granite	76
Table 7:	Optimistic estimate of penetration for BLU-113 and MOP for 110 MPa granite	76
Table 8:	Viable penetrator ordnance sizing based on nominal MOP for 400 MPa granite	77
Table 9:	Viable penetrator ordnance sizing based on nominal MOP for 110 MPa granite	77
Table 10:	Viable penetrator ordnance sizing based on B-1B capability for 400 MPa granite	77
Table 11:	Viable penetrator ordnance sizing based on B-1B capability for 110 MPa granite	78
Table 12:	Long-rod penetrator performance with fineness ratio of ten	78
Table 13:	Long-rod penetrator performance with fineness ratio of twenty	79
Table 14:	Long-rod penetrator performance with fineness ratio of thirty	79
Table 15:	Rocket equation variables	81
Table 16:	Rocket equation assumptions.....	81

Table 17: Rocket boosted viable penetrator ordnance sizing based on B-1B capability into mean strength granite	82
Table 18: Rocket boosted from zero potential velocity to 4000 ft/sec into mean strength granite.....	83
Table 19: Rocket boosted from zero potential velocity to 4000 ft/sec into maximum strength granite	83
Table 20: Optimistic estimate of maximum shaped charge performance against granite target as constrained by delivery platform maximum payload diameter.....	102
Table 21: Estimate of CSC weights vs. penetration performance to penetrate to a depth of 80 meters in granite.....	104
Table 22: Specific energy for removal of hard rock	110
Table 23: Comparison of surface drilling vs. subterrenes	111
Table 24: Morphological matrix for a thermal penetrator for DBHT defeat	120
Table 25: Maximum characteristic dimensions allowable for isotope forms to achieve various mean internal fluxes	141
Table 26: Producer price indices and historic radioisotope costs	152
Table 27: Close-contact melting variables from Kascheev	160
Table 28: Coefficient ranges for fits of granite and basalt viscosities....	163
Table 29: Some variables used in the steady state thermal analysis.....	166
Table 30: Important radioisotope characteristics	173
Table 31: Principal historically favored radioisotopes for RHS applications	175
Table 32: Potentially satisfactory isotopes.....	177
Table 33: Preferred isotopes.....	181

Table 34: Experiments demonstrating refractory metal compatibility and thulium containment at elevated temperature	183
Table 35: Thulium production summary for ATR and new isotope production reactor	190
Table 36: Thulium RHS mission characteristics and performance	190
Table 37: Production summary for ATR and commercial PWR using 80% enriched Ytterbium-168.....	191
Table 38: RHS mission characteristics and performance using 80% enriched Ytterbium-168	191
Table 39: Hazard modalities	208
Table 40: Hazard outcomes – radioisotope outcomes	208
Table 41: Hazard outcomes – radioisotope production and thermal outcomes	209
Table 42: Sample of outcome realization scenarios.....	210
Table 43: Radiation shielding results using MCNP code	227
Table 44: Variables selected to define the system space and their ranges	252
Table 45: Output variables for which Response Surface Equations were generated.	253
Table 46: Summary of fit for transformed penetration rate	255
Table 47: Summary of fit for transformed maximum mission depth	256
Table 48: Summary of fit for transformed penetrator total mass.....	257
Table 49: Summary of fit for transformed penetrator radius	258
Table 50: Summary of fit for penetrator external surface temperature ..	259
Table 51: Summary of fit for transformed penetrator power.....	261

Table 52: Uncertain variables and their assumed distributions for MCS	262
Table 53: Design variable settings for MCS	263
Table 54: Power density variables and settings	274
Table 55: Isotopes evaluated from ENDF	283
Table 56: Screening of neutron producible radioisotopes	289
Table 57: Isotope separation technologies in rough order of technical maturity	306
Table 58: Gaseous compounds of elements of possible interest for short half-life RHS	308
Table 59: Qualitative comparison of radioisotope and fissile power sources for military and scientific applications	325

LIST OF FIGURES

Figure 1:	Top-level approach used for alternative analysis, selection, and development	6
Figure 2:	General approach to analyzing DBHT/DBHT-defeat-munition system & requirements	9
Figure 3:	Some possible <i>DBHT Functions</i> , as well as a <i>Functional Diagram</i> and diagram of the <i>Physical Connectivity</i> of a DBHT (notional)	10
Figure 4:	<i>Generate Feasible Alternatives</i> – some steps in the indentification of (a) feasible alternative(s).....	12
Figure 5:	A Mutidisciplinary Analysis Formulation, depicted as an n^2 diagram, showing selected disciplinary analyses and their interdependence in terms of feed-forward and feed-back of analysis variables	20
Figure 6:	Assessing robustness of alternatives through metamodel facilitated Monte Carlo Simulation.....	22
Figure 7:	Types of strategic hard and deeply buried targets	33
Figure 8:	Concepts for munition carriage and separation	44
Figure 9:	“ <i>Beethoven-Gerat</i> ” aka “ <i>Mistel-1</i> ” composite aircraft	45
Figure 10:	Historical examples of carriage options for large unitary payloads.....	49
Figure 11:	A scale comparison of very large munitions historically separated from aircraft	50
Figure 12:	GBU-28 employing explosive filled BLU-113 warhead with fineness ratio of 10.5.....	67
Figure 13:	Anti-tank long-rod penetrator in 120 mm sabot/shell system (M829A2 APFSDS-T) with fineness ratio of about 30.....	68

Figure 14: “Mushrooming” nose of a typical steel or tungsten penetrator (left) and “self-sharpening” nose of a depleted-uranium alloy penetrator	69
Figure 15: Impact velocity in 2.4 g/cc granite vs. stagnation pressure	73
Figure 16: Unconfined compressive strength for various rocks.....	75
Figure 17: Stacked sequentially initiated propellant charges as illustrated in MetalStorm™ patent.....	88
Figure 18: Picture of gun battery using MetalStorm™ technology firing at a cyclic rate of 1,000,000 charges per minute.....	89
Figure 19: O’Dwyer reaction control concept for missile using MetalStorm™ approach to discrete propellant charge packaging/initiation.....	89
Figure 20: A system component concept for utilization of sequential propulsion charges in adaptive post-impact propulsion system.....	90
Figure 21: A traveling charge conceptual model of boosted post-impact penetration.....	92
Figure 22: Typical components of a shaped charge	95
Figure 23: Action of a shaped charge against a target	97
Figure 24: Regression on a selection of historical shaped charge data....	106
Figure 25: Notional integration of RIPTP Munition components.....	122
Figure 26: Notional RHS integration with refractory penetrator case	123
Figure 27: Sequence of events in RIPTP DBHT defeat.....	125
Figure 28: Thermal subterrene – a chronological history of some relevant prior work.....	131
Figure 29: RIPTP life-cycle flow-chart.....	137
Figure 30: Principle geometries considered for target elements	140

Figure 31: Average internal flux for an isotope target form vs. its characteristic dimension.....	140
Figure 32: Close contact melting of a sphere in a PCM.....	155
Figure 33: Validation of close-contact melting predictions using results from Emerman, Kascheev, and Yaojiang.....	158
Figure 34: Validation of penetrator surface temperatures using Emerman	158
Figure 35: Comparison of results of Emerman, Kascheev, Yaojiang, and Branscome using alternative granite properties.....	159
Figure 36: Surface temperatures using Kascheev and considering viscosity change	159
Figure 37: Rock viscosities from Bacon, Krupka, and Klett.....	164
Figure 38: Isotopes screened for RIPTP RHS application	178
Figure 39: Isotope production from thulium-169 precursor.....	180
Figure 40: Tm ₂ O ₃ wafer similar to historically produced RHS wafers....	183
Figure 41: Results for production of ¹⁷⁰ Tm at ATR.....	187
Figure 42: Baseline RIPTP life-limited penetration depth capability	188
Figure 43: Baseline RIPTP mission duration-limited penetration depth capability	189
Figure 44: Comparison of radioactivity vs. time of GPHS-RTG and baseline RIPTP	202
Figure 45: Rate of vaporization of saturated water by RIPTP vs. time ...	218
Figure 46: Equilibrium temperature vs. time for water cooled RIPTP	222
Figure 47: Equilibrium temperature vs. time for RIPTP in adverse temperature environment	223
Figure 48: Equilibrium temperature vs. time for penetrator immersed in molten granite	224

Figure 49: Equilibrium temperature vs. time for non-penetrating RIPTP immersed in non-circulating granite	225
Figure 50: Shielding thickness vs. dose rate at 1 meter from thulium-172	231
Figure 51: Dose rate from exposure to baseline RIPTP at one-meter distance.....	232
Figure 52: Radiation exposure for bulk-fragmentation.....	234
Figure 53: Distance vs. dose rate from bulk fragment of RIPTP	235
Figure 54: External radiation exposure for explosive dispersal	240
Figure 55: Internal radiation exposure for explosive dispersal	240
Figure 56: Ground shine dose rate from explosive dispersal	241
Figure 57: CEDE internal dose from explosive dispersal	242
Figure 58: Predicted vs. actual transformed penetration rate.....	255
Figure 59: Predicted vs. actual transformed maximum mission depth	256
Figure 60: Predicted vs. actual transformed penetrator total mass.....	257
Figure 61: Predicted vs. actual transformed penetrator radius.....	258
Figure 62: Predicted vs. actual penetrator external surface temperature.....	259
Figure 63: Predicted vs. actual transformed penetrator power.....	260
Figure 64: Penetration-rate distribution functions for the baseline RIPTP	264
Figure 65: Maximum mission penetration distribution functions for the baseline RIPTP.....	264
Figure 66: Melt wall temperature distribution functions for the baseline RIPTP	265

Figure 67: Case interior temperature distribution functions for the baseline RIPTP	265
Figure 68: Maximum core temperature distribution functions for the baseline RIPTP	266
Figure 69: Total mass distribution functions for the baseline RIPTP	266
Figure 70: Radius distribution functions for the baseline RIPTP	267
Figure 71: Power distribution functions for the baseline RIPTP	267
Figure 72: “Prediction Profiler” from <i>JMP</i> for RIPTP wall temperature and penetration rate as a function of system variables	269
Figure 73: “Prediction Profiler” from <i>JMP</i> for RIPTP wall temperature and penetration rate as a function of system variables with changed values	270
Figure 74: Penetration rate distribution functions for high power density RIPTP	275
Figure 75: Maximum core temperature distribution functions for high power density RIPTP	275
Figure 76: Radius distribution functions for high power density RIPTP	276
Figure 77: Total mass distribution functions for high power density RIPTP	276
Figure 78: Viscosity of granite melts	295
Figure 79: Thermal conductivity of granite.....	296
Figure 80: Heat capacity of granite	297
Figure 81: Thermal expansion of “Salisbury Pink” Granite	298
Figure 82: Rare earth oxide thermal conductivity vs. temperature	299
Figure 83: Tungsten thermal conductivity vs. temperature.....	301

Figure 84: One of the many uranium-236 fission reactions.....	303
Figure 85: Radioisotope production through neutron capture by a target isotope	303
Figure 86: Penetration rate distribution functions for 5E+04 uniform random samples of the design space	312
Figure 87: Penetration rate distribution functions for 5E+04 uniform latin-hypercube samples of the design space	312
Figure 88: Penetration rate distribution functions for 5E+04 uniform latin-hypercube samples of a design sub-space	313

LIST OF SYMBOLS, ABBREVIATIONS, AND ACRONYMS

SYMBOLS

A	Penetrator cross sectional area; linear differential equation coefficient matrix; viscosity regression fit coefficient
A_{equiv}	Area of a sphere of equivalent volume to object
A_v	Avogadro's Number
B	A viscosity regression coefficient
b	A response surface equation coefficient
c	Specific heat
c_p	Melt specific heat
$c_{p,s}$	Specific heat of solid phase
D	Depth of penetration
d	Penetrator diameter
e_f	Average recoverable energy released per ^{236}U fission
E	Number of a specified dimension class of measure polytope in a space of equal or greater number of dimensions
e_{decay}	Sensible (non-neutrino) energy of decay of radioisotope nuclei
f	Fineness Ratio of penetrator (length to diameter)
f_c'	Target unconfined compressive strength
g	Acceleration due to gravity
h_{sf}	Latent heat of melting
h'_{sf}	Effective latent heat of melting
i	A summation index
I_{sp}	Specific impulse of propellant

j	A summation index
k	Thermal conductivity; “ (of granite); dimension of a class of measure polytopes; a summation index limit
k_{bulk}	Effective thermal conductivity of RHS
k_{filler}	Thermal conductivity of filler
k_i	Bulk thermal conductivity of RHS
k_l	Thermal conductivity of melt
k_o	Thermal conductivity of RIPTP case
k_{targ}	Thermal conductivity of radioisotope target element
$k_{Tm_2O_3}$	Thermal conductivity of Tm_2O_3
L	Length of penetrator
l	Mean free path of neutron; cylinder length
L_n	Length of penetrator nose
m_f	Final mass of rocket system
m_i	Initial mass of rocket system
m_{inert}	Inert weight of rocket motor system
$m_{payload}$	Payload of rocket system
m_{prop}	Propellant weight
MW	Molecular Weight
N	Nose performance coefficient
n	Number of isotopes in Batemann Equation system; number of orthogonal dimensions of a multidimensional space
N	Linear differential equation state vector
N_0	Initial number of atoms of radioisotope
n_f	Average number of neutrons produced per ^{236}U fission
N_i	Number of atoms of isotope i

N_v	Number of neutrons
P	Power generated by isotopic decay; penetrator power generated by "
p	Hot body power per unit volume; fraction of a multidimensional space which satisfies feasibility criteria
P_0	Probability of neutron escape from an absorbing body
$P_{c,l}$	Penetrator power required for PCM temperature increase and liquefaction
p_{core}	RHS volume specific power
Pe	Peclet Number
P_k	Conduction power loss
$P_{rad.eq.}$	Penetrator emitted radiative power
p_{req}	Penetrator volume specific power required
P_{req}	Penetrator power required
$P_{thermal}$	Thermal power of nuclear reactor
Q	Rock quality
R	Hot body radius
RSE	A fitted response surface equation function
r	radius
R^2	Coefficient of determination for a regression fit
r_{equiv}	Radius of a sphere of equivalent volume to object
r_{RHS}	RIPTP case inside radius, RHS outside radius
r_m	Melt shaft radius
r_{RIPTP}	RIPTP outside radius
r_{targ}	Radius of radioisotope target element
S	Penetrability of target
Ste	Stefan's Number
t	Time; RIPTP case thickness factor $(I_{RIPTP}-I_{RHS})/I_{RIPTP}$

T	Thickness of RIPTP refractory shell; temperature
T_0	Temperature hot body surface
$t_{1/2}$	Half-life of decay
T_∞	Ambient (farfield) temperature of PCM
$T_{amb,r}$	Ambient radiative temperature
T_i	Temperature of case internal wall
T_m	Melting temperature
T_{max}	Maximum (bounding) temperature
$T_{max,targ}$	Maximum (bounding) temperature of radioisotope target element
T_S	RIPTP surface temperature
$T_{S,targ}$	Surface temperature of target element
V	Speed of penetrator relative to target at impact, or speed of thermal penetrator penetration
V_1	Speed of (thermal) penetration based on force balance
V_2	Speed of (thermal) penetration based on energy conservation
V_{avail}	RHS volume available for radioisotope compound
V_{CASE}	Volume of RIPTP Case
V_{filler}	Volume of RHS comprised of high thermal conductivity filler
V_i	Initial speed
V_{RHS}	Volume of RHS
V_{RIPTP}	Volume of RIPTP
V_{sph}	Volume of sphere of equivalent volume to object
$V_{Tm_2O_3}$	Volume of RHS comprised of Tm ₂ O ₃
W	Weight of penetrator
x	Independent variable

X	A response surface equation independent variable
Y_p	Tensile yield stress of penetrator nose
Z	Atomic mass number
α	Viscosity regression coefficient
β	Viscosity regression coefficient
δ	PCM molten layer thickness
ΔV	Change in velocity provided by rocket
$\Delta\rho$	Difference between hot body and melt densities
ε	Penetrator external surface emissivity
η_v	Fraction of excess neutrons available for isotope production
κ	Thermal diffusivity
μ	Dynamic viscosity of liquid
π	Archimedes constant
ρ	Density of a material
ρ^*	Melt to solid density ratio
ρ_l	PCM melt density
ρ_p	Hot body (penetrator) average density
ρ_s	PCM medium solid density
ρ_t	Density of penetrated material
σ	Stefan-Boltzmann Constant
σ_c	Reaction cross-section (microscopic)
Σ_t	Total macroscopic cross section
Σ	Summation
σ_t	Total reaction cross-section (microscopic)
Φ	Thermal neutron flux

ABBREVIATIONS & ACRONYMS

A	Alpha particle decay
A/C	AirCraft
AEC	Atomic Energy Commission
AMU	Atomic Mass Units
APFSDS-T	Armor Piercing Fin-Stabilized Discarding Sabot-Tracer
ASDL	Aerospace Systems Design Laboratory (of Georgia Tech)
ATR	Advanced Test Reactor
AVLIS	Atomic Vapor Laser Isotope Separation process
B-	Beta decay
B+	Positron decay
BAA	Broad Area Announcement
BEC	Bose Einstein Condensate
BLU	Bomb Live Unit
BNL	Brookhaven National Laboratory
BOS	Beginning of Service
BROACH	Bomb Royal Ordnance Augmenting Charge
C ³	Command, Control, and Communications
C ³ I	Command, Control, Communications, and Intelligence

C ⁴ ISR	Command, Control, Communication, Computer, Intelligence, Surveillance, Reconnaissance
CALCM	Conventional Air-Launched Cruise Missile
CBW	Chemical and Biological Weapons
cc	cubic-centimeters
CD	Charge Diameter
CDF	Cumulative Distribution Function
CEDE	Committed Effective Dose Equivalent
CRC	Chemical Rubber Corporation
CSC	Conical Shaped Charge
DBHT	Deeply Buried Hardened Target
DE	Directed Energy
DIA	Defense Intelligence Agency
DoD	Department of Defense
DOE	Department of Energy
DTA	Differential Thermal Analysis
DU	Depleted Uranium
DUCC	Deep Underground Command Center
EC	Electron Capture
EFP	Explosively Forged Projectile

EMP	ElectroMagnetic Pulse
ENDF	Evaluated Nuclear Data File
ENSDF	Evaluated Nuclear Structure Data Files
EOS	End of Service
FIFO	First In First Out
FIPTP	Fissile Powered Thermal Penetrators
FTI	Fissile Transuranic Isotope
GBU	Guided Bomb Unit
GEM-46 SSRM	Graphite Epoxy Motor 46, Strap on Solid Rocket Motors
GP	Gaussian Process
GPHS	General Purpose Heat Source
GPS	Global Positioning System
GTOW	Gross Take-Off Weight
GW_{th}	Gigawatt of thermal power
HDBT	Hard and Deeply Buried Targets
HE	High Explosive
HEP	High Explosive Plastic
HESH	High Explosive Squash Head
HFIR	High Flux Isotope Reactor

HOTSPOT

HPM	High Powered Microwave
HVAC	Heating, Venting, and Air Conditioning
IC	Intelligence Community
ICBM	InterContinental Ballistic Missile
ICRP	International Commission on Radiation Protection
INL	Idaho National Laboratory
INS	Inertial Navigation System
IT	Internal Transition decay
K	Kelvin
kT	kiloton
kW	kilowatt
LCSC	SNL's Largest Conical Shaped Charge
LD	Liner Diameter
LLNL	Lawrence Livermore National Laboratory
LRALT	Long Range Air-Launched Target
LTD	Limited
M	Metastable
MCNP	Monte Carlo N-Particle transport code system

MCS	Monte Carlo Simulation
MeV	Million Electron Volts
MIRD	Medical Internal Radiation Dosimetry database
MLIS	Molecular Laser Isotope Separation
MOAB	Massive Ordnance Air-Blast
MOP	Massive Ordnance Penetrator
MS	Modelling and Simulation environment
MT	Megaton
MW _{th}	MegaWatts of thermal power
NA	Natural Abundance
NASA	National Aeronautics and Space Administration
NBC	Nuclear, Biological and Chemical
NN	Neural Network
non-dim.	non-dimensional
NuDat	Nuclear Data file
ORNL	Oak Ridge National Laboratory
OSC	Orbital Sciences Corporation
PC	Personal Computer
PCM	Phase Change Material

PDF	Probability Distribution Function
PI	Precursor Isotope
PNL	Pacific Northwest Laboratory
PPI	Producer Price Index
Prec.	Precursor isotope
PSP	Plasma Separation Process
PWR	Pressurized Water Reactor
R^2	Coefficient of Determination
RDS	Robust Design Simulation methodology
RF	Radio Frequency
RHA	Rolled Homogeneous Armor
RHS	Radioisotope Heat Source
RI	RadioIsotope
RIPTP	RadioIsotope Powered Thermal Penetrator
RMSE	Root Mean Square Error
RNEP	Robust Nuclear Earth Penetrator
ROM	Rough Order of Magnitude
RSE	Response Surface Equation
RSM	Response Surface Methodology

RTG	Radioisotope Thermoelectric Generator
SAP	Semi-Armor Piercing
SDB	Small Diameter Bomb
SILEX	Proprietary MLIS process of the Silex company
SNL	Sandia National Laboratory
SO	StandOff
SRB	Solid Rocket Booster
SRL	Savannah River Laboratory
STP	Standard Temperature and Pressure
STS	Space Transportation System
Sv	Sieverts
SWU	Separative Work Unit
T111	A refractory tungsten alloy
TBM	Tunnel Boring Machine
TBM	Theater Ballistic Missile
TIES	Technology Identification Evaluation and Selection methodology
TIF	Technology Impact Forecasting methodology
TNT	TriNitroToluene (a common explosive)
TRIGA	Training, Research, Isotopes, General Atomics (reactor type)

TRIZ	Theory of Inventive Problem Solving (Russian acronym ТРИЗ)
TRL	Technology Readiness Level
TZM	Tungsten-Zirconium-Molybdenum alloy
UARL	United Aircraft Research Laboratories
UAV	Unmanned Aerial Vehicle
UCAV	Unmanned Combat Air Vehicle
US	United States
USEC	United States Enrichment Corporation
USRM	Titan Upgraded Solid Rocket Motors
USSR	Union of Soviet Socialist Republics
UXO	Unexploded Ordinance
WD	Warhead Diameter
WMD	Weapons of Mass Destruction
W_{th}	Watts thermal
α	Alpha particle
β	Beta particle
γ	Gamma (photon) radiation
ν	Neutron particle, or produced via neutron transmutation

GLOSSARY OF TERMINOLOGY

acute radiation sickness

The rapid onset/short course adverse health effects associated with large ionizing radiation exposures of an individual (>~ 50 rem or .5 Sv)

adiabatic shear-banding

Formation of a weak highly plastic band in a body subjected to very high strain rate. In some penetrator materials, the phenomenon causes failure of penetrator point surface material to occur through shear such that a sharp penetrator point is maintained (as distinct from many ductile materials which tend to “mushroom” upon impact)

air blast

The blast wave propagated through air upon detonation of a weapon

alpha radiation

Radiation composed of doubly ionized helium nuclei

aquifer

An underground layer of permeable rock or unconsolidated material from which water can be extracted through a well

atom-density

Number of atoms per unit volume

barns

Unit associated with sigma, the neutron capture cross section - when physicists were first studying nuclear interactions, the probability was thought to be proportional to the cross-sectional area of the nucleus (this probability is still

called the cross-section). Upon experimenting, they discovered the interactions were far more probable than expected; the nuclei were 'as big as a barn'. The units for cross-sections were christened Barns, (10^{-24} cm^2)

basalt

A common extrusive volcanic rock produced from cooling lava, typically mafic in composition

beta radiation

Radiation composed of high energy electrons

Bose Einstein Condensate

A state of matter occurring below a critical temperature. The state is characterized by assumption of an identical quantum state by all bosons comprising the matter

Bremsstrahlung radiation

The electromagnetic radiation produced by a change in the velocity of an electrically charged subatomic particle, such as an electron, as when it interacts with another particle

BROACH

A two-stage shaped-charge/cased-explosive-charge warhead

burn rate exponent

The exponent on pressure in the Saint Robert's Law (or Vieille's Law) burn rate equation

capture cross-section

As a simple means of estimating rates of certain nuclear reactions a "cross-section" for the reaction is used which gives the reaction rate when multiplied by the flux of the initiating particle (ie neutrons)

cermet

A composite material consisting of ceramic particles bonded by a metal

cladding

A protective outside layer applied to a material

close-contact melting

The category of physical problems typified by the melting of a material's solid surface which is in close contact with a second hot solid surface

coefficient of determination

The proportion of the sample variance of a response variable explained by the predictor variables (as when a linear regression is performed)

Committed Effective Dose Equivalent

A metric for estimating the potential health impact over a 50 year period to an individual from internalized radioactive material

computed tomography

Construction of a three dimensional model of the interior of a body using computer analysis of a radiography data set

conventional weapons

Weapons utilizing solely conventional effects to neutralize a target such as blast, fire, shrapnel, etc. -- and specifically excluding weapons with notable and/or intentional pathogenic, chemical toxicity, or radiological effects.

criticality (nuclear reactor)

The point at which a nuclear reaction is self-sustaining

decay chain

Chain of isotopes which are produced from the decay of an initial radioisotope

desalination

The removal of salt (as from seawater to make potable water)

design load factor (aircraft)

The loading in units of g's which an aircraft structure is designed to withstand during flight

detonation wave

The wave-front of supersonic combustion propagated through an exploding substance by a shock

dielectric

A substance that is highly resistant to the flow of electric current

Differential Thermal Analysis

A thermoanalytic technique which measures the heat needed to raise the temperature of a sample vs. temperature

dirty bomb

A bomb designed to distribute radioactive debris over a wide area so as to create a dispersed radiological hazard

drag bit drilling

Drilling with a bit that shears rock with a continuous scraping motion

drill and blast

Mining technique characterized by the drilling of holes in which explosives are placed and detonated to fracture the rock, enabling its removal

dynamic viscosity

Viscosity of a fluid, with the SI unit of Pascal seconds

enduring nuclear stockpile

The US stockpile of nuclear weapons post Cold War, categorized by level of readiness into "Active Service," "Hedge," and "Inactive Reserve" stockpiles

enrichment (isotope)

To concentrate a particular isotope with respect to the fraction of the total number of same-element nuclei it comprises

epithermal neutrons

Neutrons of medium energy, of somewhat greater energy than thermal neutrons

Euler buckling

Longitudinal buckling of a long, slender ideal column under axial loading

fallout

Suspended material which "falls-out" of the atmosphere, typically referring to the radioactive particles produced by a nuclear detonation and injected into the atmosphere which produce the "residual" or delayed radiation hazard associated with an uncontained nuclear detonation.

Faraday Cage

A conductive enclosure designed to exclude electromagnetic fields

feasibility

Possible according to the laws of physics

felsic

Rocks (usually lighter in color) enriched in lighter elements such as silica, oxygen, aluminum, sodium, and potassium

fines

Fine particulate material, used in the context of powdery material as produced by a sintered ceramic form

fissile material

A material capable of undergoing nuclear fission

fission daughter products

Isotopes resulting from the fission of a parent nucleus

flux trap

Space in a reactor core designed to provide a high ambient neutron flux for the purpose of subjecting specimens to high neutron fluxes

frangibility

Tendency to break or crumble

full-functional defeat

Defeat of a target such that it is incapable of providing any of its intended functions

gabbro

A type of intrusive igneous rock chemically equivalent to basalt

gamma radiation

Radiation composed of high energy photons of energies consistent with nuclear energy levels

gas-check

A cup, typically of metal and lubricated with oil or wax, that expands under the action of pressure so as to form a gas-tight seal in a bore

gas-generator

A component of an engine which produces high pressure gas, such as may be used to turn a turbine or drive a piston system

gastrointestinal

The digestive tract

granite

A common type of intrusive felsic igneous rock

granodiorite

An intrusive igneous rock similar to granite but with more plagioclase than potassium feldspar

gravitometer

An instrument that measures the strength of a gravitational field

gravity gradiometer

An instrument that measures the gradient of the local gravitational field in space

gray

*SI Unit of absorbed dose, being equal to an absorbed dose of 1 joule/kilogram
(100 rads)*

ground-shine

Radiation emitted from radioactive material distributed on the ground plane

half-life

Time required for one-half of an initial population to undergo decay

hazard

A possible undesirable outcome or consequence

heat pipe

A heat transfer mechanism capable of transporting large quantities of heat between a hot and cold surface with a small temperature difference

heavy metal toxicity

Adverse health effects arising from accumulation of excessive quantities of heavy metals in the body

hedge component of enduring nuclear stockpile

The component of the US enduring nuclear stockpile comprised of those nuclear warheads not installed on any delivery system which are either fully operational or can be made so on short notice

homogeneity

The state or quality of being uniform in composition and/or structure

Hopkinson fracture

Tensile fracture resulting from the interaction of a compression wave and a free face

hydrodynamic impact regime

The regime of impacts occurring at velocities sufficiently high that inertial stresses are large with respect to the strength of materials and interacting materials behave like interacting incompressible fluids

hydrostatic pressure

Pressure due to the weight of the fluid above the fluid level of interest

hypervelocity

Velocities sufficiently high that inertial stresses are large with respect to the strength of materials, typically greater than 2500 m/sec for structural metals

inhalable particles

Particles of a size able to enter the head

initial radiation

Initial pulse of radiation (principally of gamma, x-ray, and neutron radiation) produced by a nuclear detonation

insoluble

Of low solubility

interbedded rock

Layers of rock lying between or alternating with layers of a different rock

interferometer

An instrument that uses interference phenomena of interacting waves to measure some property such as speed, wavelength, distance, etc.

irradiation

The act of exposing to radiation

isotropic

Invariant with respect to direction

kinetic penetrator

Penetrators which utilize their kinetic energy, and not explosives, to penetrate a target

latin-hypercube sampling

A type of space-filling method for stochastic sampling

levelized annual cost

The present value of the total cost of building and operating a plant over its economic life converted to equal payments in real dollars

limestone

A sedimentary rock composed largely of calcite, typically from the shells of marine organisms.

liquefaction

The process of liquefying

liquefactive

Relating to liquefaction (e.g. liquefactive power: power required to liquefy)

long-rod penetrator

A type of kinetic penetrator employing the inertia of a long-rod to penetrate an impacted material

lubricity

The quality of slipperiness

mafic

Rocks enriched in heavier elements such as magnesium and iron, typically characterized by darker colors, higher densities and lower melt viscosities as compared to felsic rocks

MATLab

A popular commercial engineering analysis and programming software

measure polytope

A term from n -dimensional geometry, denoting the class of convex closed figures consisting of opposite groups of parallel unit-length line segments, at right angles

*to each other, and aligned with each of the n-dimensional space's dimensions.
Unit lines, squares, cubes, and tesseracts are the measure-polytopes for
dimensions 1 through 4, respectively.*

metamodel

*A model of a model -- typically an easy to evaluate model fitted to the results of a
more expensive model or process*

micron

One millionth of a meter

modality

*A grouping of similar alternative implementations by basic physical processes by
which a specified physical outcome is produced*

monopropellant

A single constituent propellant, such as monomethyl hydrazine

Monte-Carlo Simulation

*A stochastic simulation method for determining probability distribution functions
of a system with uncertain inputs*

morphological matrix

*A matrical tool for depicting alternative compositions of a system by selection
from alternatives for implementing various system components*

mothballed

Inactive protective storage

mudstone

*A fine grained sedimentary rock whose original constituents were fine grained
clays or muds*

multidisciplinary analysis

Engineering analysis incorporating multiple coupled disciplinary analyses

n² matrix

A matrical tool for depicting the interdependence and iterative sequencing of dependent processes.

natural isotopic abundance

The fraction of all naturally occurring nuclei of an element consisting of a particular isotope of an element

Neogene (pre-Neogene)

A unit of geologic time, preceding the current period (Quaternary) and succeeding the Paleogene. Pre-Neogene would indicate times of more than about 23 million years ago.

neutron activation

Transmutation of stable isotopes by neutron capture into radioisotopes

neutron flux

Flux of neutron particles

neutron moderator

A material which slows neutrons down via nuclear collisions to speeds more consistent with the momentum distribution of the moderator's atoms

neutron spectrum

The velocity distribution spectrum of a neutron population

non-Newtonian Fluid

A fluid in which the viscosity changes with the applied shear force

nuclear reactor core

Central part of a nuclear reactor where fission occurs

nuclear reactor fuel-cycle

Here, the cycle of fueling, operating, defueling, and refueling a nuclear reactor

optical isolator

A device using an optical transmission path to transfer a signal between elements of a circuit while keeping them electrically isolated, often employing a Light Emitting Diode (LED) coupled with a photodiode

Ostwald-de-Waele non-Newtonian Fluid

A power-law, generalized Newtonian fluid

packing efficiency

Fraction of available volume occupied by a substance

pebble bed nuclear reactor

An advanced nuclear reactor design which utilizes a collection of spherical fuel elements

percussive drilling

Drill bit is forced into material by repeated blows

photogrammetry

Estimation of the actual dimensions of an object through analysis of one or more images of the object

photographic scaling

Scaling of all dimensions of an object by an identical factor

poise

A centimeter-gram-second unit of dynamic viscosity equal to one dyne-second per square centimeter.

prediction profiler

An interactive graphical tool for simultaneously exploring the effects of a number of independent variables on one or more responses

prompt radiation fatalities

Fatalities resulting from the acute effects of radiation exposure

pyrophoric

Exhibiting the property of spontaneously igniting upon contact with air

quality factor

A factor used to adjust the radiation dose absorbed by an individual for the relative adverse health effects of different types of radiation (quality factor for alpha, neutrons of unknown energy, high energy protons, and photons are 20, 10, 10, and 1 respectively)

rad

A unit of energy absorbed from ionizing radiation, equal to 100 ergs per gram or 0.01 joules per kilogram of irradiated material. It has been replaced as a standard scientific unit by the gray.

radiative cooling

Passive cooling through thermal radiation

radioisotope

An isotope whose nuclei are unstable, undergoing nuclear decay with a characteristic half-life

radioisotope production target elements

Individual units of encapsulated target material irradiated in a reactor to produce radioisotope, elements are contained in a target assembly

radiological effects

Effects having to do with exposure of something or someone to radiation.

radiotoxicity

The property of being a radioactive substance that is toxic to living cells or tissues

rare earth

Scandium, yttrium, and the lanthanide elements, historically referring to the elements in their naturally occurring oxide compounds

rarefaction wave

Expansion wave

reactive armor

Armor which reacts to the impact of a penetrator to mitigate its penetration, as by the propulsion of one or more metal plates by explosive reactive armor

refractory

A high melting temperature material

rem

Roentgen Equivalent Man. A unit for the amount of ionizing radiation absorbed by an individual required to produce the same biological effect as one rad of high-penetration x-rays (equivalent to 1/100th Gray)

respirable particles

Particles of a size able to enter the deep lung during nose breathing (<10 microns)

rhyolite

A type of mafic extrusive volcanic rock chemically equivalent to granite

RIPTP Munition

The integrated RIPTP, aeroshell, and guidance kit that comprise a precision guided munition DBHT defeat system

risk

A statistically expected consequence which captures both the severity of one or more hazards as well as their respective statistical likelihoods

roentgen

A unit of radiation exposure equal to the quantity of ionizing radiation that will produce one electrostatic unit of electricity in one cubic centimeter of dry air at 0°C and standard atmospheric pressure.

roller bit boring

A type of drilling mode – one or more (typically three) cones on the drill bit face covered with hardened projections exert a crushing and chipping action on the rock face

sandstone

A sedimentary rock composed of sand-size mineral or rock grains

scab

A piece separated from a face of a material due to internal stresses, as from spallation (also called spall in this instance)

sedimentary

Rocks formed from sediment

self-deterrence

The theory that the effects of existing inventory nuclear weapons are perceived as so horrific that, due to national and international political concerns, their retaliatory use in response to a limited WMD strike would not be authorized (i.e. their use would be self-deterred)

self-shielding

The shielding of an objects core from an external flux by its outer layers

Separative Work Unit

Standard measure for enrichment services. Separating a mass m_f of feed of assay x_f into a mass m_p of product assay x_p and waste of mass m_w and assay x_w is associated with an expended effort expressed in terms of the number of Separative Work Units needed, given by the expression $SWU = m_w \cdot V(x_w) + m_p \cdot V(x_p) - m_f \cdot V(x_f)$. The value function $V(x)$ is defined as $V(x) = (1 - 2x) \ln \left[\frac{1-2x}{x} \right]$

shaped charge effect

The jet effect produced from the interaction of a supersonic detonation wave in an explosive with a concave free (lined or unlined) surface, aka “Munroe Effect,” “hollow charge,” or “cumulative charge”

shock

Strong compression wave, typically used to mean a compression wave sufficiently strong to modify the material state variables via its passage

sievert

The SI unit for the amount of ionizing radiation absorbed by an individual required to produce the same biological effect as one gray of high-penetration x-rays (equivalent to 100 rem)

spall

A piece separated from a face of a material due to internal stresses, as from spallation, or the physical process of spallation

spallation

Breaking off of pieces of a face due to internal stresses

specific impulse

The change in momentum that can be affected by a propellant per unit propellant weight

spoils

Refuse material removed from an excavation

squash warhead

An antiarmor warhead comprised of plastic explosive with a delay fuze, designed to spread out against the surface of a target prior to detonating so as to propagate a compressive wave into the target wall, hopefully resulting in spallation of the wall interior and consequent terminal effects (aka High Explosive Squah Head/HESH, or High Explosive Plastic/HEP)

subterrenes

An underground vessel or vehicle physically independent of the surface (analogous to a submarine)

super hard DBHT

A Deeply Buried Hardened Target expected to be robust to attack by nuclear weapons

tachylite

A vitreous form of basaltic glass

target assembly

The physical assembly which is inserted into a reactor for irradiation

Technology Readiness Level

A technology maturity metric, TRL is a classification system which enables comparison of technological maturity between different technologies

terminal effects

Effects produced by a munitions interaction with a target.

terminal lethality

The effects of a munition upon interaction with a target which contribute to target neutralization

Theory of Inventive Problem Solving

A method of inventive problem solving formulated by the russian Genrich Altshuller.

thermal neutrons

Neutrons possessing a velocity spectrum consistent with the ambient moderator temperature

thermal penetrator

a penetrator employing melting or other thermal effect to travel through a material

thermal radiation

Electromagnetic radiation emitted by matter that is due only to its temperature.

In terms of nuclear weapon effects, thermal radiation is produced by the superheated gases comprising the fireball after detonation.

thermal spall

Spallation of a material's surface due to fracture resulting from thermal stresses

thermal subterrene

a penetrator employing melting and physically independent of the surface

thermite

A chemical reaction or chemical mixture in which a metal is oxidized by the oxide of a second metal to produce heat (a type of exchange reaction)

thoracic particles

Particles of a size able to enter the lung during mouth breathing (<30 microns)

thrust-gravity losses

The losses to attained momentum change of a vehicle incurred due to the action of the thrust vector in opposition to the gravity vector

transmutation

Conversion of one isotope to another by some nuclear process

travelling charge gun

A gun in which the propelling charge travels with the projectile, ideally burning at a variable rate so as to maintain a constant base pressure on the projectile

tuff

A rock composed of compacted volcanic ash varying in size from fine sand to coarse gravel. Also called tufa

vaporific effect

Fuel-air explosive like effect that can be produced by the high velocity impact of combustible materials such as aluminum and uranium metals and the consequent rapid combustion of the small fuel particles produced.

viability

Capable of succeeding in actual practice (competitive in the face of practical considerations such as economics, politics, etc.)

weathered rock

Mechanical breakdown and/or chemical alteration of rock due to the effects of weather such as temperature variations, water, etc.

wipe velocity

Velocity component tangential to long axis of a penetrator, measured relative to impacted surface

SUMMARY

During the Cold War, Deeply Buried Hardened Targets (DBHTs) and the assets they protected were of great strategic and tactical concern to the Department of Defense. Megaton-class nuclear warheads were the only viable means of attacking many of these facilities, and even so, a small subset of DBHTs was anticipated to be robust even in the face of such an attack. Post Cold War, the threat posed by DBHTs has not disappeared. Rather, the conventional warfare advantages of the United States have led to an increasing emphasis by potential adversaries on the construction and use of hardened facilities such as DBHTs for protection of both conventional and unconventional assets. Further, the shift in perceived relative risk to the United States' national security from large scale all-out nuclear attack towards very limited attack by Weapons of Mass Destruction (WMD) has led some to hypothesize that "self-deterrence" may diminish the strategic value of current inventory nuclear weapons.

The objective of the work described was to identify and explore a paradigm shifting solution that could offer leap-ahead capabilities to counter current and future DBHT threats while mitigating or eliminating the "self-deterrence" issue. Systematic evaluation of DBHT defeat alternatives lead to the selection of a thermal subterrene as a hypothetical means of providing such a capability. A number of possible implementation alternatives for a thermal subterrene were investigated, resulting in the identification of the RadioIsotope Powered Thermal Penetrator (RIPTP) concept for providing an effectively unlimited hard rock penetration capability using near-term technologies.

However, the proposed approach was novel and thus required formulation and application of a physics based multidisciplinary analysis code to enable evaluation of

design alternatives and analysis of performance. Technical considerations identified as important to the feasibility of a RIPTP for DBHT defeat included: packing of RIPTP components in available volume; close-contact melting in a medium with nonlinear thermodynamic properties; radiation shielding; radiation health physics; point source plume dispersal calculations; alternative technologies for production of radioisotopes; chemical and physical properties of isotope compounds; nuclear reactor characteristics; high temperature material stability and inter-material compatibility; weapon and delivery system integration; a variety of heat transfer regimes including radiation, conduction, convection, nucleate boiling, and film boiling; thermal/mechanical stress analysis (steady-state and transient); rock physical and thermodynamic properties as a function of temperature; detection/mapping of deeply buried facility spaces; and more.

The following disciplinary analyses were composed into a multidisciplinary analysis code for a RIPTP: packing of RIPTP components in available volume; close-contact melting analysis; transmutation of isotope species by neutron activation; reactor neutron economy; radioisotope power generation through decay; modelled radiation shielding calculations for a RIPTP; and steady state thermal analyses for a RIPTP in various scenarios.

Filtering of radioisotopes for potential suitability, their possible production mechanisms, state of technological development, and multidisciplinary analysis code predicted performance lead to the identification of Thulium-170 as the best isotope for powering a RIPTP using present-day technology and technical data. Ytterbium-169 was identified as an alternative isotope offering the potential for significant potential improvements over Thulium-170 in radiological safety as well as RIPTP performance

and producibility. Production, however, was determined to require identification of a cost effective technology for highly enriching Ytterbium-168 from its low natural abundance.

Performance analysis of the identified baseline Thulium-170 RIPTP suggested that the predicted low penetration rate of about 10 meters/day could be a significant negative factor with regards to possible viability of the concept. Consequently, a survey for potentially enabling technologies was performed using an adaptation of the Technology Impact Forecasting (TIF) approach. It was found that the greatest potential for improving performance of the baseline Thulium-170 RIPTP resulted from increasing overall power density of the penetrator. Several possible technology approaches to achieving significantly increased penetration rates (approximately 50 meters/day expected penetration rate vs. original 13 meters/day) were proposed.

However, it was determined that the hypothetical technology having the greatest potential impact on thermal subterrene viability for DHBT defeat with respect to penetration rate was cost-effective enrichment for Ytterbium-168. Development of such a technology would eliminate or enormously reduce the impact of all identified RIPTP performance and producibility concerns. Alternatively, relaxation of the requirement for no radiological hazard to enemy combatants would enable selection of a fissile powered thermal subterrene to provide required power densities consistent with rapid penetration.

INTRODUCTION

This thesis documents a Multi-Disciplinary (MD) approach formulated and implemented for the identification and evaluation of a novel concept for defeat of Deeply Buried Hardened Targets (DBHTs), *thermal subterrenes*. This MD approach included consideration for: DBHT defeat alternatives; thermal subterrene concept alternative implementation analysis; definition of a baseline feasible thermal subterrene through safety and multidisciplinary analysis; and an exploration of the multidisciplinary design space to identify enabling technologies for thermal subterrene viability.

MOTIVATION

Concerns regarding DBHTs and the assets they protect were pronounced throughout the Cold War, and were generally addressed by the tasking of multi-megaton-class nuclear warheads for defeat of such targets in the event of war.^{1, 2} The end of the Cold War, however, has not caused the threat posed by DBHTs to disappear. Rather, the conventional warfare advantages of the United States have led to an increasing emphasis by potential adversaries on the construction and use of hardened facilities such as DBHTs for protection of both conventional and unconventional assets.

A report to congress submitted by the Secretary of Defense and the Secretary of Energy in 2001 states in part:³

Our potential adversary's weapons of mass destruction (WMD), long-range missiles, modern air defenses, most sophisticated command and control systems, national leadership in wartime, and a variety of tactical arms are increasingly

concealed and protected by networks of hard and deeply buried facilities. If the United States does not have the means to defeat these facilities and the threatening assets they protect, adversaries may perceive that they have a sanctuary from which to coerce or attack the United States, its allies, or its coalition partners with threats much more powerful than in past conflicts... The intelligence community (IC) suspects with reasonable certainty that there are over 10,000 potential HDBTs (Hard and Deeply Buried Targets) worldwide and their numbers will increase... There are no easy answers... and certainly no "silver bullets"... Concern is growing about use of HDBTs to protect WMD production and deployment, especially chemical and biological weapons (CBW)... (the) problems clearly overlap.

Consider, for example, a hypothetical DBHT emplaced under 80 meters of high-strength rock. The technical problem posed by defeating such a DBHT is significant because, as will be discussed later, requirements exceed the capability of virtually any traditional hard target defeat approach (other than a ground or subsurface nuclear burst) deliverable by present or projected delivery platforms. The available option of targeting such facilities with even reduced yield penetrating nuclear bombs is relatively unattractive with respect to both the political and collateral human costs. Some of the most important hardened strategic targets are emplaced hundreds of meters below the ground and are likely invulnerable to both the largest operational inventory weapons (300 kT penetrating B61-11 and 1.2 MT B83) as well as the larger "hedge" weapons (the 9 MT B53, variously reported "retired" or part of the "hedge" component of the enduring nuclear stockpile).^{2, 4, 5}

One analysis of employment of low-yield penetrating nuclear bombs for hard target defeat suggests on the order of 10^4 short-term casualties for even a 1-kiloton penetrating nuclear bomb used in an area with population density of 5000 habitants per square kilometer.⁶ This result neglects all contributors to lethality other than deaths due to fallout associated radiation poisoning in a two-month time frame and gives an approximate idea of the expected collateral damage.

Another recent analysis by the National Academy of Sciences suggests casualties of thousands to in excess of a million resulting from a nuclear strike using a Robust Nuclear Earth Penetrator (RNEP) type munition against a single HDBT in an urban area. In a rural area, the same report estimated casualties numbering from hundreds to hundreds of thousands. These results considered prompt nuclear weapon effects (air blast, thermal radiation, and initial radiation) contributions to casualties as well as those from fallout induced acute radiation sickness. Deaths were estimated to in general vary over similar orders of magnitude as serious injury.²

It is clear that a means of defeating DBHTs with more precisely controllable effects is needed given: that existing conventional weapons are unable to hold at threat many strategically important DBHTs; the expected political and human costs of nuclear attack; and that some of the most strategically important DBHTs are estimated to be robust to even nuclear attack.

PROBLEM STATEMENT

The problem considered is defeat of a hypothetical Command Control and Communication (C³) DBHT by means of an air-delivered system. Nuclear-explosives are

not an allowed alternative in so much as casualties due to radiological effects were considered unacceptable as a result of any candidate solution's nominal effects against the target. Chemical or biological agents with intended or incidental anti-personnel effects were likewise excluded. The hypothetical target DBHT was specified as: emplaced under 80 meters or more of intact high-strength granite; hardened against attack by Nuclear, Biological, and Chemical (NBC) weapons; and possessed of internal redundant utilities such as Heating, Venting, and Air-Conditioning (HVAC), power generation, food stockpiles, and an internal deep-water well.

“Full-functional” defeat of the facility is desired – that is, the facility should be rendered incapable of performing any of its intended functions that provide strategic or tactical utility to the enemy. Ideally, the manner in which this is accomplished should be such that the capabilities of the DBHT cannot be reconstituted in any tactically relevant period of time. Lastly, the means identified for attacking the DBHT should be such as to provide a leap-ahead capability – that is, the identified solution should be capable of overmatching DBHT facilities of today and the immediate future.

The resources available were specified to be existing or near-term technologies that would support an operational capability for DBHT defeat in the short-term, i.e., within the next ten years. Expenditures consistent with historical munitions programs were assumed to be acceptable *if* a plausible solution was identified.

APPROACH

The evolution of offensive air-delivered munitions for hardened target attack vs. the defensive capabilities of hardened targets to resist such attack has lead to the present

status quo, wherein DBHT hardened targets enjoy a fairly robust defensive capability with regards to attack by non-nuclear explosive munitions. A principle purpose of the present work is to step back from traditional DBHT-attack munition concepts, and ascertain whether a fresh, wide-ranging, “out-of-the-box” look at alternative DBHT defeat concepts combined with techniques borrowed from a variety of modern complex system design methods might enable identification of one or more potentially feasible alternatives for air-delivered DBHT attack which sidestep the active constraints limiting effectiveness of historical approaches.

To this end, a number of modern concept identification and complex system design methods were considered, apparently useful elements selected, and then composed into a proposed multidisciplinary approach to the problem. Some of the methods borrowed from were: TRIZ;⁷ Integrated Product/Process Design (IPPD);⁸ Robust Design Simulation;⁹ and Technology Impact Forecasting.^{10, 11} Figure 1 illustrates the approach employed for: generation of alternative concepts for DBHT defeat; selection of the preferred concept; definition of a baseline design; and analysis of the preferred concept to identify technologies potentially enabling to concept viability. The ultimate product of the process is the information developed regarding potential performance and characteristics of the preferred alternative as well as any identified associated enabling technologies. The availability of this information enables informed planning for any future research and development effort which might be undertaken for an identified concept.

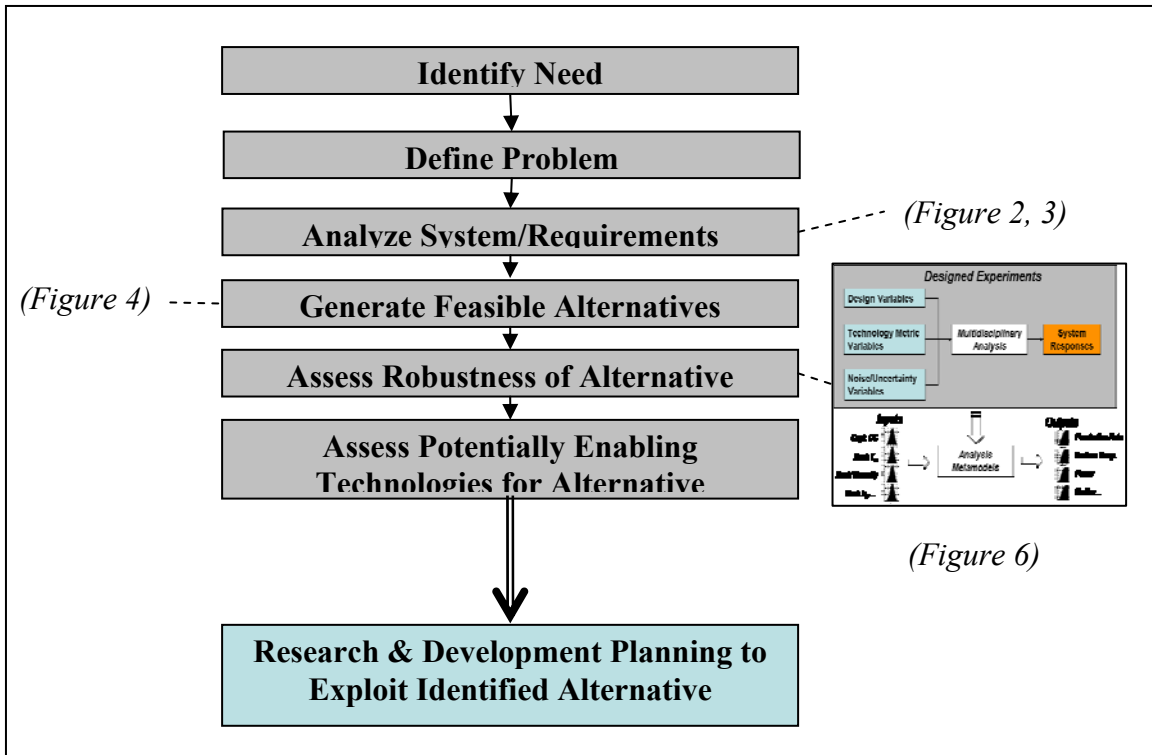


Figure 1: Top-level approach used for alternative analysis, selection, and development

Identifying need

The first step as outlined was to establish that a need exists in society. This need is evident in congressional reports, white papers, patents, history texts, etc., and can be expressed as follows. *The defeat of DBHTs is of great importance both in the event of war as well as for the purpose of strategic deterrence, and the only extant available option, nuclear explosives, are undesirable inasmuch as their use would likely be associated with significant collateral casualties and undesirable political consequences. Further, even this option may not be able to hold at risk the hardest and most strategically important DBHTs.*^{1-3, 6, 12-19}

Defining the problem

The second step in this process was to define the problem in explicit terms – what are the objectives, and what resources are available? As previously described, the objectives are:

- **Identification of an innovative means of defeating DBHTs (not consistent with evolutionary improvement of existing alternative)**
- **“Leap-ahead”/overmatch capability against DBHTs (ideally capable of engaging a target of much greater depth than specified baseline target)**
- **Full-functional defeat is desired if possible**
- **Air delivered munition**
- **No nuclear explosives utilized**
- **No radiologically, biologically, or chemically inflicted casualties as a nominal expected consequence of weapon employment**

- **Existing or near term technologies that would support an operational capability for DBHT defeat being available within the next ten years**
- **Expenditures consistent with historical munitions programs**

Part of defining the problem is also investigating the literature. In the present case, the literature investigation was principally focused on unclassified DBHT characteristics and historical approaches to hard target defeat. Both of these topics are discussed in later sections.

Analyzing system/requirements

Once a problem system has been defined, it is necessary to undertake the process of system decomposition and analysis so that the system components and subcomponents may be identified and their interdependencies considered. As shown in Figure 2, the problem system considered consists of both existing components which must be identified (such as DBHT facilities, and perhaps alternative delivery vehicles for the DBHT defeat munition) and undefined components which must be defined (the DBHT defeat munition).

For the defined problem component (DBHT targets), DBHT system analyses are undertaken such as: identification of the top-level functions; functional diagramming; and analysis of the physical connectivity of a DBHT's systems (Figure 3). These analyses: 1) identify the types of utility provided to the enemy by the DBHT which it is the objective of some candidate DBHT-attack-munition to destroy, deny, or disrupt; 2) sub-functions of the DBHT facilities components necessary to the execution of the DBHT's overall functional objective; and 3) physical connectivities of DBHT system components which might be exploited to attack DBHT functions necessary to DBHT mission execution.

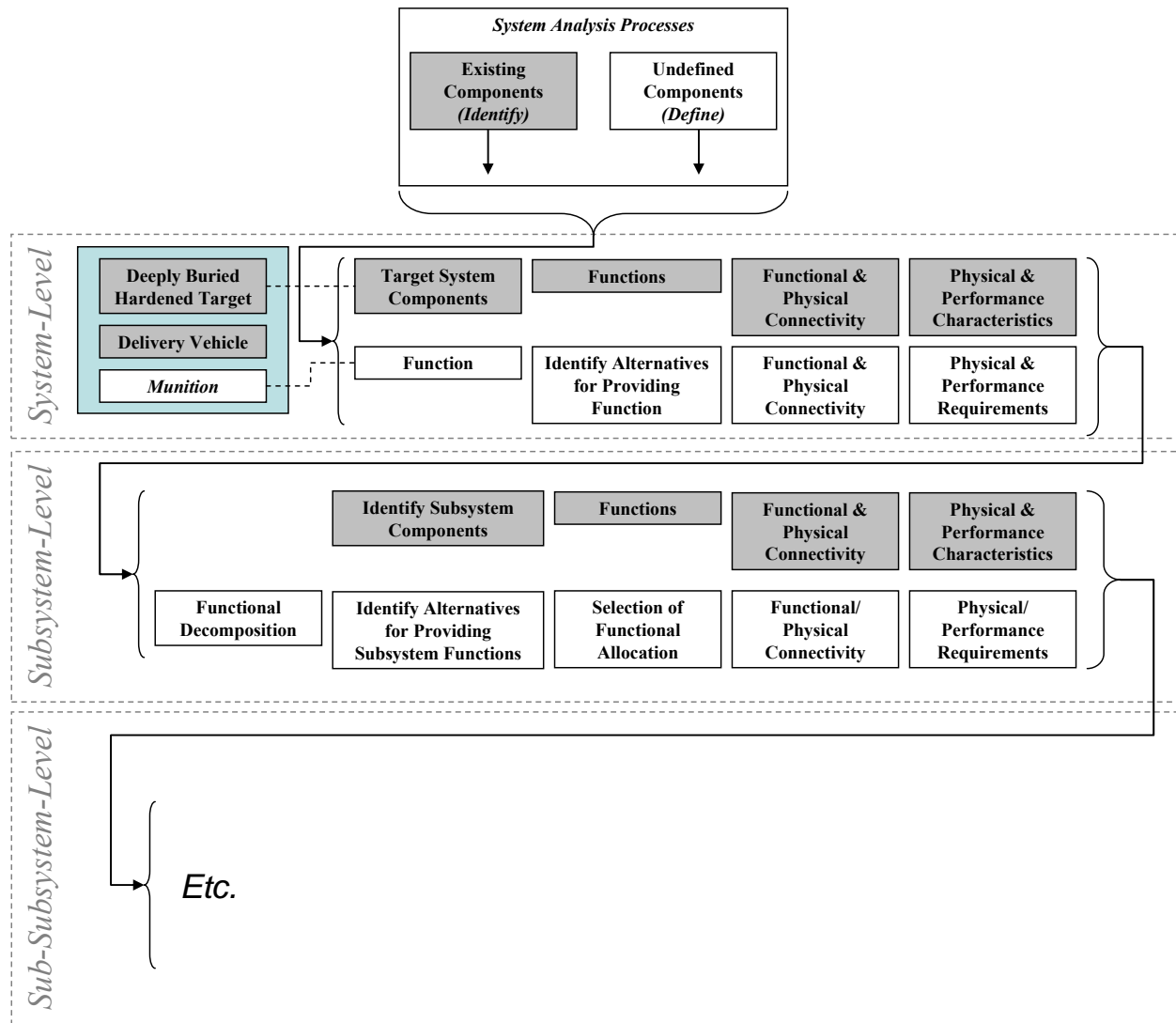
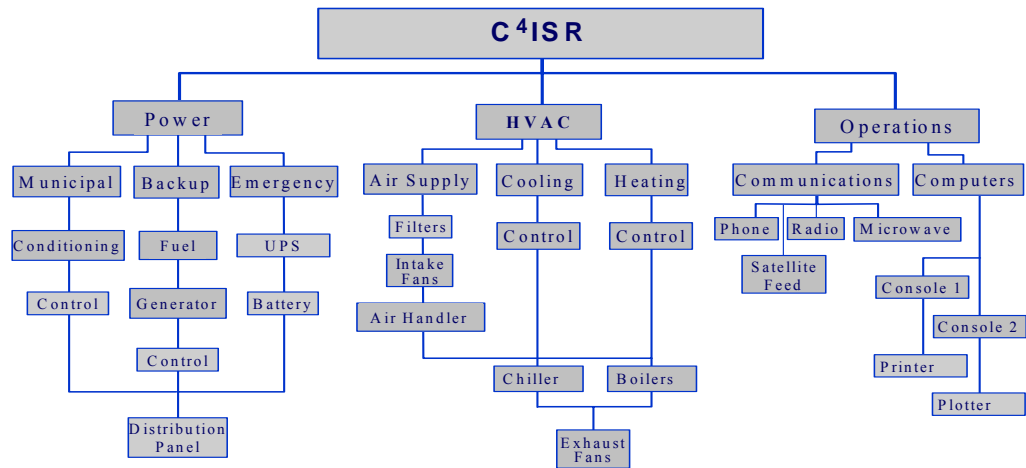


Figure 2: General approach to analyzing DBHT/DBHT-defeat-munition system & requirements

DBHT Functions

1. **Command, Control, Communication, Computer, Intelligence, Surveillance, Reconnaissance (C⁴ISR)**
 - a. **Air Defense**
 - b. **Ground, Naval, Coastal Forces**
2. **Artillery, Rocket Launching / Staging**
3. **Materiel / Weapon Storage**
4. **NBC Production, Storage**
5. **Industrial/Other**

Functional Diagram



Physical Connectivity

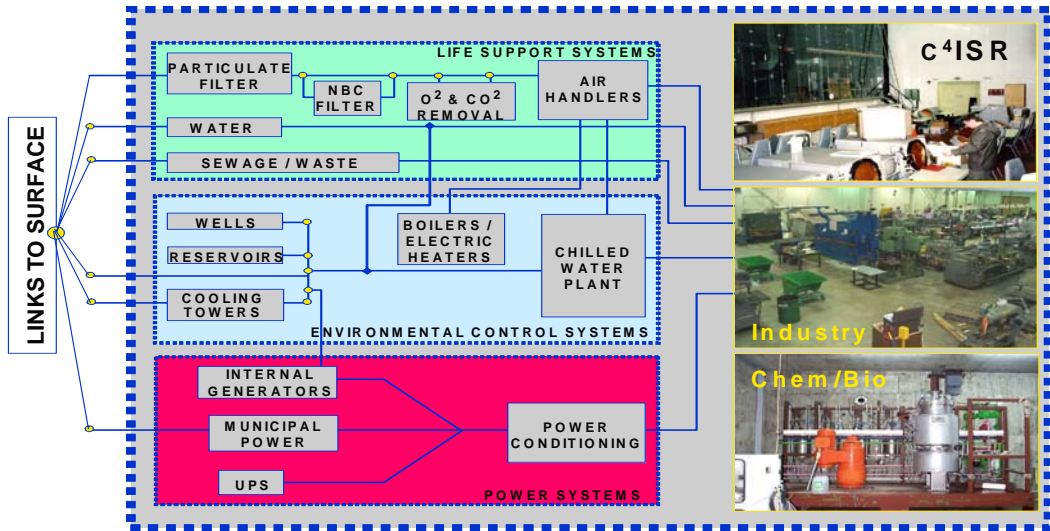


Figure 3: Some possible *DBHT Functions*, as well as a *Functional Diagram* and diagram of the *Physical Connectivity* of a DBHT (notional)

Reference²⁰

Generating feasible alternatives

It is next necessary to generate one or more feasible alternatives that could potentially solve the problem. Defining the creative component of this step – the identification and (also creative to a degree) rejection of potential solutions – in such a fashion that it would be a repeatable process with repeatable outcome is impossible. An engineer’s intuition, experience, imagination, and the resources available to him all play too great a role in the outcome. However, the expansion of the “Generate Feasible Alternatives” block in Figure 1, shown in Figure 4, is an attempt to outline some of the major elements involved in the process which leads to the identification and selection of a proposed alternative. Fundamentally, generation of feasible alternatives involves the generation, characterization, and filtering of options. It involves substantial historical research of what has been tried before, and is an iterative process.

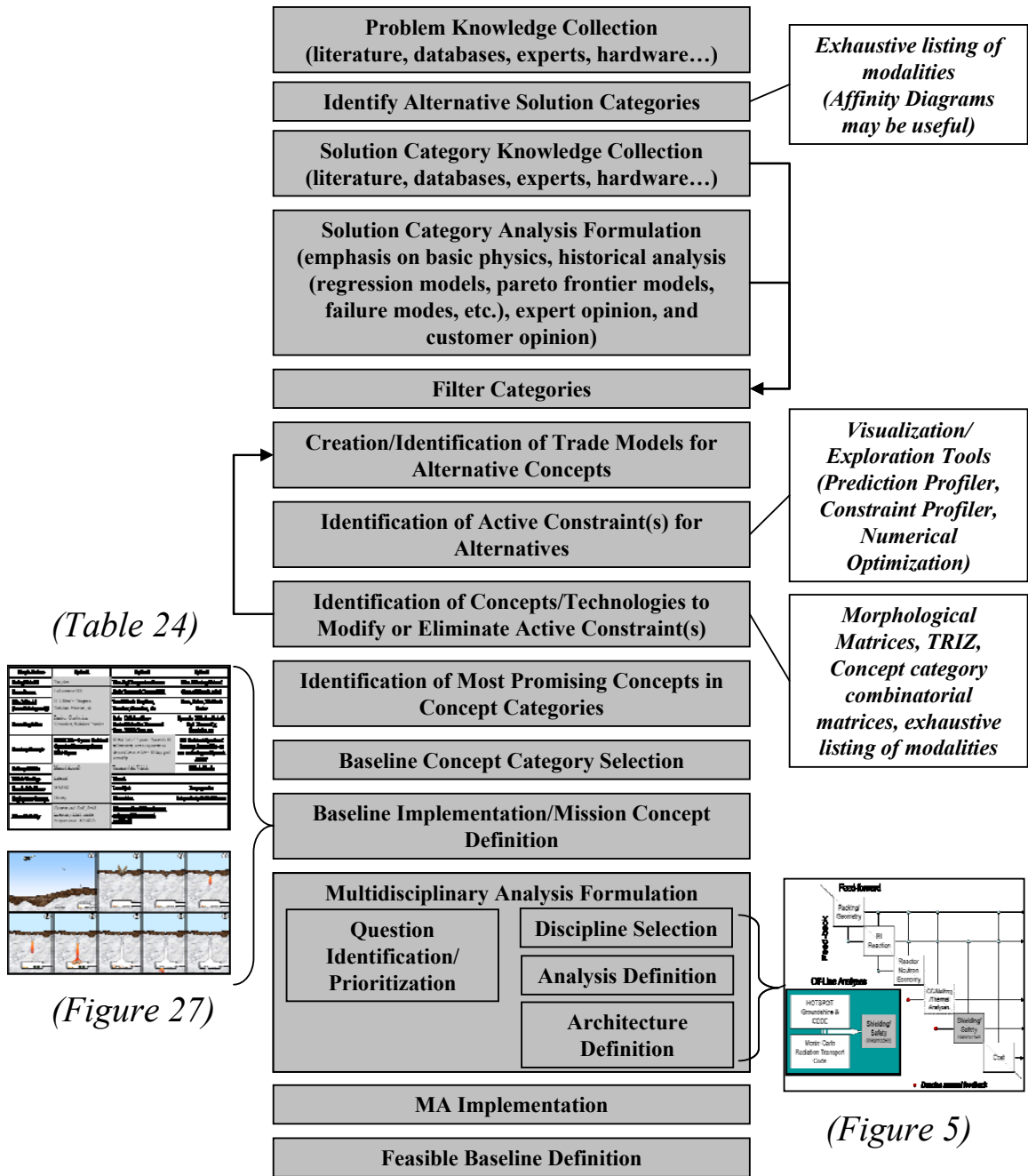


Figure 4: Generate Feasible Alternatives – some steps in the identification of (a) feasible alternative(s)

Generating alternative concepts for consideration

Generation of alternatives is in parts reactive, exhaustive, historical, and combinatorial in nature.

It is reactive in that identification of the active constraints limiting performance of historical solutions can facilitate identification of approaches for which the constraints do not apply or apply differently, enabling the potential for improvements in performance up to the point that a new active constraint is encountered. In the context of engineering design constraints, “revolutionary” engineering solutions are solutions which circumvent the constraints limiting historical solutions. Thus, revolutionary engineering solutions potentially can be identified by analysis of constraints.

This is essentially the approach used in Theory of Inventive Problem Solving (*ТРИЗ* or “TRIZ” is the popularly recognized Russian acronym of the method developed by Genrich Altshuller), although TRIZ states the identification of the active constraint as a contradiction in a dialectic framework. In TRIZ, “inventive principles” historically used to resolve “contradictions” (constraints limiting improvement) of various natures are considered in application to the contradiction at hand to attempt to identify an inventive solution.⁷

The process of identifying possible solutions is also exhaustive, in that it is often fruitful to exhaustively list means of providing one or more required functions that contribute to solving a defined problem. This can be helpful from the standpoint of identifying options for providing a function that may not have been historically considered in the context of the problem at hand. With respect to identifying innovative and potentially revolutionary solutions (for which historical constraints either do not

apply or restrict performance to a lesser degree) it can be particularly helpful to generate exhaustive lists of alternative modality* solutions.

Also, attempting to make exhaustive lists of options can help prevent one from focusing on a single possible solution too early in the design process and potentially missing more promising alternatives (this is what is meant by the old design engineer's adage "champion the problem, not a solution").²¹ It can be a strong temptation for engineers, particularly those with less experience, to become so personally invested in a single solution that they fail to fairly assess the range of alternatives available. They fall into the role of advocate for a solution approach, instead of a more appropriate role of being an advocate for the problem.

Next, efficient and thorough alternative concept identification is to a great degree historical in nature... there is little new under the sun, and very large numbers of historical approaches to solving a problem can typically be identified. The literature, the opinions of grayer heads, and surviving hardware are primary tools to inform the identification and selection of alternatives.

Creatively identifying concepts is also in part combinatorial. One reason for this is that almost all engineered systems have multiple functional requirements. Satisfaction of these requirements typically involves specification of different categories of solution

* Here, the word *modality* is used to denote similar groupings of basic physical processes by which a desired physical outcome might be achieved that contribute to the solution of the defined problem. For almost all non-trivial engineering problems, multiple modalities exist by which a desired result could be brought to pass. For example, if you need to measure the passage of time, you could utilize a host of physical phenomena (modalities) to do so: flow of a fluid (such as sand or water) through an aperture; oscillation of an electrical circuit; motion of a pendulum; decay of an isotope; etc. For each of these given modality's, various and typically different functional and/or physical components are necessary or desirable for the implementation using the given modality in a potential solution's implementation. For example, a pendulum could utilize a number of potential energy/kinetic energy coupled systems: a mass on a rigid arm swinging in a gravitational, magnetic, or electrostatic field; a mass on a spring arm; etc. Different constraints will typically apply to each of the different modalities and implementations, potentially leading to identification of a category of approach unconstrained by the performance limitations of historical systems.

characteristics. Identifying the full solution space for a given concept involves the combinatorial problem of picking one or more options for each of the characteristics that comprise a potential solution. A useful format for defining this solution space is a morphological matrix, where categories of system characteristics are listed in rows with a different option in each column (see Table 24). A single system implementation can then be composed by picking one or more compatible options from each row to define a single implementation possibility.

The process of identifying alternative concepts is also combinatorial in that sometimes it is possible to synergistically combine distinct approaches to providing a required function so that the requirement is met by the aggregate contribution of effects from different approaches. Thus when considering penetrators one may wish to consider concepts combining shaped charge and long-rod penetrator effects, long-rod and thermal penetrator effects, long-rod and explosive spallation effects, etc.

Eliminating alternatives from consideration

Just as important as identifying potential alternatives is efficiently eliminating them. Due to the large numbers of alternatives which can be generated it is necessary to eliminate alternatives from consideration as efficiently as possible. A principle approach used was to attempt to identify one or more alternative characteristics that met all of the following criteria: the characteristic was associated with a fundamental/inherent constraint limiting potential performance of the concept; and the restriction on potential performance created by the constraint could be assessed cheaply using readily available information.

Another option used for efficiently eliminating alternatives was by considering similarity of two or more alternatives – that is, if one alternative is essentially equivalent in nature to another alternative but inferior in one or more crucial respects, then the first alternative can be eliminated from consideration. If the retained alternative is ultimately found unsatisfactory, then the alternative previously eliminated due to similarity would have been as well.

Historical knowledge resources are vital to identifying favored alternatives for further consideration. Literature and expert opinion can be consulted to identify historical constraints limiting an alternative's performance, and historical data can be analyzed to extrapolate demonstrated system performance to ultimate plausible limitations. Patent literature often reveals alternative concepts of implementation that modify or eliminate the impact of one or more historically dominant constraints (for example, sequential employment of shaped charges in series modifies the shaped charge diameter constraint on maximum depth of penetration).

In summary, it is vital to not be fixated on an alternative's potential advantages, never more so than early in the design process – there are inevitably dozens, perhaps hundreds of thousands of alternatives (often more) to consider in identifying potential conceptual solutions to a problem statement. The goal is to first identify them (with particular regard to identifying the major categories of approach) then eliminate alternatives as quickly and cheaply as possible for sound engineering reasons, while at the same time giving all alternatives the benefit of the doubt as to potential performance given the fidelity of analysis employed.

Selecting a baseline concept

Ultimately it is necessary to select a baseline concept for more in-depth engineering evaluation. This decision is made based on the engineer's understanding of the problem definition, the available resources, and what is known about the identified alternative's respective characteristics. All concepts that have not been previously eliminated are then compared as to their respective merit with regard to the problem definition's performance requirements and resource limitations.

At this very conceptual level an irreconcilable lack of engineering history or required resources for analysis is an important demerit for an alternative. The overall objective is to identify a feasible alternative that is capable of satisfying the problem definition. If relevant engineering experience for a particular concept is unavailable in the literature or engineering community, then the risk of non-feasibility of the concept due to unrecognized constraints increases. Also, unfamiliar concepts can appear attractive to designers because their limitations are less familiar than those of traditional approaches. A critical eye towards historical engineering literature and a willingness to consult both diverse disciplinary experts and more experienced programmatic engineers is crucial. However, at the same time, differences in background and engineering expertise are a principle reason for seeking innovative "out of the box" solutions from individuals, organizations, and historical literature (such as patents, technical or programmatic articles, etc.) with significantly different engineering focus than those historically associated with a problem.

A deficiency in required data or theory for analysis of an alternative is also a demerit. If the deficiency in theory or data cannot be corrected with available project resources, then a reasonable engineering case arguing the feasibility of the approach may

not be possible. For example, if engineering expertise and requisite data on computer software, computer networking, and network security in use by possible target DBHTs is unavailable to an engineering effort (or the answers are diverse and specific when the problem requires a general solution), then expending resources on investigating information system attacks or similar approaches to DBHT defeat is probably unwise. The sensitivity of viability of a concept to very detailed, difficult to ascertain, and likely very target specific information make the robustness of an approach questionable.

Defining a feasible baseline design

If one is able to identify from the literature a historical system capable of satisfying the problem definition, then defining a baseline feasible design is as simple as determining the engineering definition of the historical system. If, as in the present case, a historical system capable of satisfying the problem definition is not identifiable, then defining a feasible baseline design can become quite involved, in parts qualitative and quantitative in nature.

Recall that part of the process of filtering concepts is identification of historically important constraints and expert concerns that might affect the feasibility or limit the performance of a given concept. The first part of defining the baseline feasible design in the reported work was qualitative – alternatives/assumptions defining a concepts implementation, fabrication, and utilization were selected in an attempt to avoid or mitigate known limitations of the conceptual approach.

The next part of defining the baseline feasible design was more quantitative. Defining the feasible baseline design for the concept required identification of potentially active constraints that might limit the concept's performance and formulation of

disciplinary analyses for assessing the same. Recall that part of the process of filtering concepts is identification of historically important constraints and expert concerns that might limit the performance of the given concept. Disciplinary analyses allowing assessment of these identified topics are the starting point for composing a multidisciplinary analysis to facilitate definition of a baseline design. The multidisciplinary analysis is defined by first identifying the interdependencies of the selected disciplinary analyses, and then specifying an analytical/computational architecture whereby the dependencies will be computationally resolved (Figure 5). Figure 5 defines the MDA architecture for analyzing the baseline DBHT defeat approach, whose selection will be discussed later.

Once a multidisciplinary analysis capability is created, values (or ranges) for the non-design variable parameters in the analysis are identified. This is done using engineering and scientific literature to identify parameters related to material properties, physical constants, manufacturing capabilities, etc. Manual exploration of the design space and numerical optimization are then used to identify a baseline feasible design definition.

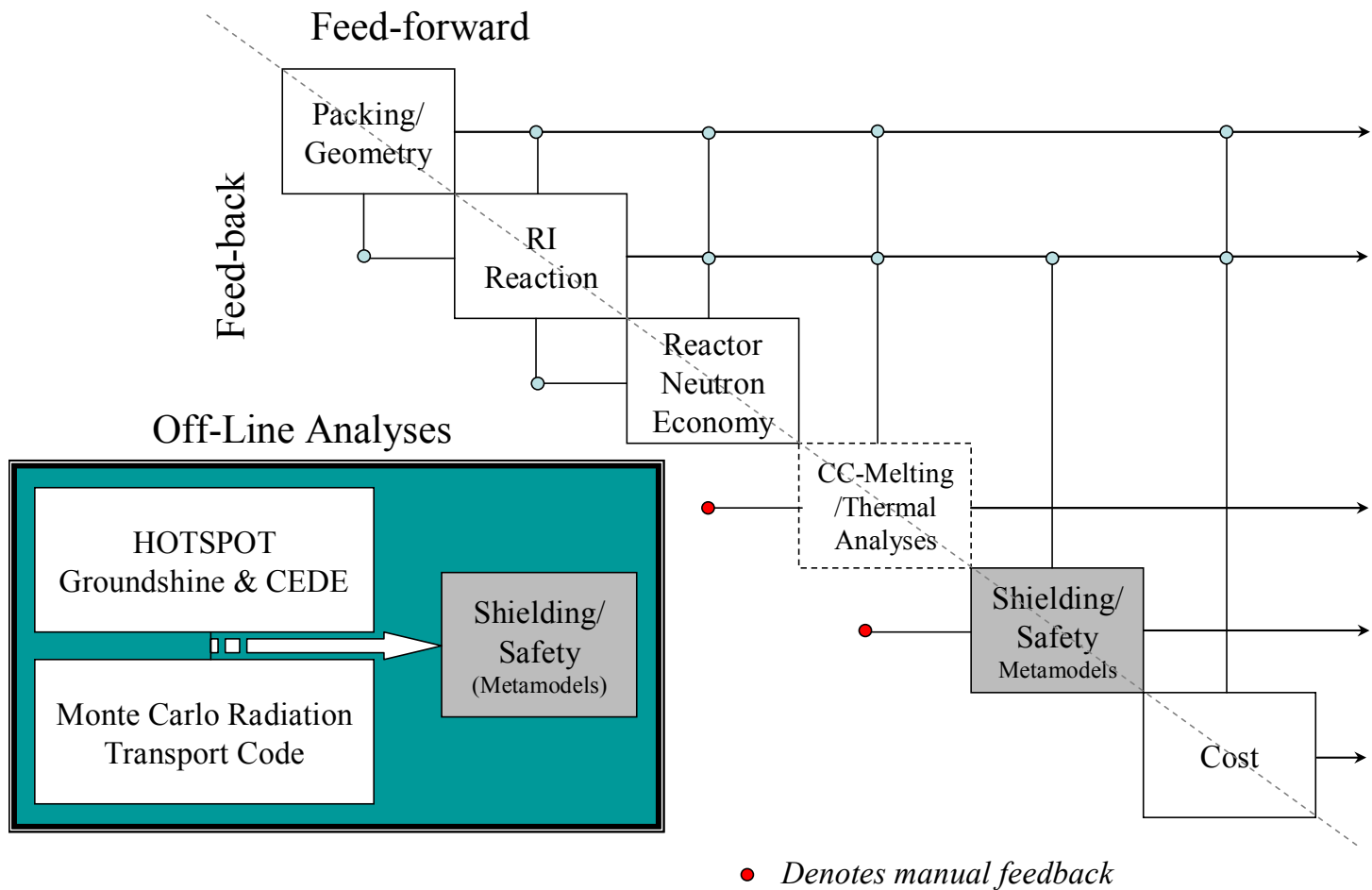


Figure 5: A Multidisciplinary Analysis Formulation, depicted as an n^2 diagram, showing selected disciplinary analyses and their interdependence in terms of feed-forward and feed-back of analysis variables

Assessing robustness of alternative

Given that a potentially feasible alternative has been found (that is, one which does not violate the laws of physics) it is next desirable to identify the *likely* performance of this concept given the presence of risks and uncertainty. One approach to doing so is through Monte Carlo Simulation, wherein probability distributions may be specified for variables in the multidisciplinary analysis previously formulated whose actual values are uncertain or noisy, and the corresponding impact on probable concept performance assessed through analysis of the resulting distributions of the output variables.

A typical issue which arises with this approach, however, is the computational expense of Monte Carlo Simulation (MCS). A typical number of draws for an MCS simulation is approximately 10,000. Considering that for an MDA code requiring one minute per case to execute a single MCS with 10^4 draws would take a week of computational time, it is clear that some more computationally efficient approach to assessing robustness is desirable.

Robust Design Simulation (RDS) is one approach to improving computational efficiency (Figure 6).⁹ In this approach, designed experiments are executed to create a dataset suitable for fitting a fast executing *metamodel* (a model of a model, such as the MDA analysis considered). The metamodel provides a regressive or interpolative approximation of the more costly model, thereby enabling more rapid execution of MCS analyses. Some types of alternative metamodels include: Response Surface Equations (RSEs); Gaussian Processes (GPs); Neural Networks (NN); and Kriging models.

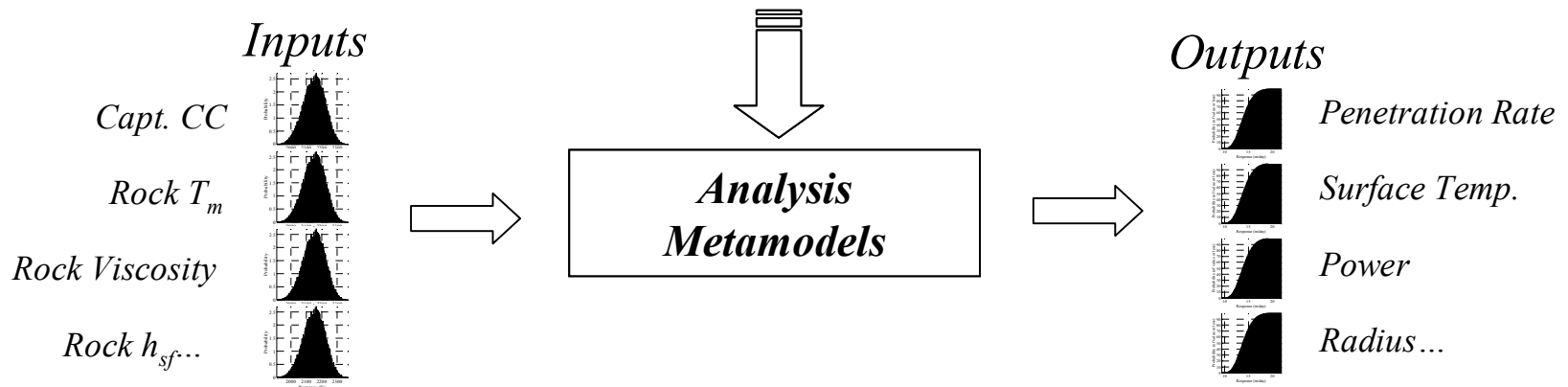
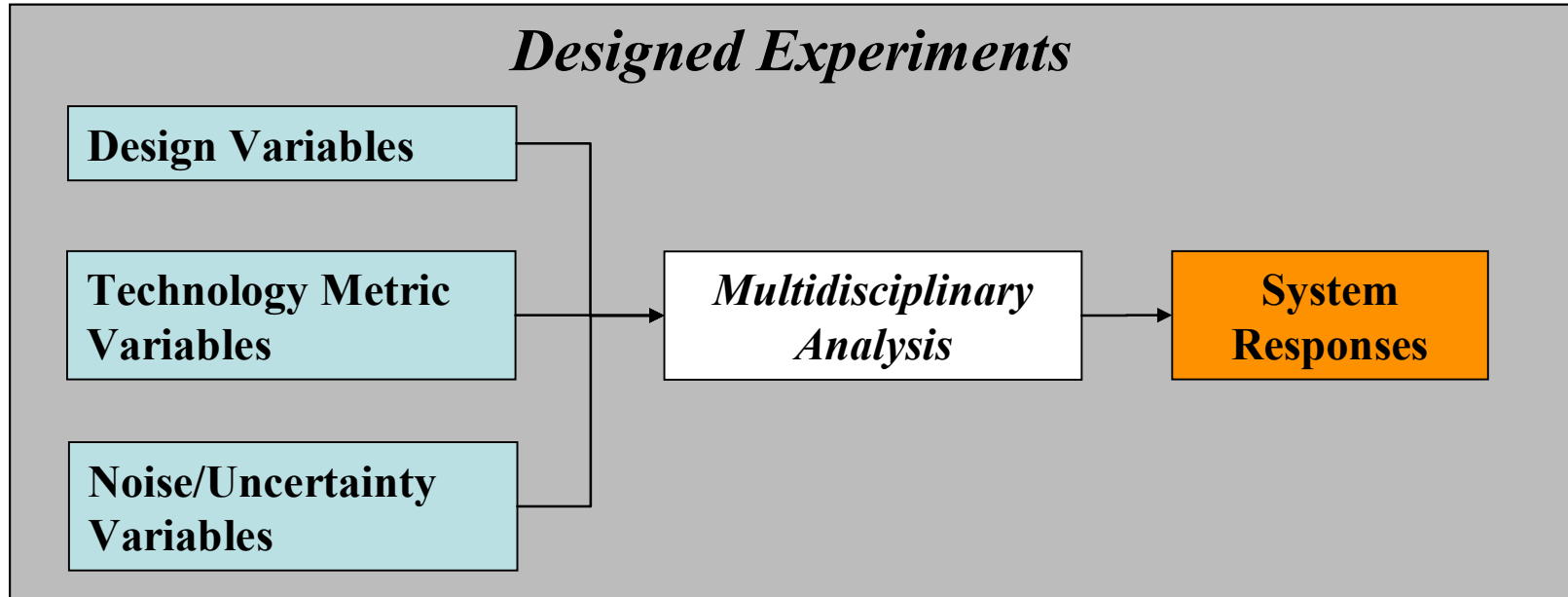


Figure 6: Assessing robustness of alternatives through metamodel facilitated Monte Carlo Simulation

Assessing potentially enabling technologies for alternative

In the present work, a feasible baseline design was defined for a thermal penetrator concept that appeared capable of satisfying the problem as defined. However, customer feedback indicated that the low rate of penetration of the baseline feasible design (approximately a week was required to defeat the baseline target) was of concern with respect to the concepts viability. As a result it was decided to perform an investigation on the baseline concepts design space to attempt to identify possible technology areas that might enable significant improvements in performance.

The approach used was similar to that of Mavris, Kirby et al's "Technology Impact Forecasting" (TIF).^{10, 11, 22} The principle steps in this approach (closely adapted from Kirby¹¹) are listed below:

1. Identify need (in terms of a military threat).
2. Define the problem in terms of a set of customer requirements.
3. Map customer requirements into mathematically quantifiable terminology – i.e., system metrics.
4. Identify a potential class of concepts that may fulfill the customer requirements and define a baseline design (datum).
5. Define a design space as control variable deviations from the baseline design.
6. Investigate the design space for technical feasibility in a modeling and simulation environment via the Response Surface Methodology (RSM)²³ combined with a Monte Carlo Simulation (MCS).

7. Next, an economic space is investigated with variations in noise variables (inflation rate and other uncertain economic parameters, uncertain physical parameters such as capture cross section, etc.).
8. If the probability of success for feasibility and viability are unacceptable, the decision-maker has the option to expand the design space further, relax the constraints, investigate other concepts, or infuse new or alternative technologies.
9. For the purposes of the TIF method, infusion of new or alternative technologies is pursued through a simulation of technology metrics. A technology metric is a standard of measurement used to define the impact of a generic technology area (or a specific technology if applying the TIES method) on the system and includes benefits and degradations.
10. The system technical feasibility and economic viability are explored again.
11. If feasible and viable solutions exist, the robustness of the best solutions can be evaluated with various techniques. One method is the Robust Design Simulation (RDS).^{24, 25}

As explained by Kirby et al, TIF and similar advanced design methods presuppose a cohesive Modeling and Simulation environment (MS) enabling evaluation of constrained technical and economic performance. Without an MS, “application of the TIF method is both arduous and qualitative in nature.”¹¹

Typically, creation of validated MS environments requires collaboration of a number of disciplinary experts using the resources of a large organization over a period of years. As the identified system concept for DBHT defeat of a radioisotope powered

thermal penetrator did not have a preexisting MS environment created for it, creation of a multidisciplinary analysis for modeling the concept using simplified and approximate disciplinary analyses comprised a large part of the reported effort. This multidisciplinary analysis was sufficient for the purpose of exploring concept characteristics and likely performance at the conceptual level with reasonable fidelity.

Given the state of the investigation of the concept, the question most relevant for determining potential viability of the thermal penetrator approach was whether or not it was theoretically possible to significantly reduce the required time to defeat the target, and if so, what technologies would be required. If reduced penetration times appeared feasible, then given the dependence of the concept on either radioisotope or fissile power any decision for further investigation of the concept is likely to be determined by political considerations outside of the scope of this engineering effort.

Consequently, the actual approach diverged from that described above:

1. Identify need (in terms of a military threat).
2. Define the problem in terms of a set of customer requirements.
3. Map customer requirements into qualitative and quantitative metrics.
4. Identify a potential class of concepts that may fulfill the customer requirements and define a baseline design.
5. Define a system space as system variable deviations from the baseline design. System variables were considered to include concept design, material property, and manufacturing variables as well as target material property variables. Ranges were selected to reflect plausible maximum deviations from the baseline values.

6. Investigate system design space to determine if points exist exhibiting the required penetration time to depth performance. If so, search for hypothetical concepts (technologies) that might provide the required deviations in system variables to achieve required penetration time to depth.
7. If points are not found to exist with the required penetration time to depth, evaluate what would be required of the system in terms of the close-contact melting analysis to provide the requisite penetration time to depth, and identify possible technologies that might provide the required characteristics.

Results of the last two steps above can then be reported for the purpose of informing any future Research and Development planning regarding the proposed concept which may occur – if and when it is decided that the concept characteristics identified in this investigation have the potential of providing a significant value to society at costs (political and otherwise) that can be accepted.

RESEARCH QUESTIONS, CONTRIBUTIONS, AND TASKS

The key research question posed at the beginning of the effort was whether or not a feasible non-nuclear explosive, air-deliverable option for defeat of an NBC hardened DBHT could be identified, using only available or near term technologies, that would comprise a significant departure from the limitations of conventional approaches to hard target defeat.

Upon the identification of the radioisotope or fissile powered thermal subterrene as a possible solution to this question, the ancillary question of feasibility arose. In particular, feasibility with regard to producing such a device that did not deliver nuclear hazard to the targeted facility under nominal employment conditions; and feasibility with regard to achievable performance, cost, producibility, and life-cycle. Multidisciplinary analysis of the concept to answer these questions lead to the conclusion that a previously unconsidered measure of merit – penetration time to depth – was important to concept viability. Consequently, the question arose of whether the impact of infusing technologies to the thermal penetrator design problem might provide substantial gains in performance with respect to penetration time to depth.

Other ancillary questions also arose during the investigation such as: is it plausible there would be significant lethality against a DBHT space intercepted by such a device; are historical refractory material and radioisotope technologies consistent with implementing such a device; and do the requisite production facilities exist for creation of such a device?

Research contributions

The novelty of the present research can be characterized as follows with respect to existing literature. First, the proposal of a thermal subterrene for DBHT defeat is unknown in the public domain. Second, a multidisciplinary approach for the sizing and characterization of such a device is unknown in the public domain. Thirdly, a feasibility study of such a device with respect to representative mission requirements is unknown in the public domain. Finally, a technology study characterizing what technologies, if any,

might contribute to the viability of a thermal penetrator for DBHT defeat is unknown in the public domain.

Research tasks

The principle research tasks undertaken to resolve the identified research questions were as follows:

1. Generate and filter alternative concepts for DBHT defeat so as to identify an innovative potential solution to the problem. Explore, evaluate, and select from alternative concept implementations to identify a baseline implementation for further investigation.

2. Develop and implement a multidisciplinary analysis and sizing code to facilitate definition of a baseline design.

Identify appropriate analyses for:

- Isotope production and power generation through nuclear decay
- Radioisotope shielding calculations
- RIPTP penetration of granite through close-contact melting
- Approximate internal temperature calculations of a RIPTP
- Radiation hazard of RIPTP
- Rough Order of Magnitude (ROM) RIPTP costs

Synthesize all of the above analyses into a RIPTP performance analysis and sizing capability

3. Acquire data necessary for analysis of RIPTP performance:

- Nuclear properties of candidate radioisotopes
- Natural abundance of precursor and adulterant isotopes

- Enrichment technologies for precursor isotopes
 - Material properties of suitable compounds of candidate radioisotopes
 - Properties of representative RIPTP materials
 - Relevant characteristics of nuclear reactors that could be used to produce RIPTP radioisotopes
 - Material properties of solid and liquid rock as a function of temperature
 - Standards and health impact for radiation exposure
4. Identify primary feasible radioisotope candidates
 - Identify characteristics of radioisotopes that may be used for determination of their infeasibility
 - Screen radioisotopes to identify potentially suitable candidates
 - Analyze approximate required characteristics of radioisotopes as produced for RIPTP feasibility
 - Analyze production characteristics of candidate radioisotopes in various candidate nuclear reactors
 - Identify feasible candidate radioisotopes
 5. Identify an optimum baseline RIPTP design configuration using existing technology.
 6. Adapt and apply a TIF-like methodology to the RIPTP concept for DBHT defeat to determine best radioisotopes for further investigation and potential technologies required to meet requirements.
 - Create top-level metamodels of system performance

- Explore feasibility vs. requirements to define current probable achievable performance
- Identify performance requirements that may not be met
- Use models to identify key metrics that most influence these performance requirements
- Identify technologies that can help modify metrics to achieve required performance

7. Document the approach employed in the effort so as to make the approach auditable and the conclusions obtained repeatable.

BACKGROUND

Analysis of and selection from the alternatives available for DBHT defeat by an air-delivered munition involved the initial research of: hard target types and characteristics; historical air-delivered munitions and aircraft capabilities; and historical approaches to defeating hard targets. Historical and non-traditional approaches to defeating a DBHT were then evaluated in light of this information and the general approach of rock drilling technologies identified as of most interest for further investigation. Investigation of historical literature pertinent to rock-drilling/penetration technologies facilitated selection of a novel DBHT defeat concept, *thermal subterrenes*. Investigation of options for implementation of a thermal subterrene by specification of a concept munition morphological matrix lead to selection of a baseline thermal subterrene concept implementation for further analysis.

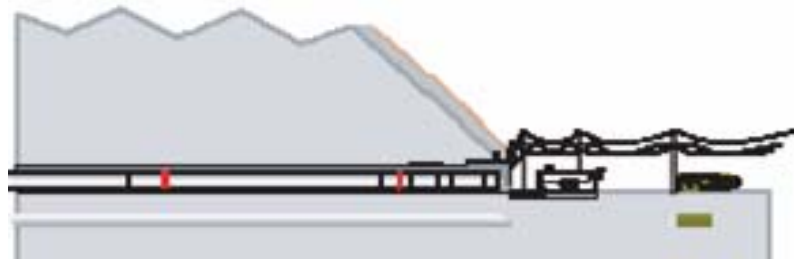
HARD TARGETS

Hard target taxonomy

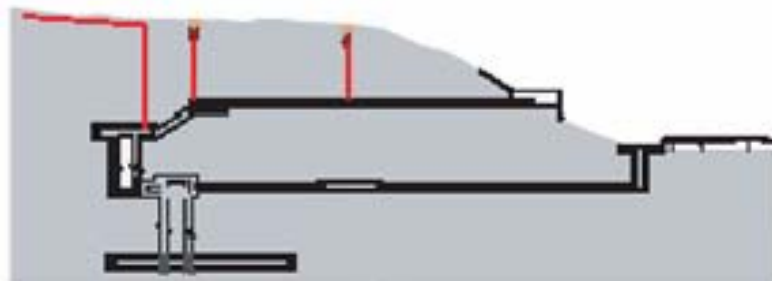
DBHTs are a subset of Hard and Deeply Buried Targets (HDBTs). HDBTs are all facility-type targets – above or below ground – intentionally hardened against the effects of offensive weapons. Types of Hard and Deeply Buried Targets include: shallow underground bunkers; above ground bunkers; basement bunkers; hardened aboveground structures such as hardened hangers and submarine pens; deep underground tunnel complexes; etc.²

Strategic HDBTs are comprised of those HDBTs that are used to protect assets which perform a strategic function, such as: command and control of military forces; protection of leaders; and preservation of strategic weapons such as Weapons of Mass Destruction (WMD). A common characteristic of many strategic HDBTs is that it is unlikely they could be defeated by an air-strike using existing conventional weapons. Some examples of strategic HDBTs hard enough to potentially withstand conventional air-delivered munition attack are illustrated in Figure 7. There are approximately 2,000 such HDBTs worldwide as estimated by the Department of Defense (DoD) and identified by the Defense Intelligence Agency (DIA). DBHTs are consistent with the first two HDBTs illustrated in Figure 7.²

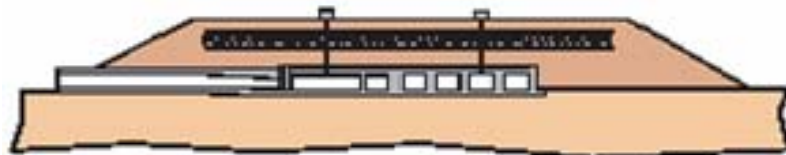
Missile Tunnel Complex



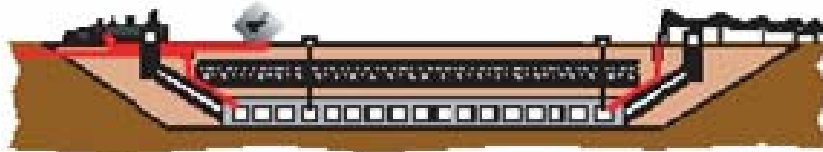
Deep Underground C³ Complex



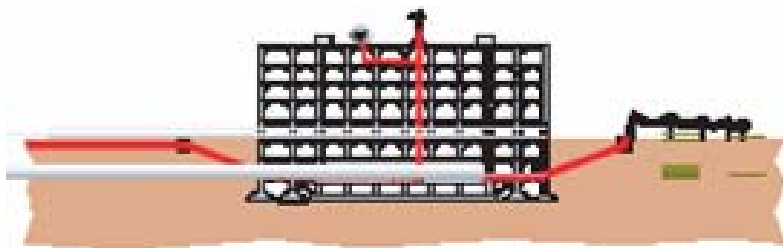
Aboveground Bunker



C³I, Shallow Underground Bunker



C³I, Basement Bunker



Shallow, Accessible Bunker/Silo

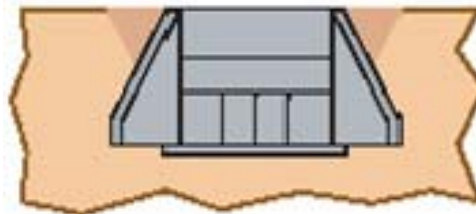


Figure 7: Types of strategic hard and deeply buried targets
Reference²

Deeply Buried Hardened Targets

Due to the enormous expense required for engineering and construction of DBHTS, production of a DBHT by a nation implies a protected asset that is considered both highly valuable and at some perceived risk. DBHTs typically include: C³ and Command, Control, Communications, and Intelligence (C³I) facilities; leadership preservation facilities; WMD production and storage facilities; and missile tunnel complexes.

C³ and missile tunnel complexes are typically between 100 and 400 meters deep, with the majority less than 250 meters deep. A few “super-hard” DBHTs are 500 meters deep or more, and may be robust against nuclear strike with even the largest existing nuclear weapons.²

As an example of a possible “super-hard” DBHT, declassified documents from the 1960’s indicate serious consideration of the construction of a Deep Underground Command Center (DUCC) DBHT in Washington, DC which would have been emplaced more than 1000 meters below the surface. The DUCC was represented as being able to withstand multiple direct hits from 200 to 300 megaton weapons detonated at the surface, and multiple direct hits from 100 megaton penetrating weapons detonating at 20 meters depth. Functional defeat of the DUCC was estimated to require a minimum of ten 100 megaton warheads to defeat communications with the surface. Costs for construction were estimated at between 110 million and 310 million \$1964Yr.²⁶

Hardening of Deeply Buried Hardened Target

A number of approaches are used to harden DBHTs, and include:

- Deep emplacement below the surface, ideally in competent, dry, high-strength rock
- Reinforcement of tunnel walls to mitigate kinetic penetration and/or spall effects (with: anchors; anchors and netting; concrete, composite, and/or steel tunnel linings, sometimes with gravel backfill);
- Use of massive blast doors on access tunnels (sometimes in series);
- Sprawl (a large geographic extent of facility increases targeting uncertainty regarding location of critical facility spaces);
- Compartmentalization of facility to limit damage in event of breach;
- Camouflage or misdirection with respect to surface indications of DBHT presence, location, and/or mission (such as tunnel openings, antennas, utilities, personnel and/or vehicle movements);
- Jogs and branches in access tunnels (to: conceal precise location of facility spaces; mitigate blast effects propagating from tunnel entrances; and facilitate removal of debris from access tunnels post attack);
- Redundant access tunnels and/or blind emergency access tunnels which approach but do not breach the surface (these provide egress in case of closure of access points by attack);
- Isolation of mission-critical systems and personnel from ground shock (for example, by suspension of systems from cable/damper systems or mounting rooms on spring/damper systems);
- Redundant and/or hardened communication infrastructure with the outside such as antennas and communications landlines;

- Redundant and/or internal utilities (including: internal deep water well; electrical power generation; HVAC; etc.);
- Drinking water and food stores;
- Blast valves on air and exhaust ducts connecting to the outside;
- Counter radiological, biological, and chemical agent processing on external air;
- Hardening of electrical systems to radiation, high power electromagnetic fields, and electrical surges;
- Automatic actuation of blast doors and/or other defensive systems based on overpressure or other attack cues.

Suppose, hypothetically, that a revolutionary means of penetrating a DBHT defeat munition through a sufficient depth of rock to threaten a DBHT's critical spaces were available, and that the penetration could be accomplished with a reasonably predictable trajectory. Two major practical challenges to defeating a DBHT would *still* remain of particular note: first, ascertaining DBHT geometry and characteristics so that aim-points could be selected; and second, determining post-strike that the DBHT had in fact been defeated.

Selecting aim point for deeply buried hardened targets

A common and critical constraint in the defeat of DBHTs is target characterization for strike planning. Strike planning ideally requires ascertaining the location, size, connectivity and function of a DBHT's internal spaces so as to determine lateral targeting of a munition. Absent direct intelligence, only limited information may be inferred from observation of surface openings. However, only modest improvements

in the current state of the art in gravimetry and/or acoustic imaging together with conventional surveillance and analysis may be required to solve this challenge.

Existing gravity gradiometer measurement capabilities coupled with GPS have been reported capable of resolving underground tunnels as little as 5 meters in diameter at 45 meters depth from a 100 meter height, with next-generation systems capable of similar resolution to a depth of 350 meters.^{16, 27} Further, new Bose-Einstein Condensate (BEC) based gravimetry concepts have been discussed as means of improving state-of-the-art gravimeter resolution by more than six orders of magnitude within the next ten years (theoretically up to 10^{11} times the resolution of light interferometer based devices).²⁸ Such improvements in resolution might provide a computed tomographic imaging capability of deeply buried facilities, possibly even enabling inference of the contents of a DBHT. Given projected improvements in sensitivity, isolation and filtering of noise from the sensor platform and interference from geological noise sources are likely constraints limiting potential resolution of the technology.²⁷

If the facility characterization problem is solved, targeting may be accomplished by Monte Carlo-type Simulations to ascertain required penetrator employment to achieve a desired probability of DBHT kill. Advanced technologies in combination with traditional surveillance and analysis make it plausible that the lateral aim-point selection challenge can be solved.

Determining Deeply Buried Hardened Target defeat

Positively determining functional defeat of a DBHT is problematic. A penetrating bomb or other weapon may induce collapse, spall, sever critical services, or otherwise disrupt the function of a hardened facility. However, externally observable collapse or

slump is unlikely for a DBHT, and without significant smoke from target openings success may be unknowable. This is a major limitation of any DBHT defeat agent not inducing significant conflagration inside the target. Smoke from a significant conflagration is likely to eventually reach the surface and be observable, and is a good indicator that surviving personnel in the facility are likely in extreme hazard and not doing their nominal functions.

HISTORICAL CAPABILITIES FOR AIR-DELIVERY OF MUNITIONS (AND OTHER PAYLOADS)

Given a sufficiently capable delivery system, several DBHT defeat options could theoretically threaten a hard rock emplaced DBHT at an arbitrary depth. Indeed, much of the history of hardened target aerial attack using conventional munitions was one of increasing bomb mass/delivery aircraft size.²⁹ The trend was actually continued after the advent of the fission nuclear bomb and through initial hydrogen bomb development, with both massive conventional bombs such as the T-12 (into the early 1950's) and massive nuclear bombs such as the TX-14 and TX-16 (late 1950's) developed for hardened target and area target defeat, along with aircraft (such as the B-36) capable of delivering them to their targets.³⁰ Thus, to bound the question of capabilities of various alternatives for DBHT defeat, it is useful to consider what is viable and feasible with regards to aerial delivery of munitions to a DBHT.

Payload capabilities of assorted aircraft

Table 1 lists the approximate internal payload carriage capability of an assortment of present day and historical (XB-70B) aircraft. These numbers are approximate as a

large number of factors differ between the states of the aircraft used to specify the quoted characteristics by various sources, such as: load distribution; specific aircraft as modified; operating conditions; regulatory directives; operational de-rating of system by end user; etc. Further, if one were to hypothesize a specific DBHT defeat agent for carriage, constraining factors such as load transfer to aircraft structure, aerial separation of the munition, etc. would modify the maximum mass and dimensions of agent that could be carried.

For a unitary internally carried payload on a present day tactical bomber, the B-2 bomber is limited to approximately 30,000 lbm based on available unclassified literature. Published maximum payload for the B-2 is approximately 50,000 lbm (25,000 lbm per bay) and the Massive Ordnance Penetrator (MOP), currently in design by Boeing for carriage on the B-2 and B-1B, is nominally ~30,000 lbm.¹⁹

For the B-1B, the limit is likely between 30,000 lbm and 50,000+ lbm. This conclusion is based on the B-1B published internal payload of 75,000 lbm distributed in three weapons bays. The bulkhead between the forward two of these bays can be removed, possibly allowing carriage of a unitary munition of 50,000 lbm+ in a space of roughly 33' x 6' x 6'.³¹

The B-52H can carry at least 30,000 lbm of munitions and associated equipment internally (8 3,250 lbm CALCM's plus ~5000 lbm of launch equipment), and perhaps as much as 50,000 lbm. During the Vietnam War, a program called "Big Belly" was undertaken to modify the B-52D to carry 84 Mk-82 500 lbm bombs internally (42,000 lbm plus whatever the required bomb racks massed).³²

The C-5, C-141, C-130J-30, C-17, An-124, and An-225 cargo aircraft comprise a representative and spanning assortment of present day military transport cargo airlift capability. The XB-70B, though never equipped with an operational bomb bay (it was present, but used for instrumentation), provides an interesting bounding historical example of a maximum energy, massive conventional payload delivery capability.³³ The Boeing 747-200F and Lockheed L-1011-200F provide representative examples of large civilian freighter capabilities. The 377SGT “Super Guppy” provides an example of the current largest diameter outside payload air transport. Future planned oversized cargo aircraft (747 and possible A330 variants) could increase outside cargo dimensions further.³⁴

Table 1: Approximate aircraft system capabilities

System	Length (ft)	Width (ft)	Height (ft)	Internal Payload Mass (lbm)	Altitude (ft)	Speed (ft/s)	Max. Specific Energy (ft/s slug)
B-2	~23	>~6	>~6	2x25,000 ³⁵	50,000 ³⁵	895 ³⁵	2690
B-52H	28	6	6	30,000 – 50,000 ^{32, 36}	50,000 ³⁶	953 ³⁶	2750
B-1B	~33 ³⁵	~6 ³⁷	~6 ³⁷	~30,000 ³⁵	50,000 ³⁵	1264 ³⁵	3060
XB-70B ³³				20,000	70,000	3000	5120
C-5	107 ³⁷	19 ³⁷	13 ³⁷	265,000 ³⁸	34,000 ³⁹	836 ³⁹	2320
C-141	70 ³⁷	10 ³⁷	9 ³⁷	94,500 ³⁷	25,000 ³⁷	676	1950
C-130J-30	55.5 ³⁷	10 ³⁷	9 ³⁷	46,800 ³⁷	20,000 ³⁷	540	1680
C-17	65 ³⁷	18 ³⁷	12 ³⁷	170,900 ³⁷	45,000 ⁴⁰	757 ⁴⁰	2460
An-124 ^{41, 42}	120	21	14.5	265,000	38,000	775	2340
An-225 ^{41, 42}	142	21	14.5	550,000	38,000	775	2340
747-200F ^{43, 44}	~150	21	13.5	250,000	35,000	814	2320
L-1011-200F	>122 ⁴⁵	>16 ⁴⁵	>10 ⁴⁵	140,720 ⁴⁵	~33,000	874 ⁴⁶	2330
377SGT “Super Guppy” ^{34, 47}	111	25	25	54,500	25,000	425	1700

Concepts for munition carriage/separation

Requirements for munition carriage/separation vary depending on the defeat agent considered. For example, a long-rod penetrator munition would ideally be separated from the delivery aircraft at maximum possible total energy so as to maximize terminal velocity. Terminal velocity of squash, shaped charge, and ElectroMagnetic Pulse (EMP) warheads, however, is irrelevant to warhead performance (given proper delivery to the target).

Figure 8 illustrates a variety of alternatives for carriage/separation of massive unitary munitions from a delivery aircraft. Included under each caption is the maximum known demonstrated unitary payload separated using each approach. Options “A” and “B” are most attractive for existing bombers from the standpoint of requiring the least modification to the aircraft. Option “C” could potentially be utilized with bombers, military airlift, or civilian freighter aircraft. Option “D” has advantages from the standpoint of precision delivery of massive and/or outsized payloads from standoff ranges using smaller, relatively unmodified tactical aircraft such as the C-130. Option “E” has advantages with respect to carriage and separation of outsized payloads, and includes the largest known payload (the 150,000 lbm orbiter test vehicle *Enterprise*) separated from an aircraft in mid-flight. Option “F” is applicable to current military transport aircraft with airdrop capabilities.

Options “G” through “I” represent a concept for separation of a massive payload from an expendable unmanned aircraft with minimal modifications. Consider that safe separation issues and required structural modifications will likely preclude exploitation of the maximum theoretically feasible cargo weight for a given aircraft, and that large

numbers of old and/or mothballed military and civilian transport aircraft exist in the national inventory and world aircraft market. Further, a high value target such as a DBHT is almost certain to have significant air defenses allocated to protect it, increasing the risk to an aircrew in a piloted attack. Given these considerations, internal integration of a munition on the main deck of a transport might provide a technically low-risk, low-cost solution as aircraft aerodynamics would not be affected and minimal structural modifications required. Retrofit of an aircraft guidance package (such as used to convert F-4's to QF-4 targets) would turn the aircraft into an expendable Unmanned Combat Air Vehicle (UCAV)/cruise missile. Conversion to remote piloting of a jet airliner has previously been performed by NASA in 1984 for the *Controlled Impact Dynamics Program* using a Boeing 720 airliner for a flight crash test.⁴⁸ Autonomous flight would remove risk to pilots when attacking a high value asset such as a DBHT. Lastly, since the vehicle would be used in one-way unmanned flight, structural margins might be relaxed to exploit the structural capability implicit in the design load factor and maximize payload.

For separation of a massive kinetic penetrator or other DBHT defeat agent, the delivery aircraft could be disassembled in a controlled manner in midair using shaped charges to cut the skin, bulkheads, and/or spars. Aerodynamic forces, inertia, and cabin pressure could be used to separate aircraft structure from the munition. This approach seems particularly feasible in the context of a massive kinetic penetrator, which should be comparatively easy to make robust to possible contact with the separating aircraft structure due to the penetrator's massive construction.

Alternatively, with a unitary penetrator munition, one could run the projectile down internal rails installed on the main deck and punch it through either the nose or aft bulkhead. Using some variation on these concepts, a munition with a mass of up to 500,000 lbs could feasibly be deliverable over long range with comparatively low incremental cost and short programmatic timeline using existing airframes (MD-8, L-1011, C-141, 747, An-225, etc.). Viable limits of this approach have not been explored.

Options not depicted in Figure 8 are some composite aircraft configurations such as wingtip-to-wingtip joined aircraft, or integration of the warhead with an aircraft and intact delivery of same to a target. One example of the latter was the German “Beethoven-Gerat” aka “Mistel-1” weapon of World War II (Figure 9). This interesting composite aircraft was comprised of an unmanned “tired” (high-time) Ju-88 bomber mated below an FW-190 or Bf-109 fighter. Several dozen Ju-88’s were recycled by replacing their cockpit/forward-fuselage with a two meter diameter 3500 kg shaped charge warhead (the largest historical shaped charge warhead of which the author is aware). The piggy-back FW-190 delivered the Ju-88 to the target on a glide-slope of about 15 degrees, separating from the Ju-88 prior to impact.⁴⁹

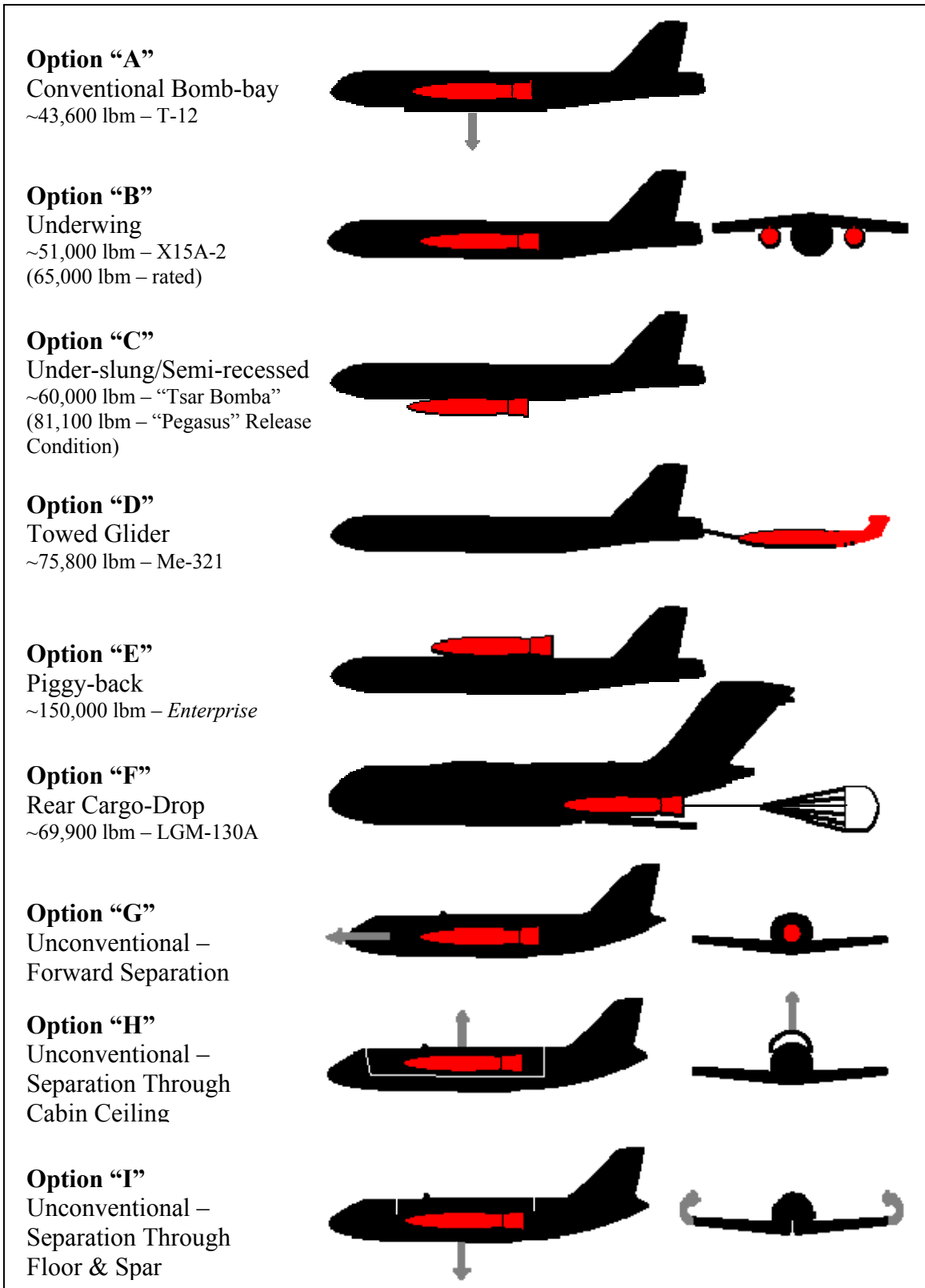


Figure 8: Concepts for munition carriage and separation

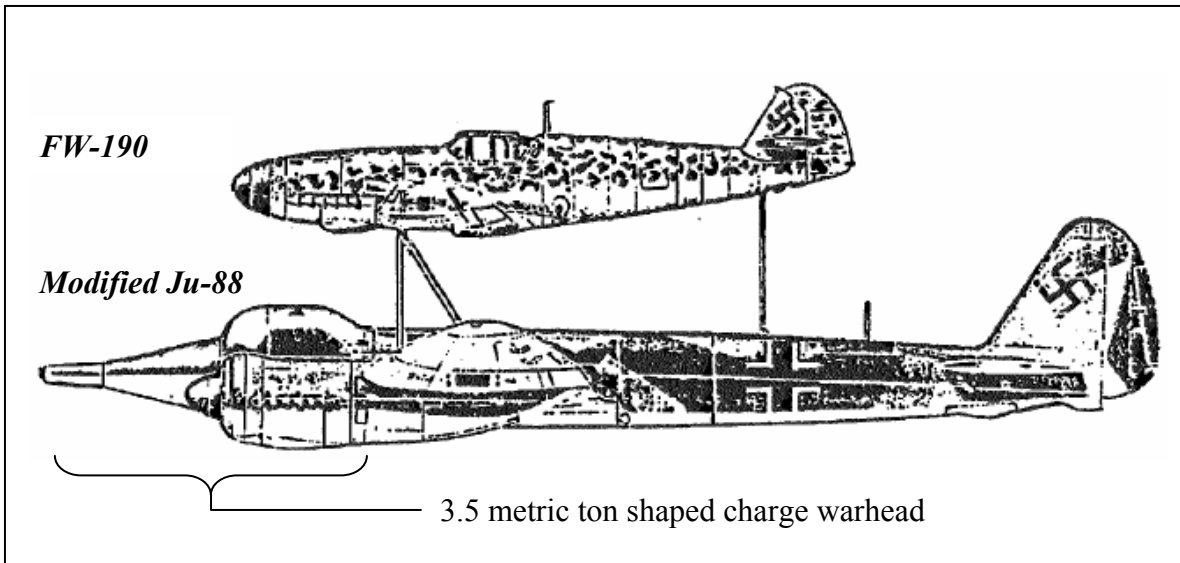


Figure 9: “Beethoven-Gerat” aka “Mistel-1” composite aircraft
Reference⁴⁹

Historically demonstrated unitary payload separation capability

Figure 10 depicts selected historical examples of some of the payload carriage and separation concepts listed in Figure 8. Figure 11 depicts scaled examples of various very large historical munitions dropped from aircraft. Table 2 lists some of these historical examples with approximate dimensions and estimates of possible release conditions.

“Option A”: The T-12 was a massive conventional unitary bomb developed for hardened target attack, two of which could be carried internally on the B-36 bomber.²⁹ During the early 1950’s mock-ups of TX-14’s and TX-16’s, some of the first hydrogen bomb designs, were dropped from B-36’s. They were carried internally in the bomb bay. At roughly 40,000 to 50,000 pounds, the T-12, TX-14, and TX-16 were the largest unitary bomb’s carried entirely within a conventional bomb bay of which the author is aware. If the Massive Ordnance Penetrator’s (MOP) final weight when it is developed is consistent with the 30,000 pounds discussed in open literature, it will be a sizeable step back from what has been historically demonstrated for internally carried unitary

munitions (probably reflecting reductions in single weapons bay maximum length and weight capabilities for the latest strategic bomber, the B-2).

“Option B”: The Tallboy “Medium’s”, X-15A-2, and Pegasus Launch vehicle represent some of the largest under-wing payloads ever successfully carried and separated. The X-15A-2, at approximately 51,000 lbm, was the largest of the three with the pylon/NB-52 combination modified to carry it rated for 65,000 lbm.⁵⁰

“Option C”: The “Grand Slam” conventional bomb, and the “Tsar Bomba” (the highest yield nuclear bomb ever detonated – USSR) are two of the heaviest bombs ever carried semi-recessed in the bay of a carrier aircraft.⁵¹ With regards to centerline under-slung/pylon carriage, the Pegasus XL and perhaps the secret Anti-SATellite (ASAT) launcher the Russian “Burlak” was supposedly based on were two of the largest of their class. The Russian “Burlak” space launch vehicle, carried on a Tu-160 “Blackjack,” was proposed in the early 1990’s by the Russians to the German government as a satellite launch vehicle with extremely low development cost, and was rumored to be based on a classified Soviet anti-satellite missile. If one presumes that the anti-satellite missile was actually tested and closely resembled the proposed “Burlak” design, then this missile, at ~60,000 pounds, might have been the heaviest munition ever carried and separated from a centerline pylon (and at a very high total energy state). As it stands, the Pegasus XL, dropped from an L-1011, is the largest centerline pylon carried payload identified by the author (53,000 lbm).⁵²

“Option D”: Gliders have advantages as compared to other means of payload transport by an aircraft: the glider provides its own lift; it can be designed to wrap around an outsized payload; precise delivery of the payload is possible by incorporating a

guidance system into the glider; cheaply built/expendable construction can be used for the glider; higher payload/Gross Take-Off Weight (GTOW) fractions can be achieved as fuel, propulsion systems, and landing gear are not required; and gliders can be more stealthy than other aircraft due both to their lack of a propulsion system as well as the materials used in their construction. The largest glider known to have been flown is the World War II German Me-321, with a GTOW of approximately 75,800 pounds, and a payload of about 45,000 pounds.⁵³

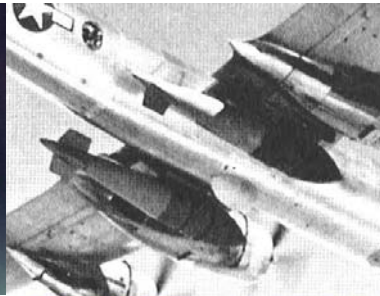
“Option E”: The absolute heaviest unitary payload ever separated in mid-air was likely the *Enterprise* orbiter test vehicle at approximately 150,000 pounds.⁵⁴ The *Enterprise* was carried piggy-back on a modified Boeing 747 and used for manned glide tests of a full-scale Space Transportation System (STS) orbiter. Note that unlike the *Enterprise*, the USSR’s “Buran” orbiter was never separated from its An-225 carrier aircraft for glide tests – instead, an orbiter test vehicle with jet engines installed was used.

“Option F”: Finally, a selection of massive payloads airdropped from large transports is listed. These include: a Minuteman I ICBM dropped as part of the *Air Mobile Feasibility Demonstration*;⁵⁵ 40,000 pound “Sheridan” tanks; 60,000 pound pallets; and the latest generation of massive bombs (Massive Ordnance Air-Burst, MOAB), air-launched ballistic missile targets (Long Range Air-Launched Target, LRALT) and launch vehicles (“Quick Reach 1” or “Falcon”).

Based on the demonstrated history and proposed new efforts, 30,000 pounds is viable for delivery using existing inventory bombers, 20,000 pounds is viable for tactically capable transport aircraft, and 70,000 pounds is viable using the C-5. Using various munition integration approaches (with attention only to feasibility and not

viability), munition weights approaching 500,000 pounds are feasible using existing transport aircraft.

Based on these general assumptions and data regarding a delivery system, some calculations can be made regarding maximum depths of defeat for various DBHT defeat approaches such as long rod, shaped charge, and High-Explosive “Squash” Head (HESH, or High Explosive Plastic/HEP) type warheads.



Option “B” Underwing – X-15/NB-52, Two Tallboys/B-29
Photo Credit: NASA, USAF



Option “E” Piggy-back – Buran/AN-225, Enterprise/747-100
Photo Credit: Mark Wade, NASA



Option “C” Under-slung/Semi-recessed – Grand Slam/B-29A, Pegasus/L1011
Photo Credit: Thien Collection of the Kansas Aviation Museum, OSC



Option “D” Towed Glider – Me-321 “Gigante”
Photo Credit: www.waffenhq.de



Option “F” Rear Cargo-Drop – Quick Reach 1 Demo/C-17, LGM-30B “Minuteman I”/C-5A
Photo Credit: USAF

Figure 10: Historical examples of carriage options for large unitary payloads

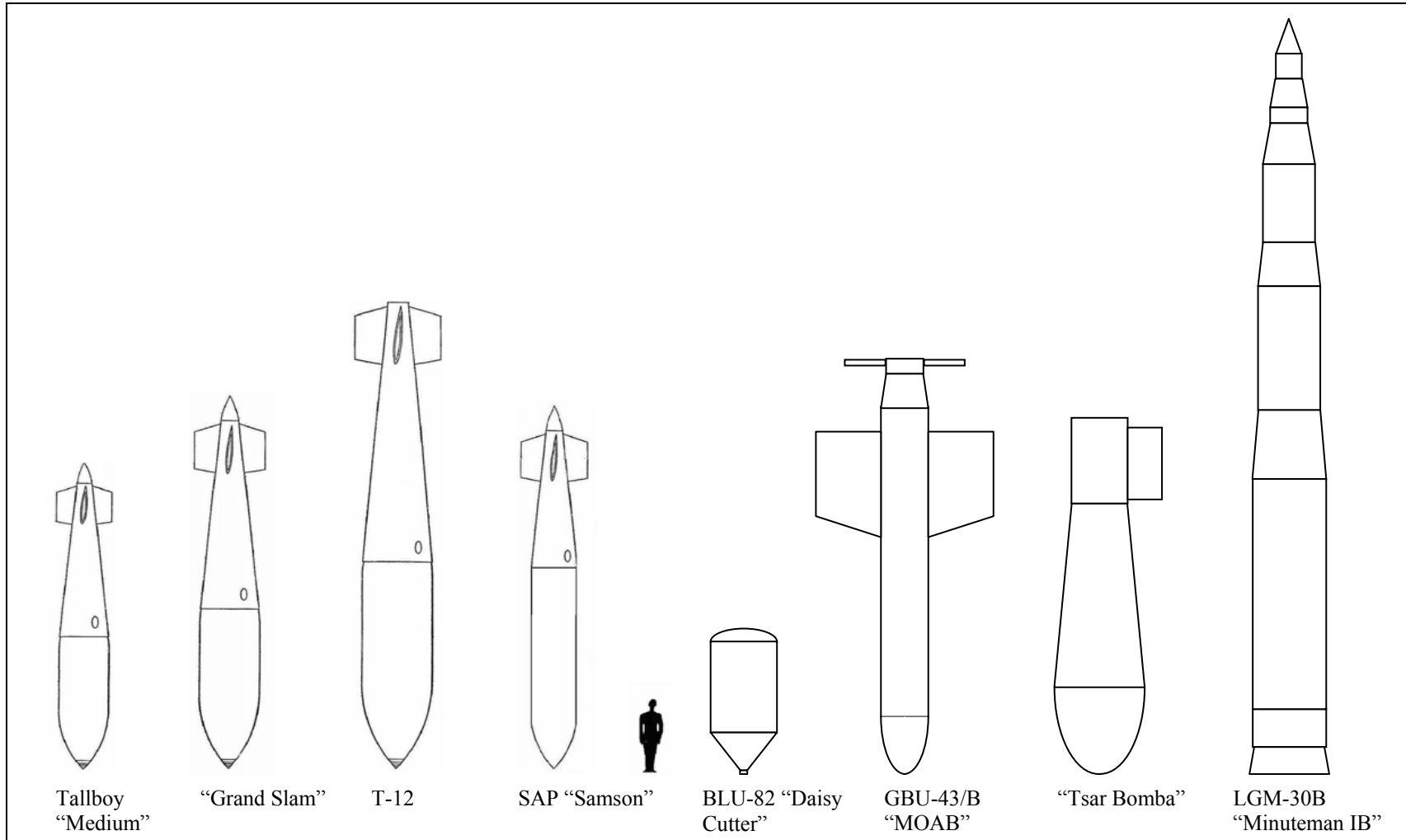


Figure 11: A scale comparison of very large munitions historically separated from aircraft

From left to right: Tallboy "Medium"²⁹; Grand Slam²⁹; T-12²⁹; SAP Samson²⁹; BLU-82⁵⁶; GBU-43/B⁵⁶; Tsar Bomba⁵¹; LGM-30B⁵⁷.

Table 2: A selection of large unitary payloads separated mid-air

System	Approx. Yr of Dev. Initiation	A/C Carriage	Mass (lbm)	Max. Diameter (in)	Length (ft)	Estimated Max. Release Conditions
T-12 ²⁹	1942	B-29A; B-36	43,600	54	26.8	40,000 ft
TX-14, TX-16 mock-ups ³⁰	Dropped 1953	B-36	~50,000	~61	~25	36,000 ft; 506 fps
MOP ¹⁹	2005	B-2; B-1B	~30,000	?	?	
X-15A-2	Dropped 1967 ⁵⁰	NB-52B ⁵⁰	51,000 (NB-52 rated to 65,000) ⁵⁰	56 ⁵⁸	50.8 ⁵⁸	44,000 ft; 840 fps ⁵⁰
Tallboy "Medium" ²⁹	1943	Lancaster Mk 1; B-29A	12,622	38	21	30,000 ft
Samson SAP ²⁹	1946	B-29	25,000	32	~25.4	30,000 ft
Grand Slam ²⁹	1944	Lancaster Mk 1; B-29A	22,000	46	25.4	16,000 ft (30,000 ft?)
Tsar Bomba	1961 ⁵⁹	Tu-95 "Bear" ⁵⁹	~60,000 ⁵¹	~80 ⁵¹	~26 ⁵¹	34,500 ft ⁵⁹
Burlak ⁶⁰	1992	Tu-160	60,400	63	62.4	44,300 ft; 1790 fps
Pegasus XL ⁵²	Dropped 1994	L-1011	53,000 (81,100 spec'd as separation condition)	50 (311)	57.8	39,000 ft; 844 fps
ME-321 ⁶¹	1941 (first flight) ⁵³	Towed, Bf-110 ⁶²	75,800 (48,000 payload) ⁵³	~140 (payload) ⁶²	92 ⁵³	
Enterprise ⁵⁴	Dropped 1977	747-100	150,000	190 (960)	123	26,000 ft; 460 fps
LGM-30A	Dropped 1974 ⁶³	C-5A "Galaxy" ⁶³	69,900 ⁵⁵	~66 ⁵⁷	55.9 ⁵⁷	20,000 ft ⁶³
Sheridan Tanks ⁶⁴	Dropped 1989	C-5B	4x42,000	111	20	
Pallets ⁶⁴	Dropped ?	C-5	2x60,000			
LRALT ⁶⁵	Dropped 2004	C-17	33,000	52	50.9	
MOAB	2002 ⁶⁶	MC-130E ⁵⁶	21,700 ⁶⁶	40.5 ⁶⁶	30.5 ⁶⁶	
Quick Reach 1 ⁶⁷	2004	C-17	72,000 proposed (50,000 demonstrated)	97	65	33,000 ft; 190KEAS

ALTERNATIVES CONSIDERED FOR DEFEAT OF A HARD TARGET

The first five options listed in Table 3 include those conventional alternatives typically considered for defeat of a hard target, whereas the next seven list unconventional and/or undeveloped hard target defeat alternatives. A cursory discussion of several options will be made, followed by a more in-depth analysis of the options of long-rod penetrators, shaped charges, and rock drilling modes. Further discussion will then be made of the rock drilling mode employed by a thermal subterrene, its implementation alternatives and conceptual advantages.

“Finesse” alternatives

The author considers many of the concepts listed to be finesse approaches to hard target defeat as compared to more traditional approaches – given sufficient knowledge of a target they might conceivably exploit vulnerabilities to disrupt it with less force than might otherwise be required. Concepts the author would lump in this category include: robotic systems; ElectroMagnetic Pulse (EMP); High Power Microwave (HPM); or other Directed Energy (DE) concept; information system attack; target isolation; macrobiotic attack; and various NBC-type concepts.

A common difficulty with analyzing feasibility of such approaches is that compared to more brute force approaches (such as: nuclear strike; or to a lesser degree kinetic/mechanical penetration) their potential for success tends to be very sensitive to target specific detail. Given intimate knowledge of a facility’s physical design, systems, and/or operation one may be able to conceive of a concept implementation and a method for employment that theoretically could succeed. Given intimate knowledge for a large

number of targets, common vulnerabilities may be identifiable enabling identification of a concept implementation and method for employment of potentially broader applicability and robustness.

However, for the current project such information was not available, making identification of such alternatives and discussion of viability extremely speculative. Further, the extent to which an approach to DBHT defeat is dependent on target specific characteristics tends to reduce the robustness of the approach. This simultaneous *sensitivity to, and limited availability of,* details of target and concept capabilities was a primary reason for not considering these concepts in greater depth.

Isolation through closure of known surface openings and communications utilities disruption by bombardment

One possible conventional hard target defeat solution – closure of known surface openings and disruption of utility entrance points by bombardment – is a technically low-risk means of functionally degrading a DBHT. This capability presently exists and will continue to be improved by currently planned developments in precision munitions guidance and remote sensing and mapping. The principal reason for elimination of this approach was that it was not considered to be “innovative” or “revolutionary” due to the fact that it is already a nascent capability. Further, this option is inadequate to assure robust denial of many possible DBHT facility functions and is intelligence, surveillance, and airpower intensive.

Also, such attack is generally considered in the design of DBHTs. Among other approaches, some facilities include one or more tunnels drilled to within a small distance of the surface which can be breached if necessary to provide additional facility access in

the event of closure of primary access points. In the case of a command and control DBHT, land-lines may be hardened to the point that they are difficult to interrupt, and antennas may be installed sub-surface to the rock such that they are nearly as difficult to destroy as the facility spaces themselves.

Radiological, Biological, and Chemical alternatives

The primary available option for robust DBHT defeat of targeting with nuclear bombs is relatively unattractive with respect to both the political and collateral human costs, and was precluded by the problem statement. Radiological, biological and chemical human-targeted toxins options have similar political drawbacks. Biological weapons, while having enormous and as yet unexploited potential for selective targeting and tailoring of effects, are potentially far worse than either nuclear-explosive, radiological-toxin, or chemical-toxin options in that their collateral damage can be unlimited in both geographic scope and duration.

Most attractive concept identified

Nonlethal chemical incapacitants are possibly the least politically problematic of the options considered. Further, the effects of powerful anesthetics, cognescent disruptants, and/or hallucinogenics can be insidious with regards to both recognition of onset and effective management of counter-action. However, the problem remains that the DBHT considered in the problem statement is assumed hardened against such attack, and even nonlethal chemical options have historically been politically problematic.

HPM, EMP, and other RF DE options

An alternate approach to degrading or functionally defeating a DBHT is to attack the electrical and electronic systems necessary to the function of the facility using RadioFrequency (RF) DE weapons such as HPM, EMP, or similar concepts.

This is a conceptually attractive approach, as kinetic penetration of the rock in which a DBHT is emplaced is not necessary. Hypothetically, electromagnetic energy might be transmitted through the granite or propagated along power, communications, HVAC and other conduits to attack DBHT equipment. Terminal effects would be realized principally by the production of voltages across semiconductor junctions sufficient to cause dielectric break-down and permanent damage. Transient switch state errors in computers are also possible, resulting in computer crashes or less severe faults.

Realistic analytical or empirical assessment of this category of approaches is difficult, particularly with regards to the available unclassified literature. On the offensive side of the problem, capabilities and characteristics of HPM and EMP weapons are generally not available in unclassified literature. On the defensive side of the problem, techniques and performance of hardening of electrical systems as employed in DBHTs are likewise of limited availability.

Regardless, it is known that one aspect of nuclear hardening of a facility is hardening against both EMP and the hard radiations potentially inflicted on a DBHT by a nuclear detonation. Further, seemingly obvious measures for hardening critical DBHT equipment and spaces against EMP or HPM attack (such as enclosure in a Faraday Cage and electrical isolation of external data lines using optical isolators) appear both conceptually simple and likely to be effective.

A further drawback to this category of approach is the difficulty in assessing the effectiveness of an attack, as no major apparent changes in a DBHT's condition would necessarily result even from a successful attack, aside perhaps from an alteration or cessation of communications traffic. The absence of apparent communications, however, is obviously no guarantee that even a C³ facility is either not performing its mission or will not resume doing so at any moment. Also, the problem statement specified that full-functional defeat was desired, if possible.

Most attractive concept identified

Coupling losses from an external (attacking) source of electrical or electromagnetic energy into an arbitrary target electrical system are a principal limitation of any RF or other electrical brute-force attack. Given a capability for precision delivery, one might conceivably deliver a vehicle (designed to induce a damaging overvoltage to a target system) into direct- or close-contact with a conductive path of such a system – for example: an antenna; effective wave-guide; metallic enclosure; or hard transmission line. A: low wing-loading munition; lightweight submunition; or other mobile delivery unit might lodge in contact with such a coupling point and induce (perhaps responsively and repetitively) a damaging power to connecting systems.

Robotic options

Conceivably robotic systems of some variety might be able to utilize man-ways or the various conduits which supply service and access to a DBHT to infiltrate and/or attack by force. This approach is potentially advantageous in that physical obstacles to a munitions kinetic breach of a DBHT might be avoided or bypassed. Further, robotic systems are *potentially*: more robust to functional degradation than humans from

weapons and adverse environments; present lower signature of presence; have faster reaction times; and can be capable of carrying more payload.

In terms of a stealthy infiltration attack a robot might be infiltrated into a facility in manners dangerous or impossible for a human. This might be done in advance of apparent armed conflict and the robot left dormant, pre-positioned to disrupt the target upon command.

In terms of an attack by force it seems likely that, given the sort of door used to secure nuclear-hardened DBHT man-ways, any robotic attack making use of them would be over if an attack was detected and the doors shut before they were passed. From this perspective, the potential for high speed and rapid engagement of targets possible with a robotic system might be an enabling characteristic for robotic attack – if lethal autonomous attack were ever permitted.

Most attractive concept identified

Besides a ground robotic system, this approach might also be employed, perhaps more effectively, by a flying swarm of small missiles capable of navigating tight corridors at speed and carrying one or more small warheads (explosive and/or electrical in nature).[†] Elements of the swarm might penetrate the facilities corridors and rapidly

[†] Bats or similar animal might conceivably carry out such an attack. Perhaps an additional category of DBHT defeat option should be listed as *macrobiotic* attack, ie, using animals such as insects, rodents, or bats to infiltrate and attack a facility. Natural inclination of species might be exploited such that they sought the darkness/enclosure of air and exhaust vents and man-ways (and eventually utility cabinets or other sensitive equipment). Though apparently speculative, there is a history of fairly successful investigation of such approaches.^{68, 69} For example, in World War II an aircraft delivered bomb deploying approximately 1000 bats each as submunitions was developed by the United States for use against the cities of Japan. Each bat carried an individual incendiary bomb with a time delay fuze of sufficient length that the bats would have time to find a dark roost within a city. Significant potential for success in the approach was evidenced both by the accidental ignition of part of the Carlsbad New Mexico Auxiliary Army Air Base in 1943 (control tower, barracks, and some other buildings as a result of an accidental release of some armed bats) as well as a successful test against a mock-up of a Japanese city.^{68, 69} Alternatively, biomimetic flying

disperse small grenade-type warheads within the facility to attack systems and personnel. Triggering of automatic blast doors might be avoided by delayed simultaneous detonation of all charges once emplaced.

Barring secure shut doors or other effective barricades such a rapid surprise attack might conceivably succeed. Unfortunately, it seems reasonable to assume that something as basic to security as effective secured doors would be fundamental to high-value DBHT targets. Consider in a typical minimum or no-security building how many doors, stairs, or other *non-deliberate* obstacles to a rapid autonomous attack can exist. The difference between this sort of target and a DBHT is both large and likely to be unfavorable in nature. Absent detailed intelligence regarding a given facility and an autonomous operational capability of a more robust nature than usually seen it seems improbable that a robotic attack by force would succeed.

Robotic solutions were also dropped from consideration in part due to the author's lack of expertise in the area as well as the apparent sensitivity of the approach to details of a DBHT's defenses. DBHTs are typically designed to be robust to hostile entrance by men and the historical machines they can wield in time of war. While robotic systems have potential advantages with regards to their expendability, tolerance of adverse (or boring) environments, and reaction times, historically they have shown a lack of robustness in variable environments even without active, intelligent opposition. This is particularly true of autonomous systems. In the case of remote controlled or semi-autonomous systems, the significant challenge of reliably transmitting or receiving from within a DBHT would have to be overcome. This said, robotic surprise attack in force or

robots might overcome some of the practical biological impediments encountered with the *Project X-Ray* bat bomb.

by infiltration conceptually could be a promising approach, and should continue to be evaluated by those qualified to do so in light of future advancements.

Information system attack

If present, information systems necessary to the function of an hypothetical DBHT such as communications, environmental controls, command systems, etc. might plausibly be compromised or rendered inoperative by introducing malicious software, communications, or data designed for such effect. If a DBHT happened to utilize vulnerable and accessible information systems critical to performance of its primary mission, an information systems approach to attacking a DBHT would still require target-specific intelligence and planning. Robustness of a specific information system attack alternative against a spectrum of DBHT targets might be poor. Further, full-functional defeat appears unlikely – the physical systems such as motors or warheads with potential energies capable of accomplishing full-functional defeat if (in-)appropriately triggered via an information system attack typically have physical interlocks to prevent inadvertent activations that would not be directly subject to information system attack. For disruption attacks there also is the issue of the time required to reconstitute the DBHT (perhaps not long if possible by switching to a back-up system or rebooting).

Most attractive concept identified

No one specific concept was identified as most attractive for DBHT attack, however, by the nature of the problem it appears that a cadre of skilled specialists with a suite of exploit tools would be the best concept for waging information attack on a DBHT. The author's conversations with subject matter specialists suggests (typically confident) conviction that nearly any system connected to an accessible network is

pragmatically vulnerable to information system attack.⁷⁰ The author at the time of this writing lacks the expertise or experience to credibly question this confidence in the vulnerability of an arbitrary networked system.

In response to an inquiry regarding what challenge might be posed by language differences between the attacking country and the target-country one response made is that information-system architectures are language independent – and consequently, common architecture vulnerabilities exist across national boundaries. Also, ultimately, compilers reduce high-level-languages to machine code, which is abstracted beyond human dialects to a more uniform consistency. Further, the historical technological leadership of western companies in miniaturized electronics and digital communications systems has often lead to the co-option/adoption of western computational and/or communications systems to adversary systems with only minor changes.⁷⁰

For a varied discussion of contemporary approaches to information systems attack the author suggests (as a starting point) the referenced text.⁷¹ For more up to date information, the reader should go online to one of the many websites which maintain offensive/defensive subject matter (see referenced examples).⁷²⁻⁷⁵ Also, consider the following referenced toolsets for network exploitation and mapping.⁷⁶⁻⁷⁹

Squash warheads

HESH warheads function by spreading a high explosive plastic charge across a targets surface prior to detonating the explosive charge. The compressive shock produced by the explosive propagates through the target's walls until it reflects from the internal wall or cavity surface of the target as a rarefaction wave. The interaction of the rarefaction wave and the tail of the incident shock wave create a state of tension in the

target material. If the tension is sufficiently great the wall material fails and the internal surface separates from the rest of the wall in a phenomena known as “Hopkinson fracture” or spallation.⁸⁰⁻⁸²

The “scab” or “spall” produced can possess significant kinetic energy and function as a behind armor kill mechanism. Hardening against spall can take the form of: measures to increase effective tensile strength of the wall such as rock anchors and/or compressive pre-loading of the free face; anchored netting or other mechanisms to retain scabs; air or other low-density gaps separating an outer wall from an inner wall such that spall doesn’t penetrate the working space of the target; and/or one or more internal wall coating layers possessing varying speeds of sound attached to the internal wall surface such that multiple weaker partial reflections occur. Wall coatings such as plastic can be used that pose little kinetic hazard if they spall themselves, and help contain potential fragments of the material behind them.

In the context of NBC hardened DBHT defeat, nuclear and extremely large point detonated “squash” high explosive plastic warheads are equivalent on an order of magnitude basis. Both accomplish kill of DBHT spaces by coupling blast energy into the rock where it propagates as a shock wave. This shock wave eventually reflects from free surfaces in the target and causes tensile failure of the wall material and consequent spall and/or collapse of the space.^{2, 6, 16, 83}

From this blast-coupled damage perspective, the limitations and capabilities of nuclear and conventional explosive approaches to DBHT defeat can be assessed as approximately equivalent. If one calculates the yield required by a shallow penetrating nuclear bomb to compromise a target – say one kiloton – a similar order of magnitude

conventional explosion would be required – about 10^6 pounds of high explosive. From the literature reviewed, it appears that a DBHT emplaced under 80 meters of granite is likely to require greater than a kiloton of yield.^{2, 6, 16} With respect to a conventional explosive warhead, more than 10^6 pounds of explosive content alone in a munition exceeds the greatest demonstrated payload carried by an aircraft. The concept of shock coupling of conventional explosives at the surface to defeat a deeply buried DBHT appears infeasible.

Most attractive concept identified

Either a means of obtaining vastly higher explosive yields per unit explosive weight (as in metastable nuclear isotope explosive concepts) or some means of changing the overpressure/distance scaling relationship would be required for this to be an attractive approach without fissile nuclear explosives.

One possible approach would be to distribute an array of charges over the target and time their detonation such that pressure waves reinforce at the target space to effect spall damage and space collapse. Such an approach to defeating an 80 meter granite emplaced DBHT might have some promise, but even an order of magnitude reduction in explosive yield required would imply a payload requiring multiple fully loaded bombers to deploy. However, the approach would have the advantage of scalability and modularity.

Another possible approach would be to use a fluid explosive delivered into a DBHT air intake or exhaust duct. Using precision delivery, an amount on the order of 10,000 pounds might be delivered at a surface opening for such a duct. Detonation of the explosive at the DBHT end of the duct might well overcome blast valves and other

equipment by brute force. Based on the available unclassified literature, the author would classify this alternative as the most attractive of the squash warhead type of approaches.

Table 3: Hard target defeat concepts and their limitations

DEFEAT AGENT	DISRUPTION MECHANISMS	LIMITING CONSTRAINTS FOR MAX PENETRATION DEPTH	REASON FOR ELIMINATION	COUNTERMEASURES
Shaped Charge	Shrapnel, pyrophoric agent	Maximum Diameter, Maximum Weight, Jet instability	Non-innovative, marginal feasibility	Bury deeper, compartmentalize
Long rod	Explosive overpressure, shrapnel, pyrophoric agent.	Maximum Weight, Maximum Length, Max. impact velocity	Non-innovative, marginal feasibility	Bury deeper, compartmentalize
“Squash” warhead	Explosive shockwave creates internal spall	Maximum Weight	Infeasible w/ conventional explosives	Wall design mitigates spall, Bury bunker deeper
Repeated Bombing	Explosive excavation of bunker	# of req’d munitions increases as the cube of the depth or worse.	Non-innovative, marginal feasibility	Bury deeper, pile rubble into crater, target delivery system.
Collapse Openings	Neutralization through isolation	Intelligence	Non-innovative existing capability	Hidden /redundant / armored entrances, excavate & repair.
EMP/ HPM/RF	Neutralization of Electronic Assets	High frequencies propagate poorly through rock.	Apparent non-robustness, lack of data/expertise	Shielding/isolation / transient protection of external lines.
Robotics	Infiltration of facility followed by targeted disruption of utilities.	Introduction to facility and control. Lack of effectiveness & robustness due to small size.	Apparent non-robustness, lack of data/expertise	Standard hardening / NBC precautions sufficient. Sentries / close doors.
NBC agents	Disable personnel, C-fiber / powders can defeat elect.	Introduction and dispersion in facility	Lack of data; politics similar to nuclear bombs.	Seal, filter air, alternate air supply, compartmentalize.
Nuclear bomb	Blast, EMP, spall, radiological	Politically unacceptable, escalation of conflict, collateral damage, long term contamination.	Precluded by problem statement. Some facilities are too deep.	Bury bunker deeper
Surface Drilling	Introduced agents such as explosives	Disruption by enemy forces – historically demonstrated maximum drilling rates for hard rock are approximately 5 meters/hour.	Non-robustness due to likelihood of detection and sensitivity to disruption.	Enemy interference, compartmentalization, seeding of surface layers above DHBT with high hardness abrasive materials.
Mechanical Subterrene	Payload transported by subterrene (explosive or incendiary).	Energy density of power source... chemical power requires >100:1 power source length : hole diameter.	Infeasible based on reviewed historical capabilities.	Compartmentalization, seeding of surface layers above DBHT with high hardness abrasive materials
Thermal Subterrene	<i>High pressure melt bubble yields pressure explosion, spall, incendiary effects</i>	<i>Limited only by total energy/power density of selected power source.</i>	...	<i>Potentially heat sinks and some refractory materials.</i>

Long rod penetrators

Heuze presented a survey paper in 1990 for prediction of penetration of a projectile into geological materials.⁸⁴ Empirical, analytical, and numerical methods for penetration prediction are discussed. This paper also cites work relevant to shaped charges and rock properties. Based on this paper and the resources available, the empirical penetration equations of C.W. Young were selected for an optimistic estimation of the potential depth of penetration of a long-rod penetrator in granite.

Young's equations are an accepted empirical back-of-the-envelope approach to estimating penetration – as long as consideration is given to the assumptions made and limitations of the data used in derivation of the equations. Young's equations have recently been employed by two papers on nuclear earth penetrator weapons, including a report by the National Academy of Sciences.^{2,6}

It should be emphasized that Young's equations, as well as prediction methods in general, are unreliable for predicting penetration in non-homogeneous and fractured materials (as is typical of geological materials). Non-homogeneity can cause gross deflections in the penetrator's path, penetrator deformation, and/or break-up. Cracks and joints in rock can cause both enormous stress on a penetrator (potentially resulting in structural failure) as well as greatly influence the penetrator's path. Further, these characteristics of geological materials are difficult to characterize *a priori* even when a site is fully accessible, making prediction of penetrator performance in a real world scenario even more uncertain. Real-world effects such as these, however, typically tend to limit reliable penetrator performance to less than what might otherwise be predicted (as long as the bulk material characteristics of the site are adequately characterized).

Young's empirical penetration equations are listed below, with variables defined in Table 4.

Long-rod penetration equations:

$$D = 0.00178 \cdot S \cdot N (W/A)^7 (V - 100)$$

$$N = .25 L_n / d + .56$$

$$S = 12 (f_c' / Q)^{-3}$$

Assumed geometry (cone-tipped cylinder)

$$W = g \cdot \rho_p \cdot \left(\frac{\pi d^2}{4} \cdot \left(L - \frac{2}{3} L_n \right) \right)$$

$$A = \frac{\pi d^2}{4}$$

Table 4: Penetration equation variables

Parameter	Name	Units
D	Depth of Penetration	ft
S	Penetrability of Target	non-dim.
N	Nose Performance Coefficient	non-dim.
W	Weight of Penetrator	lbs
A	Cross Sectional Area	in ²
V	Impact Velocity	fps
L	Length of Penetrator	in
L _n	Length of Penetrator Nose	in
d	Penetrator Diameter	in
f	Fineness Ratio (L/d)	non-dim.
f _c '	Target Unconfined Compressive Strength	psi
Q	Rock Quality	no units
ρ _p	Penetrator Average Density	slugs
g	Gravitational Constant	ft/sec ²

In all scenarios evaluated it is assumed that there exists: zero angle of incidence at impact; no “wipe” velocity; homogeneous granite properties without joints or cracks; impact velocity 4000 fps or less; penetrator remains intact during penetration; and that

the penetrator follows a basically stable trajectory during penetration (no “J-hook,” tumbling, or changes in direction).

Viable fineness ratios for long-rod penetrators

Two types of long-rod penetrators in current inventory are air-delivered explosive filled penetrator warheads and gun fired Armor Piercing Fin-Stabilized Discarding Sabot – Tracer (APFSDS-T). The first category includes the Guided Bomb Unit-28 (GBU-28, Figure 12) BLU-113 warhead, and the Small Diameter Bomb (SDB) warhead. These warheads are intended to be suitable for employment against earth and reinforced concrete type hard targets, employ steel cases with an explosive fill for terminal effect, and typically have a fineness ratio of around ten (~10.5 for the BLU-113, and ~12 for the SDB warhead). Maximum impact velocities are supersonic and probably on the order of 2000 fps or less, depending on separation altitude, velocity, and energy loss from maneuvers/drag during descent.



Figure 12: GBU-28 employing explosive filled BLU-113 warhead with fineness ratio of 10.5

Reference^{85, 86}

A key difference between these warheads and an anti-tank type long-rod penetrator is that the former must maintain structural integrity of the warhead so as to preserve their explosive payload and function as intended upon penetrating the target.

Due to the impacted materials (armor) and impact velocities involved with anti-tank long-rod type penetrators, these penetrators are typically expected to erode/flow from the nose rearwards during impact with a target. Note that Young's Penetration Equations are not generally applicable to the penetration performance of anti-tank long-rod type penetrators (even when employed against geological materials or concrete) due to impact velocities typically in excess of the 4000 fps limit of the equations.

The current generation APFSDS-T round for the M-1 "Abrams" main battle tank is the M829A2 (Figure 13). Based on unclassified numbers for earlier US versions of the APFSDS and specifications for the current Russian export 120mm APFSDS (1850 m/sec), muzzle velocity of the M829A2 is expected to be greater than 1500 m/sec and probably closer to 2 km/sec. These velocities are in excess of what is sustainable without penetrator nose deformation/erosion and therefore out of family with the test data Young's penetration equations are derived from. From photogrammetry the M829A2 penetrator is measured to have a fineness ratio of approximately 30.



Figure 13: Anti-tank long-rod penetrator in 120 mm sabot/shell system (M829A2 APFSDS-T) with fineness ratio of about 30

Reference⁸⁷

A solid penetrator cross-section enables use of a higher fineness ratio design without concern of structural or warhead failure as compared to a penetrator with explosive fill. A high fineness ratio is further enabled by the Depleted Uranium (DU) alloy used in construction of such penetrators. The alloy self-sharpens during penetration at high velocities due to adiabatic shear-banding whereas the steels typically used in penetrating bomb-bodies (or tungsten alloys in long-rod penetrators) tend to mushroom.^{88‡} Also, the lower bar speed of sound in these alloys as compared to steel helps to limit gross deformation of the penetrator to the target/penetrator interaction zone.⁸⁹

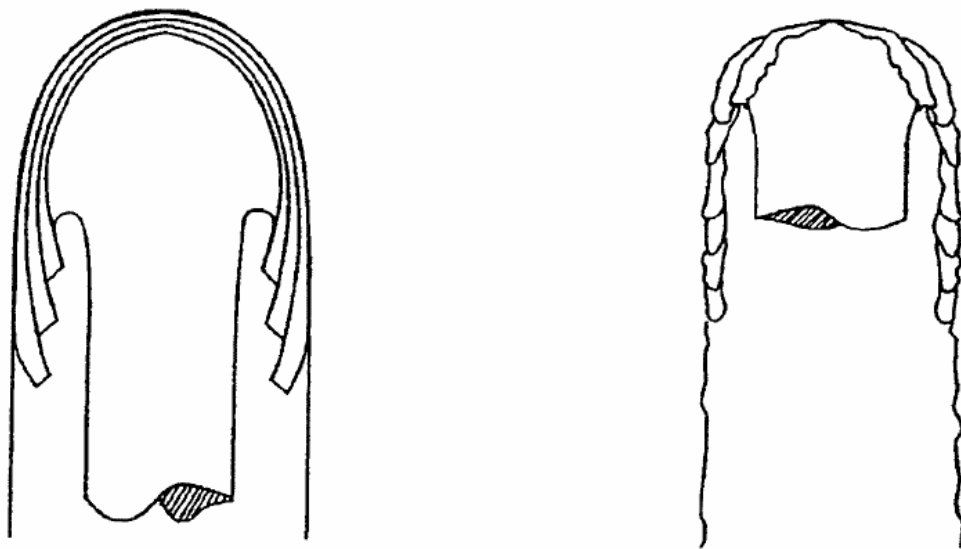


Figure 14: “Mushrooming” nose of a typical steel or tungsten penetrator (left) and “self-sharpening” nose of a depleted-uranium alloy penetrator
Reference⁸⁸

Note that the constraint limiting maximum fineness ratio in an anti-tank round appears to be in-gun/launch considerations such as: total shot weight; load transfer between sabot and penetrator; launch angle of attack; and flexure of the penetrator rod.⁹⁰

[‡] An additional advantage of DU is that at high impact velocities the “vaporific” and incendiary effects from small uranium particles can significantly contribute to behind armor lethality.

For a rocket-boosted and/or aircraft delivered munition such constraints should not apply, potentially enabling significantly higher fineness ratios.

A further option for improving performance of high-fineness ratio/high-impact velocity penetrators is the use of an extending rod penetrator design. Such a penetrator is comprised of two or more axially translating sections which extend and lock prior to impact so as to increase the total length of the penetrator and thus increase total penetration depth.^{88, 90}

Scaling considerations for structural integrity of a long rod penetrator

Consider a photographically scaled long-rod penetrator. The area moment of inertia of the penetrator scales as the fourth power of length – if the scale of the penetrator is increased by a factor of two, then the area moment of inertia increases by a factor of sixteen. Further, the critical force required for buckling scales linearly with the area moment of inertia and the inverse of the length squared (according to the Euler column buckling formula). Thus, critical force required for buckling increases as the square of the penetrator scale.

The deceleration force experienced by a penetrator impacting at a given velocity in a given material scales proportionally to the square of the penetrator scale. Therefore, while critical force required for buckling increases as the square of the penetrator scale, the force decelerating the penetrator also increases as the square of penetrator scale.

In a similar fashion, consider the scaling of stresses in a photographically scaled penetrator. As previously discussed, decelerating forces in a homogeneous medium should scale as the square of the penetrator scale. Sectional area of the structure to transmit these forces will also scale as the square. One would therefore expect – based

solely on column buckling considerations and structural stress in penetration of a homogeneous medium – that a penetrator photographically scaled up from a proven structural design and impacting similar materials at similar velocities would also be structurally sound.

In truth, real-world materials possess non-homogeneities of a variety of scales. In geological materials, these are principally crystal grains, variations in composition and weathering (often layered), and cracks/joints in the material. To the extent that a material appears more homogeneous with increasing scale one would expect a photographically scaled penetrator to be more survivable with increasing scale as loading of the penetrator would be more uniform with time and with lower lateral accelerations.

Increasing apparent homogeneity is often but not always the case with geological materials over the scales considered – it would be reasonable to expect the effects of grains, inclusions, and small scale cracks and joints on penetration would decrease with increasing scale. However, with increasing penetrator scale the depth of material penetrated would also increase, potentially increasing the likelihood of encountering layers in the material as well as encountering less fractured/weathered (and therefore higher strength material) – potentially reducing total depth of penetration relative to scaled penetrator predictions.

All in all, in the context contemplated, it seems reasonable to expect a photographically scaled penetrator impacting similar materials at similar velocities to scale well with respect to penetration equation predicted performance.

Material considerations for structural integrity of a long rod penetrator

Assuming a penetrator is harder than the target it is impacting, several considerations can contribute to the failure of a long-rod penetrator to achieve theoretical performance.

If the impact speed of the penetrator is such that the stagnation pressure of the target material exceeds the tensile yield stress of the penetrator material, the penetrator nose will typically begin to mushroom and deform – potentially resulting in penetrator deformation and/or break-up. The equation for the approximate maximum impact velocity without deformation, V , is given below, where Y_p is the tensile yield stress of the penetrator material and ρ_t is the target density.

$$V \leq \sqrt{\frac{2Y_p}{\rho_t}}$$

Figure 15 illustrates the dependence of stagnation pressure vs. velocity for an assumed granite density of 2.4 grams/cc. A kinetic penetrator steel, E4340, has a tensile yield strength of about 1000 MPa,⁶ and oil quenched and tempered tool steels can have tensile yield strengths of around 2000 MPa.⁹¹

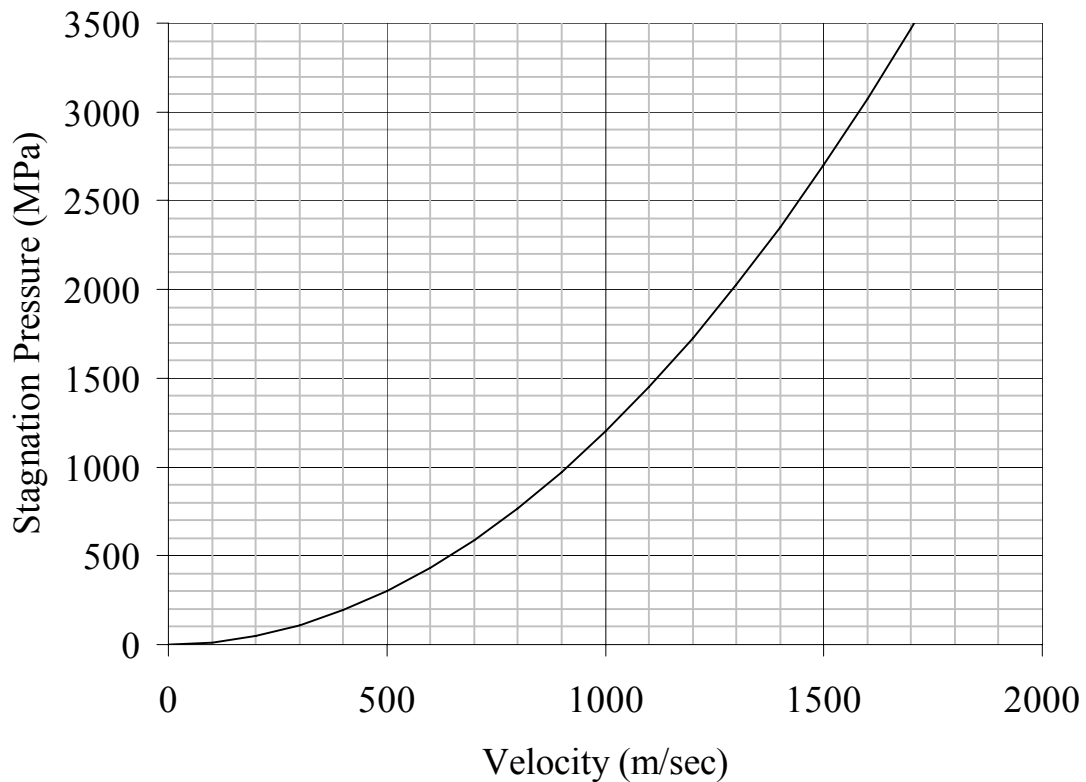


Figure 15: Impact velocity in 2.4 g/cc granite vs. stagnation pressure

Tougher penetrators will tend to first fail in deformation/erosion while harder penetrators will tend to break-up. One modification to this general rule is for DU penetrators. The uranium alloy used in these penetrators exhibits the phenomenon of self-sharpening at high impact velocities, which is attributed to adiabatic shear-banding. Self-sharpening decreases the loads/drag on the penetrator delaying deformation/break-up while increasing penetration depth.

Other scenarios resulting in less than theoretical predicted performance are when a penetrator impacts the target: at an oblique incidence; with a velocity not normal to the target surface; or penetrates angled strata of varying material properties. In these instances the asymmetric loading of the penetrator can induce yaw, trajectory deflection,

and/or loads resulting in penetrator structural failure – all of which tend to reduce penetration depth.

Granite properties

In the problem statement it was specified that the hypothetical DBHT was emplaced under 80 meters of intact high strength granite. To use Young's equations it is necessary to specify an unconfined compressive strength f_c' and a rock quality factor, Q . Maximum unconfined compressive strength of high strength granite was estimated to be approximately 400 MPa (58,000 psi) or less based on Figure 16.⁹² Mean unconfined compressive strength of high strength granite was estimated to be approximately 110 MPa (16,000 psi).

The rock quality factor Q is a descriptive estimated parameter, ranging from .9 to .1, that is not defined in terms of an equation. Instead, it is estimated based on descriptive categories for various qualities of rock. For example, a Q of .9 is specified for massive rock bodies, .6 for interbedded, ranging all the way down to .2 or even .1 for highly fractured or weathered rock.⁹³ A rock quality factor of .9 was assumed as consistent with the problem statements specification of intact, high strength rock.

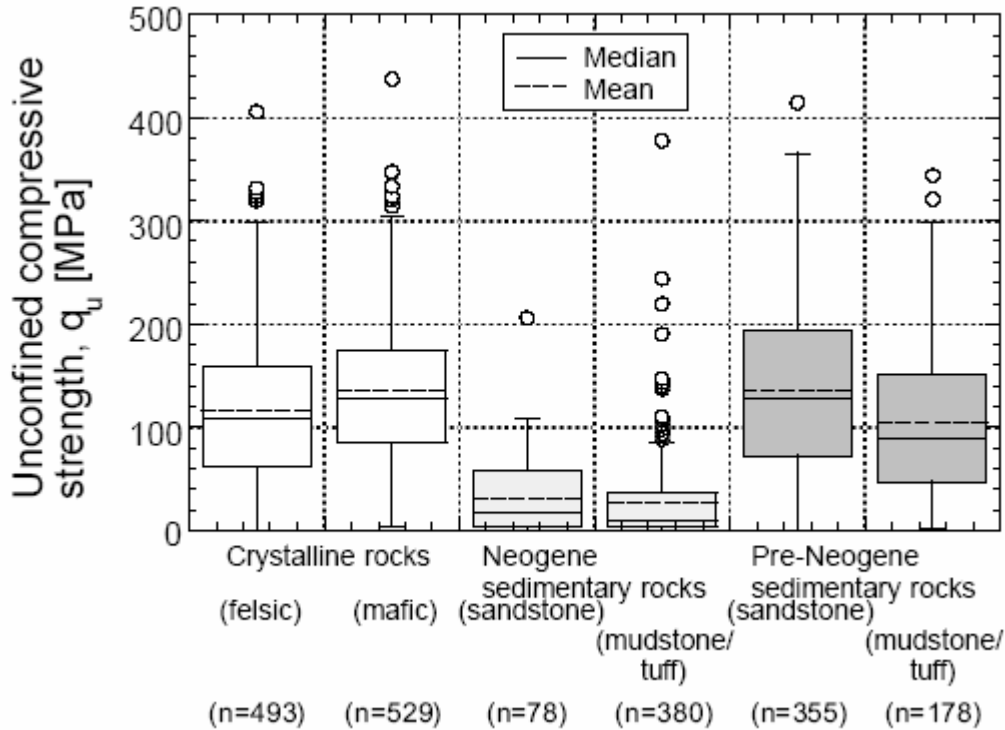


Figure 16: Unconfined compressive strength for various rocks

Felsic rocks include the varieties of granite, and mafic the varieties of basalt. In the above figure, n denotes the number of samples used to create the figure, the boxes denote $\pm 25\%$ of samples above and below the median value, upper and lower lines show the range from the upper and lower quartile to 1.5 times the interquartile difference (obviously not a physically significant metric as it can be negative), and circles show the outlying data points. The dashed line in each box illustrates the mean sample strength. Note that these samples were collected from surface outcrops and mines throughout Japan. Though the distribution of sample strengths is not universally representative of strengths in other regions, the upper limit of strength listed is expected to be representative for the purpose of a conservative penetration analysis.

Unboosted and boosted long rod penetrator

Table 5 lists assumed values for various parameters in Young's penetration equations. A nose fineness ratio of three for the nose was selected as this was believed to be an optimistic upper value for a hard material such as rock. An average penetrator density of either $.199 \text{ lbm/in}^3$ or $.686 \text{ lbm/in}^3$ was assumed where specified. This is consistent with a typical explosive filled penetrating bomb or the heaviest density metals

that might be used. The granite unconfined compressive strength and rock quality factors were selected as discussed previously.

Table 5: Penetration equation assumptions

Parameter	Name	Units	Value
L_n/d	Fineness of Penetrator Nose	in	3
ρ_p	Penetrator Average Density	lbm/in ³	.199 / .686
f'_c	Target Unconfined Compressive Strength	psi	58,000/16,000
Q	Rock Quality	no units	.9

For comparison purposes, rough estimates of the maximum penetration of the BLU-113 and MOP for a granite target for the assumptions made are given in Table 6 and Table 7. It can be seen that they are quite short of breaching a space of the hypothetical target. Also, the specified impact velocities are likely in excess of those achievable (estimated potential velocities at release from Table 1 are 2690 ft/s for the B-2 and 2750 ft/s for the B-52). MOP is an interesting baseline as it provides an estimate of maximum penetration against the hypothetical target given requirements that have been approved by the military and therefore one would assume are considered viable by the Air Force community using existing bombers.

Table 6: Optimistic estimate of penetration for BLU-113 and MOP for 400 MPa granite

Weapon	f	L_n/d	ρ_p , g/cc	V, ft/s	d, in	L, ft	Mass, lbm	Depth (m)
BLU-113	10.55	2	5.5	2700	14.5	12.7	4,400	<7
MOP(1)	10.55	3	8.0	2700	25	22	30,000	<16
MOP(2)	10.55	3	5.5	2700	28	25	30,000	<13

Estimated performance of existing BLU-113 and planned MOP warheads given penetration assumptions. MOP(1): High density estimate (similar to solid steel). MOP(2): Density similar to that of BLU-113 estimate.

Table 7: Optimistic estimate of penetration for BLU-113 and MOP for 110 MPa granite

Weapon	f	L_n/d	ρ_p , g/cc	V, ft/s	d, in	L, ft	Mass, lbm	Depth (m)
BLU-113	10.55	2	5.5	2700	14.5	12.7	4,400	<11
MOP(1)	10.55	3	8.0	2700	25	22	30,000	<23

MOP(2)	10.55	3	5.5	2700	28	25	30,000	<20
--------	-------	---	-----	------	----	----	--------	-----

Estimated performance of existing BLU-113 and planned MOP warheads given penetration assumptions. MOP(1): High density estimate (similar to solid steel). MOP(2): Density similar to that of BLU-113 estimate.

Table 8 and Table 9 assume the proposed MOP mass, a MOP penetrator density consistent with DU, a nose fineness of 3, and varying fineness ratios. Note that the density specified would preclude an explosive payload (it might be possible to extract some pyrophoric effect from the DU for terminal lethality). Based on length constraints for the B-2 for internal carriage (approximately 25 feet from photogrammetry), it would appear that a maximum depth of approximately 30 to 50 meters could be obtained.

Table 8: Viable penetrator ordnance sizing based on nominal MOP for 400 MPa granite

Scenario	Potential Velocity, ft/s	L, ft	Mass, lbm	Depth (m)
Subsonic bomber, $f=10$	2700	16	30,000	22
Subsonic bomber, $f=20$	2700	24	30,000	33
Subsonic bomber, $f=30$	2700	31	30,000	40

Table 9: Viable penetrator ordnance sizing based on nominal MOP for 110 MPa granite

Scenario	Potential Velocity, ft/s	L, ft	Mass, lbm	Depth (m)
Subsonic bomber, $f=10$	2700	16	30,000	33
Subsonic bomber, $f=20$	2700	24	30,000	48
Subsonic bomber, $f=30$	2700	31	30,000	59

Table 10 and Table 11 list estimated maximum (upper-bounding) performance given a penetrator sized following expected maximum B-1B capability. Considering both length and weight constraints for internal carriage, it would appear that a depth of about 40 to 70 meters might be obtainable.

Table 10: Viable penetrator ordnance sizing based on B-1B capability for 400 MPa granite

Scenario	Potential V, ft/s	L, ft	Mass, lbm	Depth (m)
Supersonic bomber, $f=10$	3100	19	50,000	29
Supersonic bomber, $f=20$	3100	29	50,000	43

Supersonic bomber, $f=30$	3100	37	50,000	52
---------------------------	------	----	--------	----

Table 11: Viable penetrator ordnance sizing based on B-1B capability for 110 MPa granite

Scenario	Potential V, ft/s	L, ft	Mass, lbm	Depth (m)
Supersonic bomber, $f=10$	3100	19	50,000	43
Supersonic bomber, $f=20$	3100	29	50,000	63
Supersonic bomber, $f=30$	3100	37	50,000	77

Based on Table 8 through Table 11, it would appear that internal carriage by an existing bomber of an unboosted long-rod penetrator with fineness ratio of 30 or less capable of penetrating to 80 meters in high strength granite is not plausible. This being the case, roughly how large would a penetrator have to be for various fineness ratios and deployed from various aircraft types, so as to penetrate to the specified 80 meter depth? Table 12 lists the penetrator masses and lengths obtained for various (optimistic) impact velocities and penetrator fineness ratio of ten. Comparing Table 12 and Table 1, it is apparent that the penetrator masses obtained are inconsistent by *at least an order of magnitude* with any historically demonstrated airlift capability.

The results listed in Table 13 suggest that a DU penetrator with a fineness ratio of 20 is borderline feasible for carriage by a An-225 class transport aircraft for penetration to 80 meters in nominal expected strength granite. Table 14 suggests that a DU penetrator with fineness ratio of 30 delivered by an XB-70B-like or heavy transport (C-5 or C-17) class aircraft might be able to penetrate to the required depth in mean or weaker strength granite targets.

Table 12: Long-rod penetrator performance with fineness ratio of ten

Scenario	Impact Velocity, ft/s	L^1 , ft	Mass ¹ , lbm	L^2 , ft	Mass ² , lbm
Subsonic bomber	2700	98	7,000,000	56	1,300,000
Supersonic bomber	3100	80	3,800,000	46	720,000
High-supersonic “	4000 (5120)	55	1,200,000	32	240,000

Transport	2400	117	12,000,000	67	2,300,000
-----------	------	-----	------------	----	-----------

(1) Bounding unconfined granite tensile strength of 400 MPa; (2) Mean unconfined granite tensile strength of 110 MPa.

Table 13: Long-rod penetrator performance with fineness ratio of twenty

Scenario	Impact Velocity, ft/s	L ¹ , ft	Mass ¹ , lbm	L ² , ft	Mass ² , lbm
Subsonic bomber	2700	87	1,400,000	50	260,000
Supersonic bomber	3100	71	750,000	41	140,000
High-supersonic “	4000 (5120)	49	240,000	28	46,000
Transport	2400	103	2,300,000	60	450,000

(1) Bounding unconfined granite tensile strength of 400 MPa; (2) Mean unconfined granite tensile strength of 110 MPa.

Table 14: Long-rod penetrator performance with fineness ratio of thirty

Scenario	Impact Velocity, ft/s	L ¹ , ft	Mass ¹ , lbm	L ² , ft	Mass ² , lbm
Subsonic bomber	2700	84	570,000	48	110,000
Supersonic bomber	3100	69	310,000	39	59,000
High-supersonic “	4000 (5120)	47	100,000	27	19,000
Transport	2400	100	970,000	58	180,000

(1) Bounding unconfined granite tensile strength of 400 MPa; (2) Mean unconfined granite tensile strength of 110 MPa.

Table 12 through Table 14 suggest the importance of both higher fineness ratio penetrators and higher impact velocities on both the feasibility and viability of penetrating to 80 meters in granite with an air-delivered kinetic penetrator. While it is not evident from the unclassified literature what maximum fineness ratio of penetrator is viable against granite without penetrator failure, as far as can be ascertained it might be possible to produce a DU very high fineness long rod penetrator ($f > 30$) capable of penetrating to 80 meters in average strength granite when delivered from a B1-B. However, use of DU (or tungsten) in the quantities and massive construction required would be costly, technologically challenging from a manufacturing perspective, and environmentally hazardous.

Rocket boosted long rod penetrator

Up to the point of penetrator erosion/break-up, greater penetration depths are theoretically obtainable given higher penetrator impact velocities. An obvious and historically demonstrated approach to getting such velocities for a penetrator deployed from an aircraft is to use a rocket to boost the penetrator prior to impact. Two regimes can be considered – impact at velocities similar to or less than those for which the penetrator will remain intact, and higher impact velocities at which the impact begins to most resemble a hydrodynamic process for which penetration occurs through a mutual erosion of penetrator and target.

The first regime will be considered first. Assuming the impact velocity is the maximum specified for Young’s penetration equations, and sizing the penetrator booster to match, the initial weapon package weight can be approximated as the solid rocket motor weight plus the penetrator weight:

The rocket equation was used to estimate rocket motor weight as described below, with variables defined in Table 15.

Rocket Equation:

$$\Delta V = g \cdot I_{sp} \ln \left(\frac{m_i}{m_f} \right) \quad (1)$$

$$m_i = m_f + m_{prop} \quad (2)$$

$$m_f = m_{inert} + m_{payload} \quad (3)$$

$$k_s \equiv \frac{m_{inert}}{m_{inert} + m_{prop}} \quad (4)$$

$$V = V_i + \Delta V$$

Table 15: Rocket equation variables

Parameter	Name	Units
ΔV	Change in velocity of rocket system	m/s
I_{sp}	Effective specific impulse	seconds
g	Gravitational constant	m/s^2
m_i	Initial mass of rocket system	kg
m_f	Burn-out mass of rocket system	kg
m_{inert}	Inert mass of rocket motor	kg
$m_{payload}$	Payload mass	kg
m_{prop}	Fuel mass	kg
k_s	Inert mass-fraction	non-dim.

Combining and rearranging equations (1) through (4), the initial required mass for a rocket with payload can be shown to be equal to that given by equation (5) below.

$$m_i = m_{payload} \frac{(1 - k_s) e^{\Delta V / g I_{sp}}}{1 - k_s e^{\Delta V / g I_{sp}}} \quad (5)$$

The rocket motor was assumed to be a solid. Large solid motors have specific impulses and inert mass fractions generally consistent with those listed in Table 16.

Table 16: Rocket equation assumptions

Parameter	Name	Units	Value
I_{sp}	Effective specific impulse	seconds	255
k_s	Inert mass fraction of rocket motor	non-dim.	.13
g	Acceleration of gravity	m/s^2	9.8

Assume that a B-1B carries a boosted penetrator with a rocket motor sized to provide an impact velocity (neglecting drag, maneuver, and thrust-gravity losses) of 4000 fps. Given the above assumptions, Table 17 lists the estimated maximum (optimistic) depth of penetration in mean strength granite along with penetrator length and mass/total-mass. It would appear to be possible that such a system might be capable of reaching the

minimum required depths. Note that an equivalent performance/lower density steel penetrator without booster would weigh in excess of 100,000 lbm.

Table 17: Rocket boosted viable penetrator ordnance sizing based on B-1B capability into mean strength granite

Scenario	Potential V, fps	L, ft	Mass, lbm	Depth (m)
Supersonic bomber, $f=30$	Boosted to 4000	28	20,000/23,000	80

The apparent benefit of boosting a penetrator to a higher velocity than could be obtained using unboosted delivery from an existing platform raises the question of exactly how much benefit is derived from delivering the penetrator from an aircraft in the first place. In this context it is interesting to examine the approximate system size required for various rocket boosted penetrator systems launched from zero initial altitude and velocity.

Table 18 and Table 19 suggests that, given the assumptions (which neglect a number of sources of terminal velocity losses that would be incurred), a rocket boosted penetrator system capable of penetrating to eighty meters depth would not be inconsistent with the current state of the art in solid rocket motor technology. Shuttle Solid Rocket Boosters (SRBs) produce approximately 2,300,000 pounds of sea-level thrust, and have a gross weight of about 1,300,000 pounds. Titan IV Upgraded Solid Rocket Motors (USRMs) produce approximately 1,500,000 pounds of sea-level thrust and have a gross weight of about 790,000 pounds. For the lower penetrator weights, an increasing number of clusterable commercial strap-on boosters and surplus ICBM first stages become feasible. For example, the clusterable 141,000 pounds thrust GEM 46 Strap on Solid Rocket Motor (SSRM) grossing 42,000 pounds weight, or the Peacekeeper ICBM first stage motor.

Range of such a hypothetical Theater Ballistic Missile (TBM) would be limited, particularly given the velocity losses neglected in this analysis that would detract from obtainable impact velocity as well as the flight profile required to obtain a suitable orientation and velocity vector at impact. Assuming a flat-earth/zero-drag trajectory and impulsive acceleration to 4,000 fps, the range would be on the order of 80 nautical miles. For a very high fineness ratio penetrator of 30, the total system weight and dimensions would be relatively close to the Minuteman IB ICBMs and space launch vehicle simulators that have previously been successfully air-dropped from C-5 and C-17 cargo aircraft. Writing off the initial total energy of the booster/penetrator system at aircraft separation, it might be feasible to produce a munition weighing approximately 100,000 pounds capable of penetrating to 80 meters depth in granite. Given the small diameter of the penetrator and SSRMs, such a munition might be carried on a centerline pylon beneath an adapted commercial freighter akin to OSC's L-1011.

Table 18: Rocket boosted from zero potential velocity to 4000 ft/sec into mean strength granite

Scenario	L, ft	Mass Penetrator, lbm	Total Mass, lbm
$f=10$	32	250,000	450,000
$f=20$	29	50,000	89,000
$f=30$	28	20,000	37,000

Table 19: Rocket boosted from zero potential velocity to 4000 ft/sec into maximum strength granite

Scenario	L, ft	Mass Penetrator, lbm	Total Mass, lbm
$f=10$	56	1,300,000	2,400,000
$f=20$	50	260,000	470,000
$f=30$	48	110,000	190,000

Compared to any other of the boosted or unboosted long-rod scenarios discussed, this is by far the most plausible. However: 1) a 20,000 to 100,000 lbm DU penetrator is

about three orders of magnitude heavier and one order of magnitude larger than any previously manufactured; 2) it is very uncertain as to what path a penetrator would travel over eighty meters distance in an actual non-homogeneous geological structure (or whether the penetrator would remain intact); 3) the separated booster(s) would be a potential source of collateral casualty; and 4) the terminal lethality of such a weapon is uncertain (though not implausible, DU being pyrophoric).

Hypervelocity rocket boosted long rod penetrator

A penetrator could be boosted to a velocity at which the strength of material of target vs. penetrator was relatively unimportant to the penetration performance as compared to inertial forces. Tungsten long rod penetrator performance against steel at 2+ km/sec impact velocities is about 1.3 according to one reference.⁹⁰ Scaling this to tungsten against granite, a penetrator length to penetrated depth ratio of about 3.7 is obtained. This suggests that to penetrate 80 meters of granite would require a penetrator of 22 meters length. For a rocket booster using the previously stated assumptions to accelerate a penetrator from 2700 fps to 6600 fps (2 km/sec) the mass ratio would be 1.6. For such a boosted penetrator to weigh around 50,000 lbm a fineness ratio of more than 105 would be required. Even for an extending rod penetrator design, such a high fineness ratio seems intuitively likely to result in inadequate stiffness/structural stability prior to impact. Further, the extrapolation of penetration of comparatively low penetration depth to penetrator diameter ratios (~40) to such high penetration depth to penetrator diameter ratios (~400) seems unlikely to hold.

Relaxing the weight constraint to a total of 100,000 lbm, a penetrator fineness ratio of around 75 would be predicted. This is still more than twice the fineness ratio of the state of the art APFSDS anti-tank round, but might be feasible.

Post-impact adaptively boosted long rod penetrator

Hypothetically, a penetrator could be integrated with a rocket engine that fired during the process of penetration to increase total penetration depth without exceeding penetration velocities that would result in structural failure of the penetrator. However, the practical impediment exists that the rocket motor will likely become choked by the penetrated material. Once choking occurs for a motor using a propellant with positive burn rate exponent a situation may occur where: 1) chamber pressure rises in the rocket engine; 2) propellant burn rate increases as a result – further increasing chamber pressure; until, 3) the combustion chamber fails.

One means of getting around this difficulty is to control, actively or passively, the rate of gas generation by the propulsion system based either on the acceleration of the penetrator or the sensible reaction gas pressure.

If the vents(s) of the gas generator system were moved to the forward end of the penetrator body and a tapered profile incorporated in the aft penetrator body, several potential benefits can be hypothesized: reduction of contact friction between the rock and penetrator (perhaps through enhancement of a supercavitation effect)¹⁵; propulsive force resulting from gas pressure on the penetrator exterior; and the possibility of reactive control of penetrator direction by varying radial distribution of vented mass flow. Conceivably, the propulsion efficiency might be augmented both by: the mass entrainment of rock by the propulsion gas in a similar fashion by which water or other

fluid can be injected into a jet exhaust to increase thrust; and by the confinement of the propulsion gas behind the projectile in a fashion similar to that which occurs in a gun barrel.

A further conceivable advantage to this approach is that any propellant unexpended upon penetrator breach of a DBHT space could be utilized as energetic payload for terminal lethality. Utilization of energetic payload to increase penetration depths makes sense in that if the penetrator fails to reach a sufficient depth to damage the targeted DBHT space, the energetic payload is wasted. Further, high energy solid composite gun propellant chemical ingredients are by weight principally high explosives (such as nitroglycerin, nitrocellulose, and/or higher energy organic chemicals) mixed with various minority additives (to modify burn rate, mechanical strength, lubricity, chemical stability, etc).

The typical total duration of penetration from impact to rest for a penetrator is measured in tens of milliseconds for rock and hundreds of milliseconds for soil. Also, penetrators typically experience accelerations on the order of thousands to tens of thousands of g's. As a result, three major engineering impediments to implementing a suitable propulsion system are: 1) generating gas rapidly enough to counteract the experienced deceleration; 2) adaptively (whether actively or passively) controlling the rate of gas generation in response to the actual system loads to prevent penetrator rupture or explosion; 3) having propellant grain(s) capable of withstanding the shock/acceleration loads without mechanical failure.

There is a relatively simple, demonstrated approach to adaptively regulating the required high rate of gas generation which is also relatively robust with regard to

structure and function: multiple discrete solid gas generators. In this approach, many discrete gas generators would be packaged compactly in the penetrator body and electronically initiated at the rate required to maximize penetration depth without causing failure of the penetrator.

Such a system is marketed by MetalStorm™ LTD, for the purpose of rapidly firing multiple projectiles in series from an array of barrels at extremely high cyclic rates (Figure 17). One implementation of this system has demonstrated a cyclic rate of charge initiation of 1,000,000 firings a second (Figure 18). If this technology were to be adapted to penetrator post-impact propulsion, the non-energetic mass (principally bullets) within the propellant tubes would be minimized. Functionally, the bullets are used to separate propellant charges from each other and from the hot gas in the exhaust end of the tube. Any suitable system for insulating one charge from another, preventing leakage of hot gas to uninitiated charges, and preventing set-back of charges from gas pressure could functionally replace the bullets (Figure 17) used in the MetalStorm™ system as gas-checks/projectiles. O'Dwyer has in fact proposed using his MetalStorm™ concept for the related purpose of reaction control for a maneuvering missile (Figure 19).⁹⁴

If one assumes division of a penetrator's propellant into ten to a thousand individual charges, then based on the demonstrated rate of initiation of charges the entire propellant load could be initiated sequentially in 10 μ sec to 1 millisecond. This would appear to be compatible with typical order of magnitude rock penetrator impact durations (~10 milliseconds). Notionally, the actual rate of propellant charge initiation would be tailored to maximize penetration depth, possibly on the basis of estimated penetrator velocity as determined by sensed penetrator acceleration integrated with time (Figure 20).

One potential issue with this approach that might have to be addressed is accelerometer bandwidth, as sampling of acceleration would have to be of a sufficiently high rate to resolve the penetrator acceleration vs. time response during penetration.

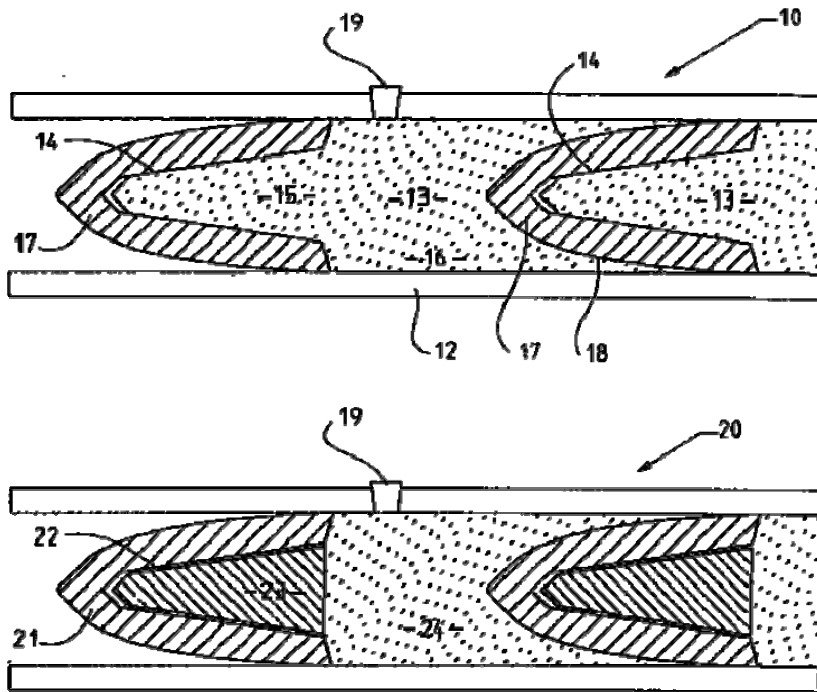


Figure 17: Stacked sequentially initiated propellant charges as illustrated in MetalStorm™ patent

10) barrel assembly; 12) barrel; 13) discrete selectively ignitable propellant charges; 14) inwardly reducing recess in rear of projectile which serves to expand base and obturate bore; 15) leading portion of propellant block shaped to expand projectile base; 16) main body of propellant block; 17) nose of next projectile in line; 18) next projectile in line; 19) external primer extending through wall of barrel; 20) alternative barrel assembly with two part projectiles; 21) two part projectile; 22) head part of projectile; 23) anvil part of projectile; 24) relatively flat faced propellant block.⁹⁵



Figure 18: Picture of gun battery using MetalStorm™ technology firing at a cyclic rate of 1,000,000 charges per minute

Reference⁹⁶

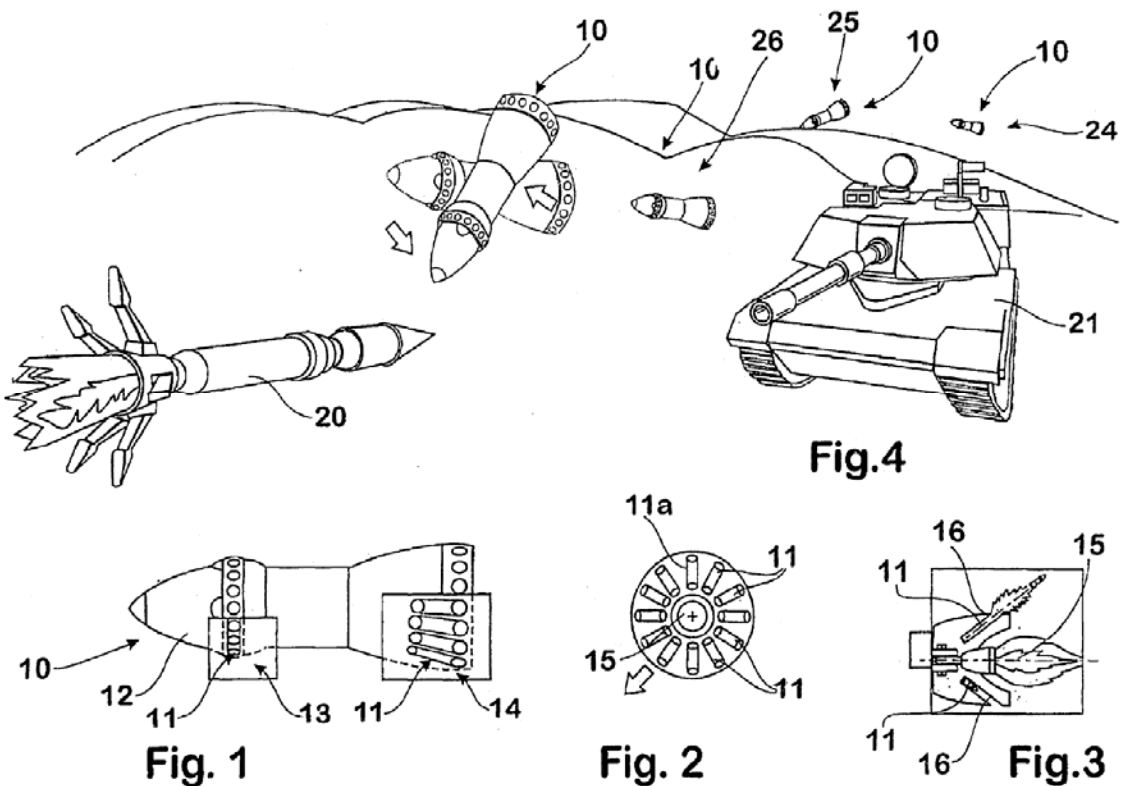


Figure 19: O'Dwyer reaction control concept for missile using MetalStorm™ approach to discrete propellant charge packaging/initiation

Reference⁹⁴

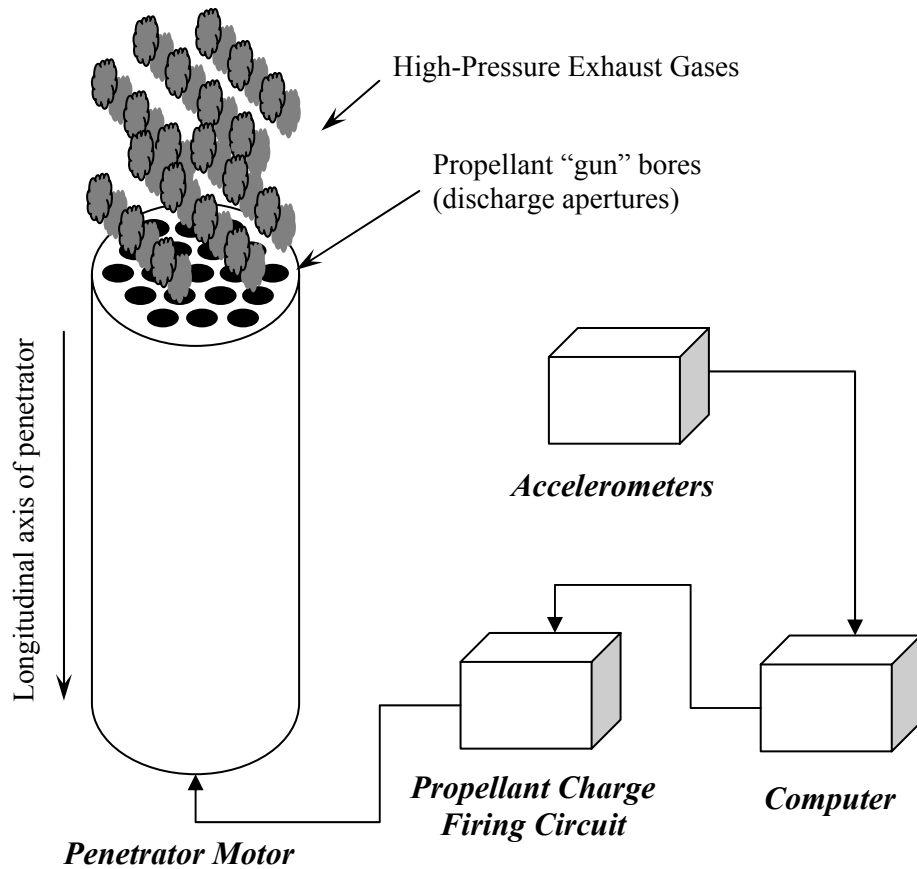


Figure 20: A system component concept for utilization of sequential propulsion charges in adaptive post-impact propulsion system

Estimation of penetration performance of a penetrator using such a system is problematic, especially at the conceptual level of investigation, because the flow field around and behind penetrators is poorly understood. A crude estimate was attempted by assuming that post penetration the shaft of penetrated material effectively forms a plugged shaft with fixed walls, and the penetrator, cavity, and plug system comprise a system analogous to a traveling charge gun. A 70% / 30% nitrocellulose/nitroglycerine double-base propellant is assumed, possessing an initial density of 1.56 grams/cm³ and producing adiabatic combustion products with a density of about .36 grams/cm³ at 345

MPa pressure. The density ratio between unburned propellant and high pressure propellant gases is therefore about 4.4.

It is further assumed that the penetrator is initially about 50% unburned propellant by volume with a fineness ratio of 10. In this case, the penetrator can maintain a constant base pressure of comparable magnitude as the average effective retarding pressure obtained from Young's Penetration Equation over a distance of about 22 diameters (or 2.2 penetrator lengths) before the base pressure begins to decay with further expansion of the cavity. Referring to Table 8, this would result in about a 135% increase in depth of penetration over an unboosted 30,000 pound steel/explosive fill penetrator impacting at 2700 fps. Referring to Table 10, the boosted penetrator penetration depth would exceed by a factor of more than 30% that of an equivalent fineness ratio DU penetrator of equivalent weight and impact velocity (DU would be similar to 1.5 penetrator lengths of penetration).

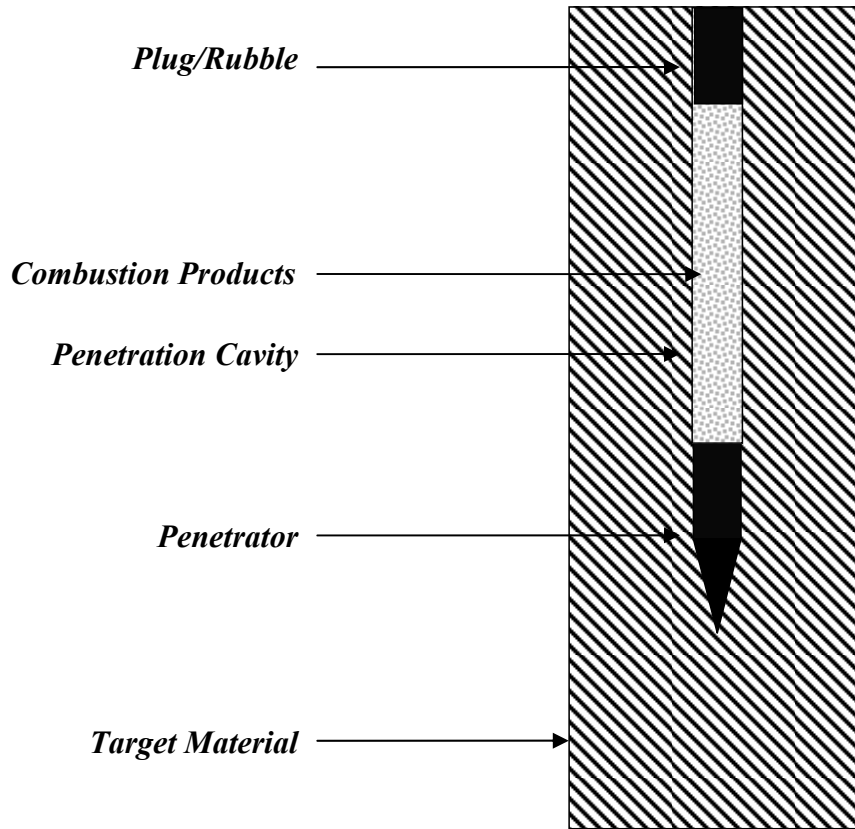


Figure 21: A traveling charge conceptual model of boosted post-impact penetration

Most attractive long-rod penetrator concepts identified

The long-rod kinetic penetrator type concepts considered most attractive to the author fall into two categories: 1) explosive filled low-fineness ratio long-rod penetrators; and 2) high fineness ratio solid long-rod penetrators.

In the first category, it seems likely to the author that *if* a substantial volume of energetic fill is to be used in a kinetic penetrator, it would be highly desirable for such fill to potentially double as a propellant for increasing total depth of penetration. An adaptively boosted penetrator as previously described might offer advantages in this respect.

In the second category the author believes a large, rocket-boosted long-rod penetrator would offer the best alternative. Rocket boosting is desirable as for an aircraft delivered kinetic penetrator system maximum penetration depth is more critically constrained by terminal velocity than by penetrator mass. Sacrificing penetrator weight to add a rocket motor providing higher impact velocity is expected to provide increased total penetration for a fixed total mass at velocities up to around 4000 fps. A very large rocket-boosted kinetic penetrator (80,000 lbm+ total mass) might be air-dropped from a large transport or cargo aircraft, might be air-mobile (using the same), or ground or ship-mobile (a Theater Ballistic Missile) and employ recycled ICBM boosters or commercial solid mainstage/solid strap-on booster technology. Such an approach has been considered in the past⁹⁷, perhaps typically on a smaller scale than what is proposed here.

Shaped charges

Explosive charges can be shaped and initiated at one or more selected locations (line and plane initiations of various geometries can be accomplished) so as to control the geometry and propagation of the detonation wave and thus control the work done by the charge on some interacting material. In such a manner explosives are used for: imploding materials such as critical masses in nuclear weapons; precision forming of metal sheets into thin complex geometries; welding materials such as plates of dissimilar metals; and formation of highly directional projectiles and jets.

In the context of defeat of a hard target, the term *shaped charge* typically refers in US literature to a lined hollow charge used to produce a penetrating effect against a target. Kennedy, Eather & Griffiths, and Walters have all written introductory reports on

the subject of the shaped charge effect and its history with focus on military applications.^{49, 98-101}

Typical nomenclature for shaped charges is illustrated in Figure 22 (charge depicted in section view – typical charge is axisymmetric about long axis). Shaped charge components typically include: a detonator (frequently electrical), which initiates the main High Explosive (HE) charge via a “booster” explosive charge; a charge case; and the cavity liner (often of copper or other ductile, high density metal). More advanced shaped charge designs may include detonation wave shapers, more complex liner geometries, tandem charges, composite or bimetallic liners, or other characteristics/components. Some shaped charge characteristic parameters frequently discussed are: liner cone semi-angle (half the aperture) and Liner Diameter (LD) for conical shaped charges; Charge Diameter (CD); Warhead Diameter (WD); and StandOff (SO) distance from the charge face to the target.

The general principle by which shaped charges operate is as follows: 1) the initiation of the HE charge opposite the charge cavity liner results in the propagation of a longitudinally symmetric (wrt the charge axis) supersonic detonation wave through the charge towards the cavity liner; 2) the immense pressures produced in the explosive behind the detonation wave progressively accelerate and collapse the liner towards and along the central axis; 3) as the liner collapses upon itself and collides along the axis of symmetry it tends to form a jet and/or slug travelling in the axial direction of the charge, and possessing a velocity ranging from one to in excess of ten kilometers per second.¹⁰¹

The specific mechanisms of liner jet formation for a shaped charge differ depending on the geometry of the cavity liner and the liner material. In the case of

metallic liners of relatively obtuse cone and hemisphere geometries, a “tubular extrusion process” appears to occur, resulting in a relatively wide jet possessing a lower velocity gradient along the jets length.¹⁰² In the case of relatively acute cones (of approximately 60° or less semi-angle), interaction of the collapsing liner with itself as it meets along the axis of the charge causes the inner wall portion (roughly 20%) of the liner to “squirt” into a fast, forward-moving jet with a relatively high velocity gradient along its length (jet tip moving fastest, potentially >10 km/sec).^{101, 102} The exterior of the liner flows into a comparatively slow moving slug (~1 km/sec).¹⁰¹

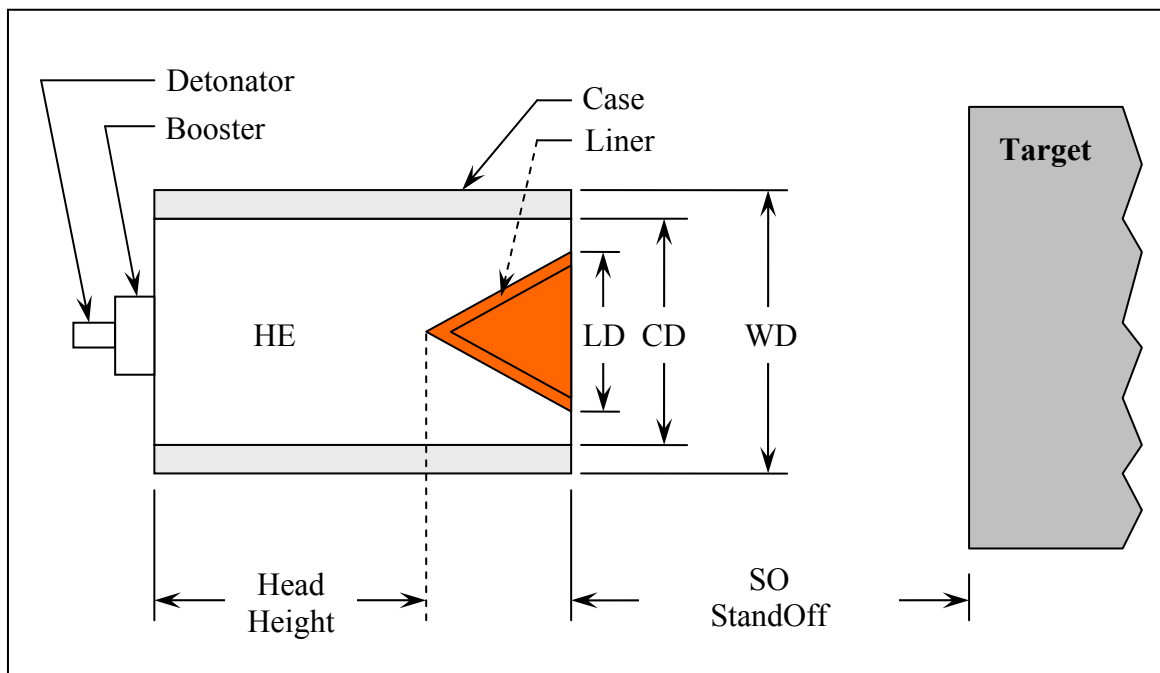


Figure 22: Typical components of a shaped charge

Proper formation of the jet for maximum penetration typically requires the charge to be detonated a minimum of around one to two charge diameters or more standoff distance from the target for best effect. Further, as compared to Explosively Forged Projectiles (EFP) the charge cannot be detonated at very long standoff distances as the jet produced has a substantial velocity gradient along its length, and therefore tends to

stretch and eventually break-up at long standoff distances. Interaction with the atmosphere at longer distances tends to slow-down, disperse, and (for some materials) substantially combust the jet particles, reducing penetration effectiveness.

Upon the resulting jet's impact of armor or other material, the pressures generated at the interface of the target and jet material exceed the yield stresses of both materials by an amount sufficient that the materials behave like fluids. Penetration is accomplished by action of this pressure pushing the target material aside, with little reduction in target mass aside from that due to ejecta and/or spall mass.^{49, 101}

Employment of a shaped charge against a target is shown in Figure 23: 1) a shaped charge is delivered to an appropriate standoff distance from the target for best effect, ideally normal to the minimum thickness of the targets armor; 2) the charge is detonated producing a jet/slug of hypervelocity material directed at the target; 3) interaction of the jet with the target material produces a hole in the target, potentially resulting in through-penetration of the target wall.

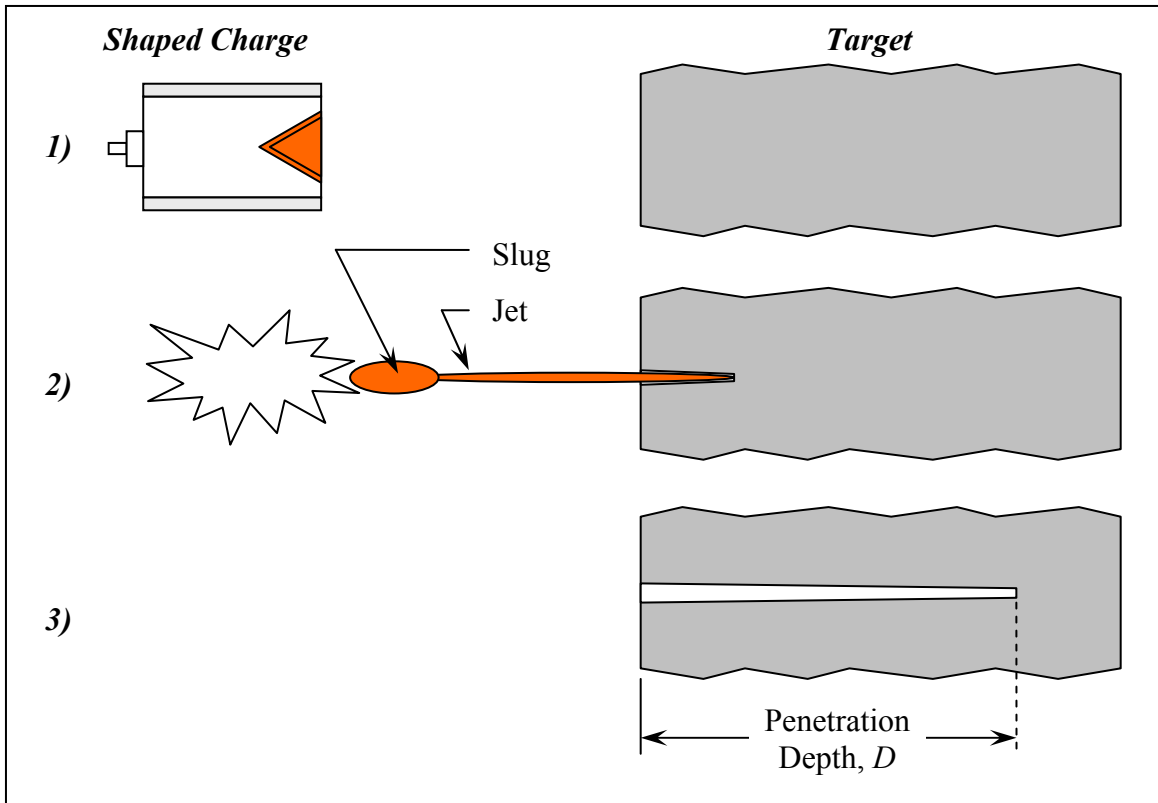


Figure 23: Action of a shaped charge against a target

Shaped charge enhancing technologies

Penetration performance of a shaped charge is generally enhanced by: use of denser explosives; denser liner materials; complex liner shapes; detonation wave shapers; lower density target material; and/or larger diameter charges.¹⁰³⁻¹¹⁰

Very dense conventional explosives are already used in shaped charges and little improvement in performance appears likely, although various concepts do exist such as: nano-thermite composite explosives; new chemical systems for high energy materials; energetic materials from radioisotope reactions (metastable radioisotopes); and use of ultrahigh pressures to create metastable energetic materials.¹¹¹

Whether called ‘metastable interstitial composites,’ ‘super-thermites,’ or ‘nano-thermite composite explosives:’ in the context of a high-explosive application, these

materials use very high energy density thermite chemical systems with nano-size reactant particles to achieve very high reaction rates (which without a gas-producing component in the reaction remain subsonic – ie, non-detonating in nature). A gas-producing component/binder such as epoxy may be added to bind the reactants together and contribute to the propagation of a detonation wave in the material (with some reduction in specific enthalpy of the energetic material consequent from the addition of the binder). Conceptually, for shaped charge applications these materials have favorable densities (higher than conventional HE) and volume specific enthalpies (two or three times higher than conventional HE).¹¹¹ The author has not yet seen, however, predictions of detonation pressures vs. volume specific enthalpies and mass densities for various candidate thermite based explosive mixtures, and it would seem intuitively that the addition of gas producing components to thermite type reactions might lower achievable energy densities to those of conventional HE or less due both to dilution effects as well as enthalpies of vaporization for the gas donor.

New HE's being sought through various experimental and computational approaches have been suggested as having the potential for gains of from 10% to 200% in energy density over existing formulations. The most near-term candidates appear to be analogs of existing explosives such as HMX, RDX or similar where one or more NO₂ group has been replaced by an NF₂ group, resulting in expected increases of 10% to 20% energy density. The fluoride compounds produced upon reaction of the explosives are expected to have a synergistic fluxing effect with respect to the passivating oxide coating present on aluminum or boron fuel particles added to the organic explosive resulting in much more complete combustion of the fuels (and hence higher energy densities).¹¹¹

In concept, metastable radioisotopes such as $^{178m2}\text{Hf}$ have been proposed as potential explosives whereby the transition of excited nuclei in their metastable state to their ground state would be stimulated in a very short period of time by action of high energy photons. Publicized interest in the phenomenon appears to have derived from work by Carl B. Collins and colleagues on stimulated decay of metastable hafnium and other nuclei using low-energy gamma photons¹¹² with ongoing work by Collin's graduate students, among others.¹¹³

In principle, if a device could be created that was capable of stimulating transition to the ground state of a significant quantity of metastable isotope in a short enough period of time, then pulsed nuclear propulsion concepts such as "Orion" and plasma driven thermonuclear implosion suggest the conceptual (perhaps highly speculative) possibility of using ablation/plasma driven acceleration of a liner to form a penetrating jet. For that matter, a low-yield fission device as the driver of a very large diameter liner might be possible if nuclear explosives were not prohibited. However, a number of apparent difficulties exist that would have to be addressed. Production cross sections for nuclear metastable states are typically small, leading to problems with obtaining significant quantities of the excited state isotopes. There is the further problem of obtaining the metastable state isotopes in sufficient concentration – enriching chemically identical isotopes is quite difficult, enriching for an essentially mass-identical isotope state may well be impossible (if the metastable isotope of interest were produced directly by activation). Assuming that one can overcome these obstacles, there remains the problem of achieving stimulated emission of a sample in a short enough period of time with practical conversion efficiencies of the metastable state population. Some information in

the public domain suggests a view that the metastable radioisotope approach is of questionable feasibility with respect to providing an explosive energetic material.¹¹¹

Copper liners are typically used in shaped charges due to copper's: good ductility at high strain rates; solid state at the typical pressures and temperatures encountered; ease of formability into the required liner shapes; fairly high density; and low cost. The greatest improvement in density conceivable over copper would be on the order of from 16.5 to 22.5 grams per cubic centimeter by substituting high density metals such as molybdenum, tantalum, uranium, rhenium, tungsten, iridium or osmium. All of these are to some degree cost prohibitive, with uranium, tungsten, and possibly tantalum less so. Most have heavy metal toxicity concerns, with uranium also posing radiological concerns. Some, such as tungsten, are very difficult to form.

Shaped charge performance estimation

Bernoulli's theorem of incompressible flow can be used to develop an estimate of penetration depth. The first order penetration law, below, was developed independently by several researchers in the 1944 to 1951 timeframe.¹⁰⁵⁻¹⁰⁸ As evident from this equation, in the *hydrodynamic impact regime*, depth of penetration, D , tends to vary linearly with the square root of the density ratio between projectile and target (ρ_p/ρ_t), and linearly with the projectile scale, L .¹⁰³ This of course is an approximation, and assumes a target with no tensile strength as compared to the jet pressure, and an ideal jet.

$$D = L \cdot \left(\frac{\rho_p}{\rho_t} \right)^{\frac{1}{2}}$$

Thus, for a shaped charge of a given design interacting with a semi-infinite target of a given material, total penetration depth scales proportionally to the Charge Diameter

(CD). This constant of proportionality for penetration in Rolled Homogeneous Armor (RHA – a kind of steel plate) is a technical measure of merit for shaped charge designs. Conservative performance for a simple Conical Shaped Charge (CSC) using a copper liner against RHA is about 4.5 CD's of penetration, with modern, sophisticated shaped charge designs capable of a maximum penetration of about 8 or 10 CD's.¹¹⁴ As details of design of modern warheads are not generally in the public domain, 8 to 10 CD's with copper may be an incorrect assumption (such performance might more easily be explained by a denser metal).

Scaling for substitution of uranium or other high density metal for copper suggests penetration increase by a factor of approximately $\sqrt{\frac{\rho_{uranium}}{\rho_{copper}}} \approx 1.45$.

Granite and other common rock materials are substantially lower density than steel, at approximately 2.4 grams/cm³ versus 7.9 grams/cm³. This suggests potential penetration increase by a factor of approximately $\sqrt{\frac{\rho_{granite}}{\rho_{steel}}} \approx 1.81$. Altogether, one would expect the penetration depth to charge diameter ratio to increase by a factor of about 2.6 when switching from: a shaped charge design using a copper liner employed against steel; to a very dense metal liner shaped charge employed against stone.

Therefore, a very optimistic estimate of the penetration depth to charge diameter ratio for a sophisticated design shaped charge using very dense metal liner against rock would be about 26 charge diameters. If we assume that delivery is diameter limited, then Table 20 lists the optimistic delivery platform payload diameter constrained maximum shaped charge penetration depth performance.

Table 20: Optimistic estimate of maximum shaped charge performance against granite target as constrained by delivery platform maximum payload diameter

Delivery platform	Liner	Depth (m)
B-52, B-1B, B-2	DU	~50
C-5, C-17	DU	~100
“Super Guppy”	DU	~200
B-52, B-1B, B-2	Copper	~35
C-5, C-17	Copper	~70
“Super Guppy”	Copper	~140

This estimate is very optimistic in that it neglects a number of real world concerns that affect scaled performance of a shaped charge. Among them are the following considerations.

During jet penetration of a homogeneous medium an annular counter-flow of material occurs in the shaft created by the jet, comprised of both jet and target materials. As depth of penetration of the jet increases, interaction of annular jet/target debris material increasingly interferes with and tends to disrupt the fresh incoming jet material. Eventually, this effect can disrupt the jet and limit penetration compared to what might be expected based on density scaling. Inhomogeneities in the target and or jet can lead to disruption of the jet. Chemical reactions between jet and target materials can disrupt the annular debris and thereby the jet, diminishing penetration. Another consideration affecting scalability of shaped charges is the precise dimensional and material property requirements that must be met in charge manufacture to achieve expected charge performance. Manufacturing explosive charges and metal liners to precise dimensions and maintaining homogeneous material properties becomes increasingly difficult with scale.

To attempt to get a conservative bounding estimate of shaped charge performance, consider the large CSC designed, assembled, and tested by Sandia National Laboratories (SNL) in 2002. This copper lined CSC was designed to be carried on a cruise missile as part of a compound warhead to produce a large diameter, deep hole in concrete or rock. The shaped charge would function as a precursor warhead for a tandem-carried following cased penetrating warhead.¹⁰⁴ This CSC was reported by SNL to be the Largest known CSC (LCSC).[§] Its diameter was 28 inches, length was 28.5 inches, and weight was 900 pounds. The tuff rock in SNL's test had a dry density of approximately 1.8 to 2.0 g/cm³. A maximum depth of penetration of about 19.5 feet, or 8.4 charge diameters was demonstrated. Note that this charge was designed to produce a relatively large diameter hole to enable the entrance of a follow-on penetrator warhead (similar to the BROACH warhead) and was not optimized for maximum penetration depth.

Other CSC designs were parametrically explored in the SNL's design study prior to selection of the demonstrated design, including some using tungsten. Maximum penetration depth for CSCs using tungsten was predicted to be in excess of 30 feet for a comparable diameter design (note this is consistent with the expected ratio of about 1.5 for maximum penetration for tungsten vs. copper).

These results give a good baseline expected performance for a simple geometry, relatively low-cost of manufacture shaped charge design.

[§] While extraordinarily large, SNL's "largest" CSC is not the largest known CSC, except perhaps in the contemporary sense. The warhead employed by the Nazi Germany "Mistel-1" composite aircraft during WWII was more than two and a half times the diameter and weighed about eight times as much.⁴⁹

Whereas penetration depth scales linearly with charge diameter, shaped charge weight scales with volume as the third power of diameter (Figure 24).^{**} Thus, while it is reasonable to estimate feasible performance of smaller diameter shaped charges on the basis of maximum viable charge diameter, at some point charge weight will become the dominant constraint limiting performance achievable. This is illustrated in Table 21. In this table, four different performance levels for a hypothetical shaped charge have been assumed. The first two are very optimistically derived from target/liner density ratio scaling from the reported state of the art of 8 to 10 charge diameters of penetration against RHA. The second two are based on the results demonstrated by SNL against Sidewinder Tuff Rock using the LCSC.

Based on these penetrator performance numbers, a required charge diameter was estimated. Next, using the regression relation illustrated in Figure 24, the approximate shaped charge weight is estimated. As seen from the last column of the table, even for the most optimistic shaped charge performance, the required charge size would be incompatible with existing inventory bombers and marginal with respect to weight as compared to the largest payloads ever historically separated from inventory cargo transport aircraft. Further, based on demonstrated LCSC performance against rock, a CSC theoretically capable of penetrating 80 meters of granite would be too massive for any existing or historical aircraft to deliver.

Table 21: Estimate of CSC weights vs. penetration performance to penetrate to a depth of 80 meters in granite

^{**} Note in this figure the paucity of data for larger diameter shaped charges. The 2 meter diameter 7700 pound “Mistel” shaped charge warhead from WWII would be an interesting addition to the data set, except that its liner has been variously reported as being of steel, aluminum, or copper. Given the scarcity (and strategic importance) of copper during WWII Germany, it seems probable that either steel or aluminum were used for the liner. Aluminum is consistent with the regression results which would suggest a nominal 20,000 pound weight for the charge as compared to its reported weight of ~8,000 pounds.

Penetration (Charge Diameters)	Diameter (in)	Mass (lbm)	Delivery platform
26 (DU Optimistic)	121	73,400	C-5, C-17, large civil freighter, purpose-built glider
18 (Copper Optimistic)	175	220,000	An-124, An-225?
11.7 (Sandia LCSC Tungsten)	270	806,000	<i>None</i>
7.6 (Sandia LCSC Copper)	415	2,400,000	<i>None</i>

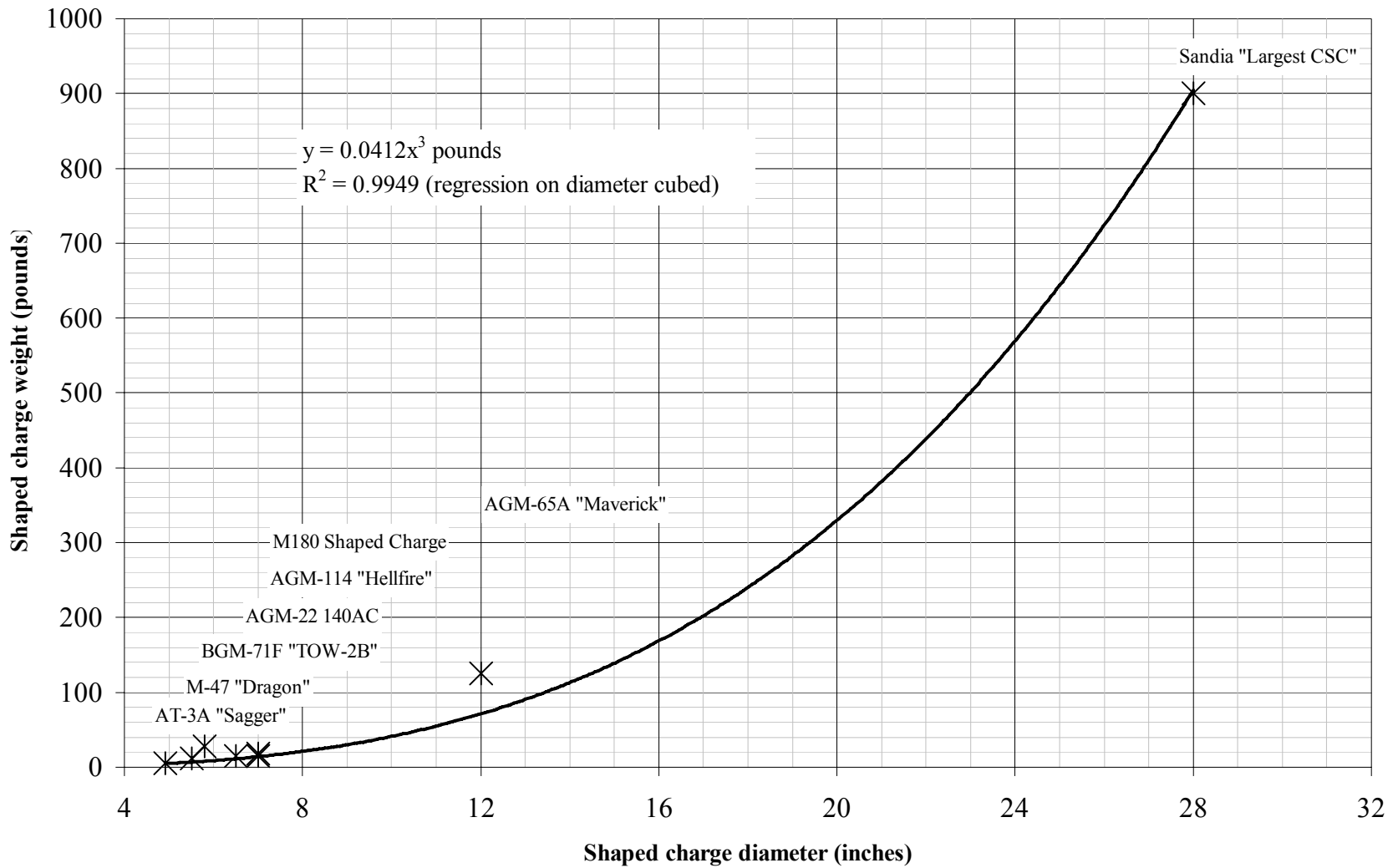


Figure 24: Regression on a selection of historical shaped charge data

Stacked shaped charges

Since penetration depth scales linearly with diameter, and shaped charge mass scales as the cube of diameter, an obvious approach to improve penetration efficiency with respect to weight is by stacking shaped charges in series. This approach is documented in the US patent literature and shaped charge histories.^{49, 99-101, 115} In this general approach the shaped charge most distant to the target is detonated first with the forward charges detonated progressively in sequence so that the slow moving slugs produced will not disrupt the fast moving jets.^{††}

When considering application of this approach to increasing penetration depth against a DBHT, two apparent difficulties are: the disruption of the second shaped charge by the effects of the first; and achieving precise axial alignment of the charges. The incremental advantage of adding additional charges for deepening a very slender hole are likely to diminish rapidly. For the sake of argument, suppose that four shaped charges could be employed with four times the effect of a single charge, and that each charge provided 12 charge diameters of penetration. In this example, the four shaped charges used to penetrate 80 meters would weigh a total of about 47,000 lbm and be about 5.5 feet in diameter. Aggregate performance required would 48 charge diameters. Minimum overall length for the warheads alone would likely exceed the maximum weapons bay length of a B-2 or B-52. However, such a device might very well be deployable from a cargo aircraft.

^{††}Note that this approach is distinct from that of the fairly ubiquitous precursor shaped charge employed by modern anti-tank munitions. In this application a coaxial smaller initial shaped charge attached to a probe is detonated prior to the main charge to initiate a tank's reactive armor, after which the main charge fires its jet through the gap in the tank's reactive armor. In this application the leading shaped charge is relatively small and separated by a relatively large distance from the following charge.

Most attractive shaped charge concept identified

Given the performance/weight scaling relations of shaped charges, the author favors sequential employment of multiple shaped charges as the best shaped charge approach to defeating the baseline DBHT.

One approach would be to use multiple integrated, coaxial shaped charges, detonated rapidly in sequence from the rear forwards to attempt to achieve enhanced penetration effects without disruption of the fast-moving jets by the slow-moving slugs (or slower-moving tails of the jets). If the composite shaped charge were of too great a size and weight for delivery from an existing-inventory bomber, it might be deployed on a sled from a cargo aircraft. However, the absence of historical evidence (in the public domain) of adoption of multiple coaxial integrated shaped charges in a fielded system may indicate that implementation of the approach is problematic.

However, there is an alternative concept providing precision delivery, compressed carriage, precision alignment capability, and multiple non-interfering jets. Consider the following two technological capabilities: delivery of massive sled mounted payloads by cargo aircraft; and GPS guided parachutes for precision delivery of the massive payload sleds from cargo aircraft to a designated point on the ground. Using these two capabilities it might be possible to deliver a massive shaped charge drilling machine incorporating: an aimable armored cradle for receiving and aligning shaped charges; an armored shock-hardened magazine for carriage of multiple large-diameter shaped charges; a number of these large diameter shaped-charges. Each large diameter shaped charge might incorporate: disintegrating fiber-wound cases with flanges providing radial standoff from the armored alignment cradle (to prevent excessive damage to the cradle); as well as

progressively varying liner designs optimized for progressively increasing standoff; and a chassis for transporting, leveling and anchoring the same on the target surface.

If it is assumed that each shaped charge produces a debris-free and straight hole (the former in particular seems an unreasonable assumption) and ignoring the negative impact of increasing standoff distance with penetration (probably not reasonable even with individually optimized charge liner profiles) it is conceivable that such a system might penetrate 80 meters or more of hard rock. Eight one-meter diameter copper lined charges (under such assumptions) might penetrate 80 meters of granite while weighting around 10,000 lbm. Survivability of the chassis with respect to repeated ~1000 lbm HE detonations seems a challenging problem within the weight constraints of an air-delivered system, but given sufficient armoring, careful profiling of blast-impinged surfaces, and shock-attenuation for sensitive components it does not seem impossible.

Alternative rock removal/displacement technologies

The last three alternatives listed in Table 3 were considered attractive for further consideration. First and foremost, drilling technologies of sufficiently small size have historically been demonstrated to have the ability to penetrate to sufficient depths. They require some knowledge of a DHBT facility's layout so that lateral targeting can be chosen. Otherwise, they appear comparatively robust to details of a DBHTs implementation.

As the three alternatives considered attractive for further consideration embody some of the various alternatives that may be employed for penetration of rock, it makes sense to explore a more general and comprehensive categorization of possible alternatives.

In order to define a rock penetration concept it is necessary to specify one of the possible technologies for removal or displacement of rock. One means of assessing the potential performance of these various rock penetration/mining related technologies is by their respective energies required for removal of a given volume of hard rock (Table 22).¹¹⁶ Further insight into the respective performance can be gained by estimation of the mechanical complexity required for implementation, historical performance achieved, as well as specific power and energy density available for implementation.

Table 22: Specific energy for removal of hard rock

TECHNOLOGY	SPECIFIC ENERGY <i>(MJ/m³)</i>
Mechanical	
Drill and blast	6
Kinetic penetrator	<i>Not Available</i>
Drag bit cutting	80
Percussive drilling	180
Roller bit boring (TBM)	210
Diamond cutting	1,120
Hydraulic (fluid jets)	
Coarse-grained rock (granite)	5,000
Fine-grained rock (welded tuff)	50,000
Thermal	
Thermal spall (flame jet)	3,000
Melt (heated penetrator)	18,000
Vaporization (lasers, plasma torches)	30,000

For example, consider hydraulic removal of rock, which employs jets of extremely high pressure fluid to cut and break up rock, flushing the resulting debris from the rock working face. Hydraulic removal of rock can require specific energies comparable to thermal penetration and requires a large volume of working fluid. A smaller volume of working fluid might be continuously recycled to attempt to produce a more compact air-deliverable system, however it is likely impractical to filter and pump

recycled working fluid at the high flow rates required for rapid penetration. In general characteristics of implementation, a hydraulic rock penetration system is likely to share many limitations of mechanical boring technologies while being less efficient. The one notable potential advantage is an increase in drill life and specific power achievable for high penetration rates through a decrease in coupling between the rate of work done on the rock face and the rate of work done on the drilling hardware (wear). Overall, however, the author believes mechanical or thermal technologies are the superior classes of options. Mechanical technologies are preferable to hydraulic technologies as they are the more efficient, and thermal technologies are preferable to hydraulic as they may offer greater robustness, mechanical simplicity, and have lethality advantages in their terminal effect upon a DBHT.

Surface drilling vs. subterrenes

Another way of categorizing options for rock penetration by a body are as: 1) surface drilling systems; and 2) “subterrenes.” Surface drilling systems are the principle rock penetrating mode employed in industry, whereas subterrenes are an underground vessel or vehicle physically independent of the surface, analogous to a submarine (note that a traditional kinetic penetrator would fall into the subterrene category). The key relative advantages and disadvantages of surface drilling and subterrene penetration approaches are summarized in Table 23.

Table 23: Comparison of surface drilling vs. subterrenes

Surface Drilling

Pros

- 👍 Volume limitation for overall system unrestrictive – energy source, engine, transmission, etc. don’t have to fit down the bore-hole.
- 👍 Advanced state of technology as of *enormous* industrial importance – principle role in nearly *all* mineral resource extraction endeavors

- 👉 Commercial hardware widely available
- 👉 No lack of industrial technology base

Cons

- 👉 Conspicuous presence at target making stealthy attack difficult or impossible
- 👉 Enemy can stop penetration by interfering at surface – penetration rate therefore *critical*
- 👉 Maximum demonstrated penetration rate for hard rock is on the order of 5 meters/hour
- 👉 Bulk and mechanical complexity makes high speed/ballistic delivery highly challenging, leading to vulnerability in delivery-to-target phase
- 👉 Bulk/vulnerability makes simultaneous air-attack using multiple drills challenging
- 👉 Targeting errors/facility compartmentalization more difficult to compensate for with multiple attack points
- 👉 Technology well developed – large improvement over best past performance unlikely

Subterrene	<i>Pros</i>
-------------------	-------------

- 👉 Less subject to interference from surface – penetration rate is less critical
- 👉 Stealthy attack of target may be possible – penetration rate is less critical.
- 👉 Compact size/form required for subterrene by requirement for having all components fit in borehole may be more consistent with air-delivered attack
- 👉 “ may enable ballistic delivery – thus less vulnerable during deployment
- 👉 “ likely to be more consistent with multiple simultaneous air-delivered attack.

Cons

- 👉 Comparatively low technological maturity other than for extremely large tunnel boring machine requiring very large support infrastructure
- 👉 Little well-developed industrial technology base (rocket gas-generator/turbomachinery, conventional drilling, nuclear waste disposal, and other technologies may be applicable)
- 👉 Little applicable off-the-shelf hardware
- 👉 Maximum penetration rates likely to be less than those for surface drilling systems
- 👉 Low available volume may drive structural specific power requirements up leading to less reliability for mechanical subterrene systems than similar surface drilling systems

While mechanical boring technologies offer the most energy efficient rock removal, they also have historical limitations that will likely be difficult to surmount. Consider first the penetration by a drill with power source, engine, transmission, and chassis located on the surface. As mentioned in Table 23, such a system is subject to interference by enemy combatants on the surface and hence maximizing penetration rate is essential to minimize vulnerability to enemy interference. However, despite extremely

substantial investments by the drilling industry and numerous national governments, the maximum penetration rate in hard rock achieved to date is only on the order of five meters per hour. Higher drilling rates may be achievable but orders of magnitude reduction in required drilling times for rotary systems seems unlikely due to the mechanical stresses and thermal loads involved and the fairly advanced state of the art.

Next consider a subterrene mechanical penetrator using one of the more efficient rock drilling technologies. For such a system penetration rate may be significantly less critical as compared to a surface drilling system as post penetration it might be both: less likely to be detected; and if detected, more robust to attempts at interference from the surface.

The author performed a rough assessment of the subterrene volume fraction required for a chemically powered subterrene rotary drill which suggests that the volume of propellant required relative to bore diameter would be impractical – for a 12.7 cm diameter hole, *at least* 16 meters of bore length would be required to accommodate chemical propellant alone. This calculation assumes: a 100 Megajoules/m³ specific energy for rock removal; 5000 joules/cm³ chemical propellant energy density (this is very optimistic for a monopropellant gas-generator type fuel); a 10% efficiency factor for conversion of chemical energy to mechanical energy; and an 80 meter required hole depth. Volume required for diversion of rock spoils around the subterrene are ignored.

The resulting fineness ratio for the subterrene fuel required would be >126:1 (length to bore-diameter), which appears impractical. Additional potential problems with such a system could include: removal of spoils from the surface to prevent pressurization of the bore/loss of propulsive efficiency; vulnerability to surface interference by

explosives or projectiles fired down bore; and poor mechanical reliability (particularly for higher penetration rates).

Thermal subterrenes

As compared to the previously discussed alternatives, a subterrene employing melting for penetration of rock might offer significant advantages if it employed an extremely high energy density, air-independent power source (such as radioisotopes or fission power) to melt rock. First of all, little or no moving parts would be required for its implementation as thermal power conversion to mechanical power would not be required. This would tend to facilitate both ballistic deployment from the air and more robust operation (nothing mechanical to fail). Second, melting of rock would enable the filling of the bore behind the penetrator with melt which would eventually re-solidify, potentially making interference with the penetrator more difficult than for a subterrene leaving an open bore. Third, thermal penetration of rock produces less acoustic signature than most other rock drilling or removal technique. Fourth, igneous rocks are excellent insulators and generally very dense, which means that a significant fraction of the thermal energy released during a thermal subterrene's descent might be recoverable upon penetration for terminal lethality against the DBHT target space. Finally, use of a high energy density nuclear power source could enable the penetration of huge depths of rock completely independent of the surface.

After reviewing the various rock penetration/mining technologies, the author's conclusion was that a thermally penetrating subterrene offers the potential for: an effectively depth independent DBHT defeat capability; minimum vulnerability to surface

interference; potential lethality to DBHT spaces; a ballistic delivery capability; and minimum mechanical complexity and new technology.

Alternative thermal subterrene implementations and baseline concept selection

Table 24 lists alternatives considered for the implementation of a thermal subterrene, with preferred baseline options highlighted in gray. It is interesting to note that this table specifies 40,000 possible alternative concept configurations.

One of the most important categories with respect to impact to overall system characteristics is the thermal power source selected. Options considered were RadioIsotopes (RI), Fissile Transuranic Isotopes (FTI), or energetic chemical systems.

Energetic chemical systems were discarded as they do not have the requisite energy density for a thermal penetrator. Thermite type exchange reactions such as ($\text{Fe}_2\text{O}_3 + 2\text{Al} \Rightarrow 2\text{Fe} + \text{Al}_2\text{O}_3$) are the most plausible candidates for a chemical power source as they possess both very high energy density and in some cases non-gaseous reaction products. Non-gaseous reaction products are a positive characteristic because liquid and solid reaction products tend to better couple heat into the system being melted (gaseous reaction products tend to escape and carry heat away, and also may reduce the adiabatic reaction temperature due to their heats of vaporization).

Obviously, the highest possible energy density for a thermite power source for a thermal penetrator would be if the material which was being penetrated provided the oxidizing agent. For example, the Iron (III) Oxide/Aluminum reaction mentioned above has a relatively high heat (426 kJ per mol of Al) as compared to many thermite systems. However, heat per cubic centimeter (cc) of the combined reactants at 100% theoretical density (3.55 g/cc) is about 14 kJoules/cc. In contrast if the density of aluminum only

were being considered (because the material being penetrated contributed the oxidizer) an aluminum penetrator could be considered to have an energy density of about 43 kJ/cc.

Granites are about 70% to 80% SiO₂. For the sake of a simple optimistic analysis the compounds comprising the balance can be ignored and possible fuels for a silicon dioxide exchange reaction identified. Some representative possibilities are Aluminum ($4Al + 3SiO_2 \Rightarrow 2Al_2O_3 + 3Si$), and Uranium ($SiO_2 + U \Rightarrow Si + UO_2$). Heats of reaction for the two are 155 kJ and 174 kJ per mol of metal, which translates to about 15.5 kJ/cc and 13.9 kJ/cc respectively. Taking the heat of fusion of granite as 130 J/g, heat capacity as 1 J/g K, and density 2.5 g/cc and assuming a temperature change effected on the granite by a thermal penetrator to be 1400 K, the corresponding heat imparted to the granite melt by the thermal penetrator is about 3825 J/cc. Ignoring all losses such as heat required to raise the reactants to temperature and conduction of heat into the surrounding rock, and taking heat available from the metal fuel as about 15 kJ/cc, a maximum possible ratio of rock melt to penetrator fuel volume of about 4 is implied.

Given the above assumptions as well as that the penetrator is of constant cross section and melting a matching channel (no room for melt passage – an optimistic assumption), eighty meters of penetration in granite implies a minimum of 20 meters of fuel. Assuming a cylindrical shape and a fineness ratio of thirty, diameter would be .66 meters. Minimum mass for a uranium metal thermal penetrator would be about 130,000 kg (286,000 lbm) and 18,500 kg (41,000 lbm) for aluminum. Uranium would clearly be infeasible, except perhaps as a combined mode kinetic/thermal penetrator (for which depth of penetration would be reduced). Aluminum would appear to not be eliminated from consideration.

Consider, however, that this is an extraordinarily optimistic analysis. Volume specific energy actually available is probably at least a third less than assumed above due to the heat unrecoverable from the hot (1700 K) fuel reaction product, reaction efficiency, etc. Power lost to conduction into rock is about the same magnitude as that required to produce the granite melt for moderate penetration rates and sub-meter diameter penetrators. Further, assume the sectional area melted in the rock is about 25% larger in area than the sectional area of the penetrator to allow for passage of melt and fuel reaction products. The new ratio of penetrated depth to penetrator length would be about one. An 80 meter long aluminum penetrator with fineness ratio of 30 would mass 1.2 million kg (2.7 million lbm). From the above cursory analysis a chemically powered thermal subterrene appears to be clearly infeasible for penetration of 80 meters of granite. A combined effects kinetic/thermal warhead might have advantages, but issues such as obtaining sufficient mixing of the fuel with melt and the tendency of conduction of heat into the metal penetrator to extinguish the reaction make the approach apparently unattractive for penetration of great depths of rock.

Fissile options were also excluded for the sole reason that minimizing the potential of hazardous nuclear effects at the target was considered to be implied by the problem definition. Nuclear reactors are very difficult to shield as compared to some radioisotopes due to the high energy fission spectrum neutrons and high energy gamma photons produced, requiring on the order of half a meter of shielding or more to reasonably reduce emissions for a water moderated reactor. Higher temperature materials necessary for operation at the temperatures of interest are likely to moderate neutrons substantially less efficiently, requiring even larger amounts of shielding. The resultant

size of a reasonably shielded reactor would therefore be large compared to a radioisotope powered device (this is only true as a result of the assumption of a post-activation shielding requirement). Further, the fission daughter products produced by the reactor once activated would pose a significant long-term radiological hazard if they were released.

The research of radioisotopes for thermal power applications lead to the conclusion that adequate power densities had historically been achieved for thermal penetration of rock using radioisotopes that were compactly shieldable. It was therefore decided to select radioisotopes as the baseline power source for the thermal penetrator concept.

Additional alternatives for implementation of a thermal penetrator exist which are not represented in the morphological matrix. A significant potential concern is impact loading of a hybrid kinetic/thermal penetrator. Combining thermal refractory and impact toughness functional requirements may result in an insufficiently robust penetrator with respect to radioisotope containment. Further, optimal geometries and structural design for kinetic and thermal penetrators are certain to be dissimilar.

Two principle alternatives are considered as possible means of circumventing these potential issues. First of all, one might use a tandem warhead approach whereby a shaped charge type warhead creates a hole in the surface overlying a DBHT into which a RIPTP can be introduced at velocities considerably lower than those required for kinetic penetration of the same material. This would be analogous to a BROACH type warhead. Secondly, a thermal penetrator could be carried within a larger kinetic penetrator

designed as a vehicle to transport the thermal penetrator deep into the surface before allowing it to separate and begin its thermal penetration.

Table 24: Morphological matrix for a thermal penetrator for DBHT defeat

Morph. Feature	Option 1	Option 2	Option 3
Casing Material	Tungsten or other refract. metal	Ultra-High Temperature Ceramic	Other refractory material
<u>Power Source</u>	<u>Radioisotope (RI)</u>	<u>Fissile Transuranic Isotope (FTI)</u>	Chemical (thermit, other)
Filler Material (for radioisotope only)	Hi-Z metals: Tungsten, Tantalum, Rhenium, etc.	Low-Z metals: Beryllium, Vanadium, Chromium, etc.	Boron, Carbon, Nitrides & Oxides
Power Regulation	Passive: conduction, convection, radiation transfer	Static: collision-cross-section/moderation variance w/ temp., TRIGA type, etc.	Dynamic: thermal expansion, diffusion, periodic expl. disassembly, percolation, etc.
Inventory Concept	RI half life > 5 years: sustained operational inventory, service life > 3 years	RI half life < 5 years: Assemble RI w/ inventory inert components on demand, service life ~ 90 days post assembly.	FTI: Sustained operational inventory. Service life ~ to nuclear warheads, possibly much greater.
Delivery Vehicle	Manned aircraft	Unmanned Air Vehicle (UAV)	Ballistic missile
Vehicle Carriage	External	Internal	
Terminal Guidance	GPS/INS	Laser-spot	Imaging seeker
Employment Concept	Unitary	Submunition	Independently guided submun.
Allowed lethality	Conventional: spall, scald, incendiary, blast, smoke incapacitation	<i><u>(Unconventional kill mechanisms such as radiation assumed prohibited.)</u></i>	

*Z denotes the Atomic Mass Number. Low Z materials are advantageous for use with β and neutron emitting isotopes to reduce Bremsstrahlung secondary radiation and thermalize neutrons, respectively. Hi-Z materials are advantageous for stopping γ radiation in short distances. †TRIGA – (Training, Research, Isotopes, General Atomics) is an inherently stable reactor design in part due to the zirconium metal-hydride/uranium composition of its fuel.

SELECTED CONCEPT: RADIOISOTOPE POWERED THERMAL PENETRATOR

The problem statement specified a need for a solution that could offer leap-ahead capabilities to counter current and future DBHT targets. Evaluations of both historical and novel hard target defeat alternatives lead to the selection of a thermal subterrene as a possible means of providing such a capability. As previously discussed, the evaluation of a number of different configurations for a thermal subterrene resulted in the specification of a RadioIsotope Powered Thermal Penetrator (RIPTP) as the preferred concept.

System components

The term “RIPTP Munition” is used to denote the RIPTP proper along with the other integrated munition components necessary for employment of a RIPTP against a DBHT. The baseline RIPTP Munition is envisaged as consisting of the following primary components (Figure 25): 1) the thermal penetrator (RIPTP); 2) the aeroshell; and 3) a tail-kit. The aeroshell and tail-kit would serve a number of synergistic purposes, one of which would be to serve as a vehicle for delivering the thermal penetrator to a precise aim-point at the target with sufficient velocity and appropriate incidence for the thermal penetrator to kinetically penetrate into the surface overlying the DBHT. The aeroshell and tail-kit would separate from the kinetic penetrator upon impact with the surface.

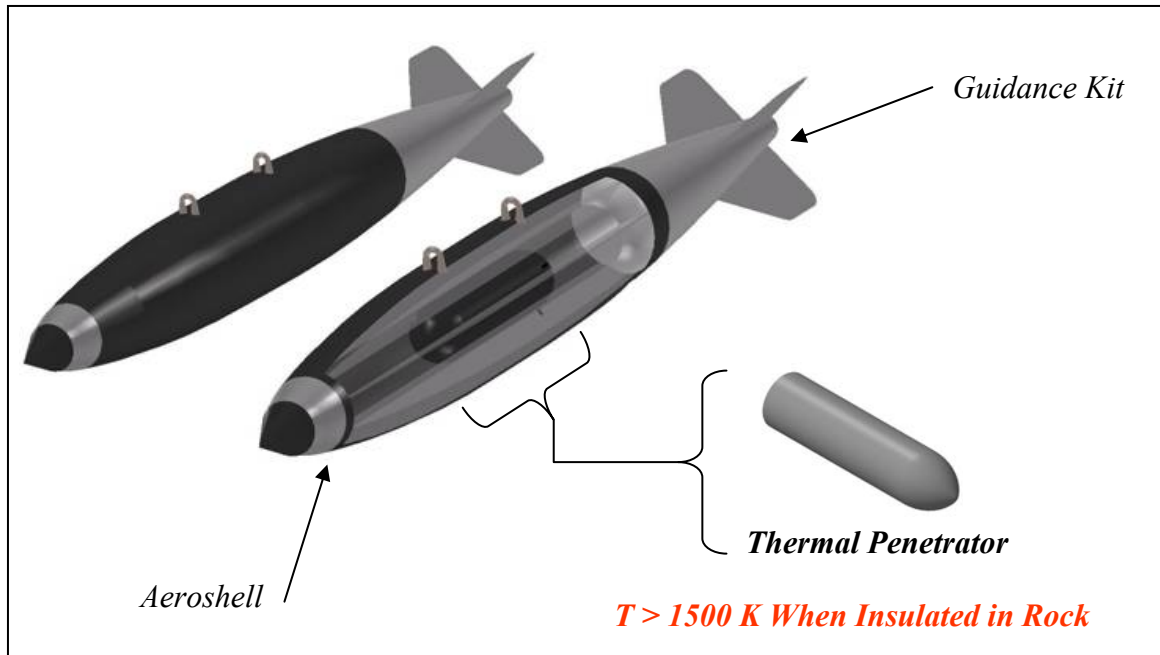


Figure 25: Notional integration of RIPTP Munition components

The aeroshell containing the RIPTP would be a means of providing a number of necessary functions. First, it may be desirable to make use of an existing guidance system with minimum modifications. As RIPTP thermal penetrators are likely to be smaller and much denser than existing guided high explosive or penetrating bombs, an aeroshell may be desirable to approximate the aerodynamic and center-of-gravity characteristics of the munitions the guidance system was originally designed for. Secondly, the aeroshell can serve as a thermal management system for rejection of heat from the thermal penetrator. Heat rejection requirements for lower power thermal penetrators would be consistent with use of an evaporative cooling system, with radiative cooling from the aeroshell surface as a redundant/back-up cooling mechanism. Thirdly, off-nominal ground impact scenarios can increase the risk of release of radioisotope from the penetrator due to impact damage to the containment system – an aeroshell could be designed to serve as an impact energy absorbing structure with engineered crush zones to reduce maximum loads

on the penetrator during oblique impacts. Finally, a concern for radioisotope containment on the battlefield will be ballistic damage from warheads and projectiles – the aeroshell can serve as additional ballistic protection to reduce the likelihood of penetrator damage leading to radioisotope release.

Like the aeroshell, the tail-kit would likely serve multiple functions besides providing guidance. Nuclear bombs have historically incorporated parachutes deployed in off-nominal aircraft separation situations to mitigate the likelihood of their catastrophic damage from impact with the ground as well as to facilitate their recovery. A RIPTP tail-kit could incorporate similar features to mitigate the danger of penetrator damage through unintended ground impact. Also, a tail-kit could incorporate an emergency beacon to facilitate location of the penetrator in accident scenarios.

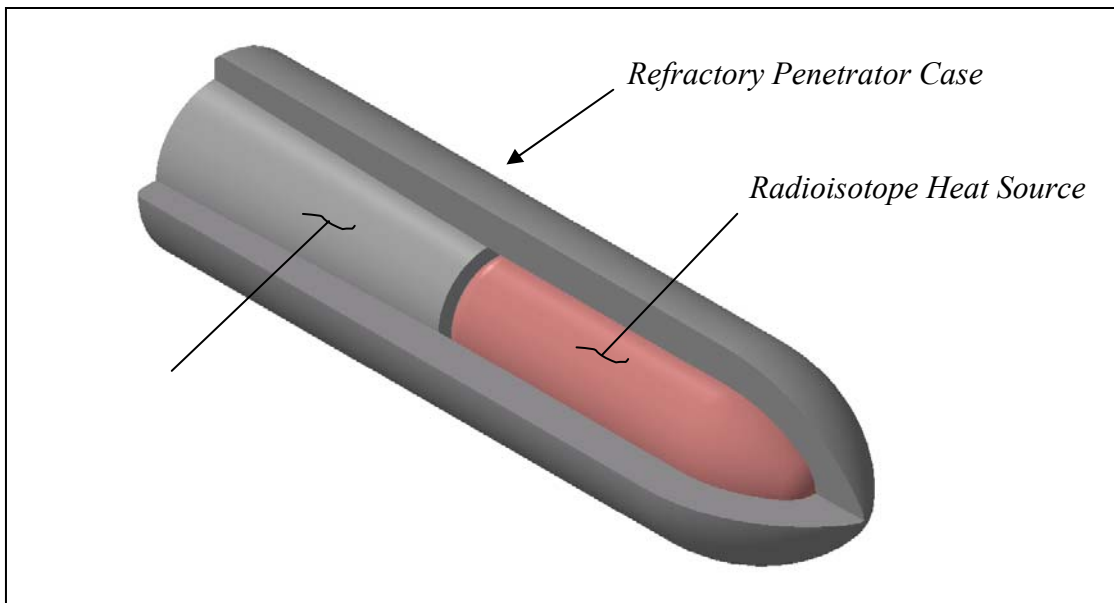


Figure 26: Notional RHS integration with refractory penetrator case

The thermal penetrator itself will be comprised of a Radioisotope Heat Source (RHS) which provides the power necessary to melt through rock, Figure 26. The RHS is

contained in a tough refractory shell which contains the RHS and enables kinetic penetration into the surface overlying the DBHT target so as to bring the penetrator into intimate contact with the hard rock in which the DBHT is emplaced.

The highest-risk concerns regarding the RIPTP concept's feasibility were expected to be production and employment of the RHS heat source in an operationally viable time-frame and for reasonable costs, as well as radiation safety concerns associated with using a RHS.

Concept of operation

The aeroshell is mated with a precision guidance kit to deliver the RIPTP to an impact point above a targeted DBHT (Figure 27, phase 1). Upon impact, the thermal penetrator separates from the aeroshell and kinetically penetrates the first few body lengths of rock or other material overlying the DBHT (2), after which it begins to melt its way down through the rock overlying the DBHT spaces (3). The penetrator descends in a nearly vertical path through the molten rock due to its much greater density (a factor of four or more) initially forming a melt shaft (4) which eventually begins to solidify behind the penetrator creating a melt-bubble (5).¹¹⁷ This melt bubble tends to pressurize due to a number of effects including thermal expansion of the surrounding rock, rock liquefaction expansion, volatile content of the rock, hydrostatic pressure, and rock ambient compressive stress.

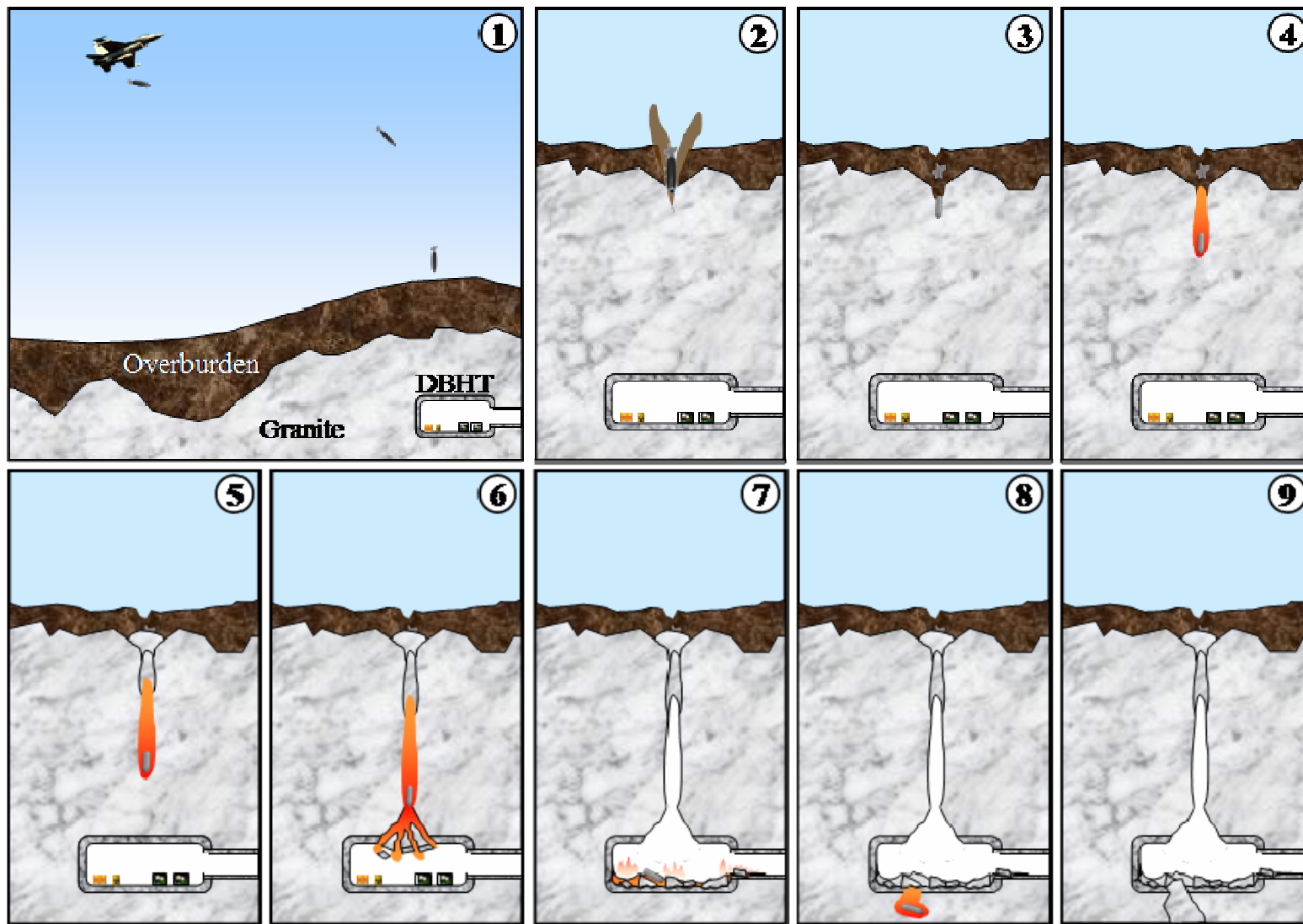


Figure 27: Sequence of events in RIPTP DBHT defeat

Melt-bubble pressurization together with rock thermal stress leads to extremely large total stresses in the surrounding rock – compressive stresses immediately around the cavity and large tensile stresses at greater distances. Induced tensile stresses result in fracture/breach of a DBHT ceiling or wall upon approach of the melt-bubble (6). Lethality against DBHT spaces results from the large quantities of thermal energy stored in the surrounding rock/melt which are liberated when a penetrator propagated melt-bubble breaches a DBHT ceiling or wall (7) contributing to initiation of confined space fires. Besides direct incendiary effect from the penetrator and molten rock, energy stored in the form of rock mechanical stress and melt bubble pressurization may be sufficiently large to make fracture of the DBHT ceiling and venting of the melt-bubble an explosive event. It is expected that a RIPTP would produce lethality mechanisms against a DBHT such as blast, crush, scald, fire, and smoke. Addition of reactive elements to a RIPTP penetrator (perhaps relatively low melt-temperature metals such as lithium, magnesium, and/or aluminum) that would be released shortly before, during, or after breaching of a DBHT space could further enhance lethality. After breaching a DBHT, it is expected that a RIPTP may continue to penetrate through the facility floor and bedrock beneath the DBHT (8-9) until power decays to a level such that it is insufficient for further thermal penetration (*post-9*). At this point the RIPTP will eventually become entombed in vitrified molten bedrock deep below the target DBHT. For the baseline RIPTP, it would become entombed on the order of several hundred meters below the DHBT, with maximum depth reached after about one year. Residual radioactivity of the entombed RIPTP decays exponentially. For the baseline design identified it decays at a high rate, with approximately 1/1000th of the radioactivity existing after 3.5 years and 1/10,000th

after 5.5 years. Creation of a long term environmental hazard in any scenario would be impossible due to the short half-life radioisotopes considered for a RIPTP.

Advantages of RIPTP concept

The chief advantages of the RIPTP concept are the ability to breach a facility at any depth, apparent mechanisms for lethality against deeply buried target spaces, minimal risk of collateral damage, and (unlike a surface or subsurface nuclear burst) no radiation hazard in nominal employment scenarios. Given the potential energy densities of radioisotope and fissile power sources, a thermal penetrator could conceivably attack the “super-hard” targets that exceed the defeat capability of even the most powerful nuclear weapons.¹ It can be argued that a pure thermal penetrator is the logical result of extrapolating the existing trend to ever lower yields for nuclear weapons that has been enabled by more accurate delivery capabilities. Thermal penetrators conceptually offer a possibility of a DBHT-lethal precision guided munition with zero explosive yield.

Performance concerns

A principle concern regarding RIPTP feasibility is the producibility of RHS heat sources in an operationally viable time-frame and for reasonable costs. Strong motivators exist for the selection of short half-life radioisotopes for an RHS, both for better thermal penetrator performance as well as radiological safety. However, selection of a short half-life radioisotope implies a very limited shelf-life for a RIPTP RHS once produced. Further, production of radioisotope to power an RHS can take a significant period of time depending on the radioisotope selected and reactor facilities used. Unless radioisotope to power a RIPTP RHS were continually being produced, significant lead times (on the

order of ten to one-hundred days) would be required for most radioisotopes prior to RHS/RIPTP availability for operational use. This of course would be a major potential impact on the operational viability of a RIPTP. For these and similar reasons it was necessary to evaluate the alternatives available for powering a RIPTP, their ROM cost, and the implications with respect to their production/employment timelines.

Safety concerns

A significant potential determinant of RIPTP viability is radiological safety. Exploring this issue was pursued through an effort to identify, prioritize, and analyze possible safety concerns that could pose a risk to concept viability with the aim of identifying “show-stoppers” that would likely render the concept non-viable.

An investigation of safety considerations was pursued in four steps: literature research of related topics such as historical high power RHSs, RTGs, and radiation sources and studies of their safety and accident history; enumeration of safety concerns; prioritization of safety concerns for investigation; and (to the extent possible with available resources) execution of rough analyses to investigate the potential hazard magnitude of the highest priority safety concerns. Potentially significant safety concerns were assessed in the context of existing alternative munition hazards and existing socially accepted radioisotope applications to arrive at an opinion regarding probable RIPTP operational viability with respect to safety.

THERMAL PENETRATOR PRIOR WORK

It is required that a doctoral thesis' contributions to the published body of knowledge be original and represent "either a substantial addition to the body of knowledge or a new and better interpretation of facts already known."¹¹⁸ The first step to establishing the originality of a work is necessarily a review of the existing body of knowledge to ascertain of what facts and theory that published body of knowledge is comprised. To this end, the literature pertaining to thermal penetration of rock and related topics was collected and reviewed. Given the collection of literature comprising the published body of knowledge, it was necessary to ascertain what if any aspects of the present work were novel additions to this body of knowledge (or a new and better interpretation of facts already known). By grouping prior work into categories of investigation, it can be ascertained that the existing work comprises an investigation of an entirely new category of system in the bodies of knowledge of both rock-melting thermal penetrators and DBHT defeat.

MORPHOLOGICAL CATEGORIES OF PUBLISHED THERMAL PENETRATOR LITERATURE

Thermal penetrators melt their way through material, accomplishing a phase change in the surrounding material by application of heat and displacement of the resulting melt. Such penetrators may either be self-contained (without external power or attachments)^{119, 120} or not,¹²¹⁻¹²⁴ and may be either tunneling (leaving a persistent tunnel)¹²¹⁻¹²³ or simply penetrating (leaving re-solidifying melt in their wake).^{119, 120}

The following categories of thermal penetrators may be found in the literature:

- Conventionally powered thermal penetrators for ice ^{120, 122, 123, 125}
- Fissile powered thermal penetrators of rock, both tunneling ¹²¹ and self-contained ¹¹⁹
- Self-contained nuclear waste powered penetrators (radioactive waste disposal) ¹²⁶⁻¹²⁹ The concept of using thermal subterrenes for disposal of high level nuclear waste in deep bedrock has recently been re-proposed in Europe with some new variations. ^{126, 127} Note that the general approach was investigated three decades earlier ^{128, 129} along with uncontained waste variants. ¹³⁰
- Conventionally powered thermal penetrators of rock for tunneling (not self-contained) ^{121, 123, 124}

Self-contained systems are generally synonymous with penetrating applications where the objective is transport of a body through a barrier. For equivalent penetration performance such systems require much higher energy-density power sources than are necessary for tunneling applications – hence chemical power sources are principally viable for self-contained ice penetration ¹²⁰ which requires lower power than penetration of rock. In order to be air-deliverable as a practical munition, a thermal penetration system for penetration through rock must be both self-contained and relatively compact. The energy density implied by these requirements dictates either a radioisotope or nuclear reactor power source. Nuclear waste and nuclear reactor powered rock penetrating subterrenes can be found in prior thermal penetrator literature (see listing of references associated with Figure 28). Non-radioactive-waste derived radioisotope powered thermal subterrenes cannot.

Further, thermal penetrators are not known in the facility-type hardened target defeat literature other than as a *conventionally*-powered *tunneling* method concept for delivery of liquid or gas defeat agents.¹²⁴

In conclusion, the RIPTP concept for DBHT defeat appears to be novel, at least as far as unclassified literature is concerned. Consequently, the solution of the multidisciplinary problems of identifying configuration specification, isotope selection, and sizing/analyzing the performance of a RIPTP is a novel contribution to the DBHT defeat literature.

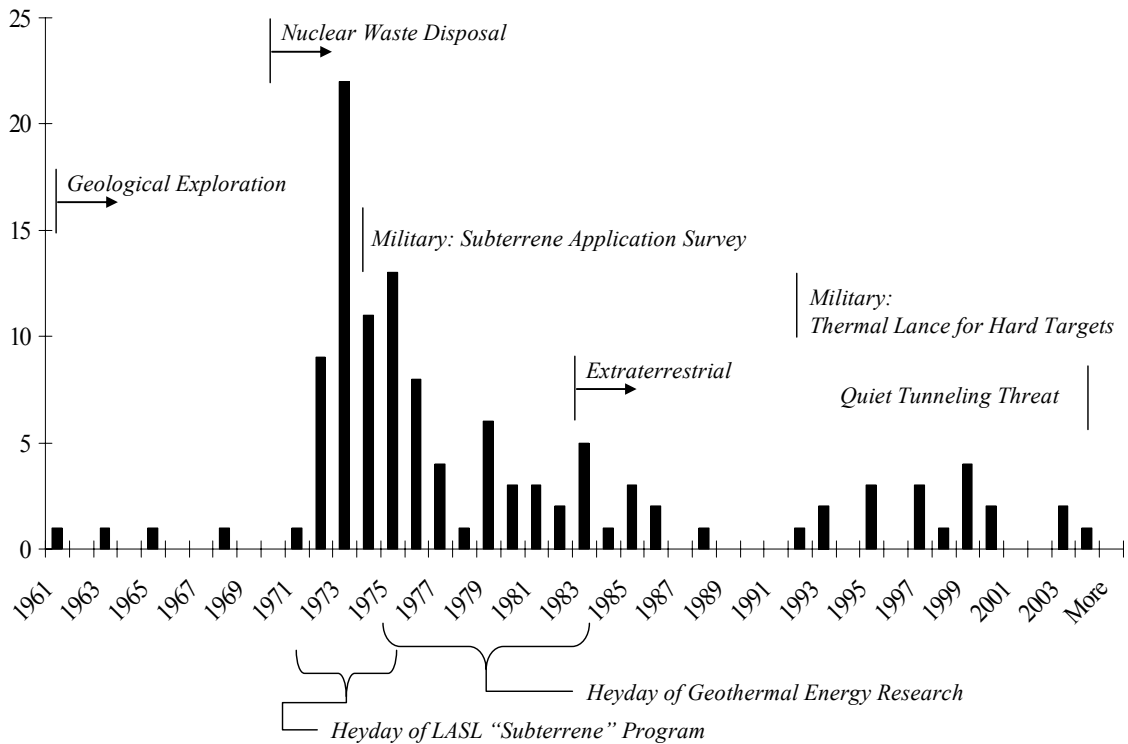


Figure 28: Thermal subterrene – a chronological history of some relevant prior work

A collection of subterrene related references^{131-180 181-230 231-250}; geological exploration^{191, 228, 231, 251}; nuclear waste disposal^{131-135, 138, 180, 218-221, 233, 235, 236, 240, 243}; nuclear (fissile) subterrene^{142, 148, 158, 159, 176-179, 215, 228, 230, 231}; LASL Subterrene Program^{134, 140-179, 181, 205, 222-225, 227}; geothermal energy research related^{162, 165, 166, 172, 181-185, 187-190, 192-194, 196-202, 204, 206-213, 242}; military subterrene/thermal penetrator including through-ice hydrophone deployment devices^{120, 124, 125, 164, 239}; extraterrestrial applications^{191, 215, 217}; quiet tunneling threat^{164, 239}; rock high temperature/melting material properties^{131, 137, 139, 149, 161, 169, 173, 174, 192, 201, 224, 240, 241, 248}; thermal penetrator material properties and compatibility^{136, 140, 141, 154, 157, 161, 175, 244}; close-contact melting^{143, 147, 163}

218, 219, 234, 236-238, 245-247, and subterrene thermal analysis^{143, 147, 150, 156, 163, 168, 169, 181, 218, 219, 229, 249, 250} (see also thermal subterrene design related documents).

PRIOR THERMAL PENETRATOR APPLICATION CATEGORIES

Figure 28 depicts a chronological history of literature relevant to rock-melting thermal penetrators. One way of grouping this literature is by the application considered – those identified from the literature were: geological exploration; geological sampling; tunneling/drilling into hard rock; nuclear waste disposal; geothermal well production; extraterrestrial exploration and construction; military drilling applications (such as a thermal lance for drilling into a bunker or similarly armored target; drilling of holes for emplacement of cratering or similar charges); production of drainage ducts for archaeological sites without site disruption; and nuclear proliferation risk analysis with respect to the potential for quiet tunneling into a nuclear waste repository.

Prior military thermal penetrator investigations in the literature

Only one published investigation of possible military applications for (electrically powered, non-self-contained) rock melting thermal penetrators was found in the unclassified literature (classified literature was not surveyed).¹⁶⁴ In this 1974 paper, the author Webster concluded “*in its present configuration and even with its projected capabilities, the subterrene does not meet a significant number of the drilling requirements of the Army.*” The potential requirements considered by Webster appear to have principally encompassed hole drilling requirements in rock for (among other things) emplacement of explosive charges. It does not appear from the survey that a possible application of a thermal penetrator (in any form) for DBHT defeat was considered.

NEW AREAS OF ENGINEERING ANALYSIS AS COMPARED TO PRIOR THERMAL SUBTERRENE LITERATURE

A substantial body of work is represented in the literature on a number of topics relevant to thermal penetrator engineering, including: calculation of thermal penetrator internal temperature distributions; heat transfer coefficients; rock penetration rates; refractory material compatibility with rock melt; refractory material fabrication methods for subterrene applications; nuclear reactor and electrical resistance heater powered thermal penetrator design and heating system integration; rock melt material characterization and chemistry; solidified rock melt material properties and chemistry; cost and economic analysis of various thermal rock penetrator systems; rock thermal fracture effected by a rock melting heat source, both stationary and moving; and high temperature heat pipe materials and design.

The most comprehensive and multidisciplinary treatise found regarding the design and analysis of rock melting thermal penetrator systems was published by Black, et al, in 1974.^{249, 250} Neither this nor any other literature found has investigated the problem of: selecting radioisotopes for powering a thermal subterrene given the problem requirements associated with defeat of a DBHT by a subterrene; analyzing and minimizing the extent of nominal and potential radiological hazard for a radioisotope powered subterrene; analyzing the performance of a neutron-activation manufactured radioisotope powered penetrator penetrating through rock; or analyzing rough cost/infrastructure feasibility for the same. Any work advancing the art in these areas constitutes a novel contribution to the body of knowledge of thermal subterrene engineering.

MULTIDISCIPLINARY ANALYSIS IMPLEMENTATION

A program was written in Matlab™ which (among other things) calculates: time-history of isotope transmutation/decay using numerical solution of the coupled Bateman Equations; sizing of a RIPTP based on user specified fineness and case thickness ratios, the available quantity of radioisotope, its density, and the packing efficiency of the target elements into the case; reactor neutron economy and (if necessary) adjustment of reactor precursor isotope load to that feasible; an estimate of RIPTP penetration rate as a function of time; ROM radioisotope costs; and calculated estimates of maximum steady state RIPTP core and case temperatures as a function of time for various scenarios. The code also plots various time-histories of interest from the data calculated. Data for granite thermal properties employed in calculations are included in “Appendix B – Properties of Granite vs. Temperature.” Data for thermal properties of case materials employed in calculations are included in “Appendix C – Thermal Conductivity of Representative Penetrator Materials.”

Important assumptions and calculations implicit to the development of the code are discussed in the following sections.

RIPTP RADIOISOTOPE PRODUCTION ASSUMPTIONS

Two routes are available for the production of radioisotope for a RIPTP – radioisotope production through neutron activation of stable isotopes, or the extraction of radioisotopes from nuclear waste (see “Appendix D – Radioisotope Production Background” for discussion on these options).

There are several important concerns common to any radioisotope extraction process from nuclear material. First of all, secondary radioactive waste is typically generated at every step of processing through contamination of equipment/materials with radioactive isotopes. Second, the processing of significant quantities of radioactive wastes is time consuming, hazardous, and expensive – particularly in the concentration and total activity required for a RIPTP RHS. Finally, if a short-lived radioisotope is desired, allowing the spent fuel to cool-down tends to limit the quantities of short-lived radioisotopes that are available for extraction at processing. Similar concerns exist for post-irradiation processing of bulk neutron-activated material.

For all of these reasons production of RIPTP RHS radioisotope via irradiation of isotope targets was assumed. The individual isotope targets are assumed to be pre-encapsulated and in final form for assembly of an RHS after irradiation in a reactor, without any requirement for post-irradiation chemical separation or enrichment of the radioisotope. This decision effectively eliminates all radioisotope candidates which are most competitively produced through fission reactions, but has good implications with respect to safety, cost, availability, required processing time, and overall environmental impact. A diagram of the assumed production approach is shown in Figure 29.

Production of a RIPTP would start with the fabrication of radioisotope production target elements consisting of individually encapsulated target isotope material. This material would be loaded into a target assembly which could be directly loaded into the reactor for irradiation. At this point two options are listed in Figure 29 for production of the radioisotope. The first is the continual production of radioisotope in a reactor in which radioisotope production targets are always kept in the reactor, and the second is

production of radioisotope on demand for which radioisotope targets would be loaded when an operational requirement for a penetrator is anticipated. Continual production is more suitable for radioisotopes that can be produced with required power densities from naturally abundant materials (for which target isotope material costs are low as compared to enriched isotope target materials).

Production on demand is likely to be operationally unsuitable for all but the most rapidly producible radioisotopes as too much time would elapse between identification of an operational need for a penetrator and penetrator availability. These rapidly producible radioisotopes generally require high enrichment extraction from the naturally occurring element and are likely to be costly.

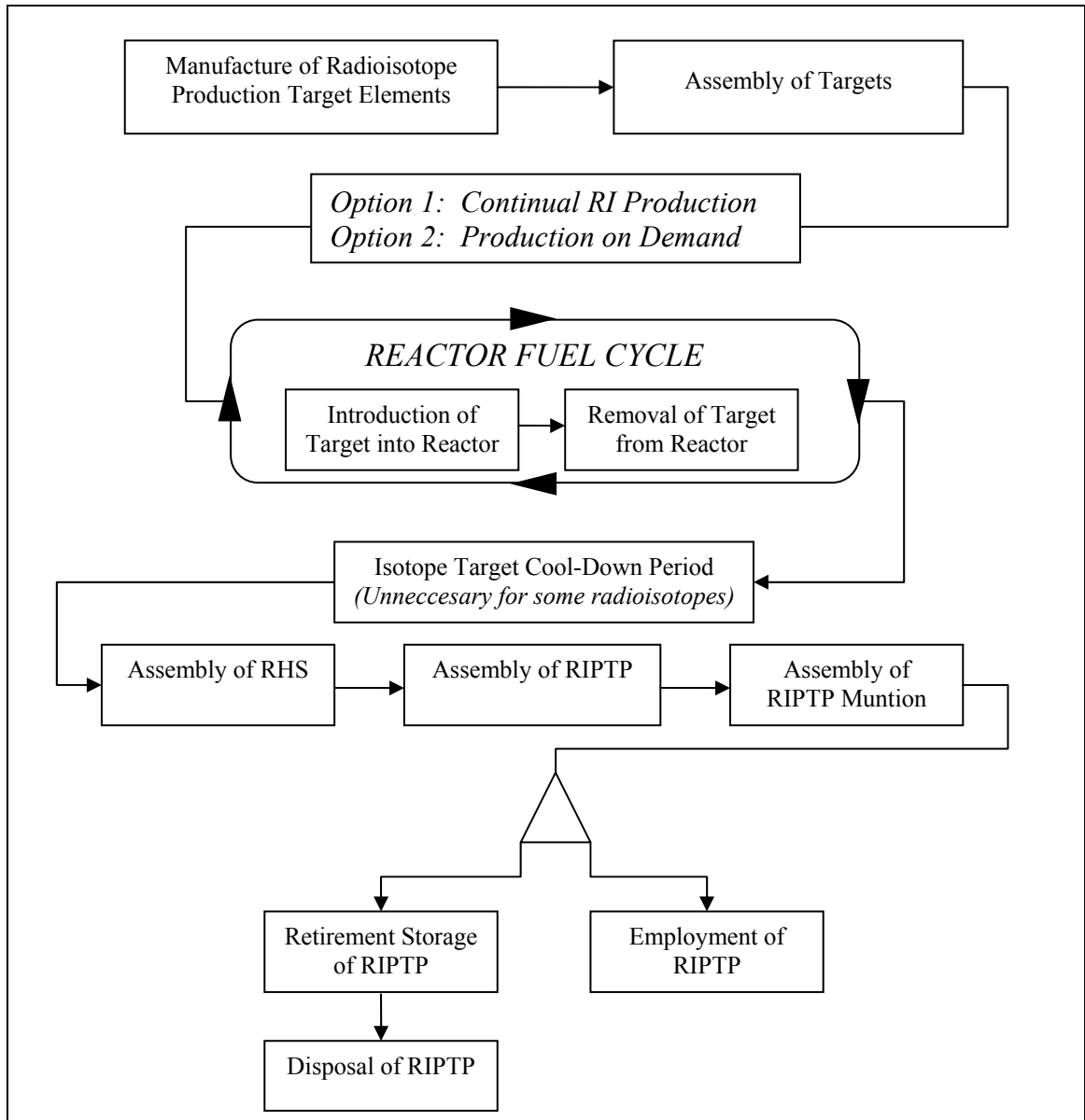


Figure 29: RIPTP life-cycle flow-chart

Regardless of the logistical production option chosen, after irradiation in the reactor the target assemblies would be removed from the reactor and the individual target elements extracted. These target elements would then be assembled into an RHS, the RHS integrated with the RIPTP, and the RIPTP integrated with the aeroshell and tail-kit components. At this point the RIPTP Muntion would be available for use.

Implications of assumptions

There are some significant production challenges implicit in a preference of a short half-life radioisotope and assumption of no post-irradiation processing that should be mentioned. Accumulation of significant quantities of a short half-life radioisotope in high concentrations requires a high rate of transmutation of the target isotope, as radioisotope decay competes with production. The rate of production of radioisotopes is determined in part by the neutron capture cross section of the target isotope, and so a high rate of radioisotope production implies a large capture cross section.

A large neutron capture cross section has two major consequences. First of all, isotopes with very large neutron capture cross-sections tend to be of low natural isotopic abundance when multiple stable isotopes of an element exist. As a result, production of the radioisotope in the concentration and quantity required is likely to require an enriched isotope target. This can potentially be very costly, but might allow production of a RIPTP RHS in a very short period of time, enabling the option of RIPTP production on demand. Second, a radioisotope production target material composed of high concentration/high neutron capture cross-section (σ_c) isotope will be largely opaque to neutrons due to “self-shielding” of the target isotope. Achieving maximum final concentration of radioisotope requires that the precursor isotope in the target be as evenly converted to radioisotope as possible. As a result, the higher the σ_c of the material, the thinner the maximum allowable target element thickness will be.

To assess the impact of self-shielding, it was assumed that: the isotope targets were immersed in a uniform isotropic bath of neutrons all traveling at a speed equal to the mean speed of thermal neutrons; neutron scattering effects were negligible as compared

to absorption; and that the targets were homogeneous. Neglect of scattering is a reasonable approximation when a target material's absorption cross section is much larger than its scattering cross section and thermalization of epithermal neutrons in the target is unimportant (Thulium-169, for example, has a thermal neutron capture cross section of 113.2 barns and a scattering cross-section of only 6.3 barns²⁵²).

In the case described above (that of an absorbing body immersed in a uniform isotropic neutron bath) it has been shown that the solution to this problem is directly related to the problem of finding the neutron escape probability, P_0 , for a body of identical geometry and capture cross section, but having a uniform internally distributed source of isotropic neutrons.²⁵³ For this problem, it has been shown that the neutron escape probability P_0 is equal to the ratio of the average neutron density in the body to the neutron density at a location far from the body in the problem of a body immersed in an isotropic neutron bath. As the speed of all neutrons is assumed to be equal, P_0 is equivalent to the ratio of the average neutron flux in the body to the unperturbed far-field flux in the moderator. Thus, P_0 provides an approximate self-shielding correction factor for the rate of isotope production.

The principle geometries considered for the isotope target element are illustrated in Figure 30. Case, Hoffman, et al's work lists tabulated values of P_0 vs. characteristic dimension for the body in mean free paths for spheres, wires, and slabs (plates).²⁵³ As can be seen from Figure 31, a sphere provides the largest form with the least reduction in average internal flux.

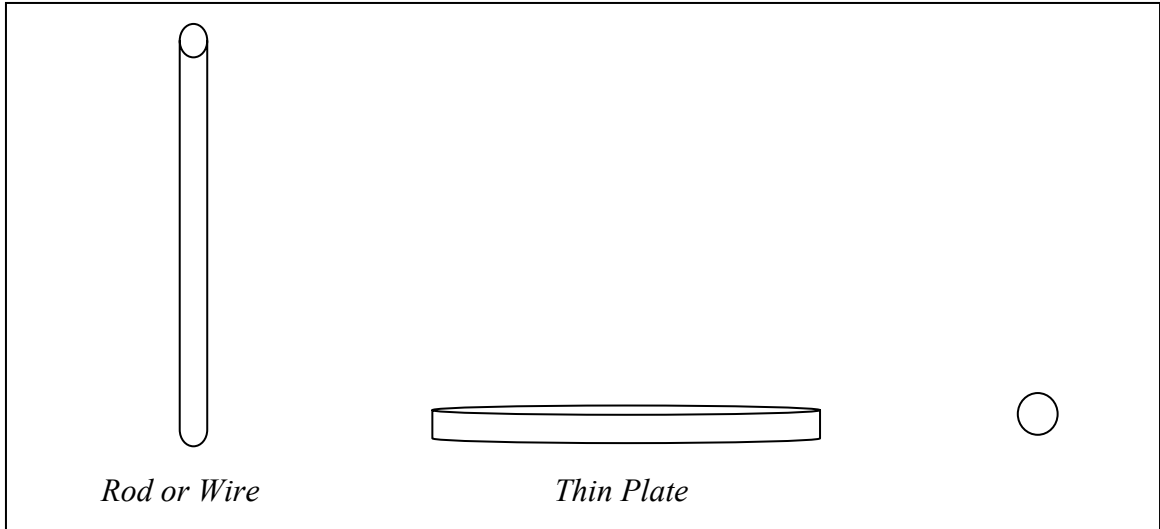


Figure 30: Principle geometries considered for target elements

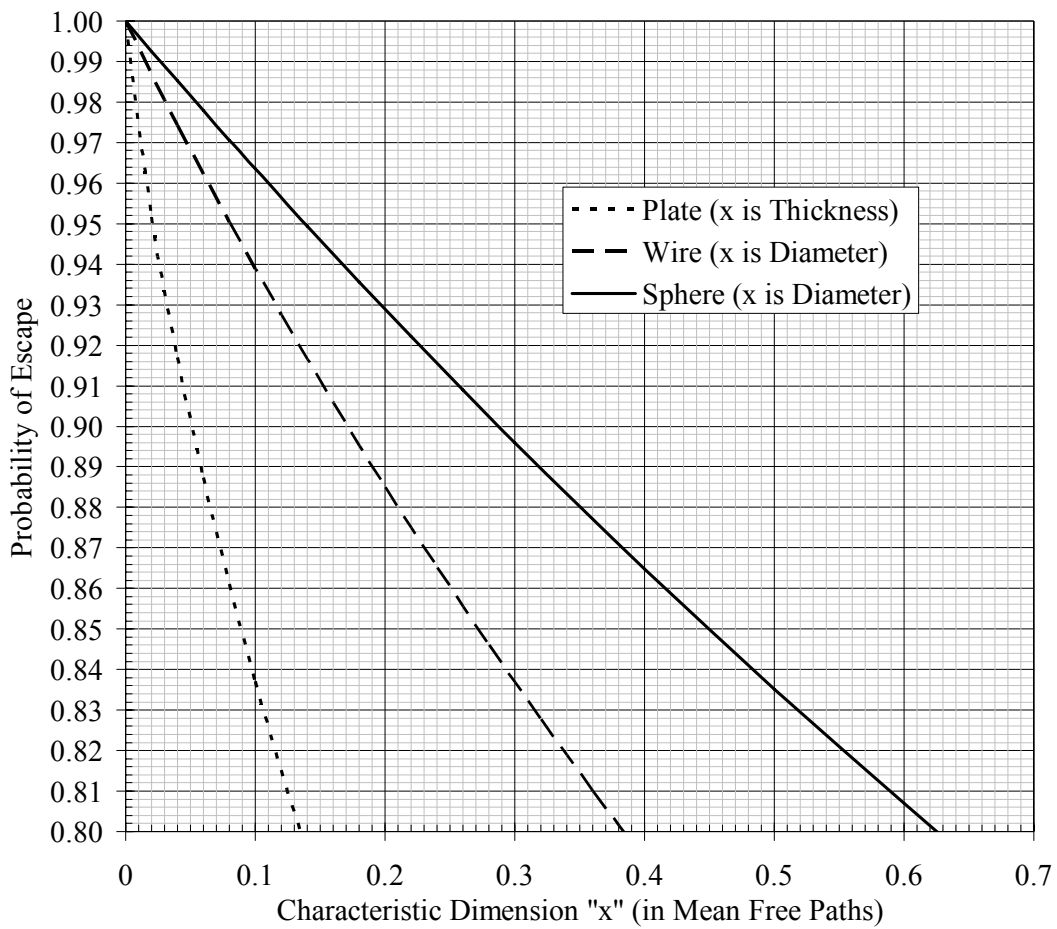


Figure 31: Average internal flux for an isotope target form vs. its characteristic dimension

Table 25: Maximum characteristic dimensions allowable for isotope forms to achieve various mean internal fluxes

P_0	Plate or Slab Thickness/ l	Wire Diameter/ l	Sphere Diameter/ l
.95	.02	.08	.14
.90	.05	.17	.29
.85	.09	.27	.45
.80	.14	.39	.63

The mean free path of a neutron in a medium, l , is just the inverse of the total macroscopic cross section for neutron interaction with the medium. For $^{169}\text{Tm}_2\text{O}_3$ the total macroscopic cross section to thermal neutrons, Σ_t , is given by the equation below, and is approximately 3.34 cm^{-1} . In the equation: Av is Avogadro's Number; MW is molecular weight; ρ is density; and σ_t is the total microscopic cross section. This corresponds to a thermal neutron mean free path of three millimeters. Similarly for $^{168}\text{Yb}_2\text{O}_3$, a compound of another isotope of interest, the mean free path in the isotopically pure compound is about .15 millimeters. Thus, a plate of $^{169}\text{Tm}_2\text{O}_3$ having a mean internal flux that was 80% that of the ambient flux in the moderator could be no thicker than four-tenths of a millimeter, whereas a sphere with the same average internal flux would be about 1.9 mm in diameter. The corresponding numbers for a target of $^{168}\text{Yb}_2\text{O}_3$ would be $1/50^{\text{th}}$ of a millimeter for a plate target and .1 mm for a spherical target.

$$\Sigma_t = Av \cdot MW_{\text{Tm}_2\text{O}_3}^{-1} \cdot \rho_{\text{Tm}_2\text{O}_3} \left(2\sigma_{t,^{169}\text{Tm}} + 3\sigma_{t,^{168}\text{O}} \right) \cdot 10^{-24}$$

Thin plates have historically been commonly used for production of high power density RHS/radiation-sources for materials with high σ_c . Thin plates stack densely and thus tend to provide good volume filling as well as good surface contact for heat transfer. However, the maximum allowed thickness for the isotopes considered is on the order of a millimeter, and the isotope will almost certainly be in a ceramic form. This results in

concerns regarding the frangibility of/production of fines from a plate form. Further, the concept of redundantly encapsulating the target element with a refractory coating or clad material is attractive. This is because such a coating or cladding could tend to reduce the likelihood of release of fines from the target element during post irradiation processing or in the event of a breach of the RIPTP casing. For some radioisotopes such cladding could further serve as a redundant radiation shield to reduce radiation emission in the event of RIPTP case breach.

A thin target form such as a plate could result in a greater likelihood of the cladding being compromised by mechanical damage. For this reason a spherical bead may be the best choice for target element geometry. Reduction in packing density and poor thermal conductivity might be corrected either by compaction at elevated temperatures of the target elements in the RHS casing, or by embedding of the activated beads in a high conductivity filler such as a refractory metal (thus forming a cermet).

Regardless of the target element geometry selected it is apparent that it would be necessary to augment the bulk thermal conductivity of any sintered ceramic used. This would be necessary to prevent the melting of the inner radioisotope core in some scenarios. Increasing bulk thermal conductivity was determined to be achievable with a modest addition of a higher thermal conductivity refractory metal, or a somewhat larger portion of conductive refractory nonmetal such as graphite. An increase in bulk conductivity of the RHS core material to approximately 20 watts/cm² K is assumed. To accommodate cladding volume a factor of .9 was used for the ratio of isotope material volume to total target element volume. To accommodate reduction in usable RHS volume due to maximum achievable packing density/filler a factor of .74 was used for the ratio of

usable target element volume to total RHS volume. This factor (74%) corresponds to the maximum theoretical packing efficiency factor for spheres of uniform size. Multiplying both assumed factors, the volume fraction of the ceramic isotope material was taken to be 66.6% of the total available RHS volume.

POSSIBLE REACTOR FACILITIES FOR PRODUCTION OF RADIOISOTOPE CONSIDERED

In order to evaluate the feasibility, cost, and time required for production of a RIPTP RHS, the reactor facilities that might be used for radioisotope production were investigated. These facilities fall into the following categories: high thermal-flux isotope production reactors; commercial power reactors; and a hypothetical new reactor for radioisotope production.

High thermal-flux reactors are attractive for radioisotope production as the rate of transmutation of an isotope is proportional to the neutron flux and macroscopic neutron capture cross-section of the isotope production target, and isotopes generally have their highest neutron capture cross sections at the lower energies of the thermal neutron spectrum. A high neutron flux is also advantageous for producing the maximum atom-density of a radioisotope in a target.

The two high flux reactors investigated (HFIR and ATR) are government operated, one of their principle missions being the production of neutron sources used for the start-up of naval nuclear reactors. Although high thermal-flux reactors offer high rates of production of radioisotope, they are typically lower power than commercial power reactors, which tends to limit the maximum quantity of target material that can be placed in the reactor without preventing the reactor from becoming critical. They also

have smaller cores with more limited volume available for the insertion of isotope production targets. A further potential drawback is that their strategically critical mission of neutron source production would be a strong competitor for other major isotope production missions unless of competitive national importance.

High Flux Isotope Reactor

The High Flux Isotope Reactor (HFIR) is part of Oak Ridge National Laboratory (ORNL). The HFIR core is cylinder shaped with the fuel comprising concentric inner and outer arrays of involute shaped highly enriched uranium (U_3O_8 —Al cermet) fuel plates. The center of the cylindrical core is a large flux trap. Outside of the cylindrical outer fuel region are annularly disposed control plates surrounded by a one-foot thick beryllium reflector. The reactor can achieve a maximum flux of approximately $2.6 \cdot 10^{15}$ neutrons/cm²-sec, and has a maximum operating thermal power of 100 Megawatts (MW_{th}) derated to 85 MW_{th} . The fuel cycle for HFIR is typically 23 to 27 days of operation followed by 4 to 7 days of down-time for refueling.^{254, 255}

Advanced Test Reactor

The Advanced Test Reactor (ATR) is part of Idaho National Laboratory (INL). ATR utilizes highly enriched uranium fuel plates in a serpentine core design. ATR's core incorporates five lobes in a clover-leaf arrangement (with a central lobe) with the power of each lobe individually tailorable. The reactor can achieve a maximum flux of approximately 10^{15} neutrons/cm²-sec, and has a listed maximum operating power of 250 MW_{th} . Although listed as 250 MW_{th} , a more typical operating power for ATR is about 110-120 MW_{th} total (with a maximum of about 25 to 30 MW_{th} in a single lobe) and a

thermal neutron flux of approximately 5×10^{14} neutrons/cm²-sec. The fuel cycle for ATR is typically 49 days of operation followed by one to two weeks of down-time for refueling (although there are occasional two-week periods of high-power operation), with a typical 7 fuel cycles per year. Though it has a lower maximum flux attainable than HFIR, ATR is in some ways more attractive as it can tolerate a greater quantity of negative reactivity and could thus accommodate more target material at one time. It also has a greater internal volume for accommodation of target assemblies.²⁵⁶

Commercial Pressurized Water Reactor

Pressurized Water Reactors (PWRs) are widely used in the United States for the commercial production of electric power. PWRs have a typical thermal neutron flux of 3×10^{13} neutrons/cm²-sec, and typically operate at around 3000 Megawatts of thermal power. Their lower flux and larger thermal power means that they can accommodate *much* greater quantities of isotope target material, although they of course produce lower maximum concentrations of isotope and take longer to reach this maximum concentration.

Hypothetical new reactor

Prior RHS production studies have proposed the construction of a new high thermal flux reactor with a thermal power of approximately 3000 Megawatts and a neutron flux on the order of 10^{15} neutrons/cm²-sec, with isotope production costs defrayed through the sale of waste heat for operation of a salt-water desalination plant. The fabrication and operation of such a reactor would cost over 10 billion dollars (2003

Yr\$) over its assumed operational life of 30 years. The levelized annual cost for such a facility including capital recovery has been estimated at \$403 Million (2003 Yr\$).²⁵⁷

Moth-balled isotope production reactors

Reactors with comparable characteristics to the hypothetical reactor discussed above have historically been operated by the DOE, but the author is unaware of any still operational. It is possible some may be moth-balled and could be reactivated, as an in depth investigation of national nuclear weapon program legacy isotope production facilities/capabilities was not performed. A prime candidate for the location of such a reactor if it does exist would be at DOE’s Savannah River Laboratory (SRL).

CALCULATION OF RADIOISOTOPE PRODUCTION – BATEMAN EQUATIONS

The rate of production of an isotope i , $\frac{dN_i}{dt}$, accounting for transmutation from isotope $i-1$ and transmutation to isotope $i+1$ as well as the rate of decay of isotope i , may be written as $\frac{dN_i}{dt} = N_{i-1}\sigma_{i-1}\Phi - N_i\sigma_i\Phi - N_i\frac{\ln(2)}{t_{1/2i}}$. In this equation σ denotes the respective neutron capture cross sections of the isotopes, Φ the neutron flux, and $t_{1/2i}$ the half-life of decay.

For a system of n isotopes this may be rewritten as the linear system of differential equations $\dot{N} = AN$ and solved in the standard way for initial conditions $N(t=0) = [N_1; N_2; \dots; N_n]$ Where $N(0)$ corresponds to the initial population of all isotope

species. The solution to this system of equations is generally known as the coupled Bateman Equations.

The appropriate values of neutron capture cross-section and isotope half-life (when available) were looked up in the online databases maintained by Brookhaven National Laboratory (BNL).^{258, 259}

CALCULATION OF RADIOISOTOPE THERMAL POWER

The power P generated by an initial quantity of N_0 atoms of isotope through decay is $P = N_0 \left(e_{decay} \cdot \frac{\ln(2)}{t_{1/2}} \cdot e^{-\frac{t \cdot \ln(2)}{t_{1/2}}} \right)$, where e_{decay} is the quantity of extractable energy released per disintegration (obtained from Medical Internal Radiation Dosimetry database/MIRD).

At a particular time for N atoms this is $P = N \cdot e_{decay} \cdot \frac{\ln(2)}{t_{1/2}}$.

CALCULATION OF RIPTP INTERNAL VOLUME

The simple symmetric geometry assumed for analysis of a RIPTP was that of a cylinder of radius r_{RIPTP} with two hemispherical end caps, also of radius r_{RIPTP} . This pill-shape defined the outer moldline of a refractory metal shell of constant thickness T , within which was the RHS. The RHS was assumed to occupy all available volume inside the refractory shell. RIPTP overall length is denoted by L .

The fineness ratio f is defined as $f = L/2r_{RIPTP}$, and was assumed to be equal to four for the baseline penetrator. A case thickness factor was defined as $t = \frac{T}{\frac{1}{2}d}$ and was assumed to .4. As a result, the radius of the RHS was specified as $r_{RHS} = (1-t) \cdot r_{RIPTP}$

Using the quantities defined above, RHS volume was calculated as

$$V_{RHS} = \frac{4\pi}{3} r_{RHS}^3 + \pi \cdot r_{RHS}^2 \cdot (2 \cdot f \cdot r_{RIPTP} - 2 \cdot r_{RIPTP})$$

RIPTP total volume was calculated as

$$V_{RIPTP} = \frac{4\pi}{3} r_{RIPTP}^3 + 2\pi \cdot r_{RIPTP}^3 \cdot (f - 1)$$

and RIPTP case volume was calculated as $V_{CASE} = V_{RIPTP} - V_{RHS}$

CALCULATION OF REACTOR NEUTRON ECONOMY

An important consideration in the bulk production of radioisotopes in a nuclear reactor is the reactor's neutron economy. Isotope target material inserted into a reactor is intended to absorb neutrons for the production of radioisotopes. However, if the target materials ability to absorb neutrons exceeds the ability of the reactor to produce neutrons, the reactor cannot sustain a nuclear chain reaction (initial become and/or remain critical). As it may be physically possible to load far more isotope target material into a reactor than the reactor can accommodate and still become critical, neglecting the neutron economy of a reactor can lead to large overestimations of the quantity of radioisotope producible in a reactor.

One simplistic approach to approximating this limitation on isotope production is by calculating the total rate of production of neutrons by a reactor and estimating the

portion of these neutrons that are available for isotope production. On average, the fission of a ^{236}U nucleus (following capture of a neutron by a ^{235}U nucleus) produces about 200 MeV of extractable thermal energy and 2.4 neutrons. Of the 2.4 neutrons produced, one of the neutrons from each fission must on average cause the fission of another nucleus for criticality to be sustained. Some portion of the remaining 1.4 neutrons per fission excess to the chain reaction can be assumed available for production of radioisotope. Thus, the rate of production of neutrons available for isotope production, $\frac{dN_v}{dt}$, may be estimated by the equation below, where e_f is the recoverable energy released per uranium-236 fission, $P_{thermal}$ is the thermal power of the reactor, n_f is the average number of neutrons produced per fission; and η_v is the fraction of excess neutrons that are available for isotope production.

$$\frac{dN_v}{dt} = P_{thermal} \cdot \frac{1}{e_f (n_f - 1) \cdot \eta_v}$$

This estimate, calculated for a reactor operating at a given power, is then compared to the estimated maximum rate of absorption of neutrons in a target assembly exposed to a specified neutron flux. If the rate of absorption of neutrons at any time exceeds the rate of production of available neutrons, the quantity of target material is excessive. The mass of isotope in the target is then adjusted by multiplying the originally assumed isotope mass times the ratio of the calculated rate of available neutron production to the maximum rate of neutron absorption by the target. Thus, the peak rate of neutron absorption by the adjusted target will not exceed that allowed by reactor economy at any point during its irradiation.

CALCULATION OF NUMBER OF RIPTPS PRODUCED

Given calculated reactor neutron economy compliance of the quantity of radioisotope production target material, two options were implemented in the RIPTP analysis code for sizing the RIPTPs produced from the irradiated target material.

The first option allows the user to specify the diameter, fineness ratio, and case thickness factor of a RIPTP. The code then calculates the number of RIPTP RHS volumes which could be filled with the total volume of irradiated target material available inflated by the packing efficiency.

Alternatively, the user can specify the fineness ratio and RIPTP case thickness factor along with a guess as to RIPTP diameter. After calculating the total volume of RHS material available the code will then adjust the RIPTP diameter so that RIPTP RHS volume matches the volume of the available RHS filler material. User specified fineness ratio and case thickness factor are maintained.

CALCULATION OF ROUGH ORDER OF MAGNITUDE RADIOISOTOPE COSTS

Radioisotope ROM costs were estimated for the purpose of comparing various alternative radioisotopes. Radioisotope costs were considered to consist of three principle components: precursor isotope material cost; cost of enriching the raw precursor isotope material (if required); and the cost of irradiating the target assemblies in the reactor. In most scenarios it is likely that the latter two components will dominate isotope production costs. In scenarios where enrichment is not required, target irradiation costs will dominate ROM cost.

The various enrichment technologies that might be used for enriching/depleting candidate radioisotopes were surveyed and a brief discussion of their characteristics is included in “Appendix E – Isotope Enrichment Technologies.” The principle conclusion from this survey was that technologies with the highest known technology readiness level for enrichment of the interesting precursor isotopes are nonviable for RIPTP RHS production. As discussed in the appendix, however, it appears possible that enrichment at moderate costs may be achievable with relatively little investment using existing gas-centrifuge or gaseous diffusion facilities. Alternatively, advanced technologies such as SILEX or AVLIS might offer a means for producing highly enriched isotopes at moderate costs, but Technology Readiness Levels (TRLs) are lower and probable technology investment costs and lead times for technology development are correspondingly longer. Costs of isotope enrichment were only considered qualitatively in estimation of ROM costs as insufficient resources were available for further investigation of enrichment technology alternatives, and the order of magnitude of potential enrichment costs was so uncertain.

Costs for irradiating the target assemblies in a reactor were estimated on the basis of two different scenarios. The first scenario considered was irradiation in one of ATR’s core flux-traps. ROM costs per year for space in a flux-trap is approximately three million dollars (2003Yr\$). The second scenario considered was irradiation in a new high-flux isotope production reactor. Cost estimates were found in two 1991 studies by Lawrence Livermore National Laboratory (LLNL) for such a reactor, and were adjusted to 2003 year-dollars using the Producer Price Index (PPI).²⁶⁰

As a check on both of these estimates, price estimates for radioisotopes from a Pacific Northwest Laboratory (PNL) report from 1973 were consulted after being adjusted by the PPI, and were found to be roughly consistent with the author's results.²⁶¹ PPIs used in adjusting isotope prices to 2003 year-dollars are listed in Table 26, below, along with comparison data used to check the price estimate obtained.

Table 26: Producer price indices and historic radioisotope costs

Year	PPI	PNL \$/gram ¹⁷⁰ Tm	LLNL \$/gram ¹⁷⁰ Tm*	ASDL \$/gram ¹⁷⁰ Tm [†]
1973	45.0	136 ²⁶²		
1991	116.5		587 to 881, ²⁶³ 270 ²⁵⁷	
2003	138.1	(417)	(696 to 1044, 320)	821

* Number quoted is for a new 3000MW_{th} high-flux isotope production reactor with assumed 30 year operational life and no other cost-defraying customers, \$/gram calculated from report using a factor of 11.7469 watts/gram; † Calculated for production at ATR using 49 day fuel cycle, 5.25" diameter flux trap, 30 MW_{th} node power, and ~3*10⁶ 2003Yr\$/year for flux-trap.

Costs for production in a commercial power reactor were not estimated, but are expected to be considerably lower than costs for production in an isotope production reactor. This is because isotope production reactors typically do not defray costs through the generation and sale of electricity (or waste heat as proposed in the LLNL studies).

DETERMINING PENETRATION RATE AND SURFACE TEMPERATURE AS A FUNCTION OF POWER

The physical class of problem to which a RIPTP melting through granite belongs is known in the literature as "close-contact melting." A good survey paper on close-contact melting has recently (1999) been presented by Fukusako et al.²⁶⁴ Other relevant phenomenology discussed in the literature includes characteristics of melt flow and melt-shaft/melt-bubble formation.^{117, 129, 265} Much work on close-contact melting has also been

performed in relation to analysis of Phase Change Material (PCM) energy storage systems which store energy through undergoing state transformations (solid to liquid and back).

Model used for preliminary analysis

The problem of close-contact melting in the context of calculating RIPTP performance is essentially that of calculating penetrator surface temperature vs. penetration rate and the associated thermal power required. For the definition of the baseline RIPTP, the author formulated a simplistic analytical model for power required vs. penetration rate which is discussed below. For the purpose of identification of potentially enabling technologies, the multidisciplinary analysis was updated to include an analytical solution of close-contact melting from the literature.

For a penetrator-fixed reference frame, the power required can be considered as that needed to transform the mass flow of the approaching granite column in front of the penetrator from a solid at ambient temperature to a liquid at the granite melt temperature. This total power can be broken into three components. Power required to: raise the mass flow to the melting temperature (capacitive power); liquefy the mass flow (liquefactive power); and overcome conduction losses into the surrounding granite (conductive power). Penetration power required for temperature increase and liquefaction as a function of penetration velocity is given below, where the terms are the change in enthalpy for liquefaction, the heat capacity, the temperature change, the granite density ρ , the penetration velocity V , and the melt shaft radius r_m .

$$P_{c,l} = (h_{sf} + c \cdot (T_m - T_\infty)) \cdot \rho \cdot \pi \cdot V \cdot r_m^2$$

Consider the two hypothetical steady-state extremes of zero penetration rate – where the temperature at the penetrator surface is just below that of the melting temperature of granite – and the opposite extreme of penetration rate very large with respect to thermal diffusivity. In the first extreme the power required for melting granite at an infinitesimally small rate is just the power lost through conduction from the penetrator surface in an infinite medium when the surface is at granite melting temperature. Assuming a spherical penetrator and temperature independent thermal conductivity for simplicity, this conduction power loss can be obtained from available steady-state analytical results of conduction in an infinite medium.²⁶⁶ In this case the conduction power loss is given by the equation below, where r_{RIPTP} is the radius, k the conductivity, T_0 the temperature of the sphere's surface, and T_∞ the temperature of the medium at infinity.

$$P_k = 4\pi \cdot r_{RIPTP} \cdot k \cdot (T_0 - T_\infty)$$

For very small penetration velocities, the total power required for melting will thus approach (for a sphere):

$$P = (h_{sf} + c \cdot (T_m - T_\infty)) \cdot \rho \cdot \pi \cdot V \cdot r_m^2 + 4\pi \cdot r_{RIPTP} \cdot k \cdot (T_0 - T_\infty)$$

Conversely penetration rate may be optimistically calculated as

$$V = \frac{P - 4\pi \cdot r_{RIPTP} \cdot k \cdot (T_0 - T_\infty)}{(h_{sf} + c \cdot (T_m - T_\infty)) \cdot \rho \cdot \pi r_m^2}$$

In reality penetration rate will potentially be lower due to the impact of viscosity on the flow of melt around the penetrator and thermal/liquefaction expansion of the penetrated material.

Close contact melting analytical solutions: Stoke's Problem with melting

A number of references with methods for calculating penetration rate and power for various geometries of close contact melting of PCMs are available in the literature. Among others, the papers of Fomin, Yaojiang, Kascheev, and Emerman were reviewed.^{117, 247, 267-269} The Fomin (et al) paper is a recent analysis of close contact melting penetration of a phase change medium with non-linearly temperature dependent properties, Yaojiang (et al) give a generalized analysis of close-contact melting which tie together several prior analyses, and Emerman and Kascheev provide similar analyses with density change of the phase change medium due to melting considered by Kascheev. Figure 32 illustrates the problem considered of a sphere of radius R melting its way through a PCM with velocity V , melt boundary layer thickness δ , and melt streamwise flow velocity u .

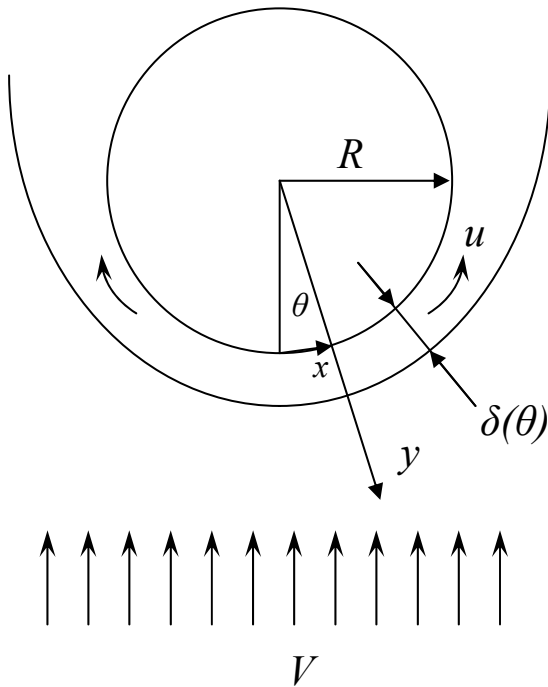


Figure 32: Close contact melting of a sphere in a PCM

All of the analyses considered make the following assumptions: viscous flow of melt around a rigid body of fixed shape; thin molten layer of thickness δ in front of the penetrator ($\delta/r_{\text{RIPTP}} \ll 1$); high Peclet number ($Pe = V^* r_{\text{RIPTP}}/\kappa$ where V is penetration speed, r_{RIPTP} is the radius or characteristic dimension of the body, and κ is the thermal diffusivity of the melt). Fomin's is the most generalized analysis, assuming an Ostwald-de-Waele type non-Newtonian fluid melt with temperature dependent viscosity and thermal conductivity and a variety of possible body geometries. Yaojiang, Emerman, and Kascheev employ a simpler model, neglecting temperature dependence of solid and melt properties such as viscosity, thermal conductivity, and density. Emerman further neglects change in density in the PCM due to melting. Kascheev follows Emerman but includes the effect of melting on density. Yaojiang et al's work is a very geometrically generalized approach, and is similar in predictions to the results of Emerman in the case of very small values of geometric heating rates (although including the effect of a change in PCM material density due to melting).

After an initial investigation of Fomin's calculation procedure, the author chose to utilize the general method outlined by Yaojiang, Kascheev, and Emerman instead. This choice was made as notational inconsistencies in Fomin's work together with the very geometrically generalized analytical approach made implementation of Fomin's results overly time consuming.

A case calculated and published by Emerman was reproduced using Emerman, Yaojiang and Kascheev's solutions for the purpose of validating the close-contact melting portion of the code and illustrating the differences in predictions between the three approaches (Figure 33). For comparison, the simplistic approach initially used by

the author is also plotted (recall that this approach predicts penetration rate on the basis of sensible power required to melt the medium plus the heat loss rate associated with conduction from a hot sphere into an infinite medium).

Using Emerman's specifications for the problem parameters (including no change in density from melting) several things may be observed. First, the solutions of Kascheev and Emerman overlay as the only difference between them is the change in density due to melting accounted for by Kascheev. Next, Emerman's published solution for melting rate in the case of very low heat production rates (not shown) is equivalent to Yaojiang's published solution. Finally, it is observed that for at least this particular set of granite properties and conditions, the simplistic melting model initially used by the author to define the baseline penetrator is both comparable and conservative in result for lower melting rates. Figure 34 shows the penetrator surface temperatures corresponding to the penetration rates shown in Figure 33, matching Emerman's predictions.

Figure 35 illustrates the predictions of these four analyses for granite properties considered more typical by the author than those used by Emerman. Note also that a change in density of the PCM due to melting is specified, so that Kascheev and Emerman's solutions no longer match. According to Kascheev's equations, the result of this change in density is a decrease in penetration rate (given that melting is accompanied by a decrease in density). Figure 36 illustrates the effect of a temperature dependent viscosity on the calculated penetrator surface temperature using Kascheev's analysis.

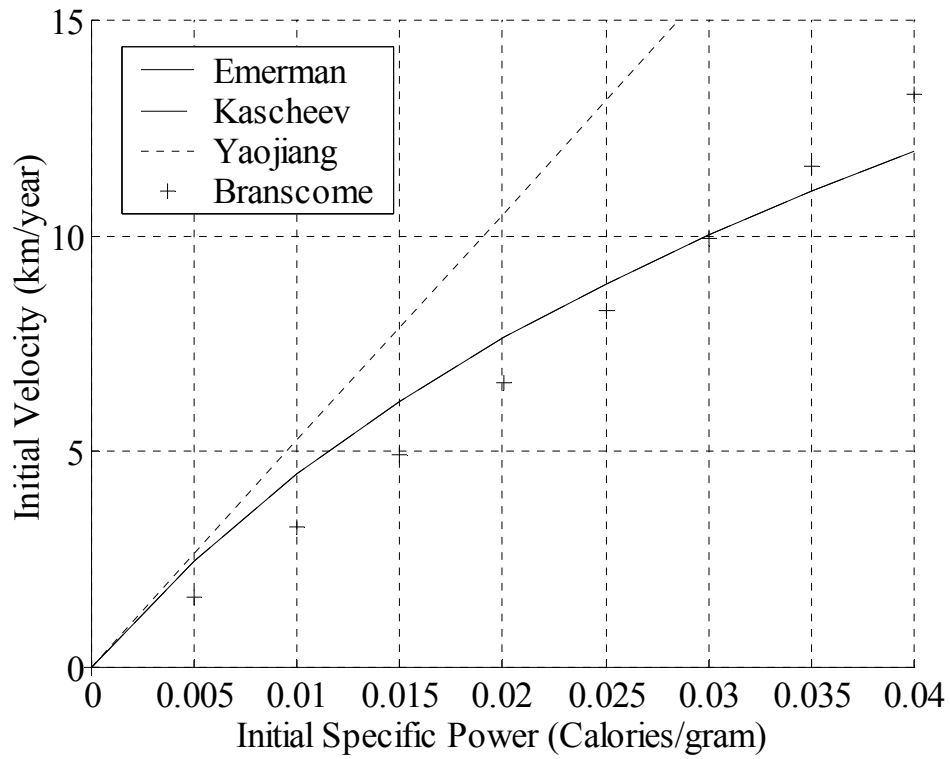


Figure 33: Validation of close-contact melting predictions using results from Emerman, Kascheev, and Yaojiang

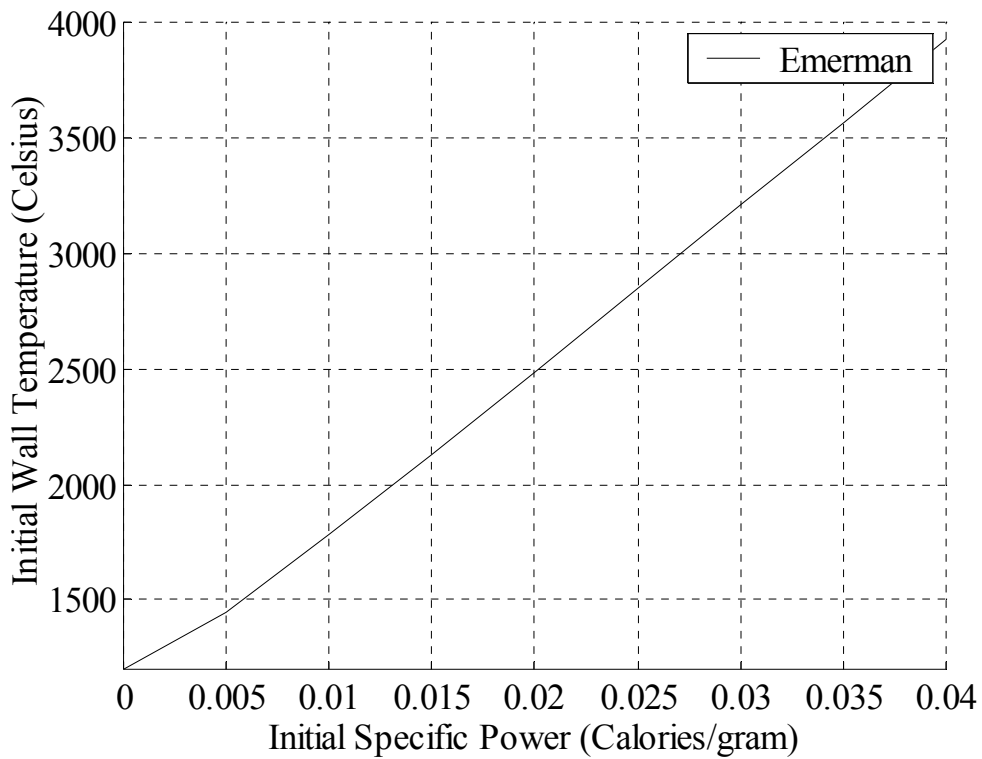


Figure 34: Validation of penetrator surface temperatures using Emerman

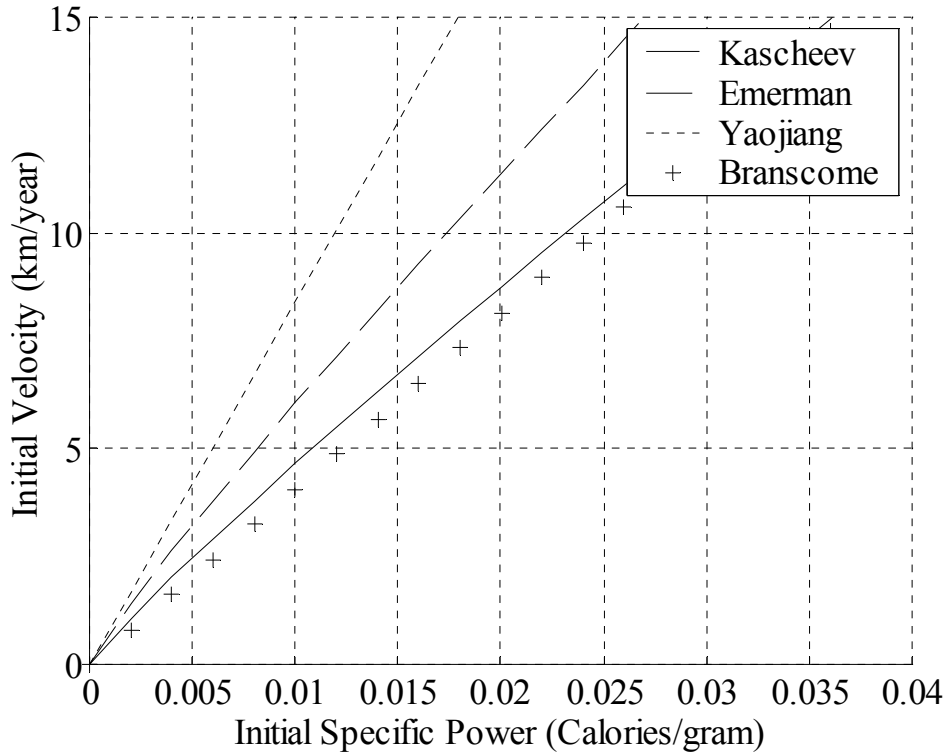


Figure 35: Comparison of results of Emerman, Kascheev, Yaojiang, and Branscome using alternative granite properties.

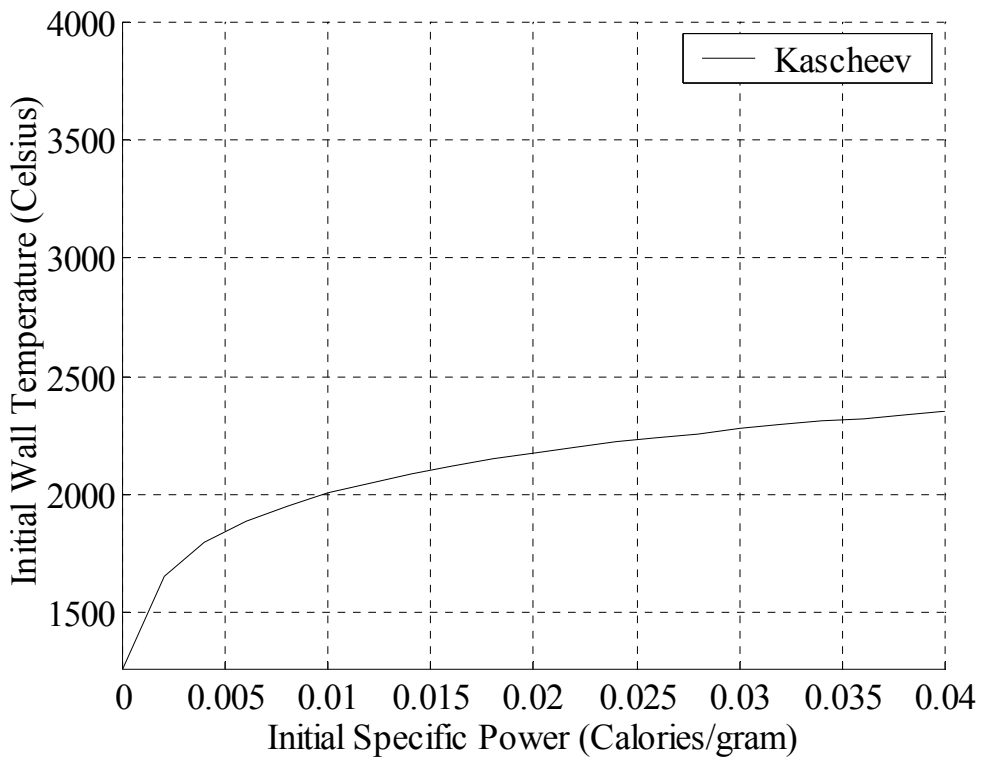


Figure 36: Surface temperatures using Kascheev and considering viscosity change

Ultimately it was decided to use Kascheev's results in the multidisciplinary analysis to account for the change in density due to melting. The pertinent equations from Kascheev are listed below, and the associated variable definitions in Table 27. The speed given by equation (1) below is the speed of penetration as derived from force balance, and that of equation (2) below is the speed of penetration as derived from energy conservation. Conservation of both momentum and energy requires that the speed obtained from both equations match. Iteratively solving for this condition allows for the determination of both surface temperature and velocity for a given penetrator power.

$$V_1 = \left[\rho^* \frac{8g\Delta\rho\kappa^3 f^3(Ste, \rho^*)}{3\mu r_{RIPTP}} \right]^{\frac{1}{4}} \quad (1)$$

$$V_2 = \frac{\frac{4r_{RIPTP} \cdot P}{3k}}{\frac{2(T_0 - T_m)}{\kappa f(Ste, \rho^*)} - \frac{\rho_s h'_{sf}}{k}} \quad (2)$$

$$\rho^* = \frac{\rho_l}{\rho_s}$$

$$\Delta\rho = \rho_p - \rho_l$$

$$Ste = \frac{c_p(T_0 - T_m)}{h'_{sf}}$$

$$f(Ste, \rho^*) = \frac{1}{2} \left\{ -\frac{10-7\rho^*}{2} Ste - 10 + \left[\frac{(10-7\rho^*)^2}{4} Ste^2 + 10(10-3\rho^*) Ste + 100 \right]^{\frac{1}{2}} \right\}$$

$$h'_{sf} = h_{sf} + c_{p,s}(T_m - T_\infty)$$

$$\kappa = \frac{k_l}{c_p \rho_l}$$

Table 27: Close-contact melting variables from Kascheev

Parameter	Name
-----------	------

δ	Boundary layer thickness
κ	Thermal diffusivity
k_l	Thermal conductivity of the melt
c_p	Melt specific heat
$c_{p,s}$	Specific heat of solid phase
$\Delta\rho$	Difference between body and melt densities
ρ_l	Melt density
ρ_s	PCM medium solid density (rock density)
ρ^*	Melt to solid PCM density ratio
ρ_p	Hot body density
μ	Dynamic viscosity of liquid
p	Power per unit volume
h_{sf}	Latent heat of melting
h'_{sf}	Effective heat of melting
V	Penetration speed
Ste	Stefan's Number
r_{RIPTP}	Radius of penetrator
g	Acceleration of gravity
T_0	Temperature of penetrator surface
T_m	Melting temperature of PCM
T_∞	Ambient temperature of PCM

The calculation procedure used for determining penetration rate is listed below. Essentially, the velocity error term $(V_1 - V_2)^2$ was minimized by changing T_0 , with new values of T_0 selected by a numerical optimizer operating on the error term as the objective to be minimized.

1. For selected rock, identify T_m , h_{sf} , ρ_s , calculate change in enthalpy to melting temperature.
2. Calculate h_{sf}'
3. Using guessed T_0 , calculate temperature averaged value for k_l , $c_{p,l}$, ρ_l , μ .
4. Calculate Stephan's number, thermal diffusivity of liquid, ρ^* , $\Delta\rho$.
5. Calculate $f(Ste, \rho^*)$
6. Calculate V_1 .
7. Calculate V_2 .

8. Calculate $(V_1 - V_2)^2$
9. Return $(V_1 - V_2)^2$ error term to optimizer (iterate until velocities match)

PARAMETRIC ROCK VISCOSITY

Most parameters in the close contact melting analysis described above vary within a single order of magnitude. In contrast, for the temperature ranges of interest (~1200K to 2100K +) rock viscosity can vary four orders of magnitude for a single igneous rock specimen and six orders of magnitude or more over the range of basaltic and granitic rock types. The impact of this variation is mitigated in that changes in velocity from the force balance equation vary as the inverse of the fourth root of viscosity.

Viscosity of a variety of rocks (including various granites and basalts, Berea Sandstone, Duluth Gabbro, Newberry Rhyolite, Tachylite, and Lunar Granodiorite) vs. temperature were found in the literature and plotted (Figure 37).^{130, 270, 271} Data for wet and dry granite were also found in a paper by Heuze, but values listed were excluded as they were: reported as “estimates”; more than an order of magnitude higher than those reported by any other source reviewed; and obtained from sources significantly earlier than Bacon, and Klett.²⁴⁸

Exponential fits for individual examples from the Granite and Basalt subsets of this data were made according to the equation below. Excellent fits were obtained.

$$\mu = A \cdot e^{-BT}$$

^{‡‡} Also considered was a discussion of rock melting characteristics and a list of temperatures for a variety of minerals listed by Krupka.²⁷¹ A significant conclusion from the viscosity and rock melting temperature data is that some sandstones and limestone can pose a significantly greater challenge for a subterrene with respect to the required melting temperature as compared to granites or basalts.

In this equation dynamic viscosity is denoted by μ , T is the temperature in Kelvins, and A , B are coefficients of the fit. Listing and plotting of the values found for A and B for the various types of granites and basalts lead to the observation that B could be fit as a function of A with reasonable correlation according to the equation below, where α , and β are coefficients of the fit, with α specified as a constant equal to .026.

$$B = \alpha \ln(A) + \beta$$

Using these two equations for the rock melt viscosity as a function of temperature and the viscosity fit coefficients enabled modeling of the range of rock viscosity variation by assigning ranges for only the parameters A and β (Table 28). Variation of these two fit parameters over their specified ranges resulted in viscosity vs. temperature functions closely spanning the range of observed granite and basalt viscosity trends.

Table 28: Coefficient ranges for fits of granite and basalt viscosities

	A (poise)	β (1/Kelvin)		A (poise)	β (1/Kelvin)
GRANITES			BASALTS		
<i>High</i>	1 E+15	.51	<i>High</i>	1.8 E+9	.51
<i>Low</i>	7 E+10	.36	<i>Low</i>	1.0 E+8	.36

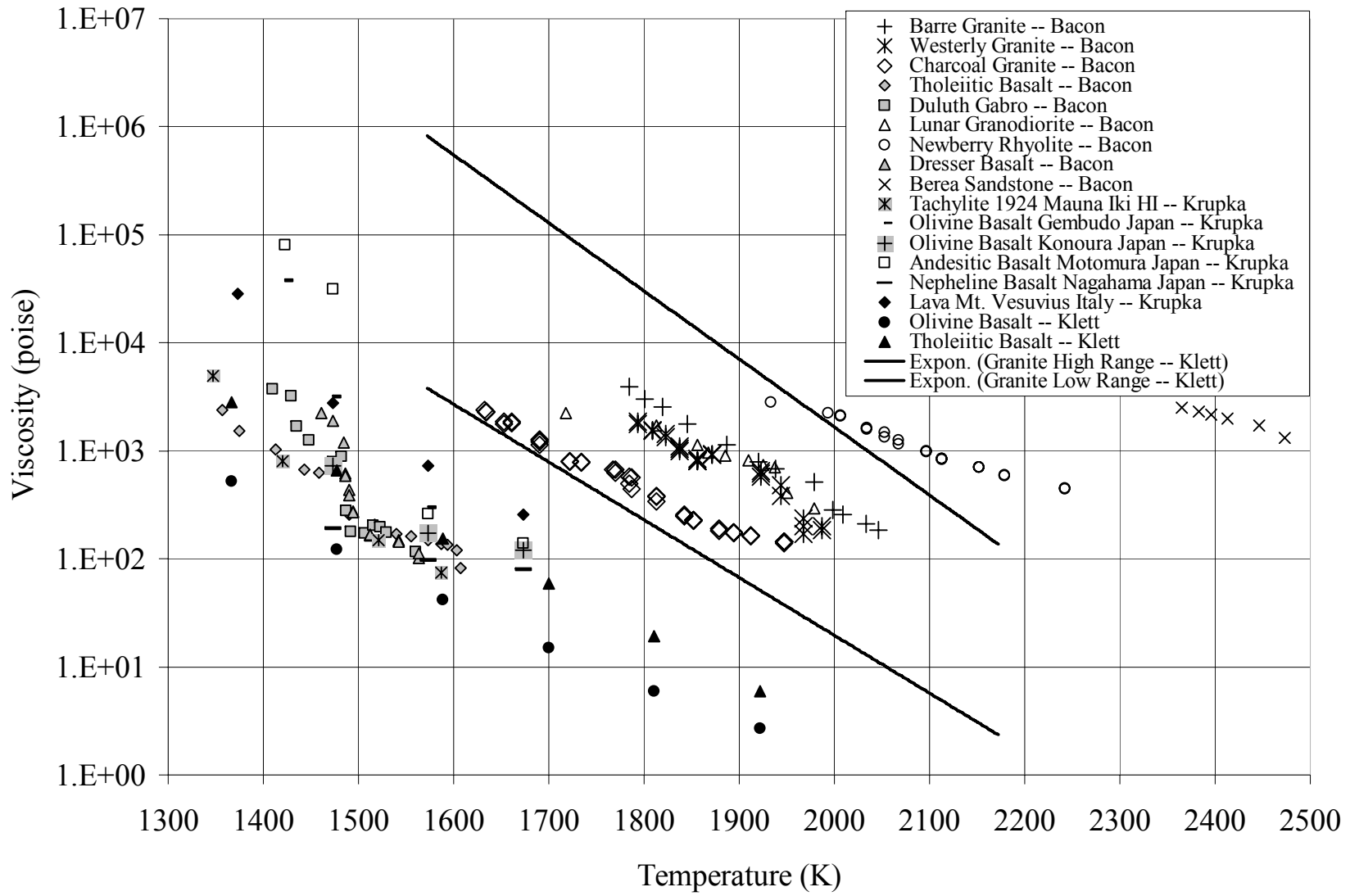


Figure 37: Rock viscosities from Bacon, Krupka, and Klett

ESTIMATION OF THERMAL PENETRATOR INTERNAL TEMPERATURES

As part of the RIPTP analysis code it was desirable to estimate maximum core and casing RIPTP temperatures in various scenarios for the purpose of determining whether RIPTP material temperature limits (such as melting temperature) would be exceeded at different points during the life of the RIPTP. The simple steady state thermal analysis outlined below was performed and used to calculate steady state temperatures for various scenarios throughout the RIPTP life. Temperatures were calculated for: RIPTP immersion in saturated (boiling) water; RIPTP with radiative cooling only in a high temperature environment; RIPTP insulated in molten granite with conductive heat transfer only; and RIPTP with radiative cooling only in Standard Temperature and Pressure (STP) environment.

Steady state thermal flux of the baseline design was compared to typical minimum thermal fluxes required to sustain film boiling. As typical RIPTP thermal fluxes appear significantly lower than those required for transition from film to nucleate boiling, a nucleate boiling regime is assumed for steady state immersion in water, and that the external case temperature would approximately be that of the surrounding water (100° C, STP). As a result, the author's approximate analysis of RIPTP immersion in boiling water would not apply for RIPTPs with greatly higher power densities as the analysis does not account for the possibility of a "boiling crisis" in which steady state thermal flux from the RIPTP surface to the surrounding water is sufficient to sustain a film boiling regime with consequently degraded heat transfer efficiency.

Note also that an estimated conservative worst-case tungsten thermal conductivity was used of 80 watts/meter-Kelvin, independent of material temperature (Appendix C – Thermal Conductivity of Representative Penetrator Materials). This pessimistic conductivity assumption together with the already conservative nature of the steady state thermal analysis should provide a conservative estimate of maximum temperatures.

Table 27 lists some of the variables used in the steady state thermal analysis.

Table 29: Some variables used in the steady state thermal analysis

Parameter	Name
P	Penetrator power produced (function of time)
p_{req}	Penetrator volume specific power required
P_{req}	Penetrator power required
V_{avail}	RHS volume available (for power source)
$P_{rad,eq}$	Penetrator emitted radiative power
ε	Emissivity
T_S	Surface temperature
$T_{amb,r}$	Ambient radiative temperature
σ	Stefan-Boltzmann constant

Penetrator volume specific power required is just $p_{req} = \frac{P_{req}}{V_{avail}}$.

Several scenarios are considered for potential compromise of the penetrator containment system due to thermal considerations with respect to both unconfined RI pellets as well as intact RIPTP penetrator: radiative equilibrium temperature throughout the life cycle; unconfined radiative equilibrium temperature of the casing throughout the life cycle, maximum sustainable ambient radiative temperature, and temperature in hot melt.

Radiative equilibrium temperature

Consider an object in thermal equilibrium with its environment producing a constant internal power P . A conservative maximum steady state external surface temperature, T_S of the object subjected to an environment with ambient radiative temperature $T_{amb,r}$ may be found by considering the case in which power is only rejected through radiation from the objects surface of area A and emissivity ε . In this case, emissive power and internal power will be equal, thus

$$P_{rad,eq.} = P = A \cdot \varepsilon \cdot \sigma (T_S^4 - T_{amb,r}^4), \text{ or } T_S = \left(\frac{P}{A \cdot \varepsilon \cdot \sigma} + T_{amb,r}^4 \right)^{1/4}$$

$$\text{where } P = p_{RHS} V_{RHS}, \text{ and } V_{RIPTP} = V_{CASE} + V_{RHS} = \frac{4}{3} \pi \cdot r_{RIPTP}^3 + 2\pi \cdot r_{RIPTP}^3 (f-1)$$

$$V_{RHS} = \frac{4}{3} \pi \cdot r_{RIPTP}^3 (1-t)^3 + 2\pi r_{RIPTP}^3 (f-1)(1-t)^2$$

If one calculates this steady state surface temperature for a sphere of equivalent volume to the object in question, the resulting estimated surface temperature is conservative as the sphere has the least available surface area for power rejection for the given volume. $A_{equiv} = 4\pi r_{equiv}^2 = 4\pi \left(\frac{3}{4\pi} V_{RIPTP} \right)^{2/3} = \pi \left(\frac{6}{\pi} V_{RIPTP} \right)^{2/3} = \left(6\sqrt{\pi} \cdot V_{RIPTP} \right)^{2/3}$

$$V_{RIPTP} \equiv V_{sph} = \frac{4}{3} \pi r_{equiv}^3, \text{ } r_{equiv} = \left(\frac{3}{4\pi} V_{RIPTP} \right)^{1/3}$$

Equivalent surface area for this conservative analysis will then be

$$A_{equiv} = 4\pi r_{equiv}^2 = \left(6\sqrt{\pi} \cdot V_{RIPTP} \right)^{2/3} \text{ and thus } T_S = \left(\frac{P}{\left(6\sqrt{\pi} \cdot V_{RIPTP} \right)^{2/3} \cdot \varepsilon \cdot \sigma} + T_{amb,r}^4 \right)^{1/4}$$

Maximum internal temperature for a body of revolution may be bounded by using a 2D heat transfer analysis for a hollow circle of radius equal to the maximum radius of

the actual penetrator and internal circle with heat source p with radius equal to the actual core. That this is a conservative estimation can be seen by considering the case of conduction in a rod of length l , constant external temperature T , and internal heat source of density p . Maximum temperature will occur in the geometric center of the cylinder and will decrease as the rod gets shorter and increase as the rod gets longer. As the rod length approaches infinity, the maximum temperature of the rod will approach that of the 2D analysis.

There are two parts to this problem. First, the temperature of the interior wall of the penetrator case must be found, and then this temperature along with the heat source of density p is used to solve for the centerline temperature.

Part one:

$$\frac{P}{l} = p \cdot \pi \cdot r_{RHS}^2 = \frac{2\pi \cdot k_o \cdot (T_i - T_S)}{\ln\left(\frac{r_{RIPTP}}{r_{RHS}}\right)} \quad (\text{second part from Lienhard}^{266}), \quad \text{thus}$$

$$T_i = \frac{p \cdot r_{RHS}^2 \cdot \ln\left(\frac{r_{RIPTP}}{r_{RHS}}\right)}{2 \cdot k_o} + T_S$$

Part two:

For a cylinder with power source of density p , outside radius r_{RHS} , and conductivity k_i , the maximum (centerline) temperature can be found by solving the

ordinary differential equation $\frac{d}{dr}\left(r \frac{dT}{dr}\right) = -\frac{rp}{k}$, which results in the solution

$$T_{\max} = T_i + \frac{pr_{RHS}^2}{4k_i} \quad \text{Thus, choosing worst case values for } k_o \text{ and } k_i, \text{ the conservative worst}$$

case radiative equilibrium temperature may be calculated as $T_{\max} = T_i + \frac{pr_{RHS}^2}{4k_i}$

In summary, for a cylinder-like body:

$$T_S = \left(\frac{P}{\left(6\sqrt{\pi} \cdot V_{pen}\right)^{2/3} \cdot \varepsilon \cdot \sigma} + T_{amb,r}^4 \right)^{1/4},$$

$$T_i = \frac{p \cdot r_{RHS}^2 \cdot \ln\left(\frac{r_{RIPTP}}{r_{RHS}}\right)}{2 \cdot k_o} + T_S$$

$$T_{max} = \frac{pr_{RHS}^2}{4k_i} + T_i$$

or

$$T_{amb,r} = \left(T_S^4 - \frac{P}{\left(6\sqrt{\pi} \cdot V_{pen}\right)^{2/3} \cdot \varepsilon \cdot \sigma} \right)^{1/4},$$

$$T_S = T_i - \frac{p \cdot r_{RHS}^2 \cdot \ln\left(\frac{r_{RIPTP}}{r_{RHS}}\right)}{2 \cdot k_o}$$

$$T_i = T_{max} - \frac{pr_{RHS}^2}{4k_i}$$

For a sphere, the above analysis may be repeated to give

$$T_S = \left(\frac{P}{4\pi r_{RIPTP}^2 \cdot \varepsilon \cdot \sigma} + T_{amb,r}^4 \right)^{1/4} \text{ as before,}$$

$$T_i = \frac{P \cdot (r_{RIPTP} - r_{RHS})}{4\pi \cdot k_o \cdot r_{RIPTP} \cdot r_{RHS}} + T_S \text{ (from Lienhard)}$$

$$T_{max} = \frac{pr_{RHS}^2}{6k_i} + T_i, \text{ from } \frac{d}{dr} \left(r^2 \frac{dT}{dr} \right) = -\frac{r^2 p}{k}$$

or

$$T_{amb,r} = \left(T_S^4 - \frac{P}{4\pi r_o^2 \cdot \varepsilon \cdot \sigma} \right)$$

$$T_S = T_i - \frac{P \cdot (r_{RIPTP} - r_{RHS})}{4\pi \cdot k_o r_{RIPTP} r_{RHS}}$$

$$T_i = T_{\max} - \frac{pr_{RHS}^2}{6k_i}$$

The last equation above may also be used for temperature calculations for individual isotope production target spheres, in which case

$$T_{\max, \text{targ}} = \frac{pr_{\text{targ}}^2}{6k_{\text{targ}}} + T_{S, \text{targ}} \quad \text{or for calculation of allowable power density } p,$$

$$p = (T_{\max, \text{targ}} - T_{S, \text{targ}}) \frac{6k_{\text{targ}}}{r_{\text{targ}}^2}, \quad \text{or the allowable surface temperature } T_{S, \text{targ}}$$

$$T_{S, \text{targ}} = T_{\max, \text{targ}} - \frac{pr_{\text{targ}}^2}{6k_{\text{targ}}}. \quad \Delta T \text{ can then be calculated from Lienhard and used to determine}$$

whether q_{\max} (the maximum heat flux prior to boiling crisis) is ever approached. Because of the small radius of the target elements as required by self-shielding considerations it is unlikely that a boiling crisis could ever be approached for target elements of the Thulium and Ytterbium radioisotopes considered.

These equations may be used in various worst case conditions to estimate maximum temperatures for the case and core materials. Worst case conditions to evaluate are likely loss of cooling scenarios such as thermal equilibrium in fire or non-penetrating/non-convecting immersion in molten granite.

Thermal Equilibrium in an Insulating Medium:

For a sphere in an infinite conducting medium with constant thermal conductivity, power due to thermal conduction through the wall of the sphere is equal to

$P = 4\pi \cdot r_{RIPTP} \cdot k_l (T_s - T_\infty)$. Thus, conservative equilibrium temperature for immersion of a penetrator in molten medium without convection is equal to

$$T_s = T_\infty + \frac{P}{4\pi \cdot \left(\frac{3}{4\pi} V_{RIPTP}\right)^{1/3} \cdot k_l}, \text{ or } T_s = T_\infty + \frac{P}{\left(48\pi^2 V_{RIPTP}\right)^{1/3} \cdot k_l}$$

$$T_i = \frac{p \cdot r_{RHS}^2 \cdot \ln\left(\frac{r_{RIPTP}}{r_{RHS}}\right)}{2 \cdot k_o} + T_s$$

$$T_{\max} = \frac{p r_{RHS}^2}{4k_i} + T_i$$

MCNP RADIATION AND HOTSPOT RADIOISOTOPE EXPOSURE CALCULATIONS

Calculation of radiation emitted in various scenarios for the purpose of shielding and hazard analysis was performed using the Monte Carlo Neutral Particle (MCNP) radiation transport code.²⁷² Calculation of the radiological hazards consequent from fine fragmentation and dispersal of RIPTP RHSs were performed using the HOTSPOT code.²⁷³ These codes were exercised by Professor Chris Wang (Nuclear Engineering Program of Georgia Tech) to produce the datasets on which regressions were performed by the author. Both calculations are discussed in detail later in the “Safety Investigation” section (pages 226-236).

BENCHMARKING

Once a preferred and apparently feasible concept has been selected for further investigation and a capability for multidisciplinary analysis of the concept created, the next step is to define a baseline feasible design. This process involves further screening of alternatives for implementation and iterative refinement of the concept definition. Eventually the multidisciplinary analysis capability is exercised to quantify predicted performance and characteristics of the concept and determine feasibility. If multiple feasible concept definitions are identified, multidisciplinary analysis results and knowledge resources are employed to filter the alternatives and select a preferred baseline definition.

FEASIBILITY INVESTIGATION

A principle concern regarding RIPTP feasibility is the producibility of RHS heat sources in an operationally viable time-frame and for reasonable costs. Strong motivators exist for the selection of short half-life radioisotopes for an RHS, both for better thermal penetrator performance as well as radiological safety. However, selection of a short half-life radioisotope implies a very limited shelf-life for a RIPTP RHS once produced. Further, production of radioisotope to power an RHS can take a significant period of time depending on the radioisotope selected and reactor facilities used. Unless radioisotope to power a RIPTP RHS were continually being produced, significant lead times (on the order of ten to one-hundred days) would be required for most radioisotopes prior to RHS/RIPTP availability for operational use. This of course would be a major potential

impact on the operational viability of a RIPTP. For these and similar reasons it was necessary to evaluate the alternatives available for powering a RIPTP, their ROM cost, and the implications with respect to their production/employment timelines.

Identification of a baseline radioisotope was also necessary for accomplishing the second primary purpose of this study – the investigation of potential RIPTP safety concerns. Thus the first step in evaluating feasibility of RIPTP RHS production as well as safety concerns was an exploration of the radioisotope alternatives that might be suitable.

Characteristics determining suitability of a radioisotope

Every radioisotope has a large number of associated characteristics which can impact its suitability (Table 30) with respect to the functional requirements for a RIPTP RHS radioisotope.

The principle functional requirements for such a radioisotope are that it must:

1. Be compactly shieldable
2. Produce adequate power density for the penetration rate desired
3. Provide power over a service life of sufficient duration so as to be operationally suitable
4. Be producible in required quantities and concentrations
5. Be producible in an operationally suitable time-frame
6. Be producible for reasonable costs
7. And have chemically-stable and phase-stable compounds at elevated temperatures

Table 30: Important radioisotope characteristics

ISOTOPIC PROPERTIES

Yield of Radiations Emitted per Decay

Total Energy of Decay

Half-Life

Yield per Fission in Reactor

Neutron Capture Cross-Section for Production

Neutron Capture Cross-Section for Transmutation
Atomic mass
<u>ELEMENTAL PROPERTIES</u>
Chemical Compounds of Isotope Available
% Abundance of Isotopes of Element/Isotopic Purity
<u>PROPERTIES OF CHEMICAL COMPOUND</u>
Chemical Stability
Chemical Reactivity
Phase Changes and Their Temperatures
% Isotope in Compound
Density

Screening of radioisotopes to power a RIPTP

A natural starting point for an evaluation of radioisotope alternatives is with those that have been previously proposed or historically utilized. Characteristics of such historically favored radioisotopes are listed in Table 31.

The author did not consider an evaluation of these radioisotopes to be sufficient, in part due to dissimilarities between historical RHS and RIPTP RHS radioisotope requirements. The principle common functional requirement driving historical radioisotope applications has been to provide power for *long durations* in inaccessible locations. Examples include power for space missions, mid-ocean buoys, sensors on the sea-floor, lighthouses on the arctic coast, pipeline sensors in the arctic, and pacemakers inside the human chest. Thus a key motivator for consideration of most of the radioisotopes listed in Table 31 was a relatively long half-life.

In contrast, the required mission duration for defeat of a DBHT is ideally within 24 hours and *at most* on the order of two weeks, so a shorter half-life radioisotope than those listed may well be feasible. Further, a principle functional requirement for a RIPTP RHS is minimal duration of any possible radiation hazard. Safety considerations thus motivate selection of radioisotopes with shorter half-lives as less time is required for

radioactivity to decay to insignificant levels. Finally, shorter half-lives also tend to result in higher power density which is critical to the penetration rate achievable by a RIPTP. For all of the above reasons investigation of radioisotopes with half-lives historically considered too short to be of interest was merited.

Table 31: Principal historically favored radioisotopes for RHS applications

Isotope	Principle Radiation	Half-Life	Watts/gm*	Watts/cm³*
Hydrogen-3	Beta	12.32 Y	.325	-
Cobalt-60	Gamma	5.24 Y	17.45	154.9
Krypton-85	Beta	10.76 Y	.590	-
Strontium-90	Beta	28.78 Y	.916	2.35
Ruthenium-106	Beta	1.020 Y	31.8	391.4
Cesium-137	Gamma & Beta	30.07 Y	.427	.780
Cerium-144	Gamma & Beta	284.6 d	25.5	14.04
Praesmodymium-144	Beta	2.6234 Y	.340	169.6
Thulium-170	Beta	128.6 d	11.86	109.5
Polonium-210	Alpha	138.38 d	141.3	1339
Plutonium-238	Alpha	87.7 Y	.558	11.08
Curium-242	Alpha	162.8 d	120	1619
Curium-244	Alpha	18.1 Y	2.78	37.6

Reference: ²⁷⁴⁻²⁷⁶

*Power density for the radioisotopes is given for 100% isotopic concentration in their pure elemental form. Most widely used radioisotopes for RHS applications are in bold.

Another motivation for a search of alternative radioisotopes was the author's determination that all radioisotopes in Table 31, except thulium-170, were unsuitable for a RIPTP RHS due to radiation shielding, power density, and/or producibility. Lastly, the search for other possible alternatives was motivated by the possibility that improved isotope enrichment technologies might make radioisotopes previously excluded from consideration for RHS applications viable.

The search for alternatives was undertaken through a screening of all isotopes listed in the BNL's online databases²⁵⁸ of radioisotope properties (represented in Figure

38).^{§§} The screening of isotopes was performed by first doing a computerized search of the online Evaluated Nuclear Data File (ENDF) database to identify all isotopes with half-lives greater than five days and shorter than ninety years, resulting in the identification of 210 radioisotopes (listed in Table 55, Appendix C).

These radioisotopes were then screened to determine those which were producible through transmutation in a nuclear reactor using the interactive nuclear decay chain display capability of the Isotope Explorer computer program.²⁷⁷ Radioisotopes principally available as fission/daughter products in nuclear fuel were not favored for reasons discussed later. If producible through neutron activation in a nuclear reactor, appropriate precursor isotopes were identified and their natural abundance determined. For the 113 isotopes remaining the maximum gamma-photon energy (if any) and production cross sections were identified, and the volume specific power calculated (Table 56, Appendix C). Maximum gamma-photon energies and extractable thermal energy per decay (for calculation of volume specific power) were obtained from the BNL's MIRD database.²⁵⁹ Thermal neutron capture cross-sections were also available at the referenced BNL website using the NuDat online feature.²⁵²

All radioisotopes were then discarded that had any of the following: maximum gamma-photon energies in excess of .5 MeV at significant yields per decay; maximum theoretical volume specific powers less than plutonium-238 (11 watts/cm³); or precursor isotope neutron capture cross sections less .5 barns. Table 32, below, lists the 13 radioisotopes remaining that were considered potentially satisfactory. Note that some

^{§§} Figure 38 was created using the Isotope Explorer software and the accompanying Evaluated Nuclear Structure Data File – 2 (ENSDF-2) database.²⁷⁷

data is missing from the table as thermal neutron capture cross-sections were not available for all isotopes in the ENDF database.

Table 32: Potentially satisfactory isotopes

RI	Half-Life	ρ	E_{Decay}	γ_{Emax}	Power	Prec.	% NA	σ
	<i>days</i>	<i>g/cm³</i>	<i>MeV</i>	<i>MeV</i>	<i>watts/cm³</i>			<i>barns</i>
¹⁷⁰ TM	128.6	9.32	0.33		109.5	¹⁶⁹ TM	100.00	105
¹⁶⁹ YB	32.12	6.90	0.43	0.31	421.1	¹⁶⁸ YB	0.13	2300
¹⁷⁵ HF	70.08	13.31	0.39	0.43	331.1	¹⁷⁴ HF	0.16	561
¹⁷⁷ LU	6.57	9.84	0.18	0.32	1171.0	¹⁷⁶ LU, ¹⁷⁶ YB	2.59	2090
¹⁹¹ OS	15.33	22.60	0.21	0.13	1242.2	¹⁹⁰ OS	26.26	13.1
¹⁰³ PD	17.16	12.00	0.06	0.50	299.7	¹⁰² PD	1.02	
¹⁴³ PR	13.51	6.77	0.32	0.74 ***	850.1	¹⁴² CE, ¹⁴¹ PR		
¹⁶⁹ ER	9.49	9.07	0.10	0.12	454.9	¹⁶⁸ ER	26.80	11
⁵¹ CR	27.74	7.19	0.04	0.32	143.7	⁵⁰ CR	4.35	15.9
^{179M} HF	25.19	13.31	1.10	0.45	2525.7	¹⁷⁸ HF	27.28	53?
⁷⁵ SE	119.72	4.79	0.40	0.40	166.2	⁷⁴ SE	0.89	51.8
²⁰³ HG	46.72	13.55	0.34	0.28	372.2	²⁰² HG	29.86	4.89
¹⁴¹ CE	32.49	6.77	0.25		282.2	¹⁴⁰ CE	88.45	0.57

RI = Radioisotope; **Half-Life** = half-life of decay for the principle radioisotope of interest; **ρ** = density of isotope in elemental form; **E_{Decay}** = energy per principle nuclear decay in Million electron-Volts; **γ_{Emax}** = maximum energy of gamma photons that can be emitted in a nuclear decay of the isotope; **Power** = power density of 100% isotopic purity radioisotope in elemental form; **Prec.** = stable precursor isotope used to produce radioisotope through neutron activation; **% NA** = Percent natural abundance (by number of nuclei) of precursor isotope with respect to all naturally occurring nuclei of element; **σ** = microscopic thermal neutron capture cross-section of precursor isotope.

*** Praesmodymium-143 is retained as it produces these photons relatively infrequently on a per-decay basis.

CHART OF THE NUCLIDES

(All ENSDF-2 Listed)

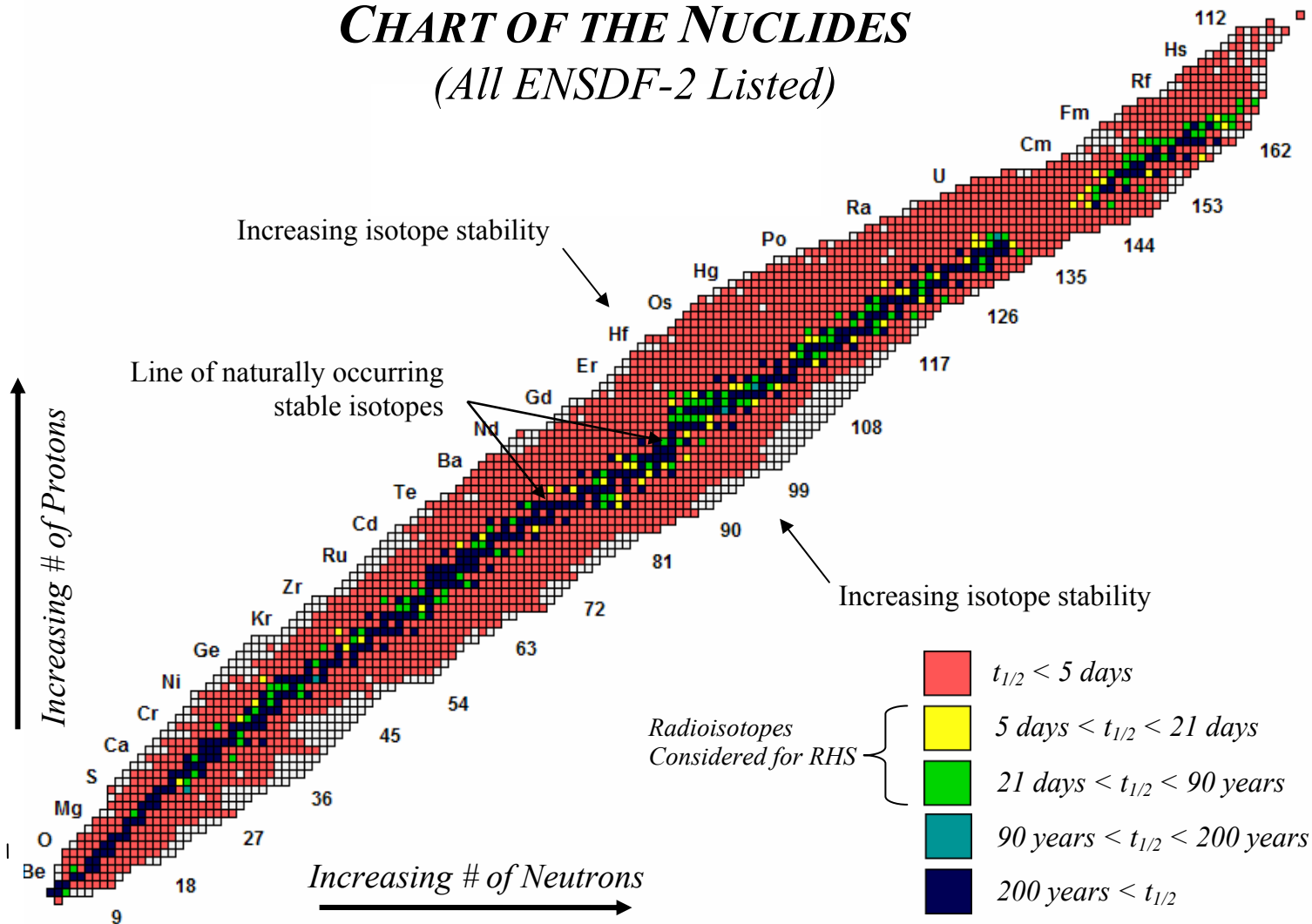


Figure 38: Isotopes screened for RIPTP RHS application

Further reductions in the number of candidate radioisotopes beyond Table 32 required more detailed development of the radioisotope production concept and the creation of a radioisotope production/RIPTP performance computer code.

RIPTP RHS baseline-radioisotope selection

Isotope transmutation/decay chains for each of the radioisotope candidates listed in Table 32 were investigated and necessary data for the evaluation of reactor isotope production collected. Figure 39 illustrates an example of such a chain for thulium-170.

For this particular isotope transmutation/decay chain, the initial precursor isotope used is thulium-169, which comprises 100% of all naturally occurring thulium. The neutron capture cross-section for this isotope is 105 barns. Upon capture of a neutron the principle desired radioisotope, thulium-170, is produced. However, thulium-170 is then removed through two independent mechanisms. First, thulium-170 decays to ytterbium-170 with a half-life of 129 days, producing .33 MeV per decay and no gamma photons. Second, thulium-170 is transmuted to thulium-171 at a rate proportional to its number density and neutron capture cross section of 92 barns. Production of thulium-171 is tolerable as it doesn't emit gamma photons, although its production is a concern with regard to time required for decay of the RHS to negligible levels of radioactivity. The last isotope in the transmutation chain produced in significant quantities is thulium-172, and its production *is* a concern with regard to thulium-170's suitability for a RIPTP as it emits a high energy gamma photon during decay. Fortunately, the half-life of this isotope is short enough that thulium-170 target assemblies could be allowed to "cool" after removal from the reactor for approximately three weeks. After this period of time, plus seven days for assembly of the RHS, RIPTP, and RIPTP Munition, sufficiently low

quantities of thulium-172 would exist such that external levels of radiation would be manageable.

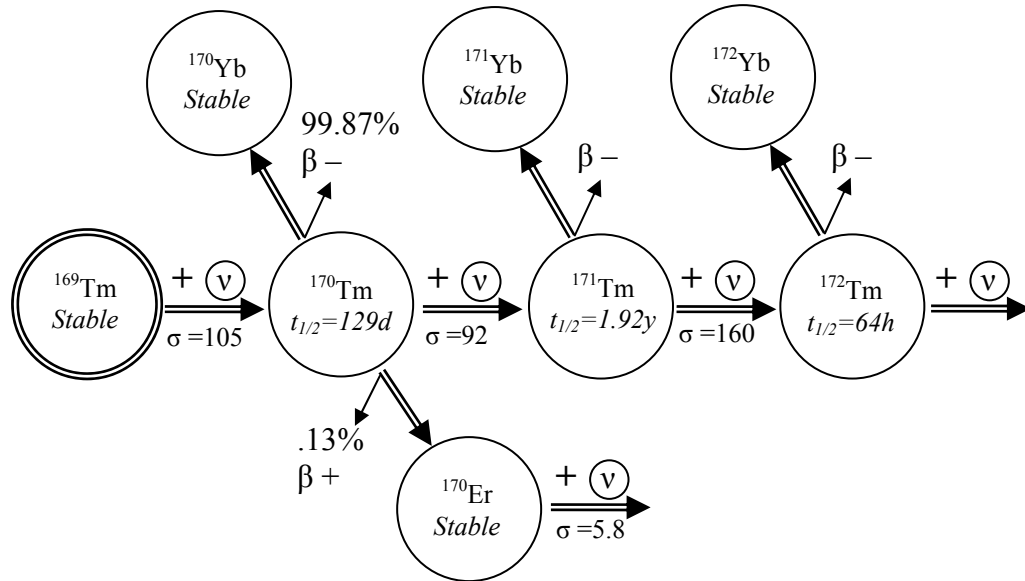


Figure 39: Isotope production from thulium-169 precursor

The previously described radioisotope production code was adapted to each of the radioisotope candidates using analogous data to that described above (when available). Analysis of code results then led to the identification of the preferred radioisotope candidates listed in Table 33. Reasons for a radioisotope not making it to Table 33 typically were that either maximum theoretically achievable radioisotope power density in a high thermal flux reactor was insufficient or that the irradiation of the precursor isotope resulted in production of difficult to shield by-product radioisotopes. Other reasons included insufficient data for complete evaluation of the radioisotope and unattractive chemical properties. Note that Lutetium-177 and Osmium-191 are likely marginal for useful RIPTP RHS service life/total penetration because of their short half-lives.

Table 33: Preferred isotopes

RI	Half-Life	ρ	E_{Decay}	γ_{Emax}	Power	Prec.	% NA	σ
	<i>days</i>	<i>g/cm³</i>	<i>MeV</i>	<i>MeV</i>	<i>watts/cm³</i>			<i>barns</i>
¹⁷⁰ TM	128.48	9.32	0.33		86.9	¹⁶⁹ TM	100	105
¹⁶⁹ YB	32.12	6.90	0.43	0.31	334.2	¹⁶⁸ YB	0.13	2300
¹⁷⁵ HF	70.08	13.31	0.39	0.43	262.8	¹⁷⁴ HF	0.16	561
¹⁷⁷ LU	6.57	9.84	0.18	0.32	929.4	¹⁷⁶ LU, ¹⁷⁶ YB	2.59	2090
¹⁹¹ OS	15.33	22.60	0.21	0.13	985.9	¹⁹⁰ OS	26.26	13.1

RI = Radioisotope; ρ = density in elemental form; E_{Decay} = energy per decay; γ_{Emax} = maximum gamma photon energy; Power = power density of radioisotope in elemental form after 1/3 of a half-life; Prec. = identity of precursor isotope that might be used to manufacture the radioisotope; % NA = natural abundance of precursor isotope.

Of the preferred radioisotopes, thulium-170 was selected as the baseline radioisotope to power a RIPTP. The reasons for its selection were that it: has a precursor isotope that is 100% of naturally occurring thulium (and thus avoids the unresolved question of the viability of precursor isotope enrichment); has good production rate; acceptable half-life; and a large body of historical data and analysis regarding its use in RHS applications.

Although thulium is the least abundant of the rare earth metals, its commercial availability is good. Thulium is 33 times more naturally abundant than gold, 5 times more abundant than silver, and half as abundant as mercury. However, it is not a noble metal and is generally present in an oxide form mixed with the other rare earth metals, increasing the cost of high-purity thulium. Thulium metal is commercially available in the required purity and quantities for RIPTP applications at a price of approximately \$2500/kg.

The next step in development of the baseline concept was selection of a thulium compound suitable for RHS application. For this purpose thulium-sequioxide (Tm_2O_3) was selected. Thulium-oxide has a number of advantages: it is much less chemically

reactive than metallic thulium; it has been previously used for production of thulium-170 RHS material in significant quantities (Figure 40); it's water insoluble; it's refractory – a 2700 K melting temperature; has no phase transitions from ambient to it's melting temperature; and is phase-stable with respect to fraction of it's ytterbium decay product.^{278, 279}

As previously mentioned, the history of prior investigation of $^{170}\text{Tm}_2\text{O}_3$ for RHS applications also makes thulium an attractive choice. Several of the most relevant results from prior related experimental work are described below. First, containment of thulium oxide has been demonstrated with refractory metals for prolonged periods and at high temperatures (Table 34) comparable to those required for a RIPTP application. Next, $^{170}\text{Tm}_2\text{O}_3$ has been demonstrated to retain mechanical integrity and possess low solubility for long-duration immersion in sea water and sediments. Together with the short half-life of thulium radioisotopes, this reduces the level of concern regarding any possibility of contamination of a body of water or underground aquifer. Reduction of fines using a small addition of calcium oxide has been demonstrated – this is advantageous with respect to radiological safety. Refractory cermets with molybdenum have been developed – a potential advantage with respect to RHS toughness and bulk thermal conductivity.²⁸⁰

In other research metallic claddings have been demonstrated for corrosion resistance/material compatibility with molten rock for similar (but somewhat lower) temperatures and longer durations than would be required for a RIPTP penetrator case. Platinum coatings have been demonstrated in molten dolerite rock during geological nuclear waste disposal experiments in the mid 1970s by DOE.¹³⁰ Other oxidation

resistant metal coatings besides platinum would also likely be suitable – experimental investigations by DOE in the 1970s and 1980s of magma energy extraction should be further reviewed for relevant materials experience.²⁸¹

Table 34: Experiments demonstrating refractory metal compatibility and thulium containment at elevated temperature

Alloy	Temperature	Test Duration	Temperature*	Test Duration
Tungsten	2273 K	21 days	1873 K	1 year, 52 days
TZM	2273 K	21 days	1873 K	1 year, 52 days
T111			1873 K	1 year, 52 days

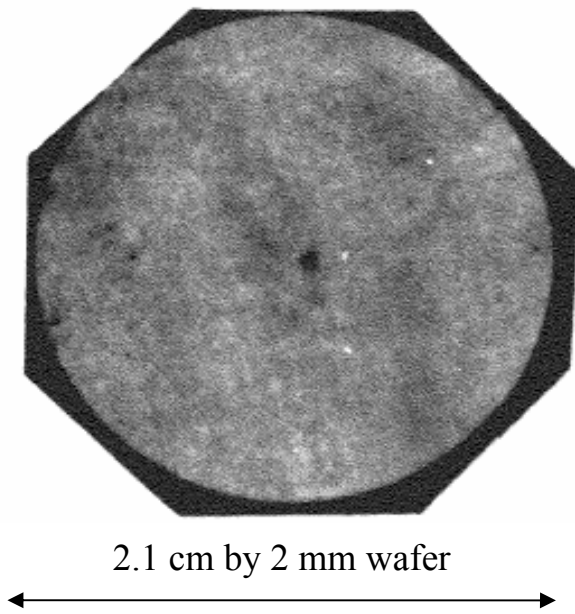


Figure 40: Tm_2O_3 wafer similar to historically produced RHS wafers

It is important to note that selection of thulium-170 is entirely premised on the concern of isotope enrichment. If cost-effective enrichment technologies were available such that precursor isotope cost was not a driving factor in radioisotope selection, then both ytterbium-169 and hafnium-175 would likely be preferable to thulium-170. Thulium-170 of sufficient power density for a RIPTP RHS could only be produced in a high flux reactor.

In contrast, ytterbium radioisotope produced in a commercial PWR would have the following advantages as compared to ATR produced thulium-170: higher achievable power densities; larger quantities producible; lower irradiation costs; much shorter required production times; no “cool-down” period required; much faster decay of post-mission radioactivity; and no external emission of radiation that would require accommodation by RIPTP handling requirements.

Further, due to the chemical similarity of ytterbium and thulium, most of the prior positive experimental experience with thulium oxide for RHS applications should hold for ytterbium oxide. All of these potential advantages emphasize the importance of a thorough investigation to identify potentially cost-effective technologies for highly enriching ytterbium-168 and other alternative candidate precursor isotopes listed in Table 33.

RIPTP baseline performance analysis results

Results of the isotope production portion of the computer code were verified in two manners. First of all, general predictions for thulium-170 production mass and concentration agree well with other published results.^{282, 283} Secondly, the code prediction results for production of plutonium-238 at ATR through irradiation of a neptunium-237 target were compared to results obtained by a detailed study of plutonium-238 production by ATR personnel.²⁸⁴ Code predicted results were 1.65 kg of plutonium-238 produced in one year as compared to ATR calculated results of approximately 1 kg.

This is considered to be a good correlation given the general level of knowledge of the assumptions used in the ATR analysis. In particular, it was assumed that the neptunium target would have plutonium extracted from it every fuel cycle, and that all

fuel cycles in a one year period would be 49 days long, and that there would be six fuel-cycles per year. If ATR's analysis assumed a multiple fuel-cycle irradiation prior to extraction, the annual production results predicted by the author's code would reduce incrementally down to an absolute minimum annual production of .27 kg of plutonium-238. A two fuel-cycle irradiation period would produce approximately .83 kg per year according to the author's code. Shorter duration fuel cycles during the year or longer reactor down-times would also result in smaller production quantities.

Mass of isotope species vs. time during RHS production are illustrated in Figure 41 for baseline RIPTP production at ATR. As previously discussed, production of the undesirable by-product radioisotope thulium-172 would require an approximately 23-day long "cool-down" period to allow decay of this radioisotope to an acceptable population consistent with easily manageable levels of external RIPTP radiation emissions. After this period, the nominal RIPTP Munition assembly time has been specified as seven days.

Maximum penetrator life-limited penetration capability is shown in Figure 42. The penetration depth shown is the maximum depth the penetrator could descend to before it became entombed, given it was dropped on the specified day. Time on the x-axis is measured in days from start of isotope target irradiation. Obviously, how long a RIPTP takes to defeat a target is important. Thus, Figure 43 illustrates a mission-duration limited penetration depth capability, with mission duration specified at 10 days. Note also the times indicated for the Beginning of Service (BOS) of a RIPTP and End of Service (EOS) of a RIPTP. BOS indicates the date of RIPTP availability for employment against a DBHT, and EOS represents the last date a RIPTP may be used and still achieve design performance within the allowed mission duration.

Thulium-170 RHS production capabilities and analysis assumptions are summarized below in Table 35 for radioisotope production at ATR and a new 3 GWth isotope production reactor. It is apparent from this table that it is unlikely that the ATR facility alone could provide an operationally viable thulium-170 RIPTP capability – only 1 RHS to power a baseline RIPTP could be produced per fuel-cycle. In contrast, larger, better performing RIPTPs could be manufactured in a new 3 GWth isotope production reactor at approximately 17 times the rate of smaller baseline RIPTP production at ATR.

Performance comparisons for ATR and a new isotope production reactor are summarized Table 36. This table shows that new-reactor-scenario RIPTPs would have almost three times better performance in terms of penetration rate (as well as better lethality as they would produce larger melt-bubbles). Note that RIPTP performance would continually decrease from its BOS date to its EOS date. Mission duration for each concept is specified as the approximate time required to defeat the baseline DBHT buried under ~80 meters of high strength granite.

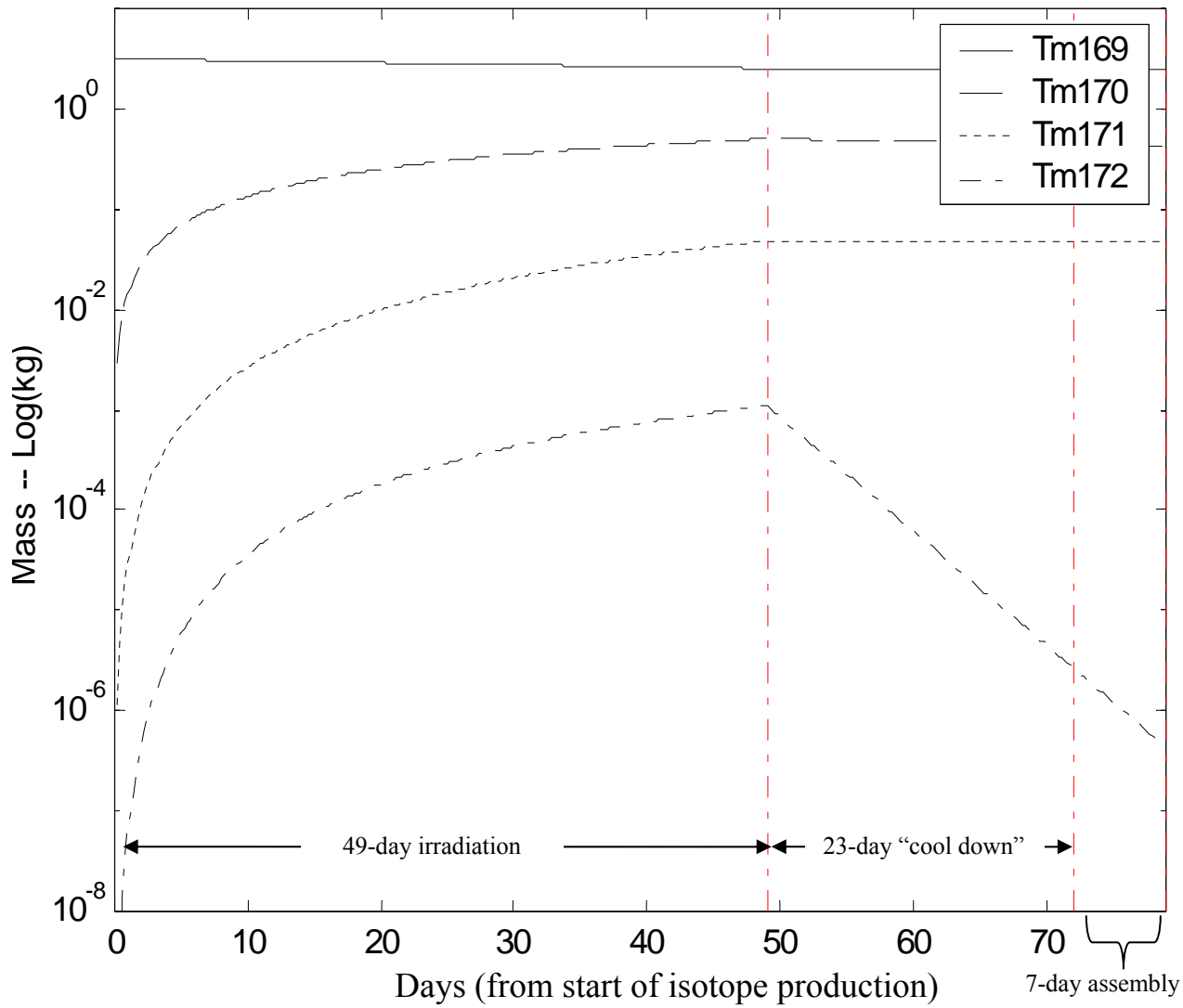


Figure 41: Results for production of ^{170}Tm at ATR

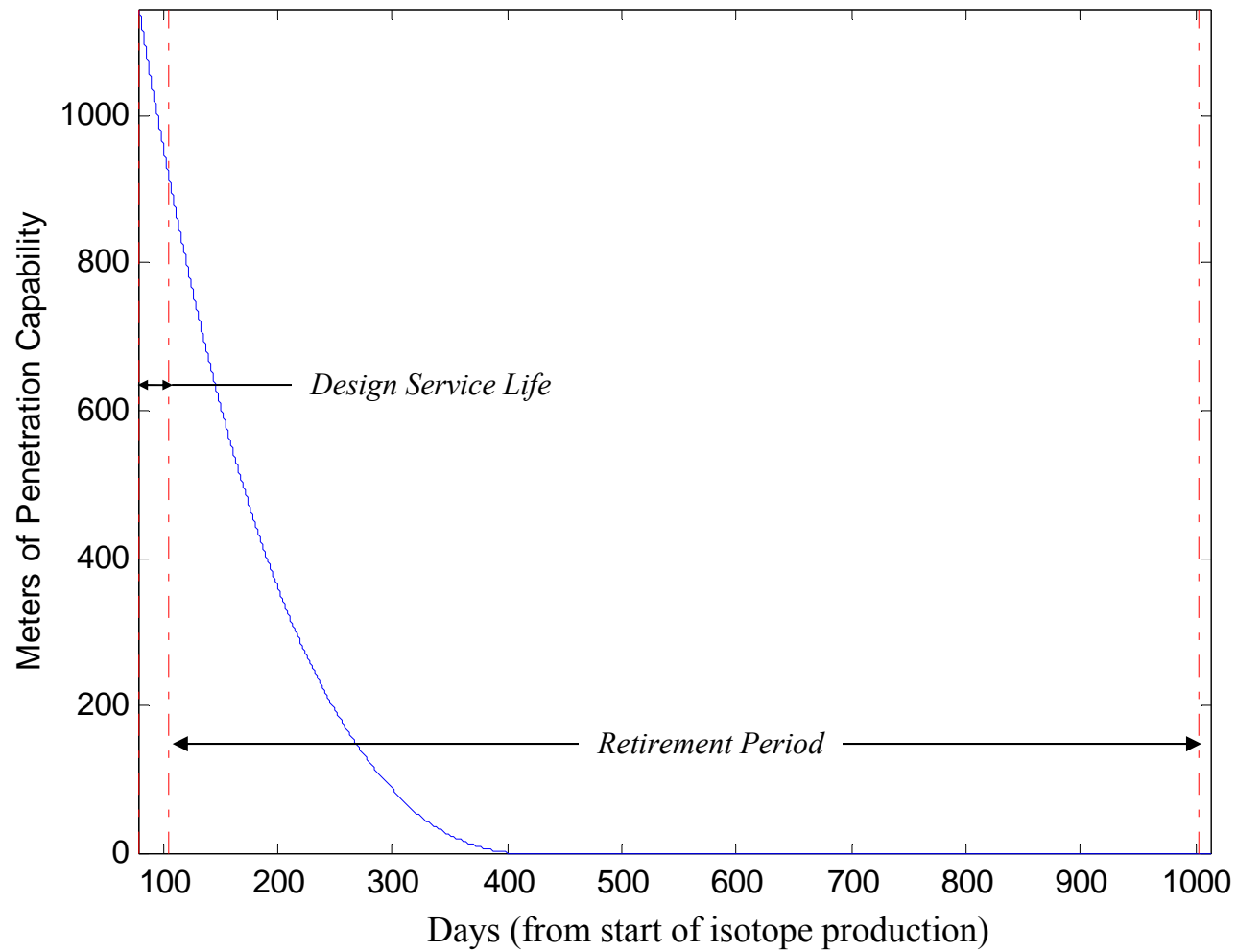


Figure 42: Baseline RIPTP life-limited penetration depth capability

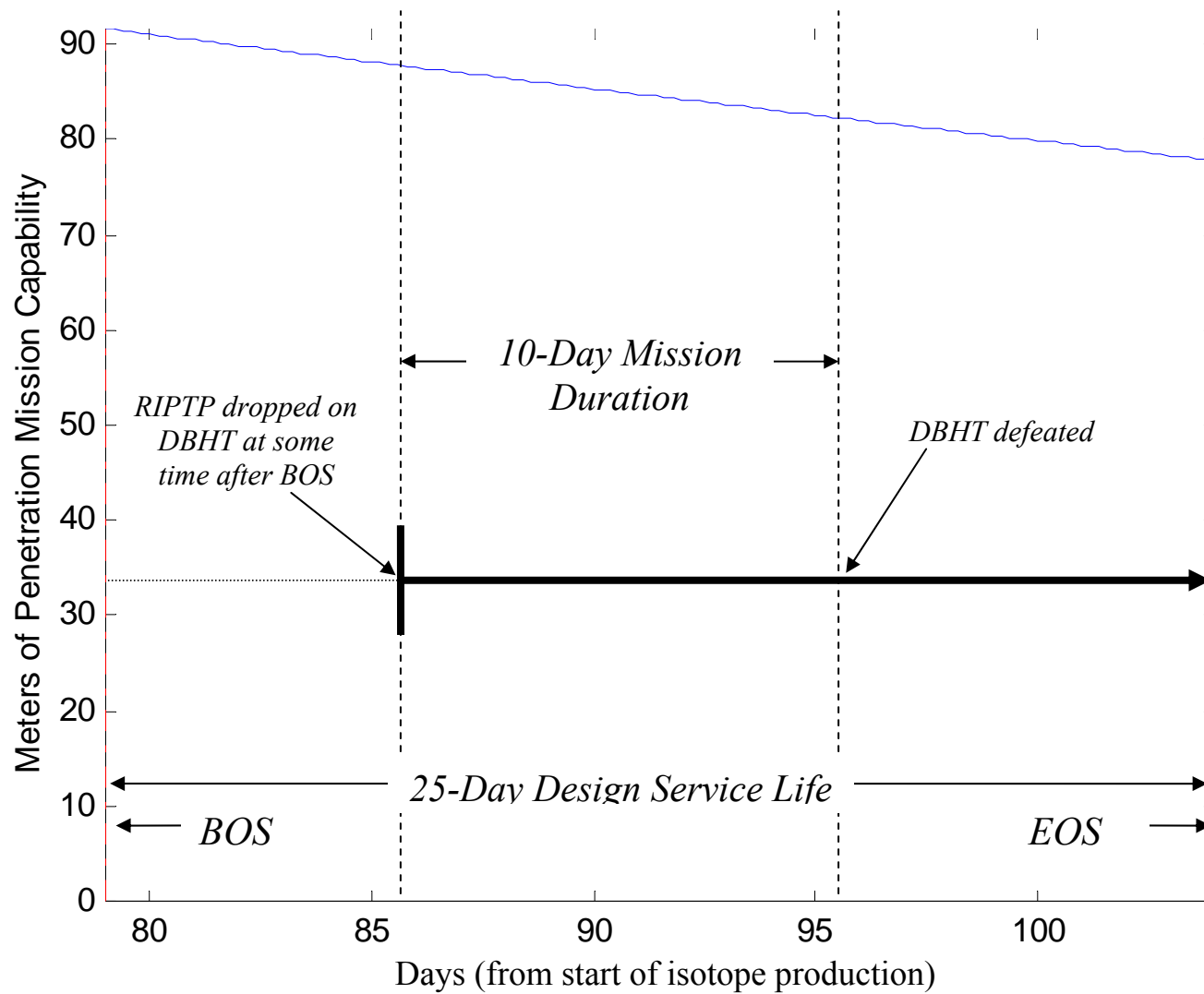


Figure 43: Baseline RIPTP mission duration-limited penetration depth capability

Table 35: Thulium production summary for ATR and new isotope production reactor

RIPTP DIMENSIONS	ATR	New 3 GW_{th} Reactor
Diameter x Length	8.7 x 34.7 cm	12.5 x 50 cm
Mass	30 kg	88.5 kg
PRODUCTION CAPABILITIES		
Batch Size	1 RHS/Fuel Cycle	17 RHS/Fuel Cycle
Production Rate	~6 per year	~100 per year
Initial Mass ¹⁶⁹Tm	3.2 kg	9.4 kg
Unit Cost for ¹⁶⁹Tm (2003Yr\$)	\$7800	\$23,600
Reactor Costs per RHS (2003Yr\$)	\$403,000	\$666,540
ASSUMPTIONS		
Flux (neutrons/cm² sec)	5*10 ¹⁴	10 ¹⁵
Thermal Power	30 MW _{th}	3 GW _{th}
Irradiation Period	49 days	49 days
Cool-Down Period	23 days	23 days
Assembly Period	7 days	7 days
Excess Neutron Percent Usable	50%	50%

Table 36: Thulium RHS mission characteristics and performance

RHS PRODUCTION/RIPTP USE TIMELINE	ATR	New 3 GW_{th} Reactor
Lead Time for Penetrator	30 days	30 days
Availability		
Service Life	25 days	25 days
Allowed Mission Duration	10 days	3.6 days
PERFORMANCE		
BOS Penetration Capability	92 m	90 m
EOS Penetration Capability	78 m	78 m
BOS Penetration Rate	10 m/day	25 m/day
EOS Penetration Rate	8 m/day	22 m/day

As previously mentioned, alternative radioisotopes identified by the author have the potential of offering significantly enhanced RIPTP performance and producibility, if a suitable isotope enrichment technology can be made available. For comparison to the baseline thulium-170 RIPTP, Table 37 provides a summary of RHS production at ATR employing ¹⁶⁸Yb enriched to 80% isotopic abundance (from a natural isotopic abundance of .13%). Use of ¹⁶⁸Yb would enable production of RIPTPs at far greater rates with much

shorter lead times. Such RIPTPs could perform at similar or better levels than could RIPTPs produced in a new 3 GW_{th} isotope production reactor (Table 38).

Further, availability of highly enriched ¹⁶⁸Yb would enable RIPTP production in a commercial PWR (also described in Table 37 and Table 38 for comparison). This would greatly reduce the constraints imposed by the limited availability of existing operational high-flux reactors such as ATR and HFIR, and could also lead to large reductions in isotope target irradiation costs. Besides being producible in larger quantities with existing facilities in shorter periods of time, such RIPTPs could have significantly better performance. The maximum performance provided by such a RIPTP would likely be limited by material temperature limitations internal to a RIPTP immersed in granite melt and/or safety considerations for other adverse cooling scenarios.

Table 37: Production summary for ATR and commercial PWR using 80% enriched Ytterbium-168

RIPTP DIMENSIONS	ATR	3 GW_{th} PWR
Diameter x Length	3.1 x 12.5 cm	12.5 x 50 cm
Mass	1.39 kg	89.6 kg
PRODUCTION CAPABILITIES		
Batch Size	1 RHS/4 days	27 RHS/14 days
Production Rate	~75 per year	~700 per year
Initial Mass ¹⁶⁸Yb	.13 kg	8.72 kg
Unit Cost for ¹⁶⁸Yb (2003Yr\$)	?	?
Reactor Costs per RHS (2003Yr\$)	\$32,900	?
ASSUMPTIONS		
Flux (neutrons/cm² sec)	5*10 ¹⁴	3*10 ¹³
Thermal Power	30 MW _{th}	3 GW _{th}
Irradiation Period	4 days	14 days
Cool-Down Period	2 days	2 days
Assembly Period	3 days	3 days
Excess Neutron Percent Usable	50%	50%

Table 38: RHS mission characteristics and performance using 80% enriched Ytterbium-168

RHS PRODUCTION/RIPTP USE TIMELINE	ATR	3 GW_{th} PWR
Lead Time for Penetrator	5 days	5 days

	Availability		
	Service Life	11 days	11 days
	Allowed Mission Duration	3.9 days	3 days
PERFORMANCE			
	BOS Penetration Capability	93 m	93 m
	EOS Penetration Capability	70 m	73 m
	BOS Penetration Rate	25 m/day	34 m/day
	EOS Penetration Rate	18 m/day	25 m/day

Heat source inventory concept for baseline radioisotope

The author proposes two different baseline radioisotope inventory concepts. The first concept is that the target assemblies would be left in the reactor for up to six fuel cycles (~ 1 year). A fresh target assembly would reach design power after the first fuel cycle. A RIPTP using this isotope would then be available for use at any time following 30 days from the time of notification of an operational requirement for a RIPTP. After being exposed for six fuel cycles in the reactor the target assembly would have to be replaced, during which time the target elements from the old target assembly would be available for use until the new target assembly had been sufficiently irradiated so as to provide the power required for mission performance.

The first inventory concept is consistent with a contingency response capability where RIPTP availability could be maintained with minimum notification time required prior to its possible employment. This approach would also be lower cost than the second proposed inventory concept.

The second inventory concept is that the target assembly would be replaced after every fuel-cycle, and the old (irradiated) target assembly used to produce a RIPTP. This RIPTP would be able to penetrate a DBHT emplaced under 80 meters of granite within some margin of design mission duration until the new target assembly was sufficiently irradiated to provide required power for a replacement RIPTP.

The second inventory concept would be most advantageous for RIPTP demonstrator development efforts (using the currently available ATR reactor) as the maximum number of penetrators could be produced and tested in a year. This approach would also provide the absolute minimum prior notification required for operational

availability of a RIPTP as a penetrator would always be assembled and available for use (if not otherwise committed for test).

With a new high flux isotope production reactor or alternative radioisotopes such as ytterbium-169 other inventory concepts would become feasible. Examples include reactor First In First Out (FIFO) radioisotope target inventory concepts, continuous target element extraction concepts, and flexible contingency planning concepts. In the FIFO inventory concept the target assemblies which had been irradiated in the reactor for the longest periods of time would be removed from the reactor periodically and replaced with new target assemblies. The target elements would be available for immediate use, while the inventory stored in the reactor would be available for use after some longer period following notification of an operational requirement. Continuous target element extraction concepts would operate in an analogous fashion to a pebble bed reactor, in that fresh target elements (or assemblies) would be continuously inserted and extracted from the reactor in small enough and sufficiently balanced insertions/withdrawals that reactor reactivity was not destabilized nor control rod reactivity control limits compromised. Other approaches would generally require the shut-down of the reactor for these reasons. The continuous concept would get around the complication of having to shut down the reactor any time the insertion or withdrawal of target assemblies was necessary. In a flexible contingency planning concept storage, reactor, and activated target assembly inventories would be adaptively adjusted based on month-to-month RIPTP operational requirements.

Feasibility conclusions

RHS radioisotope selection, performance, cost, producibility, and implied RIPTP employment timelines were investigated with respect to RIPTP feasibility. Candidate radioisotopes for powering a RIPTP were evaluated through a screening of the ENDF, NuDat, and MIRDS files of radioisotope properties, leading to the identification of thirteen potentially suitable radioisotope candidates. Sufficient information was available for the further evaluation of several of these candidates.

To evaluate performance, producibility, and costs, (and thereby facilitate selection of a particular radioisotope) a simple synthesis and sizing code was written. This code calculated radioisotope production in a nuclear reactor over the reactor's fuel-cycle, the quantity of penetrators that could be assembled from the produced radioisotope, and evaluated a simple model of the penetrators performance and thermal behavior vs. time.

Concentrations of radioisotope species vs. time as calculated by the code were then used to assess the RIPTP power density and shielding considerations with respect to both production and employment timelines, leading to the elimination of nine of the fourteen isotopes previously identified. Of the remaining five isotopes, thulium-170 was identified as the lowest-risk, safest, least-costly radioisotope for powering a development/demonstrator RIPTP capability. This determination was made on the basis of synthesis and sizing code results, available ENDF nuclear properties, and historical RHS technical reports.

Overall, the primary conclusion of the concept feasibility study is that RIPTPs capable of defeating a DBHT are producible using existing reactor facilities at unit costs comparable to those of historical munitions. RIPTPs making use of off-the-shelf and

least expensive technologies are likely to be limited to on the order of ten meters per day of penetration in igneous rock.

SAFETY INVESTIGATION

Determination of RIPTP concept feasibility and definition of a baseline conceptual design greatly facilitated an investigation of safety considerations. The overall purpose of the safety investigation was to arrive at an informed opinion regarding RIPTP viability with respect to safety. This purpose was pursued through an effort to identify, prioritize, and analyze possible safety concerns that could pose a risk to concept viability with the aim of identifying “show-stoppers” that would likely render the concept non-viable.

An investigation of safety considerations was pursued in four steps: literature research of related topics such as historical high power RHSs, RTGs, and radiation sources and studies of their safety and accident history; enumeration of safety concerns; prioritization of safety concerns for investigation; and (to the extent possible) execution of rough analyses to investigate the potential hazard magnitude of the highest priority safety concerns. Potentially significant safety concerns were assessed in the context of existing alternative munition hazards and existing socially accepted radioisotope applications to arrive at an opinion regarding probable RIPTP operational viability with respect to safety.

Background

It is necessary to define two important concepts at this point – *hazard* and *risk*. A hazard is a possible consequence, and risk is the statistically expected consequence. In

assessing RIPTP viability with respect to safety, risk is the more relevant factor as it matters little what *could* happen as compared to what's *likely* to happen.

Unfortunately, for a quantitative assessment of risk accurate to even a rough order of magnitude a great deal of information would be required about factors such as: RIPTP detail design; tactics and doctrine; operational safety procedures; delivery aircraft (and countermeasures/tactics); contingency response provisions; and enemy threat/target characteristics (air defense systems/tactics, DBHT characteristics, target geology, and procedures/doctrine/tactics). Realistically, experimental data and field trials followed by design/analysis iteration would also be required to develop practical relevant operational experience for estimating risk factors unique to a RIPTP. A quantitative risk assessment was not feasible at the present level of concept definition or with the schedule and funding available.

What could be done, however, was a qualitative assessment of safety concerns. This qualitative assessment consisted of: an identification and prioritization for further investigation of scenarios that could lead to realizing potential hazards present in a RIPTP; a quantitative assessment of worst case hazards inherent to the RIPTP concept; and a comparison of these hazards to the hazards inherent in known historical or existing systems (such as nuclear bombs, RHSs, RTGs, conventional munitions, etc.). Prioritization of concerns about various hazards was made on the basis of their: potential severity; uniqueness as compared to historically accepted munition hazards; plausibility of being a significant concern as determined in part from plausibility of their associated realization scenarios; and likely difficulty of engineering solution.

Literature research and observations

Society has employed significant numbers of high-power radioisotope devices for radiography, RHSs, food and medical instrument sterilization, RTG electrical power, and similar applications internationally for more than fifty years. Considering the widespread application of high power radioisotope devices there have been relatively few incidents of severe or fatal injury over the years, particularly within the last two decades. Further, as compared to typical historical collateral casualties from conventional munitions, typical acute casualties from radiation accidents from high power radioisotope devices have generally been comparable or significantly less in number of casualties per incident, and typically the nature of the injury has been less severe.

Historical approaches to mitigating radiation risks adopted by RIPTP

A number of typical engineering decisions/characteristics have historically been used to mitigate risk from radiation hazards. The most ubiquitous is the employment of a container which effectively shields individuals from inadvertent radiation exposure by absorbing radiation emitted by the radioisotope it contains. A robust shielding container greatly enhances safety as radiation is generally not apparent to individuals without the use of radiation detection gear.

Another engineering safety characteristic of historical RHSs, RTGs, and radiation sources is the employment of oxide, nitride, or similar chemical compound forms of radioisotopes with good chemical and thermal stability. RTGs and RHS for space applications originally took the approach of designing the radioisotope elements to completely combust during reentry and finely disperse their radioisotope at high altitudes with the intent that maximum concentrations of radioactivity on the ground would be

sufficiently diffuse as to be of negligible hazard. This approach however was less robust to other accident scenarios and was also unsatisfactory in the context of increasing levels of concern regarding low level radiation exposures. As a result, the design philosophy of safe dispersal of radioisotopes was abandoned in favor of robust containment of radioisotopes.

Instead of combustible radioisotope forms such as elemental metals, radioisotope oxides were chosen that would not support combustion and had refractory properties so they would tend not to burn, melt or volatilize and be dispersed. Low solubility compounds have also been preferred as they greatly mitigate risk from the scenario of introduction of radioisotope into groundwater or the food/ecology cycle (the relatively low risk posed by release of plutonium is due to its very low solubility in water and its low uptake rates in the gastrointestinal system in the body). These radioisotope compounds were contained as pellets within heat and chemical resistant cladding and these pellets contained within individual aeroshells capable of surviving reentry. Impact resistant shells are also typically employed in the design of radioisotope systems. Another safety related characteristic of RHS and RTG systems is employment of passive mechanisms for heat rejection to mitigate hazards that might occur due to thermal damage resulting from loss-of-coolant accidents.

This overall approach has been highly successful for space applications in preventing any significant releases of radioisotope to the environment. Later Soviet and US RHS pellet designs bear a strong resemblance to one another, suggesting that nuclear engineers of both countries believe in the same principle elements of this engineering approach. A RIPTP could also employ all of these historically proven individual

elements for robust RI containment: an external case which effectively shields all hazardous radiation emissions; an incombustible, refractory radioisotope compound of low solubility; chemical and heat resistant cladding of individual radioisotope pellets; a tough, refractory, impact-resistant containment system for the clad radioisotope pellets; and a passive cooling system capable of preventing significant thermal damage to the RI containment system.

Additional approaches to mitigating radiation risks adopted by RIPTP

As distinct from historical RHS, RTG, and other radioisotope applications, a RIPTP could incorporate a number of major characteristics that would enormously enhance its safety. For example, most historical high-power radioisotope sources have all used fairly long-lived radioisotopes. This has directly contributed to some incidents of accidental radiation exposure as radioisotope devices have been: lost track of (due to dissolution of companies or countries which own them, or change in ownership of companies); stolen from the field; stolen from safe-storage; improperly disposed of in conventional junkyards; and introduced to illegal commerce. The utilization by a RIPTP of a short-lived radioisotope enormously mitigates risk associated with all of these hazards. Instead of having to maintain secure control over a RHS for decades or several centuries to assure radiation safety, a RIPTP RHS would only have to be controlled for a period of a few years to assure radiation safety. The short half-life would further reduce the possibility for resale or diversion of a RIPTP RHS as it would so rapidly decay as to render its possible period of usefulness to illegitimate customers very transient.

Potential radiation hazard from a RIPTP would be extremely short in comparison to most historically accepted radioisotope applications due to the employment of a short

half-life radioisotope (Figure 44). Presence of long half-life radioisotopes increases the duration of potential hazard posed by some radioisotope accident scenarios as well as the potential duration of economic and social impacts (remediation/condemnation of contaminated and, long-term evacuation, etc.). For example, general consensus on the impact of a dirty bomb is that cost in lives and health would be relatively slight as compared to a conventional weapon attack, but the cost in clean-up and/or condemned property/land would likely be disproportionately large.

This assessment of relative magnitude of effects is consistent with what was seen in the Chernobyl accident, the worst accident in nuclear power history. Radiation accounted for 28 prompt fatalities, and is estimated to have accounted for on the order of ten deaths from cancer in the first 10 years following the accident. In contrast more than 370,000 people were evacuated from the surrounding land, with 4300 square kilometers condemned. Monitoring and remediation efforts continue as of the present date, eighteen years later. The duration of the impact of Chernobyl in these respects is entirely due to the presence of large quantities of long-lived radioisotopes and their associated enduring hazard. The potential for an enduring hazard is entirely absent in a RIPTP device due to the employment of short-lived radioisotopes.

Another safety principle adopted for a RIPTP device is production of radioisotope in final form. This is unique as compared to most widely fielded radioisotope devices (with the principle exception of cobalt-60 gamma-ray sources). The advantage is that production of radioactively contaminated manufacturing materials and radioisotope by-products are minimized, resulting in lower impact from manufacture to both the environment and society.

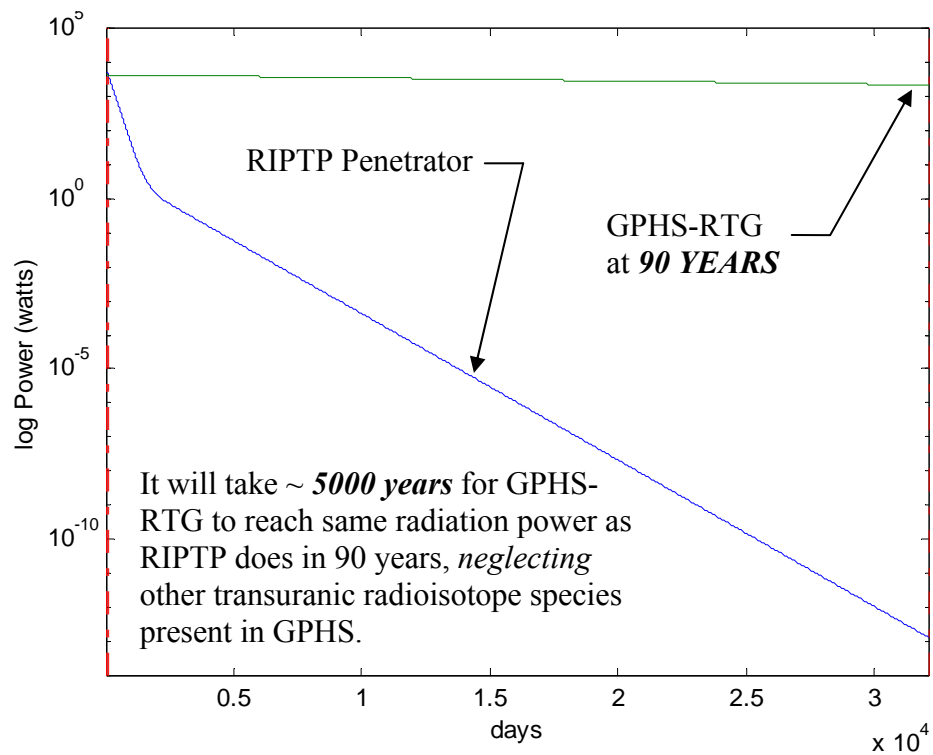
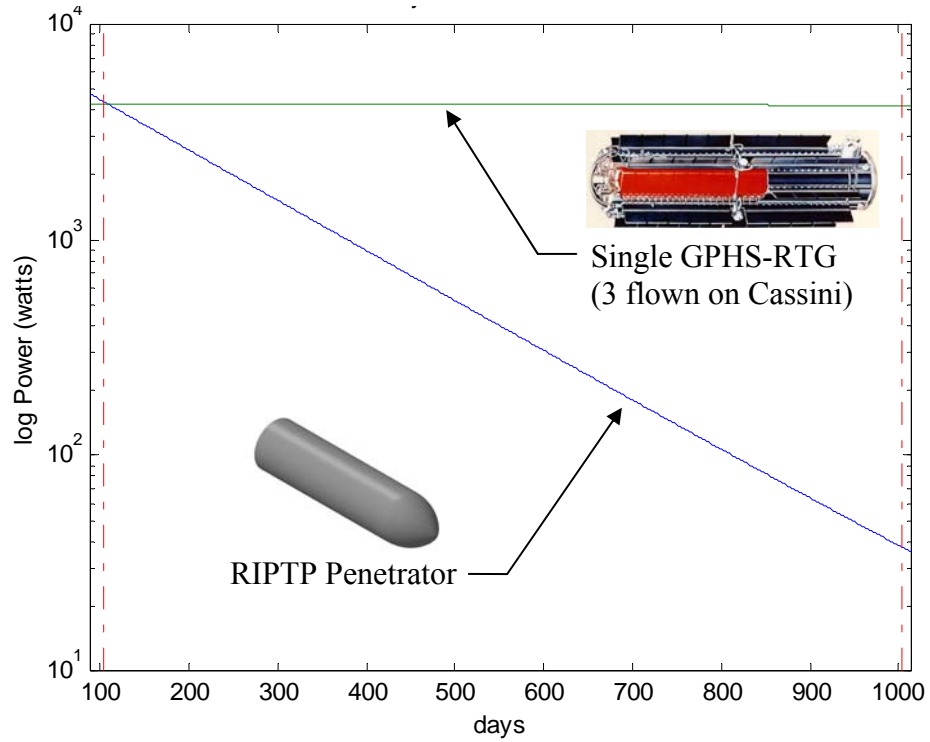


Figure 44: Comparison of radioactivity vs. time of GPHS-RTG and baseline RIPTP

Notable differences with respect to risk in characteristics of a RIPTP as compared to historical RHS systems

In some ways the engineering challenges of designing a safe RIPTP could be significantly less than those overcome by historical RHS applications, particularly for space power. This is relevant as in spite of the significant technical challenges involved in designing, building, and flying a space-rated RHS, such systems have enjoyed good operational safety records. Space RHS systems are flown on vehicles which suffer significantly higher catastrophic loss rates as compared to modern US combat aircraft in recent conflicts. Space RHS systems have to be capable of surviving hypersonic reentry prior to ground impact – hypersonic reentry is a challenging design requirement not faced by RIPTPs. Space RHS systems have more stringent weight limitations reducing the amount of structure that can be used to mitigate risk of radioisotope release and greatly limiting the materials allowable in fabrication – unlike a RIPTP, large quantities of tough refractory metals would be non-viable with respect to their impact on flight weight. Space RHSs are launched on top of vehicles with change in velocity potentials on the order of ten kilometers per second, increasing the maximum potential velocity for accelerated impacts. Launch vehicles contain many tons of highly flammable fuels and pure oxidizers, explosive in combination and with the potential of acting as accelerants for a fire or undergoing direct chemical reactions with RHS materials. RIPTPs as distinct from RHSs would also only be employed in times of war in situations specifically requiring their use when hazard to the countries involved and/or their citizens already existed and might potentially be mitigated through the option of employing a RIPTP. In these and similar ways the challenges for designing a robust RIPTP of acceptable safety

risks could be considered significantly less compared to some of the challenges of designing an RHS for space applications.

However, in some other notable ways the challenges faced in designing a robust RIPTP are unique and/or more challenging than for a space RHS application. Unlike a RIPTP, it is highly unlikely that an RHS or the vehicle which carries it will be engaged by hostile enemy forces doing their best to destroy it – high explosive charges, shaped charge jets, ballistic projectiles and high velocity shrapnel are all credible threats that might be faced by a RIPTP during delivery. Space RHSs are nominally secured and carefully controlled at all times until launched into space where they will be immune from direct human interference – a RIPTP would nominally be dropped into a hostile battlefield environment where deliberate direct human interference must be anticipated and its potential impact mitigated. Enemy diversion or co-opt of a RIPTP is also more credible (although the duration of the potential for such a hazard would be greatly less than for historical RHSs and RTGs due to the short half-life radioisotope used).

While ground RTG applications have had fair safety records and face similar potentials for human interference (as has occurred on occasion), the severity of the motivation for human interference is not as great, ground RTGs are typically used in remote locations where interference may be less likely, and the level of control over the RTG may be better than would be the case for a RIPTP. These last two considerations might actually favor a RIPTP in most nominal scenarios as a RIPTPs kinetic penetration and thermal self-burial could make it more difficult to interfere with than typical ground RTG systems. Lastly, the number of RIPTPs that might be employed at once could be larger than the number of RHS/RTGs employed at a given time.

Overall, considering similarities and dissimilarities to historical systems, the most important safety-related advantages a RIPTP would have compared to historical RHS/RTG systems would be its short half-life radioisotope, its kinetic/thermal self-burial, and its lower weight restriction. The most important safety-related disadvantages a RIPTP would have compared to historical systems are the fact that the aircraft carrying it and the RIPTP Munition itself would be targets of hostile forces employing heavy weapons, and that the RIPTP would potentially be subject to highly motivated direct enemy interference.

Other aspects of potential safety risk identified from literature

Theft of RHS, RTG, or other radiation sources have been historically identified as a cause of an important fraction of significant radiation incidents resulting in injuries. Such devices can be attractive for theft due to the large quantities of readily salable lead shielding or precious metals included in their containers, and/or for the value of the radioisotopes themselves. This has most typically been a problem in countries where appropriate material control and security provisions were not made, such as the states of the former Soviet Union, South American countries, and the like.²⁸⁵ Implementation of proper security procedures for a RIPTP could avoid such hazards prior to the devices employment, however the concern would obviously be an important one on a battlefield.

Due to the valuable refractory materials used in the RIPTP case and the novelty of a self-heating object, if a RIPTP were somehow exposed on the ground some incautious individuals might well attempt to abscond with the device, cut it up, and/or sell it (during its first year of life it would have to be a *very* incautious individual due to the high initial RIPTP temperatures). Deliberate dismantlement of dangerous radiation sources by

thieves to increase their portability has historically been seen and lead to fatal incidents of radiation poisoning.

On the other hand, the consequences of such incidents have not historically been dissimilar in severity or number of affected individuals per incident than those from similar behavior with conventional munitions – i.e. collecting, dismantling, and scavenging activities with Unexploded Ordnance (UXO) on battlefields. The maximum possible period of existence of potential hazard from such activities would be significantly less for a RIPTP than for UXO or historical RHSs/radiation sources as the radioisotope in an unrecovered RIPTP left on a battlefield would exponentially decay to very low levels within a few years. Regardless, the author assumes that reasonable provisions would be made for recovery of lost or improperly penetrating RIPTPs such that the hazard of exposed RIPTPs going unrecovered by appropriate authorities was slight.

General hazard from this type of scenario is further reduced due to the negligible levels of radiation emitted by an intact penetrator and the fact that the hazard should be slight for nominal RIPTP scenarios as the weapon will kinetically bury itself below the surface and self-dispose deep underground. Also, as compared to more typical lead radioisotope containers generally used in historical RHS or radiation source incidents, the tough refractory case proposed by a RIPTP makes it unlikely that thieves could cut up a RIPTP absent their use of capabilities typical of a well-equipped modern machine shop (diamond bits, electro-discharge machining, etc.).

Enumeration of safety concerns

Safety concerns were enumerated through four steps. First of all, as previously discussed, historical literature related to RHSs, RTGs, and radiation source safety studies/incident history was surveyed and the engineered safeguards employed in the literature and accident/incident history were used to identify potential concerns. Secondly, potentially novel safety concerns were brainstormed and sorted according to common characteristics. Thirdly, a hierarchical classification of these concerns was created and the brainstormed concerns organized according to the hierarchy. Fourthly, this hierarchical list was then used as the basis for a more methodical effort to exhaustively identify possible safety concerns by looking for gaps in the hierarchy that corresponded to analogous but unrepresented entries.

The first level of the safety concern hierarchy was hazard modalities (Table 39). The individual listings in this table represent the unique modalities through which a RIPTP could impart energy and thereby cause casualties or damage to equipment. The second level of the safety concern hierarchy was hazard outcomes (Table 40, Table 41) – that is, the general types of outcomes that could occur exhibiting the specified hazard modality. The third level of the safety concern hierarchy was outcome realization scenarios, Table 42. These scenarios are the general categories of events that might result in the corresponding hazard outcome.

As an example of how gaps in the hierarchical list were used to identify additional possible safety concerns, suppose that only Radiation and Thermal hazard modalities have been identified. It is apparent that both of these modalities represent modes for the accomplishment of work – an obvious corresponding question to ask is what other modes

for accomplishing work exist? Logically both chemical and kinetic hazard modalities are then identified. At the two lower levels in the hierarchy (hazard outcomes and realization scenarios), analogous or similar outcomes can be used to identify additional potential hazard outcomes or realization scenarios within or between hierarchy categories.

Table 39: Hazard modalities

TYPES OF EFFECTS	DISPOSITION
Radiation hazard	Significant and unique* to RIPTP
Thermal hazard	Constant power production by RIPTP makes thermal hazard inherent and significant
Kinetic hazard	Non-unique – hazard to non-combatants similar to a concrete bomb
Chemical hazard	Non-unique and comparable to or less severe than conventional munitions ²⁸⁶

* as compared to conventional munition...

Besides listing outcomes corresponding to the various hazard modalities, Table 40 and Table 41 list approaches identified by the author for mitigating the risk posed by each identified hazard outcome. Those relevant to the present conceptual level investigation of a RIPTP were adopted by the author for the baseline RIPTP design.

Table 40: Hazard outcomes – radioisotope outcomes

RADIOISOTOPE OUTCOMES	ENGINEERING ROUTES TO MITIGATE RISK
Human exposure to intact RIPTP radiation	Selection of RI with shield-able emissions Design with adequate/redundant shielding
Release of RI into aquifer	Design RI containment to be robust Redundant containment mechanisms Select short half-life RI Select RI compound with low solubility Select RI compound with low chemical reactivity
Release of RI into groundwater	“ same as above
Release of RI into rock melt	Select RI containment material to be robust to solution/corrosion/embrittlement by rock melt Select short half-life RI Select RI compound with low chemical reactivity Select RI compound with low solubility in rock
Explosive RI dispersal in air	Design RI containment for blast resistance Protection of RIPTP by aeroshell

	<p>Low frangibility RI form/material</p> <p>Anti-missile countermeasures for aircraft and/or RIPTP</p> <p>Mission profile design to mitigate hazard from enemy missiles</p> <p>RIPTP employment tactics to mitigate probability of enemy interception/ interference</p>
Evaporative RI dispersal in air	<p>Select non-volatile, non-chemically reactive RI compound</p> <p>Select RI with radiation emissions with minimal kinetic energy deposition (alpha radiation not preferred)</p> <p>Limit maximum RI power density</p>
Combustive RI dispersal in air	<p>Select non-volatile, non-chemically reactive RI compound</p> <p>Limit maximum RI power density</p>
Fragmentation and dispersal over ground	<p>Explosive/ballistic resistance of RI containment</p> <p>Protection of RIPTP by aeroshell</p> <p>Low frangibility RI form</p> <p>Anti-missile countermeasures for aircraft and/or RIPTP</p> <p>Mission profile design to mitigate hazard from enemy missiles</p> <p>RIPTP employment tactics to mitigate probability of enemy interception/ interference</p>

Table 41: Hazard outcomes – radioisotope production and thermal outcomes

RADIOISOTOPE PRODUCTION OUTCOMES	
Reactor excursion outcomes due to isotope production target induced reactivity fluctuations	Standard isotope target design, safety analysis, and reactor operation practices sufficient.
Hazard outcomes associated with increased fissile radioactive waste inventory due to radioisotope production	Most mitigated by use of existing PWR reactor facilities or replacement of reactivity shims in isotope production reactors with RI production targets... would result in production of little or no incremental high level nuclear waste
THERMAL OUTCOMES	
Contact burns to individuals	Active cooling during general storage/ground-handling + insulation of designated handling points (RIPTP munition lift-points, etc.) Ground-handling and storage procedures

	Appropriate ground-handling and storage equipment Appropriate personnel training.
Burns/smoke inhalation resulting from induced fire	Active cooling during general storage/ground-handling Fail-safe cooling with redundant passive cooling mechanisms Ground-handling and storage procedures Appropriate emergency procedures and equipment Suitable personnel training Minimization of combustible/thermally decomposable materials in RIPTP design
Damage to equipment and infrastructure	“ same as above Adequate systems engineering
Damage to RIPTP munition	“ same as above Insulation/thermal isolation of heat sensitive components such as tail-kit/guidance system electronics.

A key consideration in assessing the relative likelihood of various outcomes is the scenarios which can lead to their realization. Sample outcome realization scenarios identified by the author are listed below in Table 42. The relative importance of each of the outcomes was judged on the basis of the likelihood of the scenario occurring, the difficulty of engineering solutions to avoid the scenario or mitigate the hazard resulting from the scenario, and of course the anticipated relative severity of the consequence if the hazard outcome was realized as a result of the scenario.

Table 42: Sample of outcome realization scenarios

HUMAN EXPOSURE TO INTACT RIPTP RADIATION

- Ordinary handling of munition on ground
- Inadvertent separation of munition from aircraft resulting in non-destructive/non-penetrating ground impact at unintended location
- Loss of aircraft resulting in loss of RIPTP
- Production of steam by RIPTP ejects penetrator from ground post penetration – exposure of non-combatants/recovery personnel to RIPTP w/o aeroshell
- “Fish-hooking” of RIPTP upon separation from aeroshell/penetration into ground resulting in RIPTP penetrator resting on surface above target

RELEASE OF RI INTO AQUIFER/BODY OF WATER

Thermal shock leading to RI containment fracture
Chemical corrosion of RI containment
Embrittlement of RI containment leading to containment fracture
Containment fracture in nominal impact
Deliberate enemy action recycling RIPTP for dirty bomb attack

RELEASE OF RI INTO GROUNDWATER

Thermal shock leading to RI containment fracture
Chemical corrosion of RI containment
Embrittlement of RI containment leading to containment fracture
Containment fracture in nominal impact
Deliberate enemy action recycling RIPTP for dirty bomb attack
Inadvertent enemy action (thermal shock from water immersion during fire-fighting, attempt to counter with explosives, inadvertent mechanical fracture)

EXPLOSIVE RI DISPERSAL IN AIR

Intercept of RIPTP by guided missile
Impact of RIPTP by explosive shell
Detonation of other ordnance carried by aircraft
Deliberate enemy action recycling RIPTP for dirty bomb attack

FRAGMENTATION AND DISPERSAL OVER GROUND

Intercept of RIPTP by enemy guided missile
Impact of RIPTP by explosive shell
Detonation of other ordnance carried by aircraft
Deliberate enemy action recycling RIPTP for dirty bomb attack
Nominal impact scenario + embrittlement of RIPTP case
Nominal impact scenario + weakening of RIPTP case due to cooling failure
Adverse impact scenario (attached to plane, off-nominal impact angle, of RIPTP at elevated temperature, of explosive or ballistically damaged RIPTP, etc.)

COMBUSTIVE RI DISPERSAL IN AIR

RI initiates fire resulting in adverse cooling environment, self-heating + environment is sufficient to compromise case, RI material burns
Same scenario, other than RIPTP fire initiation source
RIPTP penetrates into a coal, peat, or other seam of fuel leading to an underground fire, no/minimal penetration by the RIPTP, & insulation of the RIPTP leading to case failure and RI compound melting/volatilization
Scavengers attempt to cut RIPTP up for transport and resale of case materials/radioisotope materials initiating RI material combustion
Damage to equipment and infrastructure resulting from RIPTP thermal power (non-combustion and combustion scenarios)
Damage to RIPTP munition from thermal power – structure, guidance system, material properties, coatings

Prioritization of safety concerns

The identified safety concerns were prioritized using engineering judgment on the basis of their apparent historical importance, probable difficulty of mitigating, consequence if occurring, and qualitative likelihood of occurring. The highest priority concerns were then selected for further analysis on the basis of the difficulty of performing the analysis and the available resources so as to best support an informed opinion on RIPTP viability with respect to safety.

Hazard modality prioritization

Examination of the nature of kinetic and chemical hazards that would be present for a RIPTP lead the author to the conclusion that neither were significant with respect to the safety-related viability of a RIPTP. The potential kinetic hazards to individuals on the surface posed by a RIPTP should be greatly less than for a typical conventional munition. As far as chemical hazards, the chemically unique component of a RIPTP with respect to conventional munitions is the use of rare earth oxide materials for the RHS. Research of the toxicology of such materials indicates they are relatively benign. As a result, both of these hazard modalities were not further investigated in this study.

Radiation hazard is the principle unique hazard modality associated with a RIPTP and was judged by the author to be the principle likely discriminator regarding concept viability. Thermal hazard modalities are unique and potentially significant, but secondary to radiation hazard modalities. Of the categories of radiation hazard outcome within the radiation hazard modality, production related outcomes were neglected as safety standards in the nuclear industry are well developed and have had a good track record.

Hazard outcome prioritization

Early on, the hazard outcome of exposure of humans to intact RIPTP emissions was the priority hazard outcome of concern. This was because the author was attempting to identify a producible radioisotope that could meet performance requirements *and* be compactly shielded so as to avoid significant external radiation. Without such a radioisotope radiation hazard would be greatly higher for friendly forces, noncombatants and combatants. Further, the author had appropriate tools and resources for the analysis of shielding requirements.

The ranking of the remaining hazard outcomes in order of priority were: combustive dispersal in air; fragmentation/dispersal over ground; explosive dispersal in air; release of RI into aquifer; release of RI into groundwater; and release of RI into rock melt.

While chemical participation of thulium or ytterbium oxides in a combustive process is unlikely due to their chemical stability, vaporization and dispersal in smoke is plausible given sufficiently high temperatures as could be facilitated by a combination of fire and RI self-heating. If such scenarios were plausible, literature and engineering intuition suggests that combustive dispersal of radioisotope might transform large fractions of the radioisotope into respirable size particles which could be widely dispersed on the smoke plume. This is significant as for relatively insoluble radioisotopes inhalation is the most dangerous route of ingestion. Thus combustive dispersal was ranked highest for further analysis. Evaluation of the plausibility of combustive dispersal scenarios was a prime motivator for the chosen safety realization scenarios' prioritization described in the next section.

Fragmentation/dispersal over ground was judged to be the next worst hazard outcome due to its relative plausibility in the context of battlefield damage from heavy weapons, thermal shock, and off-nominal ground impact. The potential in such scenarios for exposure of individuals on the ground to unshielded radioisotope leads to significant concern about the potential risk.

Explosive dispersal of RI was ranked next, with its high relative ranking due to the potential for production of respirable size particles. Hazard was estimated to be less than for a combustive scenario as it would be less likely to produce respirable sized particles. Risk was judged to be less than for a bulk fragmentation scenario as more energy would be required to compromise a RIPTP case and pulverize RIPTP RHS radioisotope materials than would be required to simply compromise a RIPTP case or break a RIPTP into multiple large fragments.

Releases of RI into an aquifer or groundwater were ranked towards the end of the list. In order to pose a significant radiotoxicity hazard in such a scenario, both the RIPTP case and RI target encapsulation would have to be compromised in such a way that RI leached into the water in potentially toxic quantities, then the water-borne radioisotope would have to be transported to a location where it could be consumed. Low solubility compounds of short-lived radioisotopes have been specified for the baseline RIPTP concept. As a result there would be a relatively small radioisotope rate of contamination due to low solubility, radioisotope dilution from diffusion/mixing in the water, and exponential decay of the radioisotope with time as it was transported away from the source. It seems comparatively unlikely to the author that significant risk would exist for

a well designed RIPTP from radioisotope contamination of water, particularly in the context of the lower RI migration rates that would be expected in groundwater.

Last in the ranked list of hazard outcomes was release of radioisotope into rock melt. The author believes this outcome is relatively amenable to engineering solution. Further, due to the short half-life of the radioisotope candidates selected, as long as release occurred after the melt-shaft closed and became a melt-bubble any significant risk would principally be for occupants of a DBHT. Released radioisotope would mix with rock melt and form a vitrified or crystallized material upon cooling. Exposure to such material in a DHBT could easily result in injurious levels of exposure to occupants, but hazard to the world at large should be modest as compared to other scenarios. Absent direct exposure to the rock melt soon after RIPTP employment little risk would be associated with this scenario as heat production by the radioisotope makes intrusion/contamination of water unlikely – and otherwise the material is contained underground for longer than required for the safe decay of radioactivity. Unconfined radioisotope rock-melting schemes analogous to the described outcome of RI release into groundwater have historically been proposed and seriously evaluated for safe disposal of high-level nuclear waste, further reducing the level of concern. Also, with regard to potential corrosive compromise of a RIPTP case by rock-melt, while the literature supports concern regarding the potentially corrosive nature of rock-melts, it also suggests that corrosion issues can be dealt with using appropriate coatings/materials.

After prioritizing the hazard outcomes as discussed above, the likelihood of combustive RI dispersal was further investigated through thermal analysis of realization scenarios (detailed later). As discussed in the next section, combustive dispersal

scenarios were found to be implausible for a RIPTP with power density, total power, and materials similar to those proposed by the author for a baseline RIPTP. After resolving to their satisfaction the concern of combustive dispersal, the radiation hazard posed by bulk-fragmentation of a RIPTP was analyzed for a representative scenario. Next, the explosive dispersal radiation hazard outcome was evaluated through analysis of a scenario involving complete explosive dispersal of a RIPTP into respirable size particles and compared to the impact of an identical scenario for a Cassini type General Purpose Heat Source – Radioisotope Thermoelectric Generator (GPHS-RTG), as well as the historical results from a low-yield underground nuclear bomb detonation. After completion of these analyses, insufficient resources remained for similar investigations of the lower priority aquifer, groundwater, and rock melt hazard outcomes.

Realization scenario prioritization

The highest priority realization scenarios were judged by the author to be thermal management related scenarios as a category – particularly those having to do with fire – followed by thermal shock, ballistic damage, accelerated oblique impact into a hard material such as rock or steel plate, and blast tolerance. Resources were not available for detailed evaluation of most of the above considerations (investigation of most of these issues will require iterative analysis/design efforts at a fairly detailed level of design).

It was decided to further investigate thermal management considerations in general, however, as the observation was made that thermal management related considerations were a primary contributing factor to both the probability of occurrence of many realization scenarios as well as their likely severity. For example, melting of RHS or case materials due to fire, loss-of-coolant scenarios, and/or overheating in granite melt

all could theoretically lead to a failure of containment/shielding and potentially to release of RI materials. Further, the degree of RI self-heating would contribute both to the likelihood of containment failure as well as the severity of RI dispersal after a hypothetical containment failure. Fire was identified as a particularly important safety scenario for further analysis as the baseline RIPTP concept is *by design* intended to initiate fires in a DBHT. If a RIPTP functions as an incendiary as intended, and release of radiation even in an enemy DBHT is unacceptable, then a RIPTP *must* be capable of withstanding prolonged exposure to fire. As a result, fire was a primary safety scenario the author identified for further investigation.

In a similar vein, the degree of difficulty of providing adequate cooling for a RIPTP under nominal or off-nominal conditions could also contribute to degradations in material properties that could facilitate RI containment failure in all mechanical damage scenarios (such as ballistic impact, explosive blast, off-nominal ground impact, etc.). Thus, the importance of characterizing the requirements for cooling a RIPTP in nominal scenarios and the robustness of the RIPTP in adverse cooling scenarios were again identified as critical safety factors.

As a result, the author chose to perform a cooling analysis to investigate the difficulty of using evaporative cooling to maintain the temperature of a RIPTP at 100° C Figure 45. It can be seen that the quantity of water evaporated by a baseline thermal penetrator per hour is fairly modest and heat loads should not pose much challenge for a passive cooling system. This conclusion is further supported by the fact that the initial power of the baseline penetrator is similar to that of a Cassini-type GPHS-RTG which can safely employ passive radiative cooling.

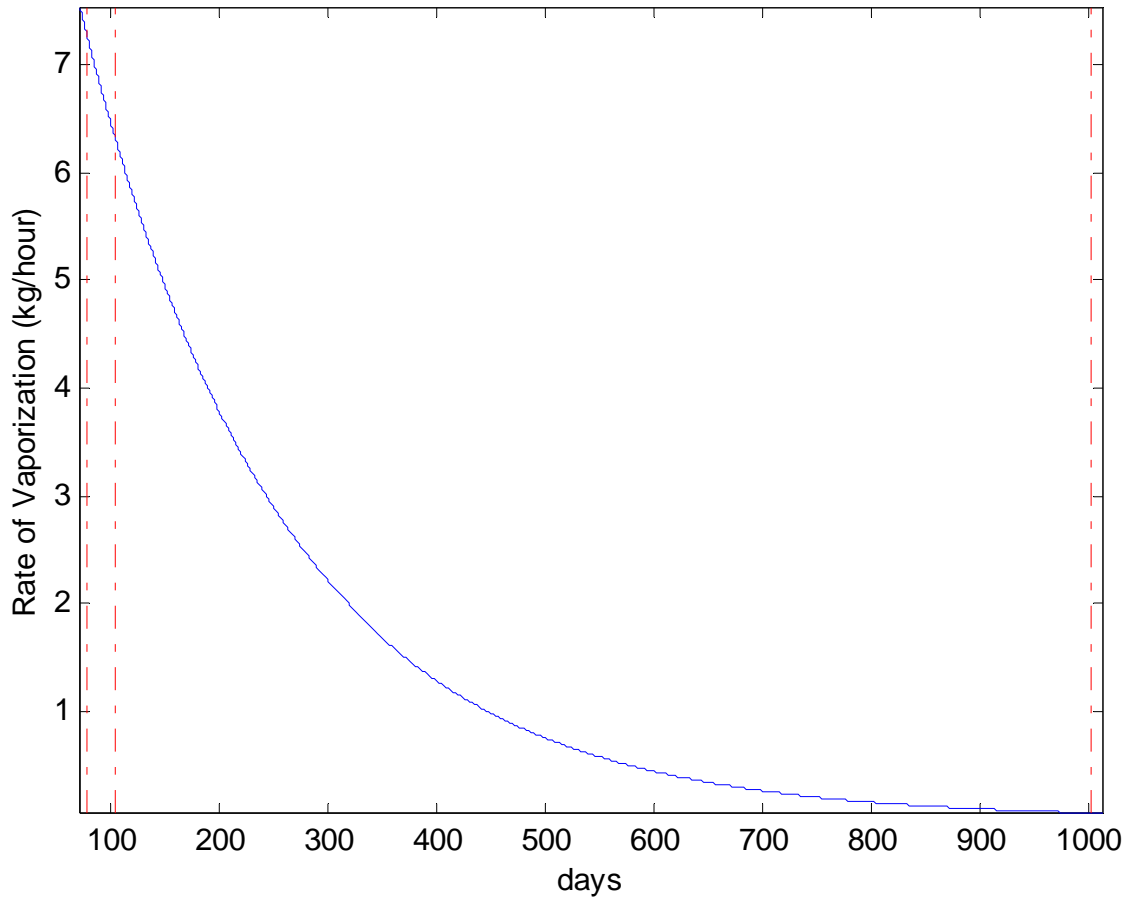


Figure 45: Rate of vaporization of saturated water by RIPTP vs. time

To further explore the degree of challenge posed by RIPTP self-heating and material temperature limitations, the author performed simple steady-state maximum temperature analyses for a RIPTP case and RHS centerline for several representative nominal and adverse cooling scenarios. The derivation of the conservative approximations for maximum steady state core and case material temperatures is given in the section “Estimation of Thermal Penetrator Internal Temperatures” on page 165. Note that these equations overestimate the maximum temperatures for a RIPTP of the baseline pill-shaped geometry.

The approximations of steady-state maximum case and core material temperatures were used to estimate the challenge of RIPTP cooling given: various RIPTP heat-transfer scenarios; RIPTP power density/total power; and representative material properties for the case, RHS, and granite melt. Scenarios considered included RIPTP: immersion in boiling water (Figure 46); exposure to an adverse radiative environment without convective cooling (intended to give a first-order estimate of the impact of a fire – Figure 47); immersion in circulating granite melt (viscosity neglected – Figure 48); and immersion in non-circulating granite melt without penetration (Figure 49). In each of the referenced figures the melting temperatures for thulia and tungsten are given as an upper bound for the maximum acceptable material temperatures.

A potentially critical design consideration identified by the author as a result of these simple thermal analyses is the poor thermal conductivity of thulium-oxide, especially at high temperatures. The author found it necessary to assume that the isotope target element encapsulation and or RHS filler (or other RHS component) materials would provide an increase in bulk RHS thermal conductivity from on the order of 2 watts/meter-Kelvin to 20 watts/meter-Kelvin.^{†††}

A check on the reasonableness of obtaining a 20 watt/meter-Kelvin bulk RHS thermal conductivity was performed as follows: an estimate of achievable bulk thermal

conductivity can be made using the rule of mixtures: $k_{bulk} \approx \frac{k_{Tm_2O_3} \cdot V_{Tm_2O_3} + k_{filler} \cdot V_{filler}}{V_{total}}$.

^{†††} Note that one implementation of an RHS the author has previously stated attractive is that of spherical radioisotope target elements close-packed to comprise the radioisotope component of an RHS. If such pellets were filled into a container to comprise an RHS, it is obvious that it would be unacceptable for the 26% minimum void space (for close-packed spheres) to be filled with vacuum as bulk thermal conductivity would be much worse than the already inadequate ~2 watts/meter-Kelvin exhibited by thulium-oxide. This argues for selection of either thin disk geometry radioisotope target elements spaced with higher thermal conductivity disks (this is the historically favored approach) or high thermal conductivity filler for the inter-sphere void space.

This can be rearranged and the desired bulk thermal conductivity, estimated filler conductivity (assumed to be the value used for tungsten), and thulium oxide thermal conductivity substituted to arrive at an estimate of volume fraction for the thulium oxide:

$$\frac{V_{Tm_2O_3}}{V_{total}} = \frac{k_{bulk} - k_{filler}}{k_{Tm_2O_3} - k_{filler}} = \frac{(20-80)w / mK}{(2-80)w / mK} = 77\%.$$

Since a baseline thulium oxide volume fraction of only 66% has already been assumed, this crude analysis suggests that the known issue of poor thulium-oxide conductivity should be correctable by employing a higher thermal conductivity refractory material in the RHS design. Options for such a material would include the refractory metals and graphite (metals ~100 watts/meter-Kelvin, graphite ~ 50 watts/meter-Kelvin). Graphite has previously been proposed by Walter and others for this purpose, and development of thulium-oxide refractory metal cermets was no doubt motivated in part by this consideration.^{280, 283} Thermal conductivity should pose less of an issue for radioisotope candidates that could reach higher power densities (such as 80% enriched ¹⁶⁸Yb Yb₂O₃), as a greater fraction of material having a high thermal conductivity could be incorporated in the RHS design without compromising power density.

Evaluation of the various cooling scenarios identified by the author suggests that robust RI containment should be manageable for most nominal scenarios and adverse scenarios. *However, the author's evaluation of cooling in molten granite identified a potential concern.* The assumption of perfect convective cooling of a RIPTP in molten rock such that the external temperature of the penetrator matches that of the molten rock (Figure 48) is obviously non-conservative given the high viscosity and very low thermal conductivity of molten granite, boundary layer effects, etc. Evaluation of the opposite extreme – non-penetrating immersion in molten granite without convection (Figure 49) is

very conservative and indicates that exceeding of the melting temperature of both the refractory isotope and case can not be ruled out without more detailed analysis.

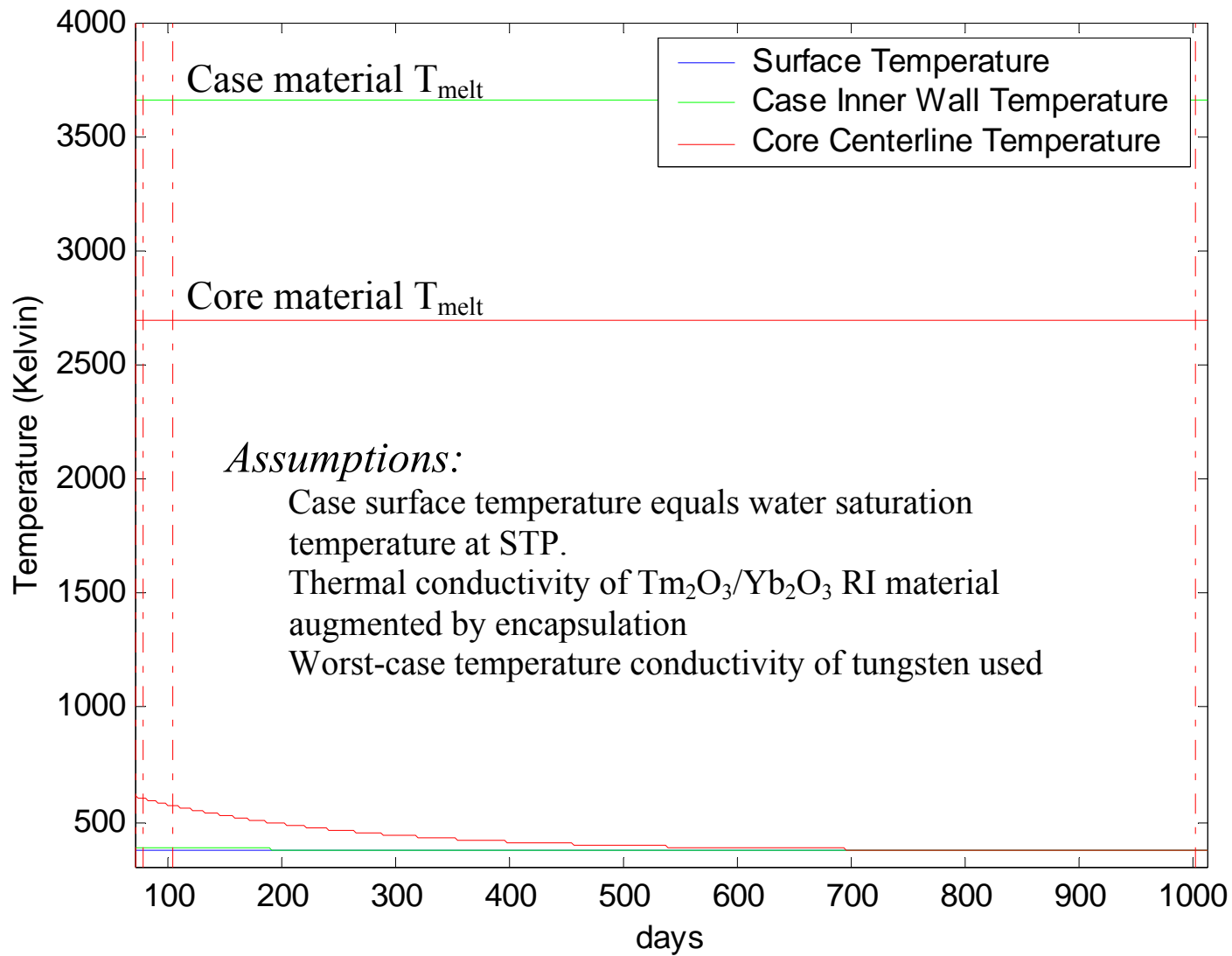


Figure 46: Equilibrium temperature vs. time for water cooled RIPTP

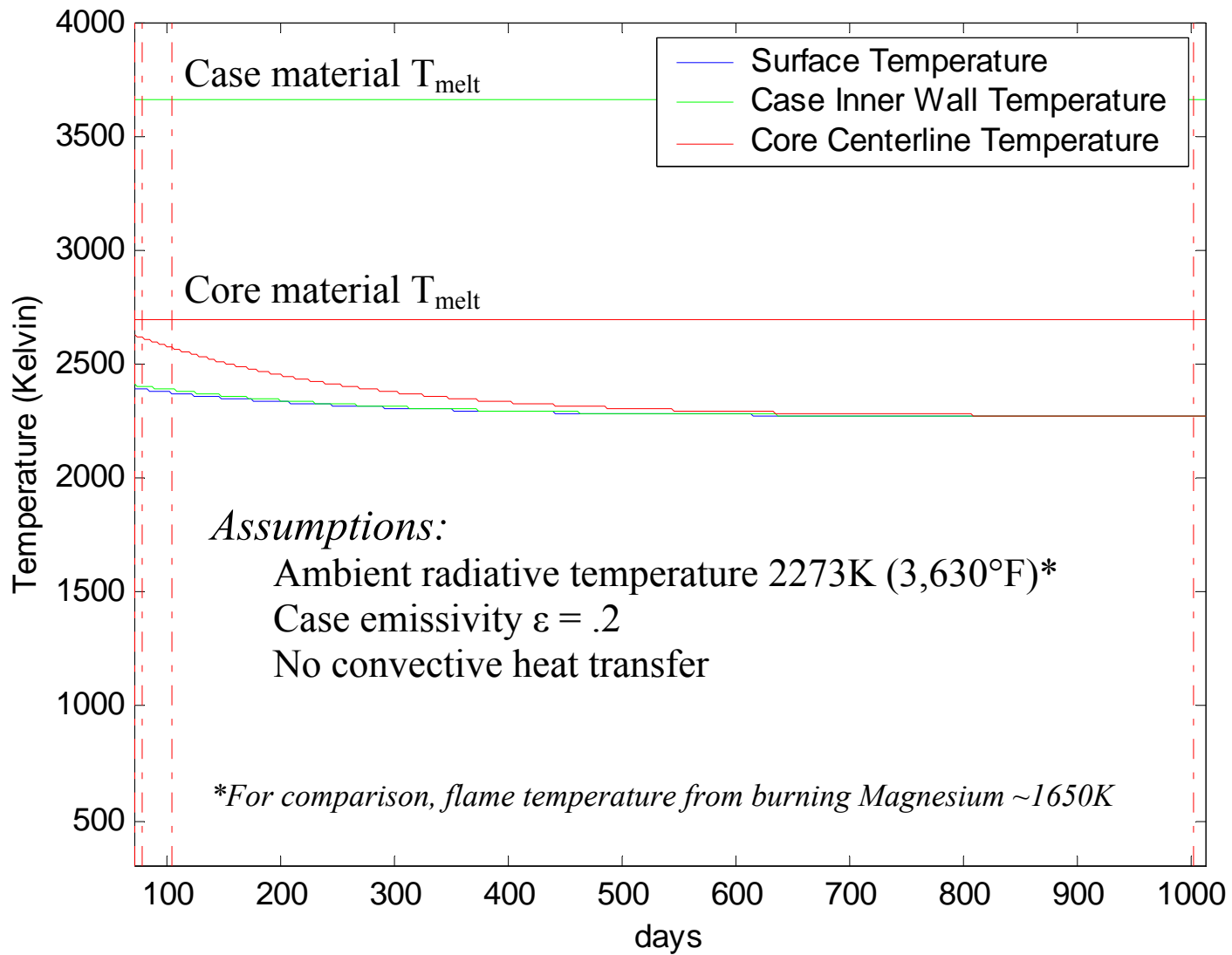


Figure 47: Equilibrium temperature vs. time for RIPTP in adverse temperature environment

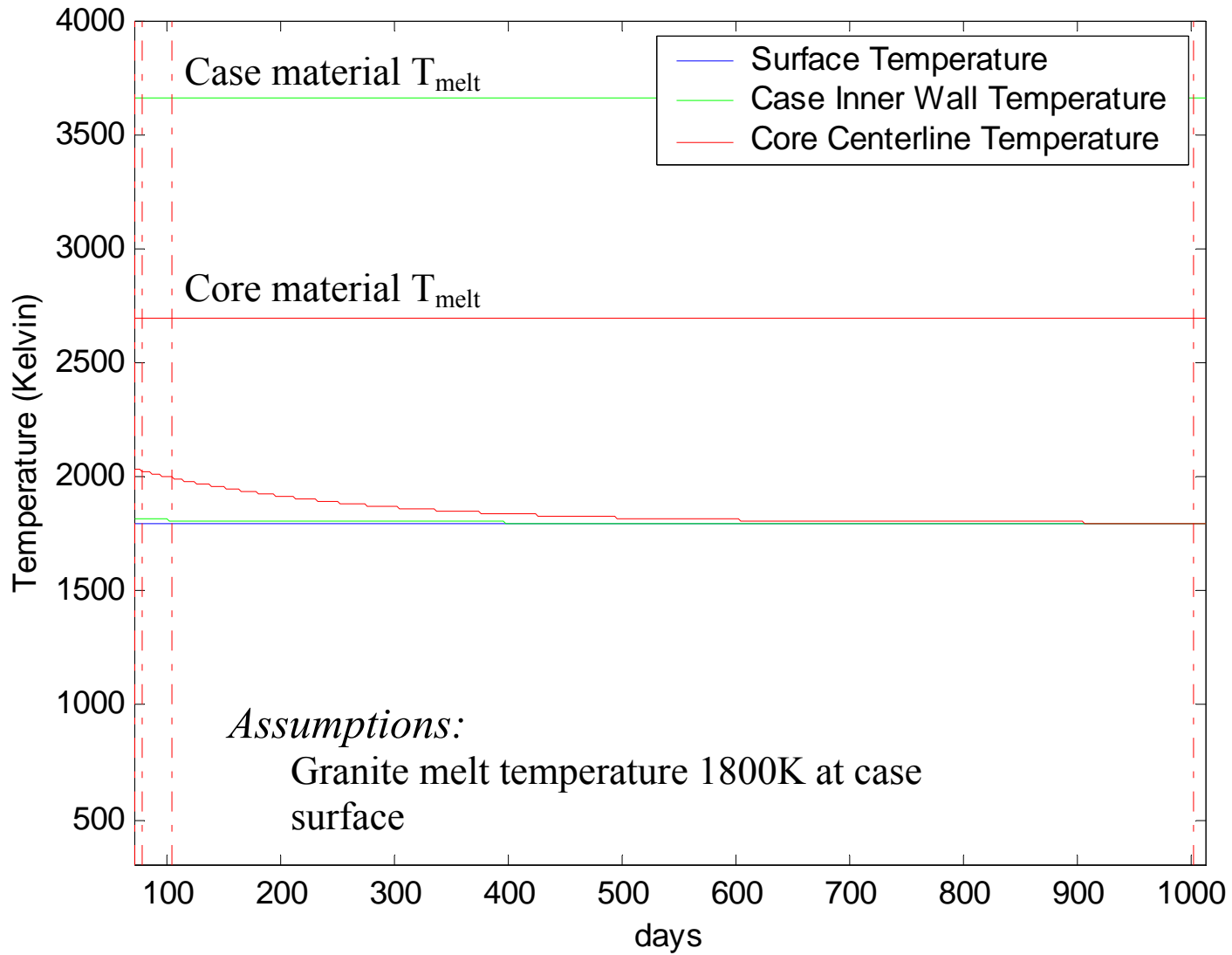


Figure 48: Equilibrium temperature vs. time for penetrator immersed in molten granite

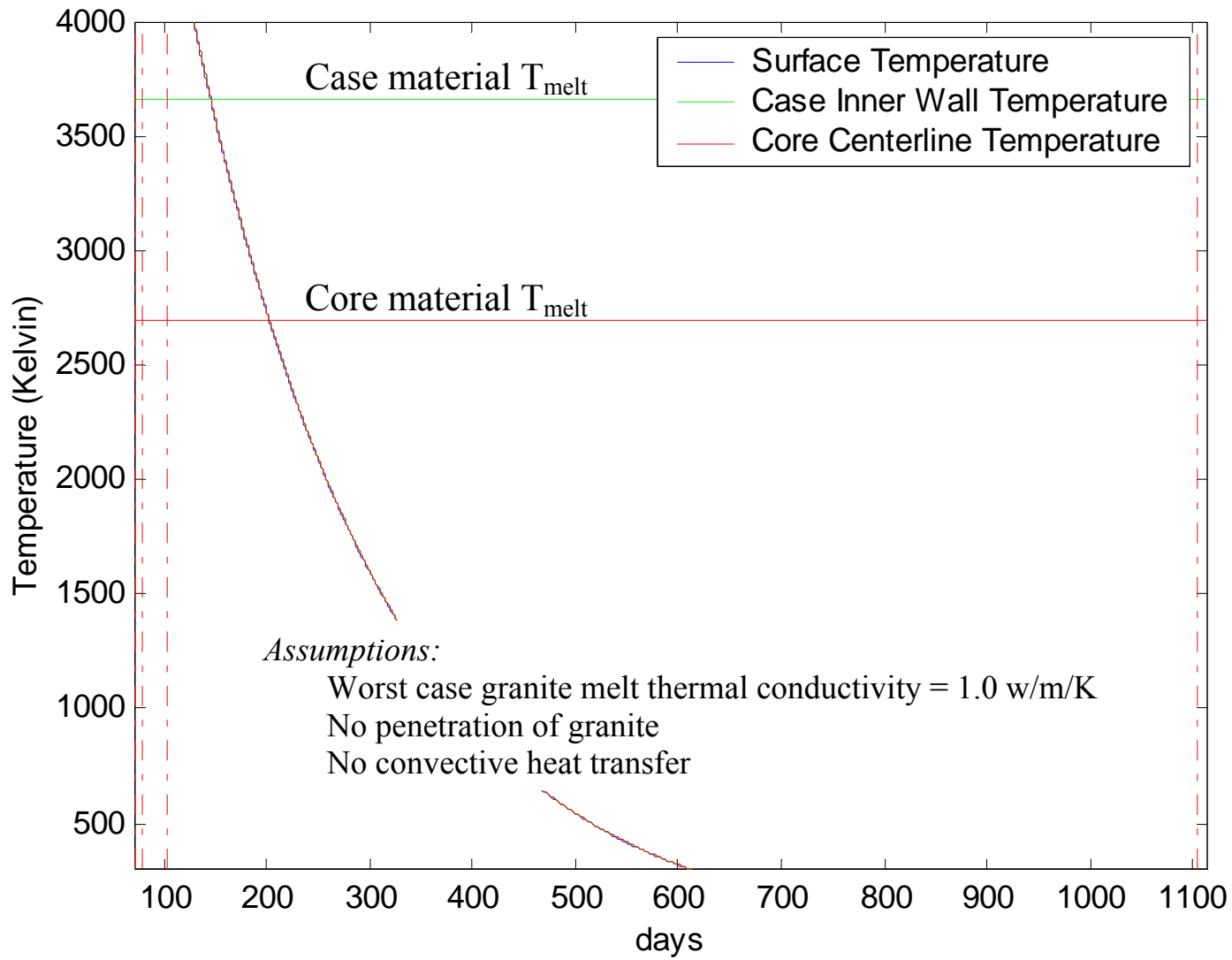


Figure 49: Equilibrium temperature vs. time for non-penetrating RIPTP immersed in non-circulating granite

Intact penetrator case radiation calculations

As previously mentioned, intact penetrator case radiation was the first major hazard evaluated as part of the radioisotope selection process during RIPTP feasibility investigation. Although a number of the radioisotope candidates considered during the feasibility investigation could provide a high power density, many were unsuitable due to the excessive shielding they required to reduce radiation emissions to safe levels.

Shielding calculations were performed with the Monte Carlo radiation transport code MCNP.²⁷² In an MCNP calculation, a large number of gamma photon histories are simulated and recorded. A photon history is initiated in the source region (i.e. the RHS), and terminated when the photon is either absorbed or escapes the system. A ring-shaped photon flux tally is placed on the mid-plane of the RIPTP at a distance of 1 meter from the RIPTP centerline. The photon transport parameters (position, energy, and traveling direction) are generated using a pseudo-random number generator and the appropriate probability density function for each parameter.

For the RIPTP intact radiation calculations, the thermal penetrator was modeled as a cylinder (the RHS) with a surrounding concentric shell (the RIPTP refractory case). Shielding results are given in Table 43 as an example of the screening process of various radioisotopes for radiation safety. In the calculation for the results in Table 43 the internal cylinder was specified as 7.5 cm in diameter and 45 cm long, within which the radioisotope was uniformly distributed. The shell was specified to be 5.0 cm thick. Both the RIPTP case and the balance of the RHS volume not occupied by radioisotope were specified to be tungsten.

Table 43 shows the gamma-ray energies, yields, intensities, and the effective dose at one meter from a thermal penetrator centerline for each of six example candidate radioisotopes. The gamma-ray intensity for each isotope is normalized in such a way that it corresponds to the amount that would produce the same power (61 kW) as that produced by one kg of ^{169}Yb . As shown, ^{169}Yb gives “zero” dose rate. This is because the low-energy gamma rays from ^{169}Yb are fully absorbed inside the thermal penetrator. The dose rates of $^{106}\text{Ru}/^{106}\text{Rh}$, $^{144}\text{Ce}/^{144}\text{Pr}$, and ^{185}Os are too high to be practically acceptable. While the dose rates of $^{170}\text{Tm}/^{172}\text{Tm}$ and ^{179}Hf are significant, they are within the acceptable range. Note that the dominant contributor to external radiation for the thulium RIPTP is thulium-172 which, unlike thulium-170, emits significant quantities of gamma photons with energies well in excess of .5 MeV.

Table 43: Radiation shielding results using MCNP code

Radioisotope	Gamma-ray energies (MeV)	Normalized gamma yield	Gamma-ray intensity (γ/sec)	Effective dose (Sv/hr)
$^{106}\text{Ru}/^{106}\text{Rh}$	0.512	0.6397	1.29×10^{17}	1.24
	0.622	0.3114	6.29×10^{16}	
	1.05	0.0489	9.88×10^{15}	
$^{144}\text{Ce}/^{144}\text{Pr}$	0.697	0.6588	1.01×10^{16}	11.8
	2.186	0.3412	5.22×10^{15}	
^{169}Yb	0.308	1.0	6.08×10^{16}	0.0
$^{170}\text{Tm}/^{172}\text{Tm}$ (after 30-day decay)	0.912	0.0496	8.28×10^{11}	2.0×10^{-2}
	1.094	0.2097	3.50×10^{12}	
	1.387	0.1951	3.26×10^{12}	
	1.466	0.2226	3.72×10^{12}	
	1.53	0.1783	2.98×10^{12}	
	1.608	0.1447	2.42×10^{12}	
	^{179}Hf	0.316	0.1358	1.74×10^{17}
	0.363	0.2656	3.40×10^{17}	
	0.41	0.1440	1.85×10^{17}	
	0.454	0.4546	5.83×10^{17}	
^{185}Os	0.592	0.0139	1.82×10^{16}	9.2

	0.646	0.8235	1.08 x 10 ¹⁸	
	0.717	0.0416	5.45 x 10 ¹⁶	
	0.878	0.121	1.59 x 10 ¹⁷	

A similar analysis was performed for the baseline thulium-170 powered RIPTP with varying RIPTP case thicknesses, the results of which are illustrated in Figure 50. The dose rates shown on the figure are for a RIPTP assembled from thulium target assemblies irradiated at ATR, 30 days after the stop of target irradiation (23 days “cool-down” for thulium-172 decay + 7 days for RIPTP assembly). Dose rates from thulium-172 would exponentially decay from the maximum shown on the figure with a half-life of 2.65 days.

Intact RIPTP radiation exposure for service personnel

Shielding would not be absolutely necessary at the start of RIPTP service life to meet nuclear industry exposure standards (10⁻³ Sieverts (Sv) when given in a single one-hour dose, .05 Sv per year total). However, unshielded dose rates from the RIPTP immediately after assembly would require close monitoring of the dose accumulated by exposed personnel and potentially cumbersome restrictions on total allowed exposure time. As a result, approximately one inch of additional shielding beyond the RIPTP case is recommended for the first seven days or so after RIPTP assembly. The RIPTP munition aeroshell/cooling structure would contribute some incremental shielding towards this one inch of additional shielding. The balance could be comprised of an additional one or two centimeters of lead plate incorporated in the RIPTPs transport/ground-handling container. By one week after RIPTP assembly potential dose

rate from an unshielded RIPTP would decay to less than 1/6th of that immediately after assembly.

As an alternative to adding additional shielding to the baseline RIPTP for its first several days of service life, the cool-down period could be increased by a week. The only downside of increasing the cool-down period is a reduction of RIPTP penetration rate performance/mission life. Either option should be satisfactory.

Intact RIPTP radiation exposure for enemy combatants

Figure 51 illustrates the dose rate at one meter distance over the service life of the penetrator. As previously discussed, the dose rate rapidly decays to low levels. As an overly conservative bound on worst case hazard from RIPTP exposure, consider an individual constantly exposed at a distance of one meter to a RIPTP without shielding and without aeroshell for *one year* from RIPTP service entry. For example, hypothetically the RIPTP is assembled, it's immediately loaded on a transport plane and then on take-off falls out the back of the plane into our individuals back yard minutes after having been cleared for service after assembly. This individual for some unknown reason (and despite the fire hazard) then spends every second of their life (eating, sleeping, working) right next to the RIPTP for an entire year. For such exposure any acute radiation effect such as radiation sickness would be impossible. Further, using conservative regulatory prediction standards for increase in cancer risk vs. accumulated radiation dose, an increase in lifetime fatal cancer risk of 1% would be predicted for the

exposed personnel... this compares to an approximately 20% natural incidence for fatal cancer in the general population.^{†††}

Consider the more credible but still conservative scenario, identical to that above but for an enemy combatant in a DBHT at the end of the runway. The enemy combatant would not be exposed to the RIPTP until it had time to penetrate down to the DBHT. Also, the enemy combatant hypothetically survives breach of the DBHT and spends every moment of the next year of his life in its close proximity. Such exposure would only result in an accumulated dose of approximately 40% the allowed annual dose for a nuclear industry worker (.02 Sv). No significant radiation associated health impact would be predicted.

It is clear from these analyses that no significant radiation hazards would be posed by the baseline thulium powered RIPTP to non-combatant or combatant personnel in nominal scenarios. Regulatory exposure standards could easily be met for service personnel by either adding a small additional amount of shielding to a RIPTP for storage and handling during its initial period of service or by increasing the cool-down period by approximately a week. Utilization of an alternative radioisotope to thulium-170 such as ytterbium-169 would result in no significant predicted external radiation emissions, thus eliminating the cool-down period required for thulium-172 and avoiding any potential requirement for initial auxiliary shielding.

^{†††} Note that the standards for prediction of increase in cancer risk were derived for flash-exposures of individuals to relatively large doses of radiation. No evidence has been documented that the dose rates and total doses such as are considered here would result in any increase in lifetime fatal cancer risk, and there are reasons, both theoretical and experimental to think they would not. No evidence for negative health effects has been documented for radiation exposures orders of magnitude above background.²⁸⁷⁻²⁸⁹

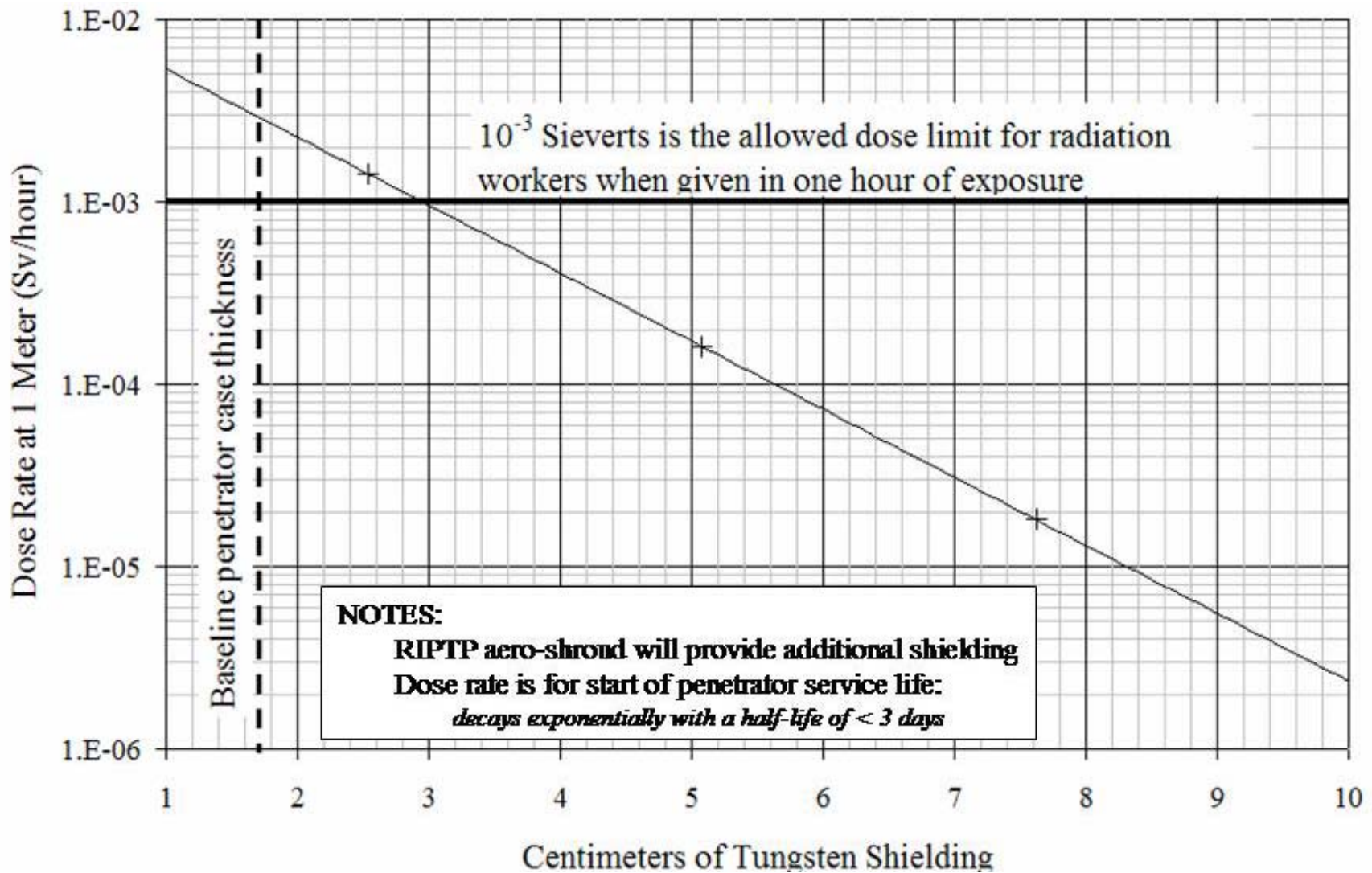


Figure 50: Shielding thickness vs. dose rate at 1 meter from thulium-172

RIPTP Poses *No Significant Unconventional Hazard* to Combatants

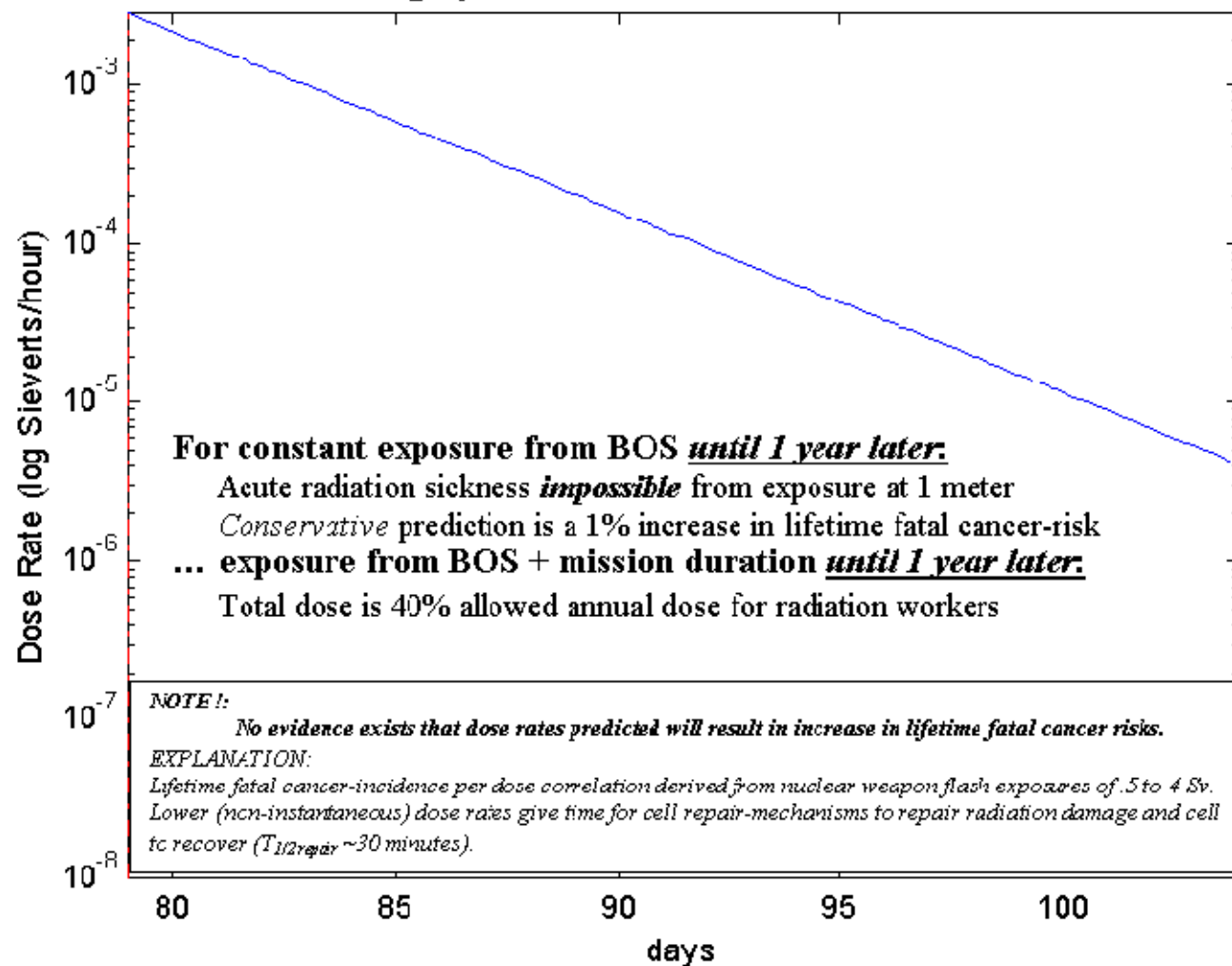


Figure 51: Dose rate from exposure to baseline RIPTP at one-meter distance

Bulk fragmentation

The category of hazard considered as posing the greatest risk is a fragmentation accident in which the RIPTP case is compromised or the RIPTP is broken into large fragments which lay exposed on the surface of the ground. To assess the potential severity of this hazard outcome, a representative scenario was analyzed in which it was assumed a RIPTP was broken in two halves with the radioactive core fully exposed. The dose rates for an individual standing at various distances from a halved RIPTP were calculated with the MCNP code. Figure 52 shows the geometric configuration modeled for the calculation of external dose rate from a RIPTP.

Figure 53 shows the results for the baseline $^{170}\text{Tm}/^{172}\text{Tm}$ RIPTP. It is apparent from the figure that significant radiation hazard exists in this scenario – exposure of an individual within several meters of the fragmented RIPTP for a period of from one to several hours might lead to acute radiation sickness. Exposure at one meter or less for a period of from 5 to 10 hours or more could potentially result in lethality from acute radiation poisoning.²⁸⁹ RIPTP exposure times required for acute effects might be significantly longer than quoted due to the lower dose rate as compared to the flash exposure data for which acute effect correlations were derived.

Dose rates *would* be high enough for standard linear dose vs. cancer risk extrapolations to be reasonable. The International Commission on Radiation Protection (ICRP) published risk-factor for radiation-induced lifetime fatal cancer is 5% per Sievert for whole-body exposure (for 50/50 male/female population and a wide range of ages – ICRP 26).²⁹⁰ Thus, exposure of a person at one meter distance for one hour would

correspond to a 3.5% predicted increase in lifetime fatal cancer risk, and exposure at six meters for one hour a .33% predicted increase in risk.

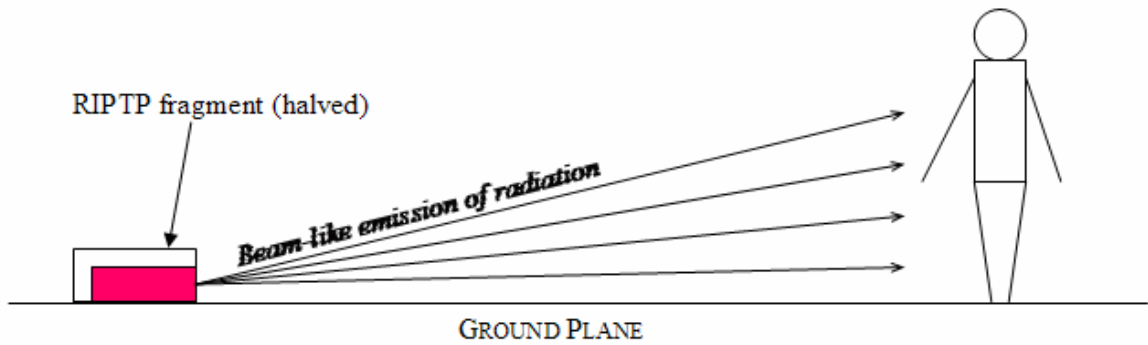


Figure 52: Radiation exposure for bulk-fragmentation

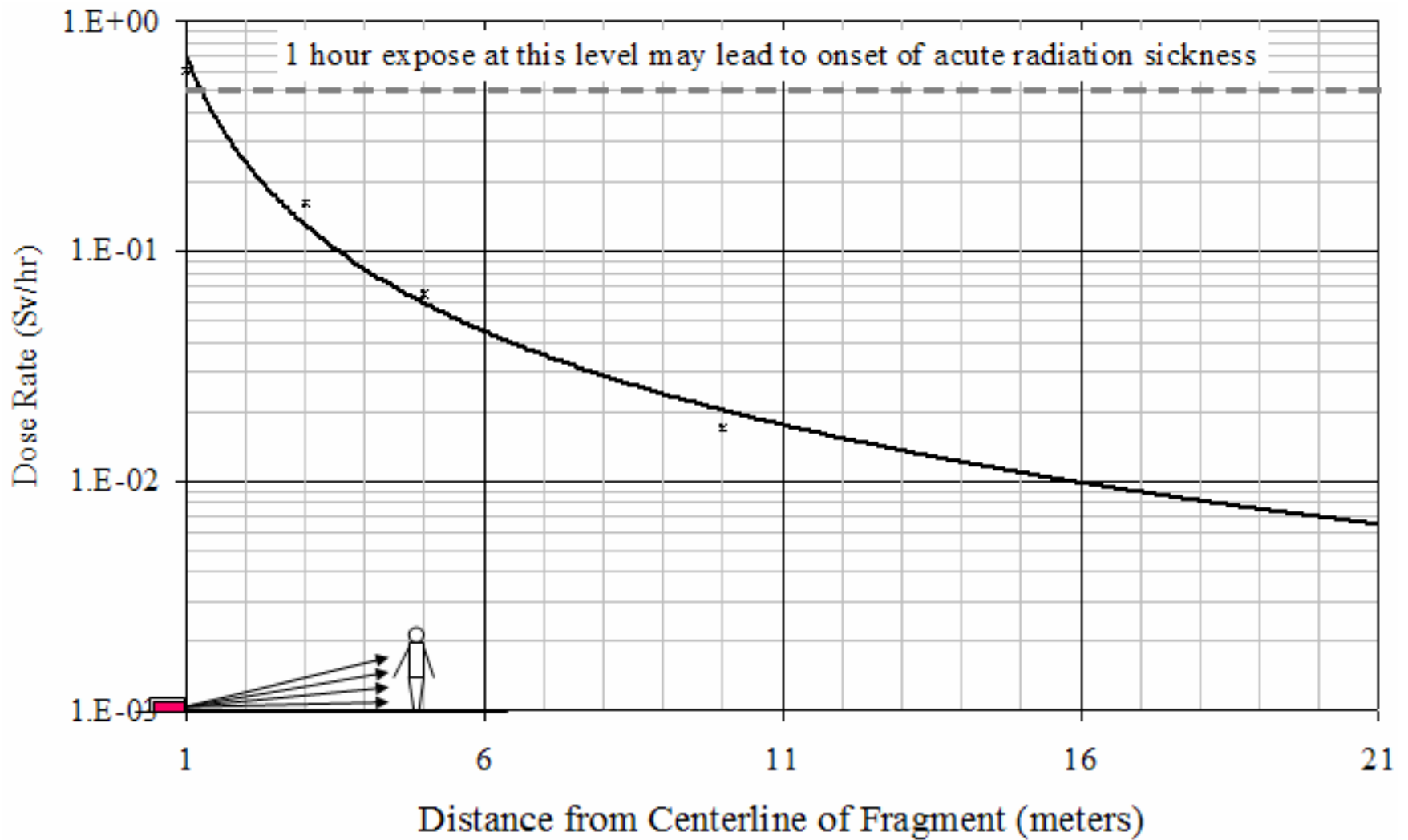


Figure 53: Distance vs. dose rate from bulk fragment of RIPTP

Explosive dispersal

The most plausible hazard scenario with the worst associated hazard magnitude for the baseline RIPTP is explosive dispersal of a large fraction of a RIPTP's RHS in airborne particles of respirable sizes. For a well designed RIPTP the risk from such a scenario is much less than that associated with the hazard of bulk fragmentation as there are few hypothetical realization scenarios that might result in reduction of a large fraction of a RIPTP's RHS to respirable sized particles. The author would not consider any scenario in which a large fraction of a RIPTP's RHS was reduced to respirable sized particles^{§§§} and dispersed to be of other than very low likelihood.

The principle category of scenario identified for realization of an explosive dispersal hazard is deliberate radioisotope dispersal in a dirty bomb. In such a scenario a large quantity of explosive might hypothetically be used by an enemy to deliberately disperse radioactivity from a RIPTP with the intent of causing radiation casualties and/or panic to the general population. It is very questionable, however, whether even the use of several hundred pounds of high explosive would be adequate to achieve pulverization of a large fraction of an RHS starting from an initially intact RIPTP – the principal production of large fragments (as previously discussed) would be more likely. The most plausible configuration for fine pulverization/explosive dispersal would be a very large shaped charge with the jet aligned along the axis of the RIPTP.

^{§§§} Radiological particles internalized through respiration can be divided into three size-selective categories: inhalable particles are particles able to enter the head; thoracic particles are particles that are able to enter the lung during mouth breathing (<30 microns); and respirable particles are particles that are able to enter the deep lung during nose breathing (<10 microns).²⁹¹ *Respirable* particles are significant as they are most likely to be retained for significant periods of time and so generally account for the bulk of accumulated internal dose not ingested from foodstuffs, particularly for the case of relatively insoluble radioisotope compounds such as the oxides of thulium or plutonium.

Mechanical pulverization of the RIPTP RHS prior to its packaging as a dirty bomb and subsequent dispersal using explosives would be theoretically possible but extremely hazardous. Whichever approach was taken by a hypothetical RIPTP RHS dirty bomb manufacturer, the end result of combining a RIPTP or RIPTP RHS with an explosive into an integrated package would likely be a device as dangerous to the creator as to the target. The high heat levels produced by a RIPTP could easily lead to accidental deflagration of chemical explosives.

Realizing a deliberate radioisotope explosive dispersal scenario would face considerable obstacles with regards to: recovery of the RIPTP by the enemy; the engineering/manufacturing challenge of modifying the RIPTP; transport of the modified RIPTP to a suitable location at a suitable time; successful fragmentation/dispersal; and suitable meteorological conditions for maximum effect. All of the above would have to be accomplished within the constraints of the short RIPTP RHS's radioisotope half-life, without detailed engineering knowledge of the RIPTP's design, probably without significant prior experimentation, and within the bounds of the political/military interests of the enemy.

The analysis of explosive dispersal is performed, however, so as to bound the absolute worst-case hazard that could theoretically be posed by a RIPTP and enable comparisons with the analogous theoretical hazard posed by existing radioisotope systems and the expected consequence of use of a low-yield penetrating nuclear bomb. The assessment was performed with the Hotspot code, which is a first order approximation of the radiation effects associated with the atmospheric release of radioactive materials.²⁷³

Hotspot calculates the downwind “ground-shine” external dose rate (Figure 54) and the internally Committed Effective Dose Equivalent (CEDE – Figure 55) due to the internalization of radioactive fallout. Ground-shine dose rate is the external radiation dose received by an individual from radioisotope deposited on the ground. CEDE is the internal dose to an individual accumulated over a 50 year period. This dose is caused by radioisotopes internalized by the individual through inhalation and ingestion and then retained (not excreted) by the individual prior to radioisotope decay. Hotspot is designed for short-term (less than a few hours) radioisotope release durations.

The total quantity of thulium-170 released in the explosive RIPTP dispersal scenario was assumed to be the total RHS radioisotope content of .5 kg, 100% of which was assumed to be in the form of respirable sized particles (the worst case possible). The explosion was assumed to be caused by 100 pounds of TNT, and wind speed was assumed to be 1 m/s at 10 m above the ground. This is a highly conservative/worst-case scenario with respect to radiation hazard as in reality it is probable that only a very small fraction of the total radioisotope content would be released in respirable size particles.

For the sake of comparison, an equivalent Hotspot calculation was also made for the quantity of plutonium-238 contained in the 3 GPHS-RTGs employed by the Cassini space mission. This scenario also assumed 100% airborne release of 20.3 kg of plutonium-238. Also, for the sake of comparison of a RIPTP to a low-yield shallow penetrating nuclear bomb (the only existing option for robust DBHT defeat) actual measured ground shine results for the “Danny Boy” nuclear detonation were obtained. “Danny Boy” was an underground test of a half-kiloton nuclear bomb buried 34 meters deep.

Figure 56 illustrates the Hotspot ground shine results for thulium-170 RIPTP, plutonium-238 RTG plotted alongside “Danny Boy” post-test measurements. The principle conclusion to draw from this figure is that the absolute worst-case RIPTP radiation hazard is enormously less hazardous than the expected hazard from employment of a penetrating low-yield nuclear bomb. From approximately .3 km to 1 km distance on the plume centerline worst case RIPTP radiation dispersal is: three to five orders-of-magnitude less hazardous than nominal hazard for a nuclear explosion; less than one order-of-magnitude more hazardous than a comparable (similarly unrealistic) worst-case Cassini RTG dispersal; and the period of hazard persistence from a RIPTP radiation dispersal is approximately four orders-of-magnitude less than that of the Cassini RTGs. The demonstrated reference nuclear bomb hazard is optimistic compared to a penetrating low-yield nuclear bomb as “Danny Boy” was buried deeper than a penetrating nuclear bomb could achieve, and was possibly lower in yield than would be tasked for DBHT defeat.

Figure 57 shows the Hotspot CEDE results for a thulium-170 RIPTP and three plutonium-238 RTGs. Analogous results for “Danny Boy” are not given as CEDE is a calculated quantity not measured in the test. This is because ^{238}Pu emits short-ranged alpha particles which do not contribute to the external dose, but do contribute to the CEDE if ^{238}Pu is inhaled into the lung. It can be seen in this figure that the predicted internalized hazard from explosive dispersal of a RIPTP would be two orders-of-magnitude less CEDE than that of Cassini type RTGs in an analogous dispersal.

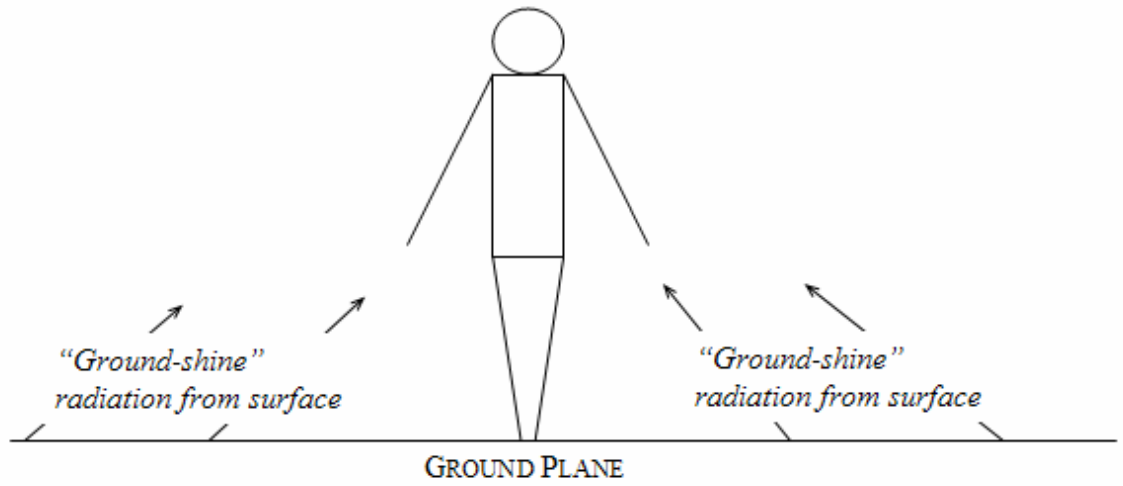


Figure 54: External radiation exposure for explosive dispersal

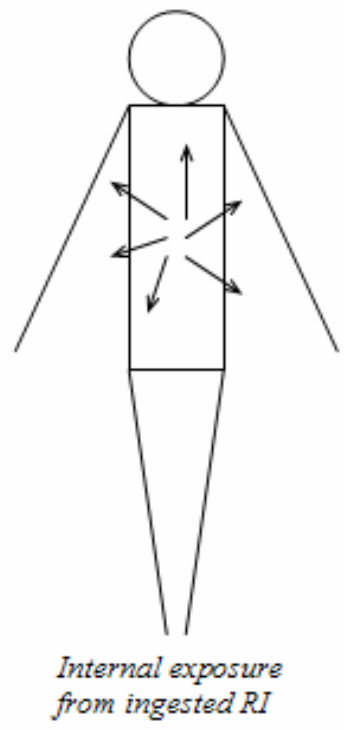


Figure 55: Internal radiation exposure for explosive dispersal

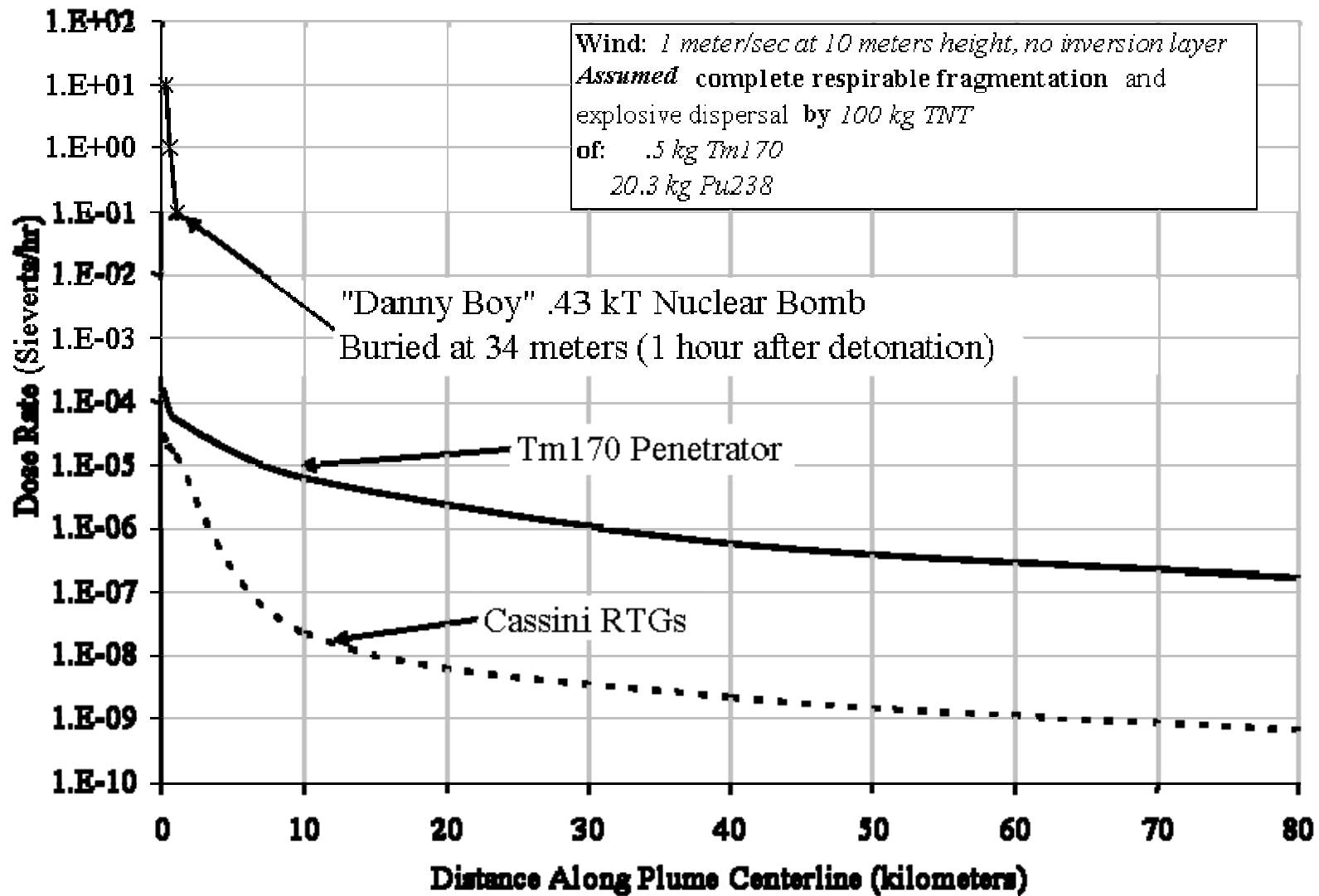


Figure 56: Ground shine dose rate from explosive dispersal

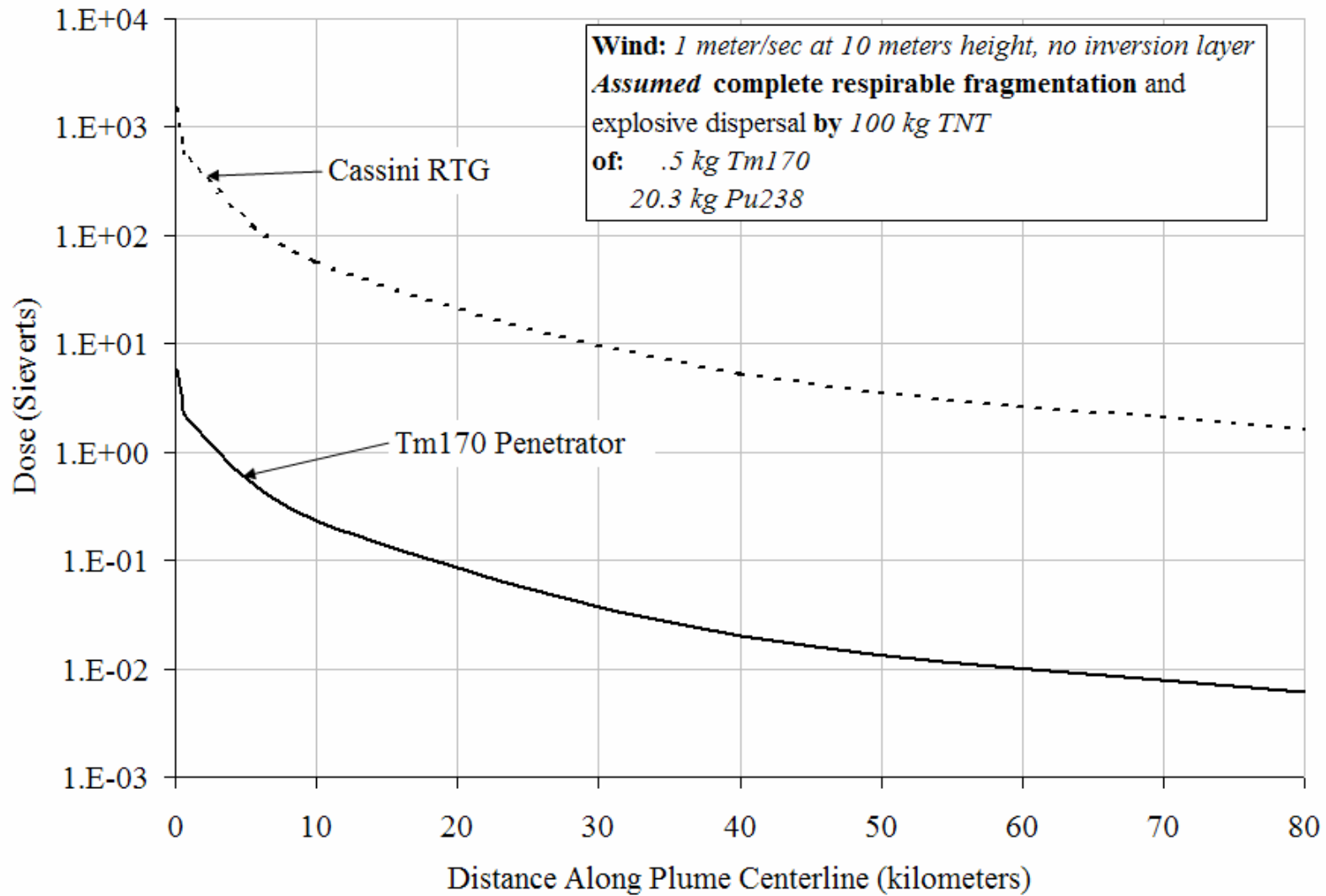


Figure 57: CEDE internal dose from explosive dispersal

Safety conclusions

At the end of the safety investigation it was concluded that no safety related reasons were identified for not pursuing a RIPTP for DBHT defeat in the context of the already accepted risks posed by either nuclear *or* conventional munitions. A RIPTP might in practice: pose less hazard to surface non-combatants; pose significantly less duration of hazard as compared to conventional UXO; might enable destruction of WMD stockpiles protected in DBHTs without invasion of a rogue nation; might deter conflict by providing a plausible means for countering DBHTs; and might reduce casualties by shortening duration of a possible war by enabling decapitation attacks and/or early elimination of even “super-hard” command and control nodes.

For RIPTPs similar in penetration performance and size to the baseline RIPTP proposed, it is believed that thermal management in adverse scenarios can be accommodated with low risk and that combustive type RI dispersal is unlikely. However, there is reason for concern regarding the maximum penetration rate in granite a RIPTP could provide without approaching RIPTP material maximum temperature limitations. Approximate identification of the maximum penetration rate for which managing this risk begins to become excessively challenging can be accomplished by integrating one of the existing close-contact melting models into the RIPTP analysis code, as was later done.

When compared to the existing principle alternative for robust DBHT defeat of a low-yield penetrating nuclear bomb, a RIPTP alternative for DBHT defeat could be significantly safer. The worst case potential casualties would be enormously less for a RIPTP, the likelihood of casualties on the surface would be vastly less for a RIPTP, and

the potential duration of environmental damage or health hazard is *many* orders of magnitude less.

Even though one potential mode of hazard presented by RIPTPs is distinct from those posed by conventional munitions (radiation), in terms of either overall collateral casualty risk or environmental risk it appears plausible that a RIPTP could be comparable to or better than a conventional munition. In the context of the risk of collateral casualties, using a single RIPTP in war might plausibly pose significantly less risk than use of a single non-penetrating high-explosive conventional bomb.

Also, although RIPTPs would share a radiation mode of hazard with nuclear bombs, both the severity of the hazard and its likelihood of occurring would be enormously less. Further, while RIPTPs would in every way considered by the analysis be safer to use in war than nuclear bombs with respect to collateral casualties, they offer a means to defeat DBHTs that at present are considered invulnerable to airstrike by anything other than a nuclear bomb.

EXAMPLE PARAMETRIC EXERCISES OF MULTIDISCIPLINARY CODE FOR ROBUSTNESS AND ENABLING TECHNOLOGY ANALYSIS

Minimization of radiological hazard to enemy combat personnel motivated the selection of a shieldable Radioisotope Heat Source. Minimization of potential hazard and maximization of power density motivated selection of a very short half-life radioisotope. A very short half-life radioisotope was specified so as to: 1) maximize power density achievable without post-irradiation target isotope extraction/enrichment processing; and 2) eliminate the potential for the creation of any enduring radiological hazard from RIPTP munition use. Minimizing cost and hazard associated with producing a short half-life radioisotope RHS and maximizing its initial power density favored selection of radioisotopes with high production cross sections and high isotopic concentration precursor isotopes. Unavailability of necessary nuclear data for analysis of some candidate isotope systems caused them to be eliminated from further consideration. Avoiding a requirement for potentially costly pre-enrichment for the desired radioisotope precursor isotope (such as would be required for $^{169}\text{Yb}_2\text{O}_3$ RHSs) together with significant prior historical technological development lead to the selection of the 100% natural abundance thulium-169 precursor isotope for production of thulium-170 RHSs.

The end result of these various decisions lead directly to the following principle limitations with respect to the viability of the $^{170}\text{Tm}_2\text{O}_3$ RIPTP DBHT defeat munition:

1. Approximately one RIPTP munition producible at a time (about 6 a year) using existing national reactor facilities. While this might be satisfactory

for a research program to explore the approach using representative test articles, it would almost certainly be impractical from an operational capability standpoint. This is because simultaneous use of multiple RIPTPs against a single target would almost certainly be desired as DBHTs can be extensive, individual DBHT spaces small and deeply emplaced, and targeting/delivery/RIPTP penetration-dispersion errors significant.

2. A nominal estimated penetration rate for a $^{170}\text{Tm}_2\text{O}_3$ RIPTP produced using existing reactor facilities of about ten meters a day.
3. Fairly long lead times for RIPTP RHS production (at least a month, assuming RHS radioisotope production target elements were already being irradiated).
4. Short shelf life once produced.
5. Initial radiation levels that, while posing minimal real risk, would still require special radiation exposure monitoring and handling procedures for the first week or two of RIPTP service life to comply with accepted regulatory standards.

The only element above which is inherent in the identified RIPTP concept is short shelf life – this is inherent by design for minimization of duration of any radiological hazard and maximization of power density for best penetration rate (a fissile thermal penetrator system would pose less potential radiological hazard prior to activation and have an indefinite shelf life, but pose greater and longer potential hazard post activation). Various technologies or possible investments have previously been discussed in the

“Feasibility Investigation” part of the “Benchmarking” section for substantially reducing or eliminating all other RIPTP limitations listed above. Below are listed the primary identified technologies for addressing the baseline $^{170}\text{Tm}_2\text{O}_3$ RIPTP viability issues.

1. Pursue cost effective enrichment technologies for producing highly enriched ^{168}Yb . If supplies of highly enriched ^{168}Yb were available, issues 1, 2, and 5 would essentially disappear. RHSs for RIPTPs having very substantially enhanced penetration rate could be produced in quantity in common PWR-type power reactors. Further, the $^{170}\text{Yb}_2\text{O}_3$ RIPTPs would have initial radiation levels not requiring any additional shielding for safe handling. With regard to item three, the lead time required could be very substantially reduced, potentially to about five days.
2. Creation of a new 3GW_{th} high flux isotope production reactor. This would only impact items one and two discussed above, potentially enabling production of several $^{170}\text{Tm}_2\text{O}_3$ type RIPTPs at a time, and/or RIPTPs of enhanced penetration capability.

These were the two already identified technologies that could be enabling of the RIPTP concept. Whether or not either or both of these technologies were pursued, however, an apparent characteristic of the thermal penetrator approach remained the slow penetration rate as compared to other penetrator technologies. While the identified baseline thermal penetrator design satisfied the problem definition as originally formulated, the question remained as to whether days to a week to defeat the baseline DBHT was satisfactory. It was apparent that the case for the RIPTP concept’s utility would be significantly enhanced if technologies could be identified that enabled

improvement in penetration time to depth to less than a day. A penetration rate of at least 80 meters a day was defined as a new constraint on the feasibility of a thermal penetrator.

Therefore it was decided to perform an investigation on the baseline concepts design space to attempt to identify possible technology areas that might enable significant improvements in performance (for the baseline thulium-170 or alternative radioisotope system). As previously discussed in the “Approach” part of the “Introduction” section, the following steps were involved:

1. Definition of a RIPTP system space as system variable deviations from the baseline design. System variables were considered to include concept design, material property, and manufacturing variables as well as target material property variables. Ranges were selected to reflect plausible maximum deviations from the baseline values.
2. Investigation of the system design space to determine if points exist exhibiting the required penetration time to depth performance.
3. If points exist exhibiting required penetration time to depth performance, attempt to identify technology concepts that might provide the required deviations in system variables to achieve required penetration time to depth.
4. If points are not found to exist with the required penetration time to depth, evaluate what would be required of the system in terms of the close-contact melting analysis to provide the requisite penetration time to depth, and identify possible technologies that might provide the required characteristics.

Step two, above, was accomplished by executing a set of computational experiments and fitting Response Surface Equation (RSE – see equation below) metamodels to the RIPTP analysis code responses of interest. A metamodel is a model of a model (in this case a second order polynomial model of a RIPTP analysis code response). In the equation below, R denotes the metamodel response which approximates the model response, the X 's are the various independent variables, and the b 's are the coefficients of the fitted polynomial equations.

$$R = b_0 + \sum_{i=1}^k b_i X_i + \sum_{i=1}^k b_{ii} X_i^2 + \sum_{i=1}^{k-1} \sum_{j=i+1}^k b_{ij} X_i X_j$$

Metamodels act as surrogates for the model to which they are fitted so as to provide the output corresponding to an input setting at much lower computational cost. The lower computational cost of the metamodel enables efficient use of various interactive system space visualization tools to facilitate rapid exploration of the system space and its responses, as well as to assess the potential impact of uncertainty through Monte-Carlo Simulations (MCS).

SYSTEM SPACE PARAMETERIZATION AND EXPERIMENTAL DESIGN

The variables and their ranges used to define the system space for the baseline Thulium-170 powered RIPTP are listed below in Table 44. Granite ambient temperature range was selected to cover from well below the freezing point of water to a temperature consistent with a very hot day. Rock density, viscosity, and thermal properties were specified to span ranges consistent with those found in the literature.

Ranges for thermal neutron capture cross sections for isotopes of thulium were specified as plus or minus twice the standard deviation of error listed for the values in the ENDF database, except for ^{172}Tm . The capture cross section for ^{172}Tm is not available. Often, but not always, thermal neutron capture cross sections are similar in magnitude for isotopes of an element within an atomic mass number of each other. The range for ^{172}Tm was therefore specified as having a maximum of 320 barns, with a minimum cross section of zero barns arbitrarily specified.

The fraction of the target element comprised of the isotope compound was specified as ranging from .7 to .95. From the standpoint of improving penetrator penetration rate it is desirable that the isotope compound fraction of the target element be as high as possible so final power density is maximized (unless there is to be some post-irradiation processing). However, this variable has several other implications. First, cladding of the target element reduces the fraction of the target element that is comprised of the target isotope compound. Second, sintered ceramics are typically limited in terms of the fraction of maximum theoretical density they can achieve (.95 to .97 would be quite good). Lastly, the thermal conductivity of the basic thulium sesquioxide material is quite poor – as power density and RIPTP size increase maximum internal temperatures are likely to exceed the melting point of even this refractory oxide in nominal scenarios. It may therefore be desirable/necessary to combine the sesquioxide with another material (such as a refractory metal in a cermet) so as to provide a higher bulk thermal conductivity.

The volumetric packing efficiency of the target elements in the RIPTP internal volume was specified to range from .5 to .97. Packing efficiency is an important

constraint on the geometry of the target elements and/or any post processing that might be required. For example, while plate target elements might achieve near 100% packing efficiency, uncompressed spheres are limited to a maximum theoretical density of 74%. Further, the remainder volume would be available for improving bulk thermal conductivity of the core.

Thermal neutron flux was specified as ranging from a low value consistent with a commercial PWR to that of a high-thermal-neutron-flux reactor such as HIFR or ATR. Thermal reactor powers were specified to range over those consistent with HIFR to that of a single lobe of ATR, and the fraction of excess neutrons available for isotope production was specified as ranging from .2 to .7. The larger a reactor's core, the less neutron leakage tends to occur, and consequently the higher the fraction of excess neutrons it may be reasonable to assume are available for isotope production. Days for irradiation in the reactor were specified to have a range consistent with the typical minimum and maximum fuel cycles for HIFR and ATR.

Ranges for cool down of isotope target elements and RIPTP processing/transport days were specified rather arbitrarily as a detailed definition of the process elements, labor, and transport times involved was not performed. Days allowed for RIPTP penetration were specified to range from half a day to ten days.

Penetrator geometry was specified to vary from a hemispherically capped cylinder with a fineness ratio of four to a sphere (a fineness ratio of one). Penetrator case thickness factor was specified to range from .1 to .5. Note that lower thickness factors are advantageous with respect to achieving higher power density and thus achievable

penetration rate, but disadvantageous with respect to radiation shielding and radioisotope containment safety.

Thermal conductivity of the penetrator core was specified to range from a value consistent with thulium-sesquioxide at elevated temperatures to one more consistent with a refractory metal like tungsten at elevated temperatures. Note that a working fluid such as lithium (as has been demonstrated in high temperature heat pipes) could substantially increase the maximum effective conductivity beyond that specified.

Thermal conductivity of the penetrator case was specified to have a range consistent with elemental tungsten at elevated temperatures. Density of the case was specified to range from a high consistent with a heavy metal alloy such as TZM to a low of ten grams per cubic centimeter. Emissivity of the penetrator case was specified to range from .9 to .1 to enable assessment of the potential importance of emissivity coating technologies to radiative cooling scenarios.

Table 44: Variables selected to define the system space and their ranges

VARIABLE	UNITS	HIGH	LOW
Granite Ambient Temperature	<i>K</i>	316	260
Rock Melting Temperature	<i>K</i>	2000	1273
Rock Density	<i>g/cc</i>	3.06	2.1
Enthalpy of Formation	<i>erg/g</i>	5.00E+09	1.00E+09
Rock Liquid Conductivity	<i>erg/(cm s K)</i>	4.50E+05	9.87E+04
Rock Liquid Density	<i>g/cc</i>	2.7	2.1
Rock Liquid Viscosity Constant A	<i>Poise</i>	1.00E+15	7.00E+10
Rock Liquid Viscosity Constant Beta	<i>1/K</i>	5.10E-03	3.60E-03
Rock Liquid Average Conductivity	<i>erg/(cm s K)</i>	4.50E+05	9.87E+04
Rock Liquid Average Heat Capacity Liquid	<i>erg/(g K)</i>	2.10E+07	6.50E+06
Rock Solid Average Heat Capacity	<i>erg/(g K)</i>	1.30E+07	6.50E+06
Rock Liquid Average Density	<i>g/cc</i>	2.5	2.1
Rock Average Conductivity	<i>erg/(cm s K)</i>	2.20E+05	1.00E+05
¹⁶⁹ Tm σ_c	<i>Barns</i>	118.5	107.9
¹⁷⁰ Tm σ_c	<i>Barns</i>	100	84
¹⁷¹ Tm σ_c	<i>Barns</i>	220	100

$^{172}\text{Tm } \sigma_c$	<i>Barns</i>	320	0
Fraction Target Element Comprised of Isotope	<i>non-dim.</i>	0.95	0.7
Vol. Packing Efficiency of Target Elements	<i>non-dim.</i>	0.97	0.5
Flux of Thermal Neutrons	<i>neut./cm²s</i>	1.00E+15	7.00E+13
Thermal Power of Nuclear Reactor	<i>Megawatts</i>	60	10
Fraction Excess Neutrons for Isotope Production	<i>non-dim.</i>	0.7	0.2
Days for Irradiation in Reactor	<i>days</i>	49	21
Days for Cool down of Target Prior to Assembly	<i>days</i>	46	11.5
Days to Process Target/Deliver Penetrator	<i>days</i>	14	2
Days Allowed for Penetration of Penetrator	<i>days</i>	10	0.5
Cost per Irradiation Cell in Reactor per Year	2003Yr\$/yr	4.00E+06	2.00E+06
Fineness Ratio of Penetrator	<i>non-dim.</i>	4	1
Case Thickness Factor of Penetrator	<i>non-dim.</i>	0.5	0.1
Thermal Conductivity of Penetrator Core	<i>erg/(cm s K)</i>	1.00E+07	2.00E+05
Conductivity of Penetrator Case	<i>erg/(cm s K)</i>	1.00E+07	4.00E+06
Density of Penetrator Case	<i>g/cc</i>	19.3	10
Emissivity of Penetrator Case	<i>non-dim.</i>	0.9	0.1

Using these variables and their specified ranges, an experimental design was created using the SAS Institute's *JMP* statistical analysis software package.²⁹² The experimental design consisted of 2,190 runs with 1,095 runs in a custom three level D-Optimal experimental design and 1,095 runs in a Latin-Hypercube space filling sample design to validate fit.

Table 45: Output variables for which Response Surface Equations were generated.

VARIABLE	UNITS
Penetration Rate	<i>m/day</i>
Maximum Mission Depth	<i>meters</i>
Total Penetrator Mass	<i>kg</i>
Penetrator Radius	<i>cm</i>
External Wall Surface Temperature	<i>Kelvin</i>
Thermal Power	<i>watts</i>

REDUCTION OF RESULTS

Each of the 2,190 unique experimental settings for the variables listed in Table 44 were run sequentially and the corresponding values of the output variables listed in Table 45 written to file in table format. After completing execution of all experiment computational runs, the output file of responses was imported into *JMP* for analysis.

It was found that the best fit for the responses was obtained by excluding experimental runs having zero penetration rates, and performing a Box-Cox Y Transformation on the remaining responses. The independent variable transformations identified were then applied to the appropriate response data and the RSE fitted. The inverse of the Box-Cox Y Transformation was then applied to the fitted RSE so as to obtain the final response metamodel.

Penetration rate

The equation below gives penetration rate as a function of the transformed penetration rate RSE.

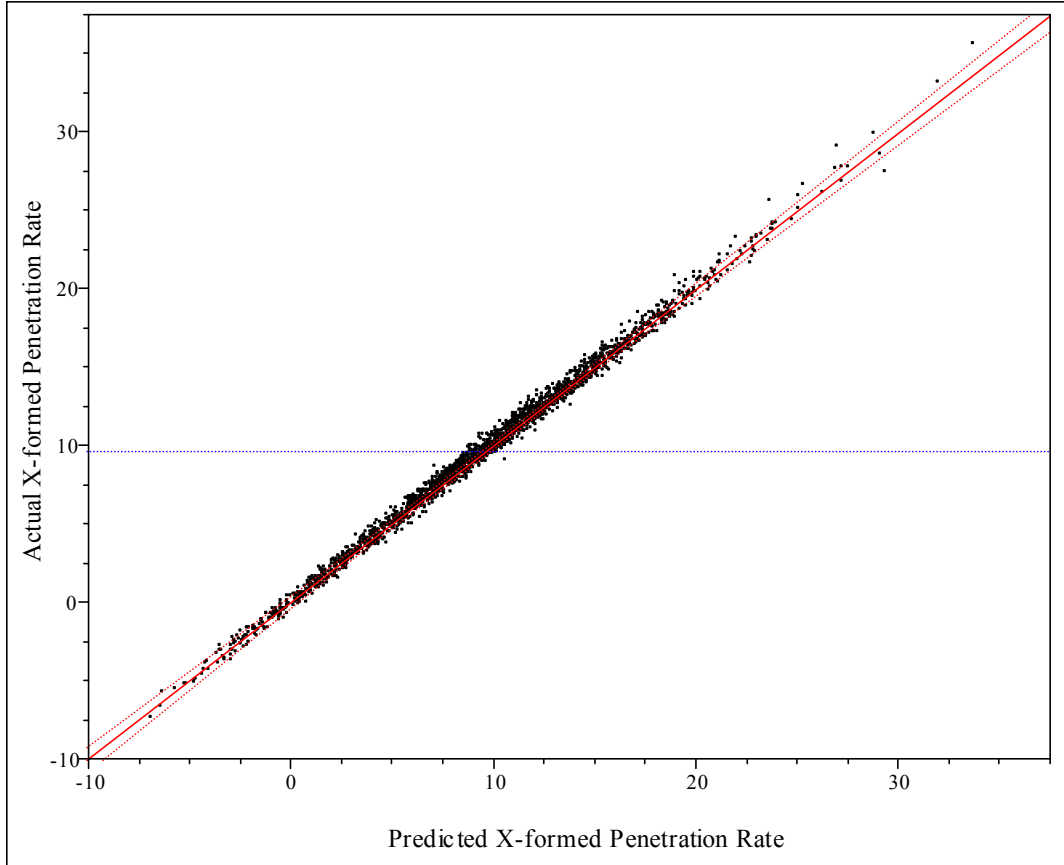


Figure 58: Predicted vs. actual transformed penetration rate

$$PenetrationRate = (RSE_{PenetrationRateX} * 0.04748 + 1)^5$$

Figure 58 shows the plot of RSE predicted vs. actual transformed penetration rate values, and Table 46 lists the corresponding RSE summary of fit metrics.

Table 46: Summary of fit for transformed penetration rate

R²:	0.995
R² Adjusted:	0.993
Root Mean Square Error:	0.466
Mean of Response:	9.676
Observations:	2098

Maximum mission depth

The equation below gives maximum mission depth as a function of the corresponding RSE.

$$MaxDepthMission = (RSE_{MaxDepthMissionX} * 0.01783 + 1)^5$$

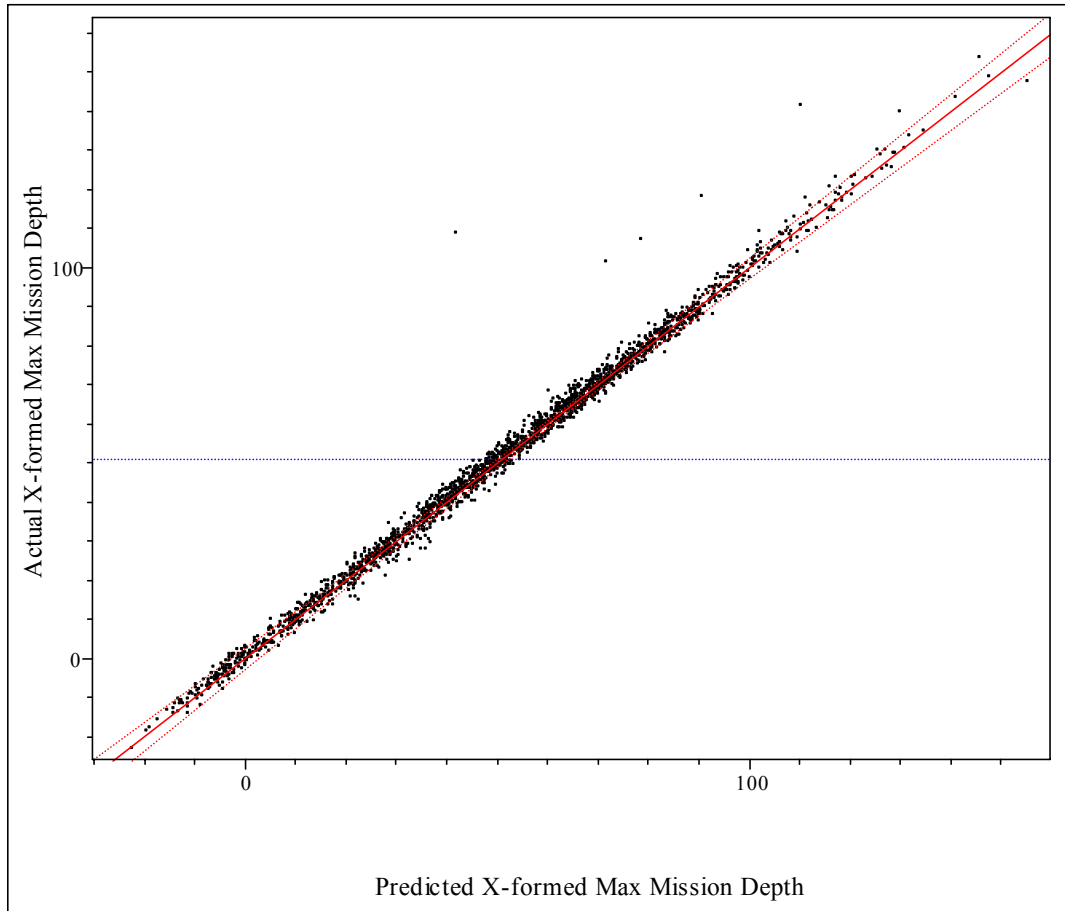


Figure 59: Predicted vs. actual transformed maximum mission depth

Figure 59 shows the plot of RSE predicted vs. actual transformed maximum mission depth, and Table 47 lists the corresponding RSE summary of fit metrics.

Table 47: Summary of fit for transformed maximum mission depth

R²:	0.992
R² Adjusted:	0.989
Root Mean Square Error:	3.124
Mean of Response:	51.19
Observations:	2098

Total penetrator mass

The equation below gives penetrator total mass as a function of the corresponding RSE.

$$TotalMass = e^{\frac{RSE_{TotalMass} \cdot X}{20.58}}$$

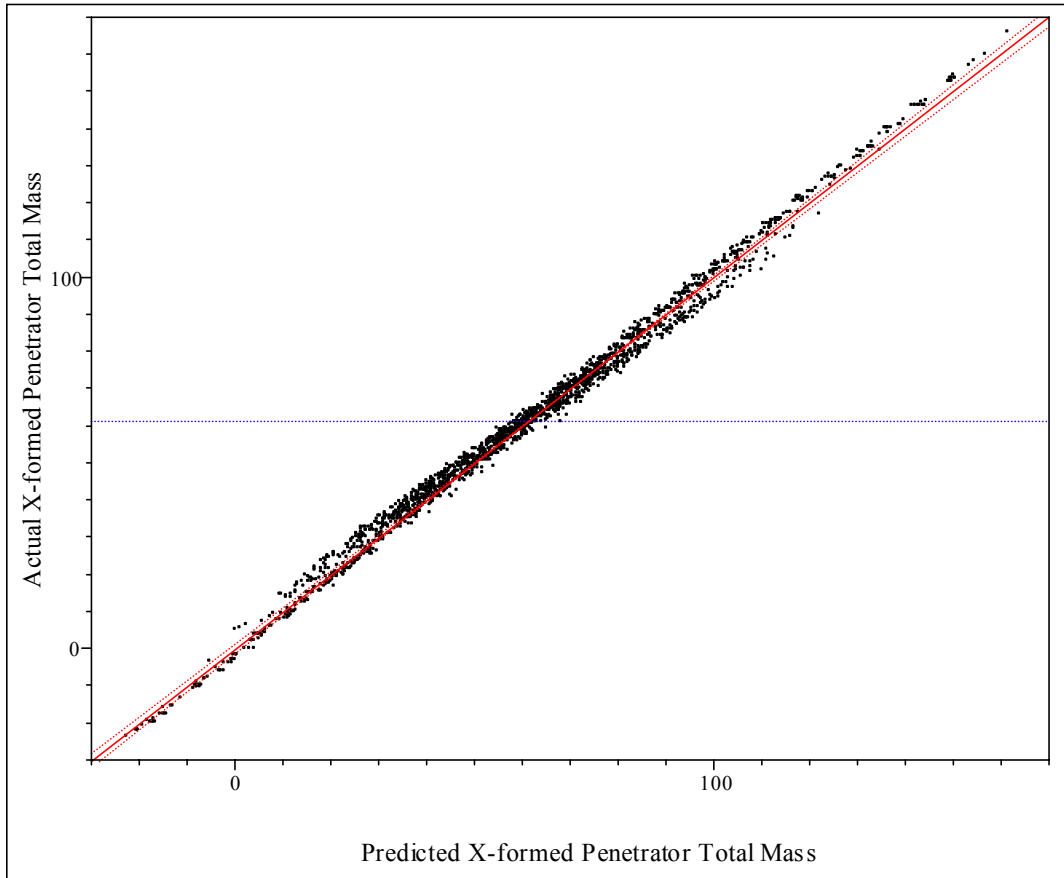


Figure 60: Predicted vs. actual transformed penetrator total mass

Figure 60 shows the plot of RSE predicted vs. actual transformed penetrator total mass, and Table 48 lists the corresponding RSE summary of fit metrics.

Table 48: Summary of fit for transformed penetrator total mass

R²:	0.994
R² Adjusted:	0.994
Root Mean Square Error:	2.504
Mean of Response:	61.20

Observations:	2098
----------------------	------

Penetrator radius

The equation below gives penetrator radius as a function of the corresponding RSE.

$$RadiusPenetrator = (RSE_{RadiusPenetratorX} * -0.03756 + 1)^{-\frac{5}{2}}$$

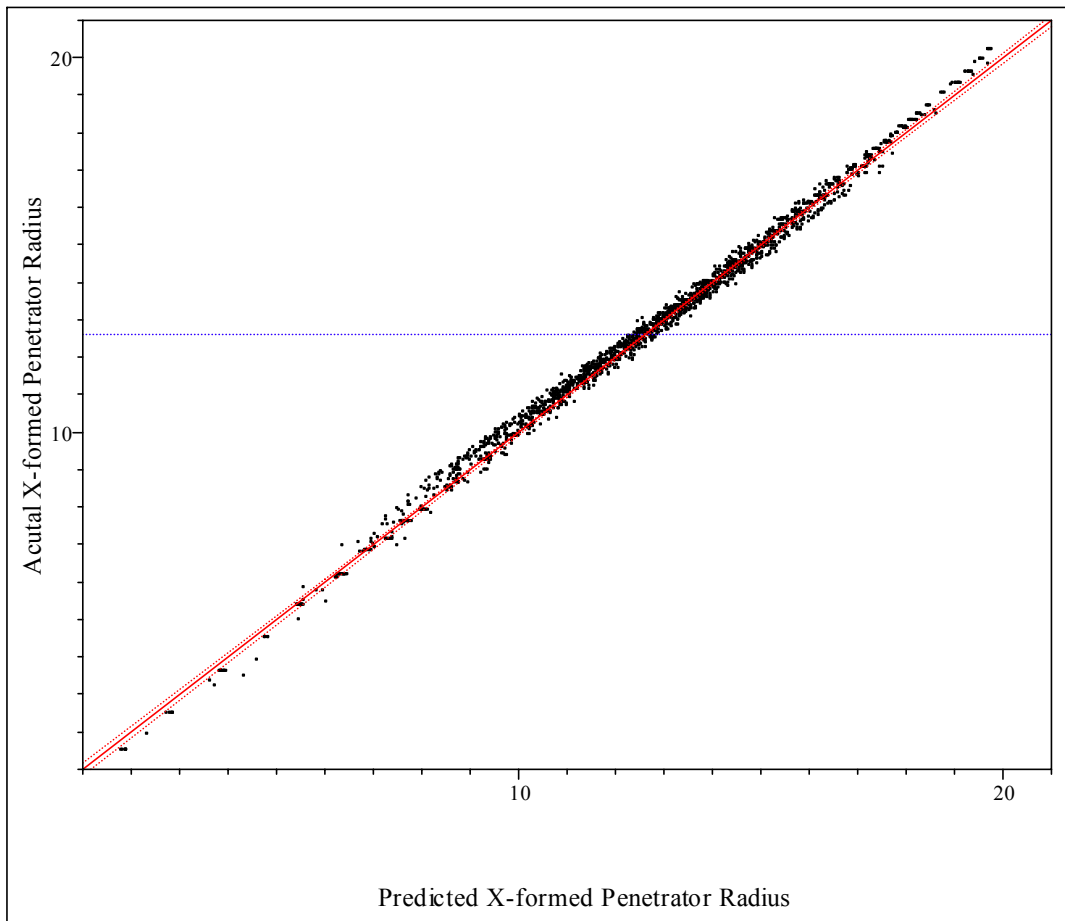


Figure 61: Predicted vs. actual transformed penetrator radius

Figure 61 shows the plot of RSE predicted vs. actual transformed penetrator radius, and Table 49 lists the corresponding RSE summary of fit metrics.

Table 49: Summary of fit for transformed penetrator radius

R²:	0.996
R² Adjusted:	0.995
Root Mean Square Error:	0.206
Mean of Response:	12.64
Observations:	2098

External wall surface temperature

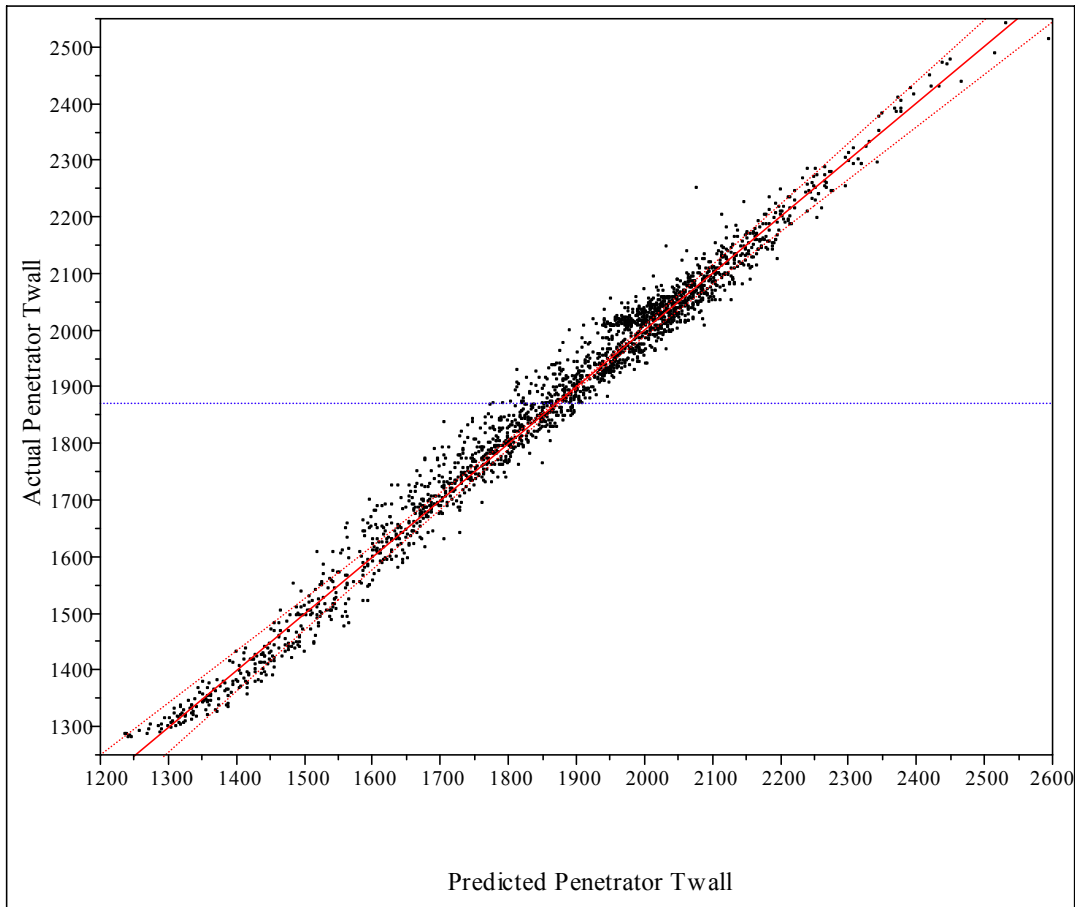


Figure 62: Predicted vs. actual penetrator external surface temperature

Figure 62 shows the plot of RSE predicted vs. actual penetrator external wall surface temperature, and Table 50 lists the corresponding RSE summary of fit metrics.

Table 50: Summary of fit for penetrator external surface temperature

R²:	0.981
R² Adjusted:	0.976

Root Mean Square Error:	35.72
Mean of Response:	1872
Observations:	2098

Thermal power

The equation below gives penetrator thermal power as a function of the corresponding RSE.

$$PenetratorPower = (RSE_{PenetratorPowerX} * 0.0003588 + 1)^5$$

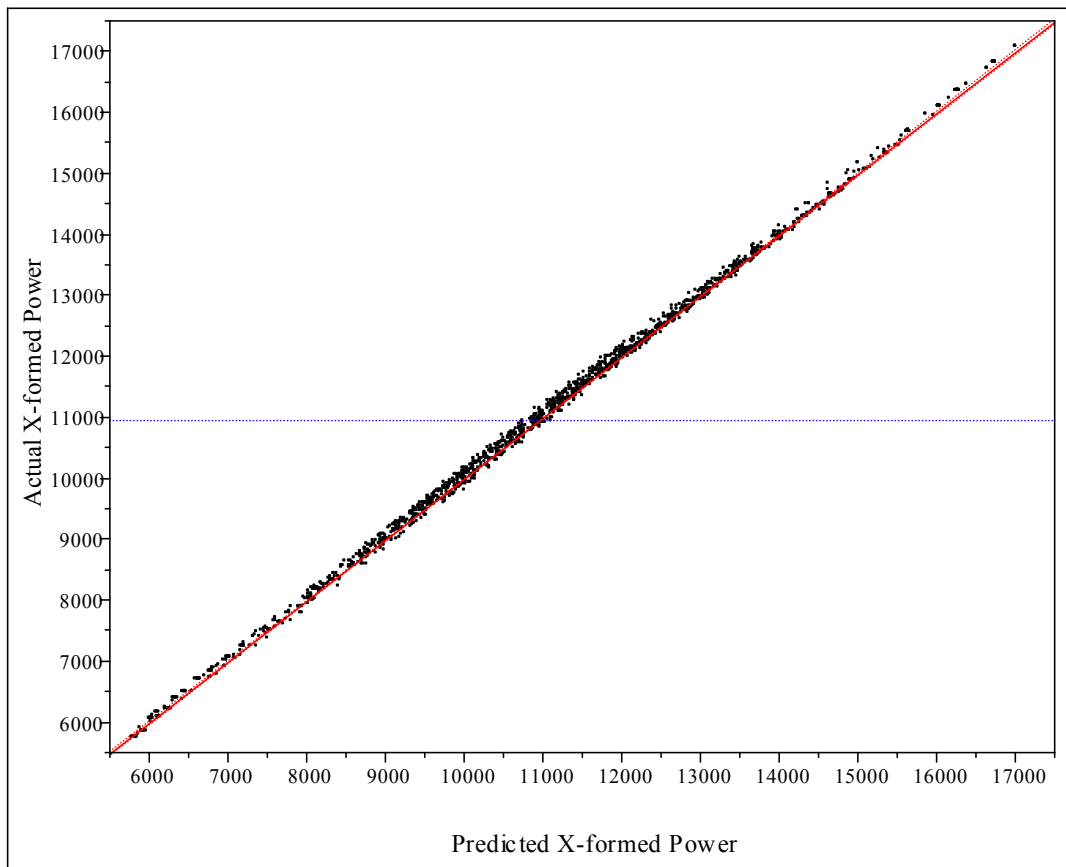


Figure 63: Predicted vs. actual transformed penetrator power

Figure 63 shows the plot of RSE predicted vs. actual transformed penetrator power, and Table 51 lists the corresponding RSE summary of fit metrics.

Table 51: Summary of fit for transformed penetrator power

R²:	0.999
R² Adjusted:	0.999
Root Mean Square Error:	73.17
Mean of Response:	10970
Observations:	2098

FEASIBILITY OF PENETRATING EIGHTY METERS OF GRANITE WITH BASELINE Tm_2O_3 RIPTP IN LESS THAN TWENTY-FOUR HOURS

Investigation of the approach to determining feasibility in the design space documented in Kirby et al's TIF and TIES methodologies led to the identification of some fundamental problems with the proposed approach (see "Appendix F – Some Notes on the Feasible Design Space Assessment Proposed in "). A more appropriate method of assessing *existence* of feasible design space as compared to the MCS suggested is through analytical solution, numerical optimization, or graphical exploration of the RSE's.

Baseline feasibility assessment

The response surface equations described above were used in *JMP's* "Response Profiler" utility to explore the system space of the baseline Thulium-170 RIPTP. It was found that given the most favorable combinations of all system variable settings (without regard to how they might practically be realized), points did exist in the baseline RIPTP system space which had sufficient penetration rate to defeat a DBHT in less than 24 hours. Given that this was so, it was decided to investigate the likely baseline penetrator

characteristics given the uncertainty in the various input variables, particularly those specifying characteristics of rock.

Baseline uncertain variable distribution definitions

The variables listed in Table 52 were identified as having significant uncertainty associated with them and assigned the specified probability distributions. All distributions were treated as independent random variables. Note that this assumption is physically indefensible for the rock property variables as variations in chemical composition of rocks are a primary cause of natural variations in the properties. Thus, if one is attempting to estimate the potential impact of rock property variability across the range of potential target geologies without knowledge or specification of relative frequency, it is still not correct to specify independent distributions on the various properties. This said, data sufficient to empirically specify distributions and their covariances were not available, nor were sufficient resources available to develop and implement a theoretical basis for specifying their covariance.

Regardless, the MCS was performed as the variability of the output variable distributions resulting from the assigned input variable distributions should still bound the distribution ranges that would result if covariances were properly specified (and assuming a sufficiently great number of samples as previously discussed in reference to Kirby’s approach to determination of feasible design space).

Table 52: Uncertain variables and their assumed distributions for MCS

VARIABLE	DISTRIBUTION	HIGH	MID	LOW
Granite Ambient Temperature	Triangular	302	291	273
Rock Melting Temperature	Uniform	1850		1600
Rock Density	Triangular	2.7	2.4	2.1
Enthalpy of Formation	Triangular	5.00E+09	1.01E+09	1.00E+09

Rock Liquid Viscosity Constant A	Uniform	1.00E+15		1.00E+12
Rock Liquid Viscosity Constant Beta	Uniform	5.10E-03		3.60E-03
Rock Liquid Average Conductivity	Triangular	4.50E+05	2.1E+05	9.87E+04
Rock Liquid Average Heat Capacity	Triangular	2.10E+07	10E+06	6.50E+06
Rock Solid Average Heat Capacity	Triangular	1.30E+07	9.75E+06	6.50E+06
Rock Liquid Average Density	Triangular	2.5	2.3	2.1
Rock Average Conductivity	Triangular	2.20E+05	1.55E+05	1.00E+05
¹⁶⁹ Tm σ_c	Normal	$\sigma=2.7$	$\mu=113.2$	
¹⁷⁰ Tm σ_c	Normal	$\sigma=4$	$\mu=92$	
¹⁷¹ Tm σ_c	Normal	$\sigma=30$	$\mu=160$	
¹⁷² Tm σ_c	Triangular	300	160	1

Table 53: Design variable settings for MCS

VARIABLE	UNITS	VALUE
Fraction Target Element Comprised of Isotope	<i>non-dim.</i>	.90
Vol. Packing Efficiency of Target Elements	<i>non-dim.</i>	.74
Flux of Thermal Neutrons	<i>neut./cm²s</i>	5E+14
Thermal Power of Nuclear Reactor	<i>Megawatts</i>	30
Fraction Excess Neutrons for Isotope Production	<i>non-dim.</i>	0.3
Days for Irradiation in Reactor	<i>days</i>	49
Days for Cool down of Target Prior to Assembly	<i>days</i>	23
Days to Process Target/Deliver Penetrator	<i>days</i>	7
Days Allowed for Penetration of Penetrator	<i>days</i>	10
Fineness Ratio of Penetrator	<i>non-dim.</i>	4
Case Thickness Factor of Penetrator	<i>non-dim.</i>	0.4
Thermal Conductivity of Penetrator Core	<i>erg/(cm s K)</i>	2E+06
Conductivity of Penetrator Case	<i>erg/(cm s K)</i>	9E+06
Density of Penetrator Case	<i>g/cc</i>	18
Emissivity of Penetrator Case	<i>non-dim.</i>	0.2

Figure 64 through Figure 71 show the resulting Probability Distribution Function (PDF) and Cumulative Distribution Function (CDF) output variable distributions for the baseline penetrator design given the assumed uncertainty in rock properties and known uncertainty in isotope transmutation cross-sections. The results suggest a somewhat better probable performance than initially estimated for the baseline penetrator given rock and nuclear property estimated uncertainties. Regardless, the CDF plots suggest a negligible

likelihood of the baseline design performing better than 20 meters/day in initial penetration rate, with a most probable initial penetration rate of about 13 meters/day. Temperature CDF distributions indicate negligible likelihood of exceeding material melting temperature limitations for case and core given the assumptions.

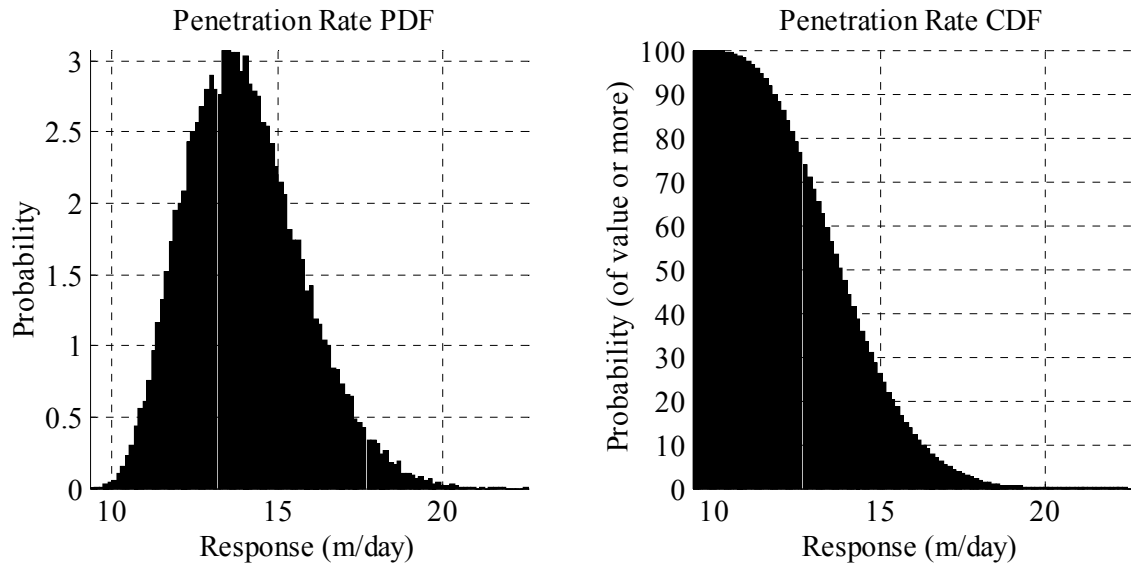


Figure 64: Penetration-rate distribution functions for the baseline RIPTP

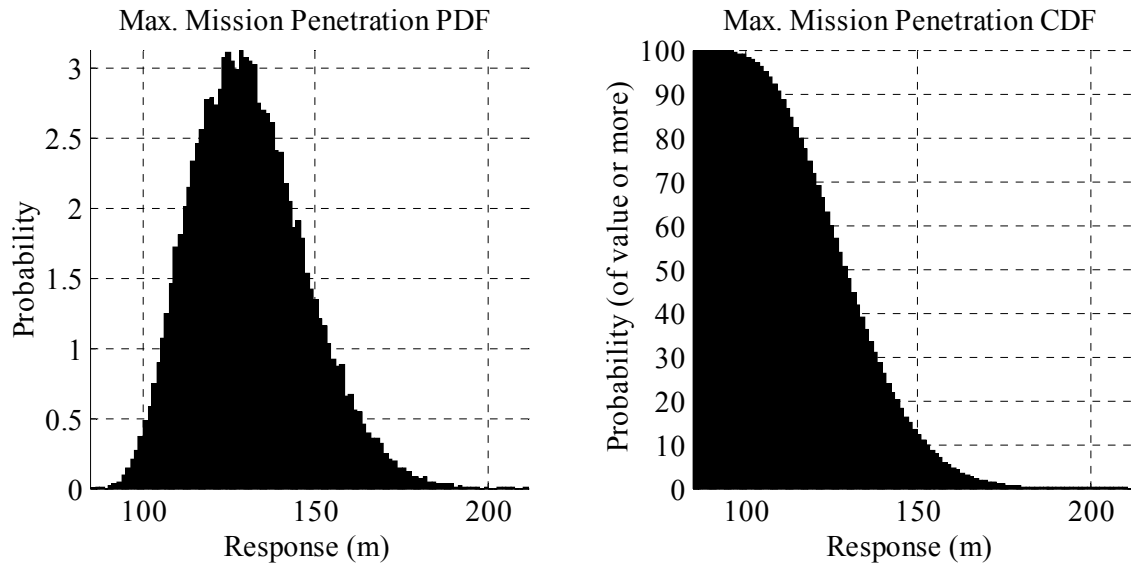


Figure 65: Maximum mission penetration distribution functions for the baseline RIPTP

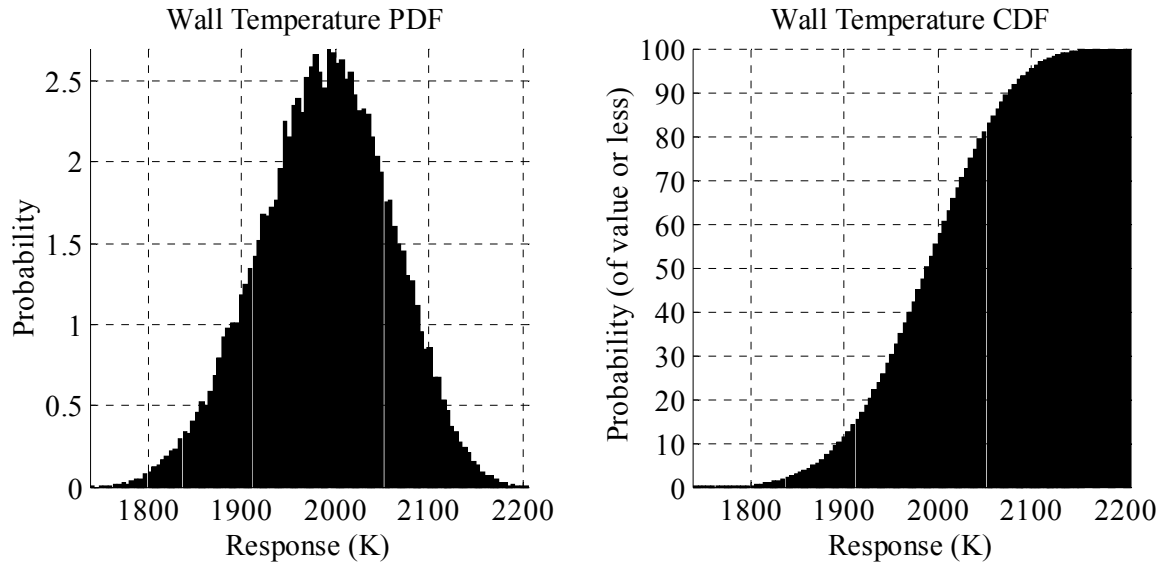


Figure 66: Melt wall temperature distribution functions for the baseline RIPTP

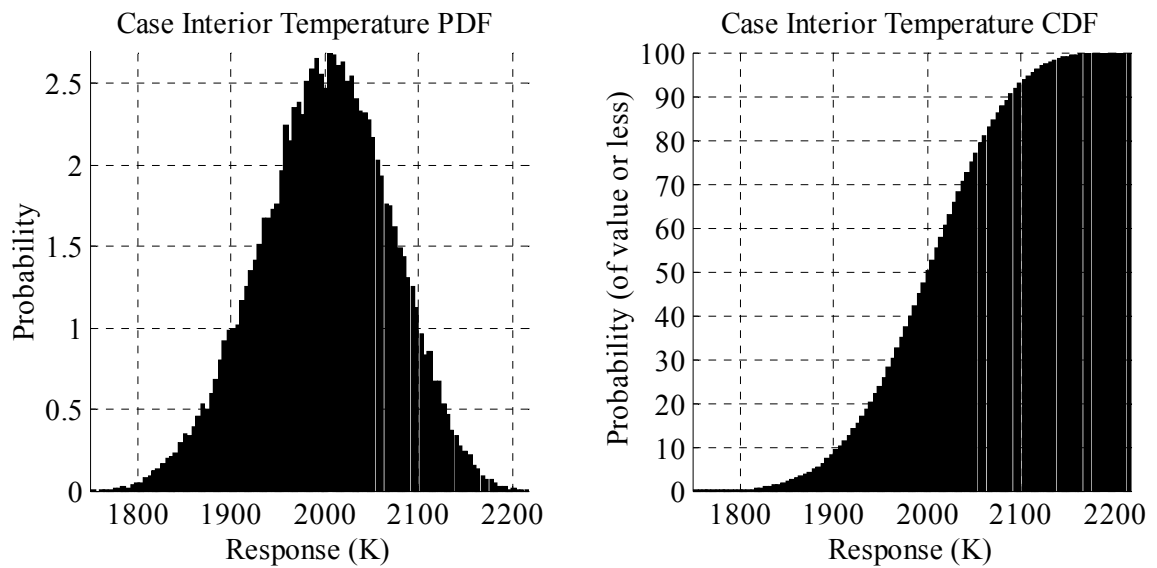


Figure 67: Case interior temperature distribution functions for the baseline RIPTP

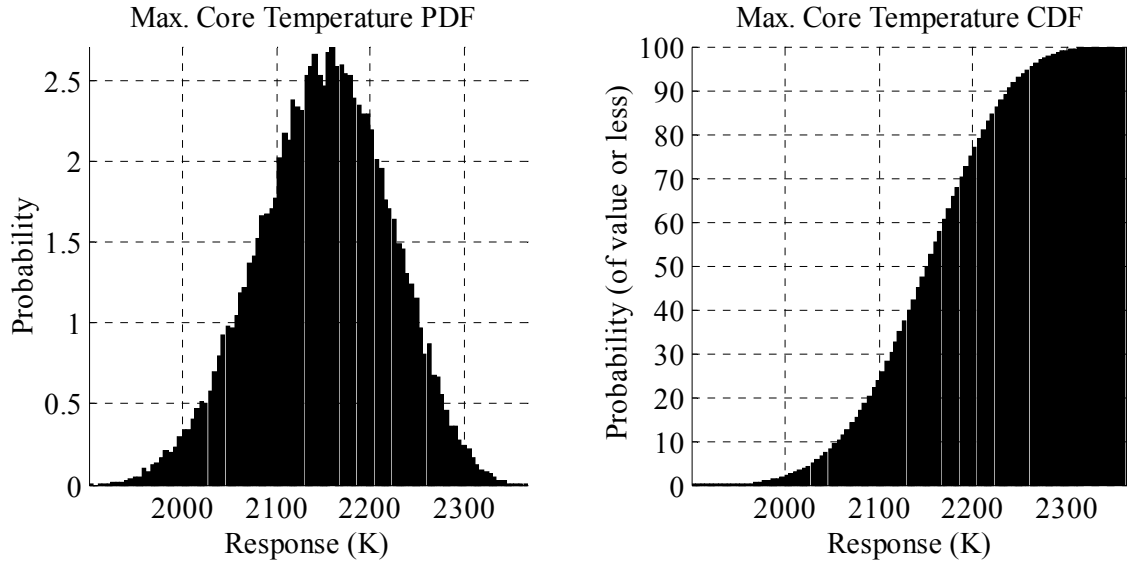


Figure 68: Maximum core temperature distribution functions for the baseline RIPTP

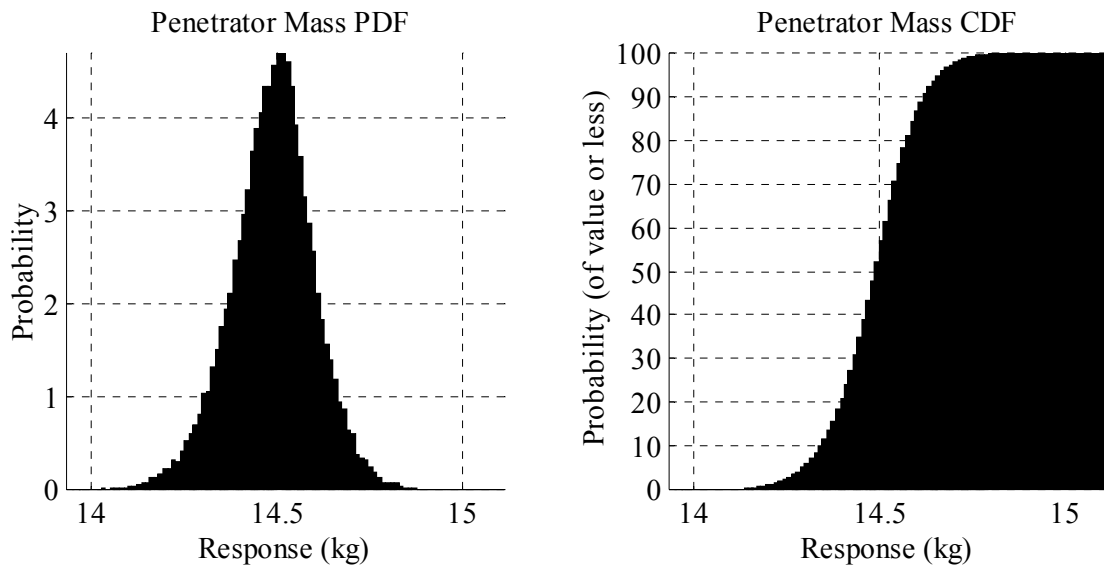


Figure 69: Total mass distribution functions for the baseline RIPTP

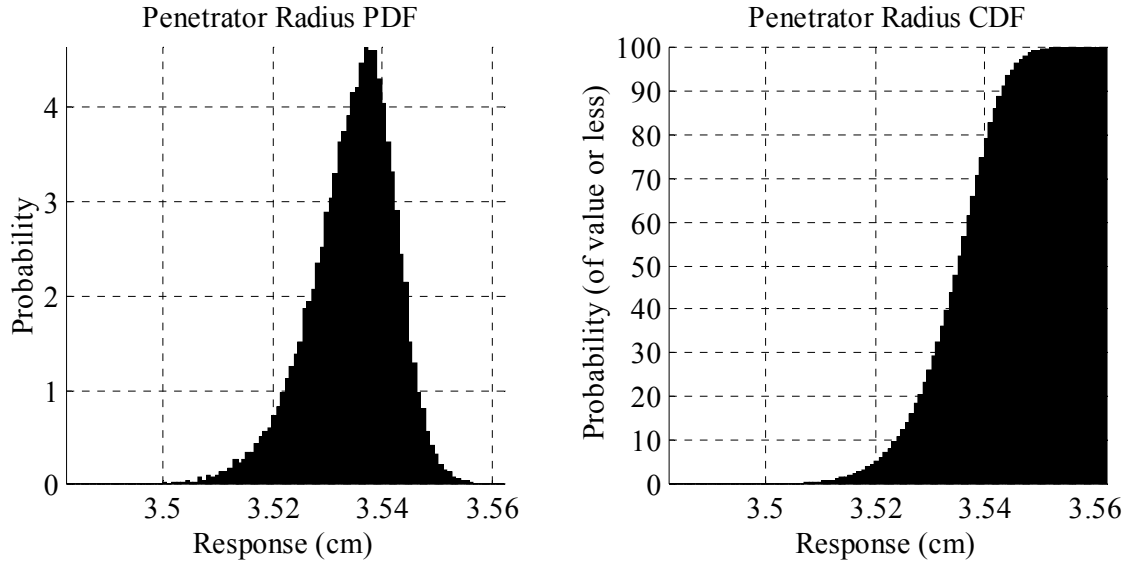


Figure 70: Radius distribution functions for the baseline RIPTP

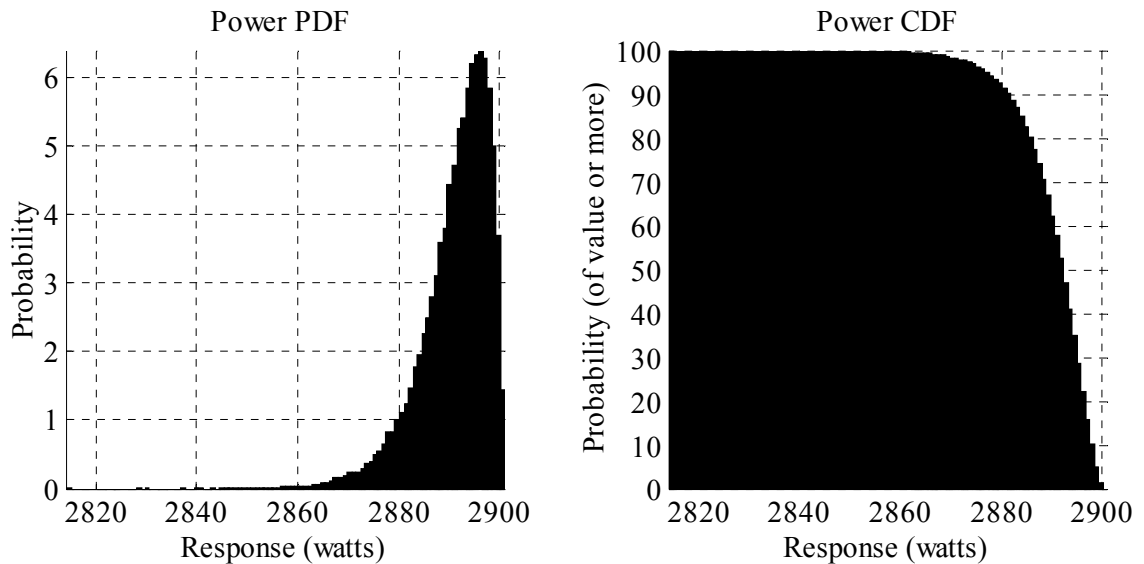


Figure 71: Power distribution functions for the baseline RIPTP

Identification of system variables most important to penetration variability

Utilization of *JMP's "Prediction Profiler"* application allowed simultaneous evaluation of the impact of all system variables on all responses of interest (see Figure 72 and Figure 73). Each row in the prediction profiler shows the variation of one response as

a function of the variation in each system variable (one per column) taken one at a time. The profiler shown in each of the two figures is split into halves to fit the page.

Figure 72 shows the penetrator wall temperature and penetration rate for the nominal settings for all variables. Figure 73 shows these two responses again, but corresponding to maximum settings for target fraction, fineness ratio, packing efficiency, reactor power, reactor neutron flux, and target irradiation days.

From exploring the design space using the prediction profiler and reviewing the magnitudes of the parameter estimates it was determined that the variables having the greatest impact on penetration rate were those having to do with: 1) maximizing penetrator power density (penetrator fineness ratio, case thickness factor, neutron flux, reactor power, irradiation days, packing efficiency of target elements in penetrator internal volume, target element fraction comprised of radioisotope target material, neutron efficiency, and cooldown days); and 2), rock properties (average heat capacity of rock, density of rock, and rock melting temperature).

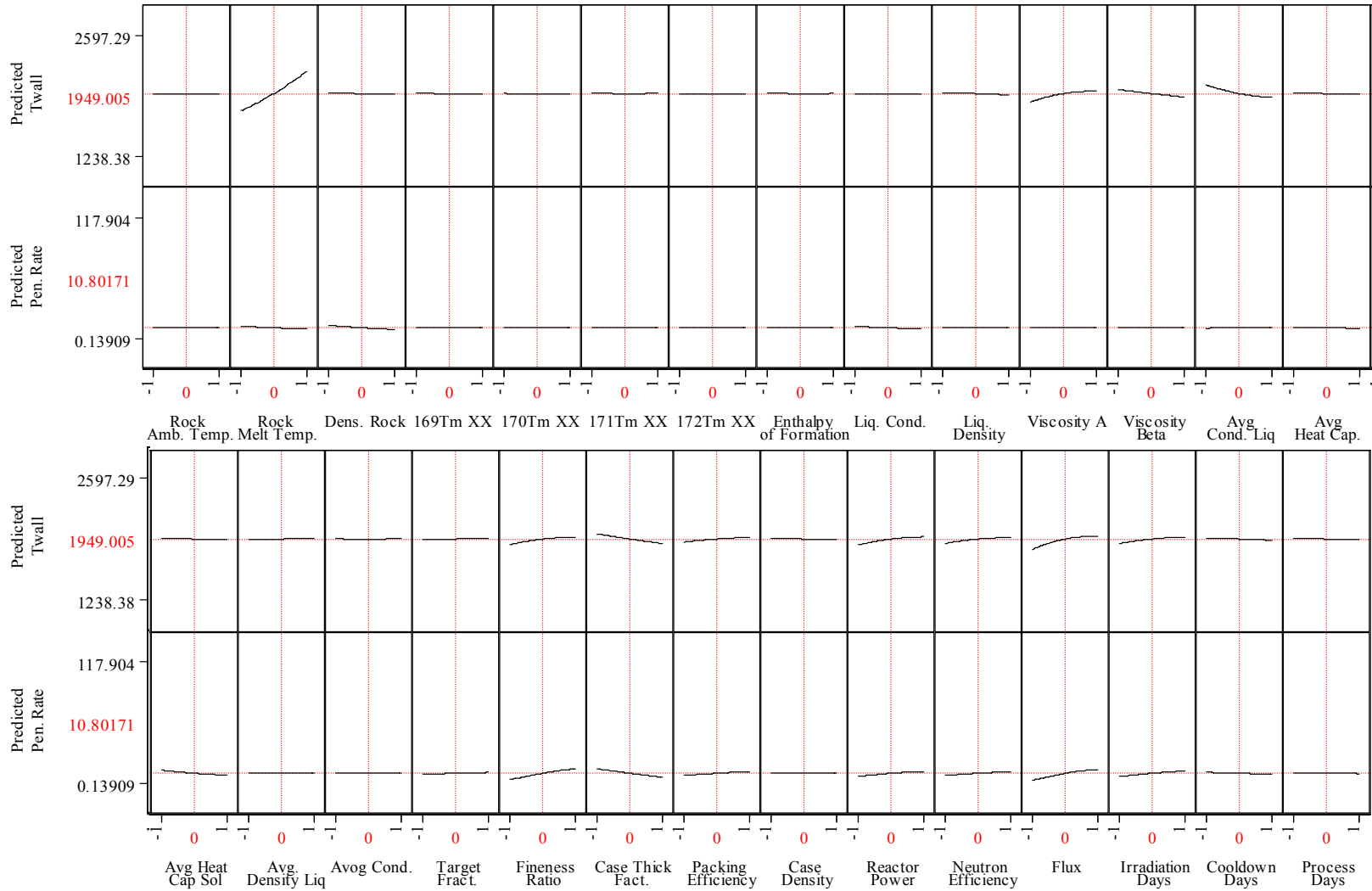


Figure 72: “Prediction Profiler” from *JMP* for RIPTP wall temperature and penetration rate as a function of system variables

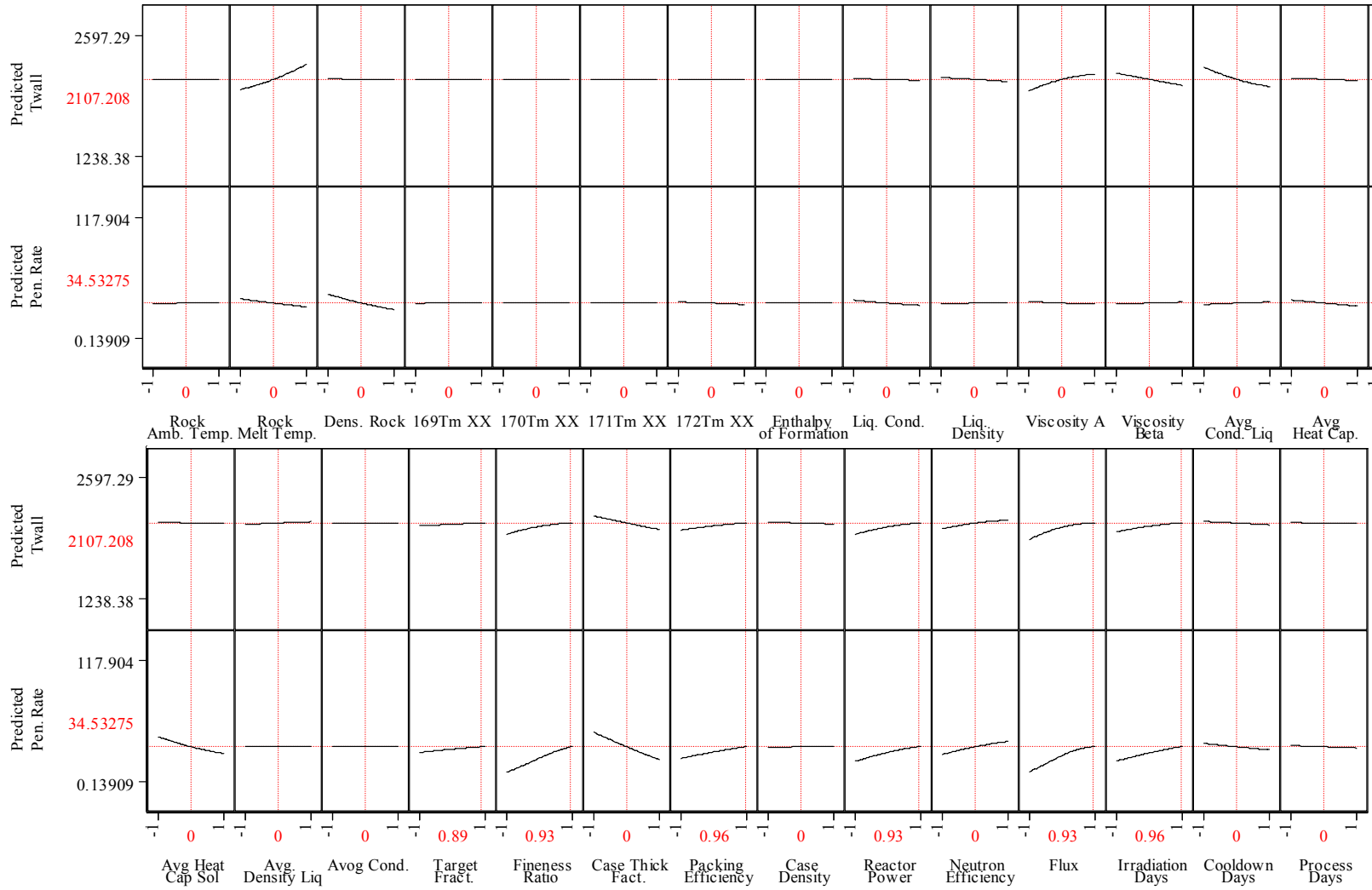


Figure 73: “Prediction Profiler” from *JMP* for RIPTP wall temperature and penetration rate as a function of system variables with changed values

Discussion of possible technologies to effect changes in identified variables

As these variables have a disproportionate effect on penetration rates achievable as compared to the other variables (given the ranges specified for each and limitations of the analysis given the assumptions made) it makes sense to consider them with respect to possible technologies that might effect advantageous changes in them to enhance rock penetration rates.

Alternatives for increasing reactor power, excess neutron utilization efficiency for production of radioisotopes, and duration of irradiation have already been identified and discussed – namely, the possibility of building a new dedicated high thermal flux radioisotope production reactor. This alternative has disadvantages with respect to justification of cost... other uses for the reactor and the thermal power generated would likely have to be found to justify such a facility.

A potentially more attractive approach to achieving the desired effect (an increase in power density) is the selection of an isotope with more advantageous production characteristics such as ytterbium-168. As irradiation of highly enriched ytterbium-168 shouldn't produce difficult to shield radioisotopes as a by-product (as occurs with thulium-172 produced during thulium-170 production), “cool-down days” could be eliminated. The higher production cross section and shorter half-life also enable shorter irradiation periods and higher power densities with lower neutron fluxes. As previously discussed, use of ytterbium-168 would require identification and development of a cost-effective enrichment technology to highly enrich the ytterbium-168 precursor isotope from its low natural abundance. Possible enrichment technologies are discussed in “Appendix E – Isotope Enrichment Technologies.”

The importance of penetrator fineness ratio and case thickness factor can both be interpreted as illustrating the importance of power density to penetration rate. They further suggest, though, that minimizing the non-RHS fraction of the penetrator (by reducing case wall thickness) and maximizing heat transport along the length of the penetrator to the melting surface are important. Minimizing case wall thickness suggests re-evaluation of the concept of a combined kinetic/thermal penetrator as withstanding kinetic impact may be a significant contributor to required penetrator wall thickness. A better approach may be to either utilize a carrier kinetic penetrator which releases the thermal penetrator after penetrating overburden and/or a shaped charge precursor warhead to create a hole in the ground into which the thermal penetrator is introduced. Also, alternative materials technologies such as refractory composites (metal or ceramic matrix) might provide significant payoff with respect to reduced wall thickness and consequently improved penetration performance.

Maximizing the overall density of radioisotope inside the penetrator conflicts with maintaining a maximum temperature in the RHS core below the melting point of the RHS material, as the sesquioxide compounds of the radioisotopes have poor thermal conductivities and would have to be somehow combined with a higher effective conductivity material or heat transport system to prevent melting. The less volume that is available for enhancing thermal transport (due to higher internal volume fraction of radioisotope), the harder it will be to prevent RHS melting. One possible approach to resolve this design conflict is a RIPTP designed to have a molten RHS core during penetration without jeopardizing radioisotope containment. This approach might

maximize density of the radioisotope in the RIPTP, and the at least partially molten core would enhance heat transfer inside the penetrator due to convective effects.

In terms of technologies potentially effecting improvements on system variables related to rock melting, the principle technology that comes to mind would be introducing elements to the system that tended to reduce rock melting onset and range temperatures (and hence reduce melt viscosity and total heat required for melting). Various compounds such as borosilicates and water are known to substantially affect silicate rock melting temperature and viscosity.^{130, 248} A survey of phase diagrams for silicate systems of varying composition could enable identification of other elements or compounds which have the greatest impact on melting temperatures/viscosities for the least variations in concentration.

Analysis and/or experiments could also be undertaken to attempt to identify elements or compounds that enhance the rate of solution of the minerals in melting rock that most impact melt viscosities. This general approach could be considered essentially a hybrid chemical/radioisotope powered thermal penetrator. It may have advantages, particularly with respect to increasing initial penetration rate and/or terminal lethality against a DHBT space (by enhancing melt reactivity with air). Given the large depth of penetration required and the relatively low energy density of chemically reactive substances as compared to radioisotopes, however, incorporation of a reactive chemical surface that enhanced melting would have to not substantially increase melt hole diameter, or impede radioisotope heat flux to the melting surface, to effect a net positive change to penetration rate.

Performance variability given best settings for power density

The variables having the greatest impact on penetrator power density per unit frontal area were set to their most advantageous values (Table 54) to observe what impact the previously specified uncertain variable distributions would have on penetration rates at higher power densities. Core conductivity was specified at its lowest value to reflect that no fraction of internal volume is available to enhance the poor thermal conductivity of the thulium-sesquioxide.

Table 54: Power density variables and settings

VARIABLE	UNITS	VALUE
Fraction Target Element Comprised of Isotope	<i>non-dim.</i>	.95
Vol. Packing Efficiency of Target Elements	<i>non-dim.</i>	.97
Flux of Thermal Neutrons	<i>neut./cm²s</i>	1E+15
Thermal Power of Nuclear Reactor	<i>Megawatts</i>	60
Days for Irradiation in Reactor	<i>days</i>	49
Fineness Ratio of Penetrator	<i>non-dim.</i>	4
Case Thickness Factor of Penetrator	<i>non-dim.</i>	0.1
Conductivity of Core	<i>erg/(cm s K)</i>	2E+05

Figure 74 through Figure 77 below show the resulting PDFs and CDFs for RIPTP penetration rate, maximum core temperature, penetrator radius, and total mass. It appears that for this RIPTP with reactor and RIPTP design variables set to maximize penetrator power density substantial improvement in expected penetration rate is achieved, with maximum samples penetration rates approaching the goal of 80 meters/day of penetration. The penetrator designs that result are very small in both dimension and weight, with diameters of around 4.7 centimeters and weights of less than seven kilograms. Note that all estimated core temperatures are well in excess of the melting point for thulia, implying an RHS core at least partially and perhaps entirely molten.

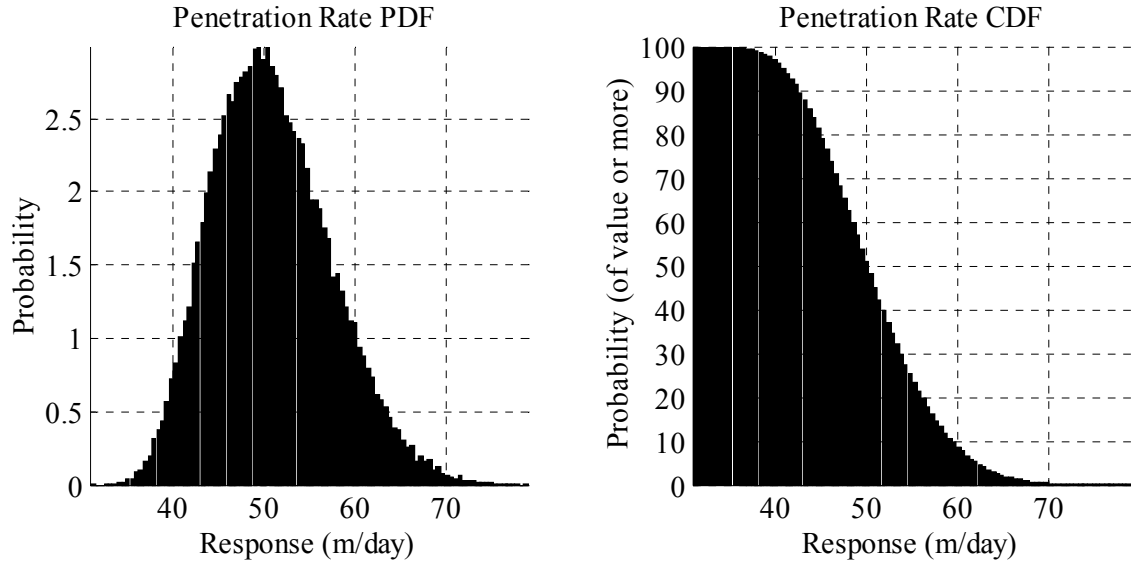


Figure 74: Penetration rate distribution functions for high power density RIPTP

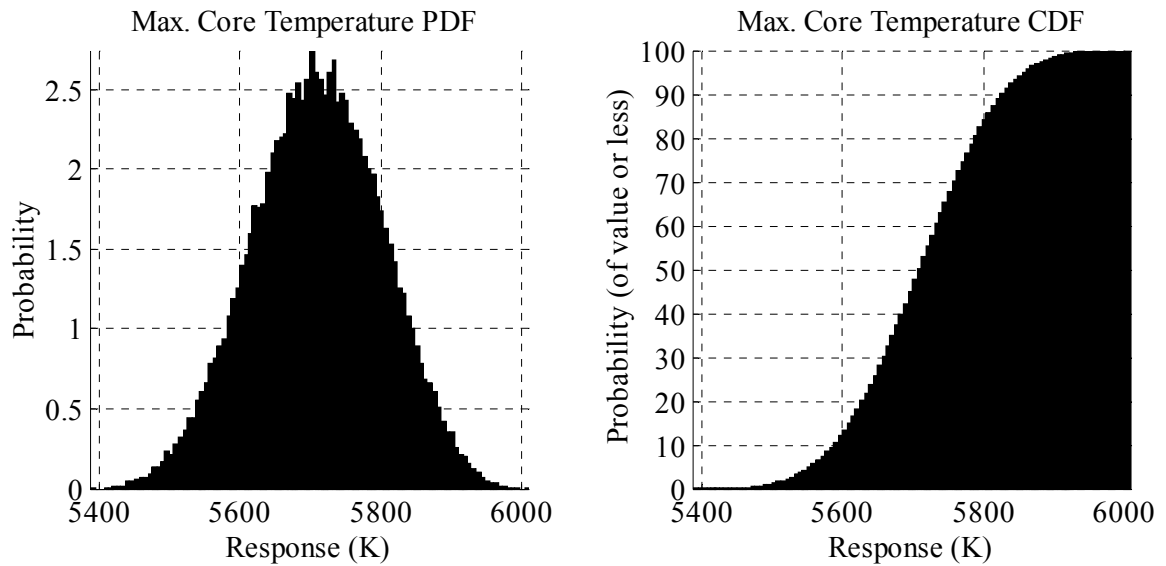


Figure 75: Maximum core temperature distribution functions for high power density RIPTP

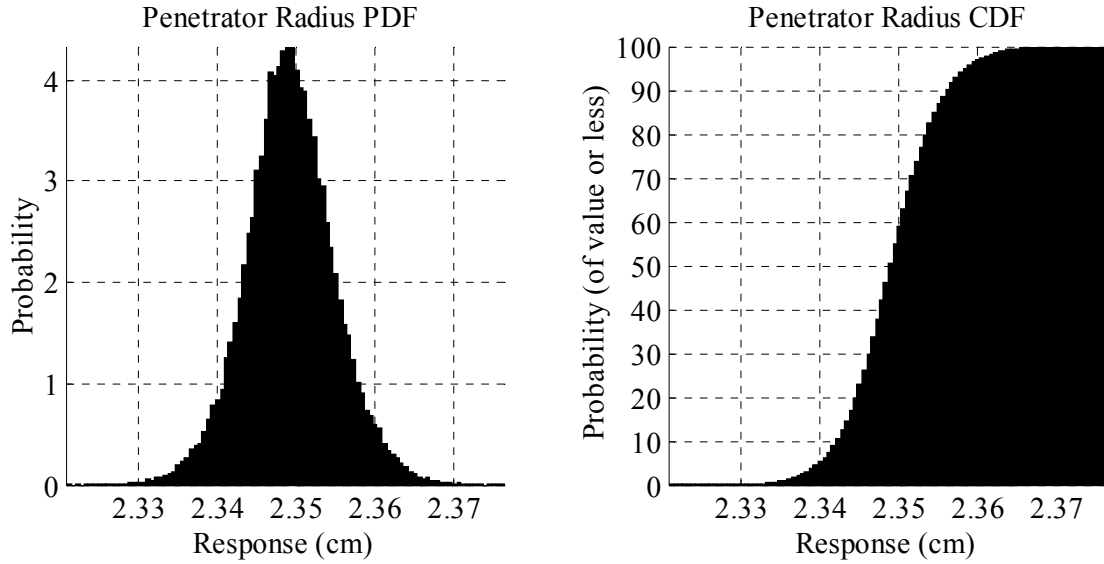


Figure 76: Radius distribution functions for high power density RIPTP

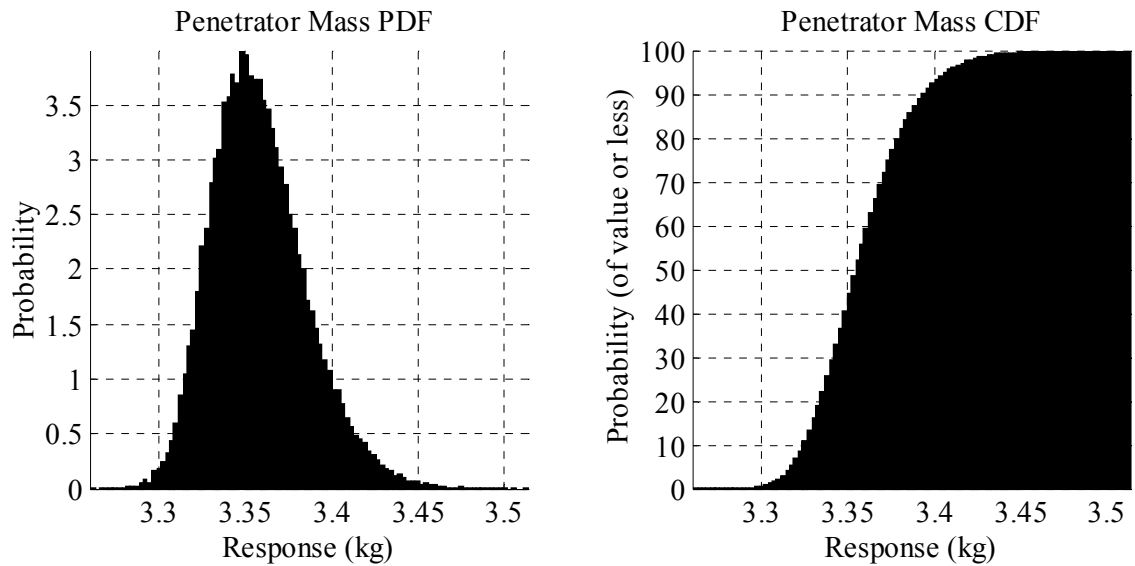


Figure 77: Total mass distribution functions for high power density RIPTP

CONCLUSIONS AND RECOMMENDATIONS

This research was initiated by the proposition that an innovative and feasible solution should be found for achieving full-functional defeat of a class of strategic hardened target using a non-nuclear explosive air-deliverable munition. It was further required that the solution found employ only technologies that would support a near-term operational capability. The class of target specified in the problem statement, NBC hardened DBHTs, have historically been considered invulnerable to anything up to (and sometimes including) a nuclear strike.

Research and analysis of alternatives lead to the identification of the novel RadioIsotope Powered Thermal Subterrene (RIPTP) concept for DBHT defeat, a method of employment against a DBHT, and multiple potential terminal effect mechanisms for achieving defeat against DBHT spaces. Definition of a baseline $^{170}\text{Tm}_2\text{O}_3$ RHS powered RIPTP was achieved through requirements analysis for a RIPTP Radioisotope Heat Source (RHS), creation of and evaluation of alternatives through a multidisciplinary analysis code, and research of historical RHS technologies and programs. Also identified was an $^{169}\text{Yb}_2\text{O}_3$ alternative radioisotope heat source with significant and unique advantages (but requiring a cost-effective precursor isotope enrichment technology) that had not previously been identified from the historical radioisotope power literature.

Production, performance, and safety analyses for both thulium and ytterbium powered RIPTP concepts were performed. These analyses demonstrated that the selected concepts were: feasible to produce; would enable a revolutionary improvement over historically demonstrated munitions hard rock penetration capabilities; posed no significant radiological hazard in nominal scenarios (in sharp contrast to the primary

existing option of nuclear explosive munitions); and in worst-case scenarios posed radiological hazards consistent with or less than those posed by historical and contemporary RHS systems.

Key potential shortcomings to the baseline design were also identified, however. While short half-life radioisotopes eliminated potential for creation by a RIPTP of long-term radiological hazard and facilitated high power densities, they also implied short usable shelf-lives for RHSs once produced and a requirement to manufacture RHSs on demand limiting the potential for operational utility. Limitations of existing national reactor facilities also meant that only one or two of the baseline thulium-170 powered RIPTP would be producible at a time. Given limitations of targeting and delivery accuracy and potential lateral deflection of a RIPTP during penetration this suggested an inadequate number of RIPTPs available for use against a single DBHT to achieve a reasonable probability of kill. Further, maximum penetration rates were expected to be on the order of ten meters a day, less than a desirable rate of 80 meters per day.

The development of cost-effective technologies for highly enriching ytterbium-168 precursor isotope for production of ytterbium RHSs was identified as a primary technology for enabling very rapid simultaneous production a large batches of high performance RIPTPs. Ytterbium RHSs would also enable the use of low thermal flux commercial pressurized reactors for radioisotope production instead of the limited resource of high thermal flux isotope production reactors such as the Advanced Test Reactor and High Flux Isotope Reactor. An alternative approach (to ytterbium enrichment) to mitigating the identified RIPTP baseline design limitations was also identified: construction of a new 3 GW_{th} high thermal flux isotope production reactor.

An approach adapted from Kirby et al's Technology Impact Forecasting (TIF) was then applied to the multidisciplinary analysis of the baseline $^{170}\text{Tm}_2\text{O}_3$ powered RIPTP to attempt to identify: if feasible design space existed to achieve RIPTP performance consistent with penetrating 80 meters of granite in less than 24 hours; probable performance of the baseline RIPTP design and performance characteristics given uncertainties in rock and nuclear properties; and metrics most affecting penetrator performance and possible associated technologies for improving RIPTP penetration rate to desired levels.

One conclusion from this portion of the work was that natural variability in rock may produce better expected penetration performance than originally estimated for the baseline design. It was also determined that any technologies which facilitated the production of higher RIPTP power densities were key to achieving significant improvements in penetration performance. The results of the investigation suggested several possible lines of investigation for achieving higher RHS power densities (other than the previously discussed options of: 1) technologies for cost-effective enrichment of ytterbium-168; 2) and/or a new high thermal power isotope production reactor). One option identified was functionally separating the requirements for kinetic and thermal penetration of rock for the RIPTP so as to facilitate a thinner, less robust RIPTP case. Case material technologies that would facilitate a thinner case would also be advantageous. High power density also tends to result in the expected melting of the refractory RHS core (which possesses poor thermal conductivity). If technology for containment of a RHS core that could be molten during RHS penetration without compromising radiological containment were available it could significantly enhance

power density by eliminating the requirement for interspersions of higher conductivity materials with the poorly thermally conductive radioisotope refractory compounds.

All in all, it was determined from the technology investigation that technology facilitated potential improvements in system variables might enable realization of a RIPTP capable of penetrating to greater than eighty meters depth in 24 hours. A probabilistic investigation of a hypothetical $^{170}\text{Tm}_2\text{O}_3$ high power density excursion from the baseline RIPTP design suggested that expected penetration rates of up to 50 meters/day might be achievable given such technologies.

Should further investigation of the thermal subterrene concept for DBHT defeat be undertaken, the following recommendations are made:

1. The potential viability of both radioisotope powered and fissile powered thermal subterrene approaches to DBHT defeat should be assessed with respect to possible operational utility vs. political costs.
2. If a potential for thermal subterrene viability as a munition is found to exist, the possible use of Fissile Powered Thermal Penetrators (FIPTPs) for strategic DBHT defeat missions should be considered by the Department of Energy in competition with RIPTPs as marked differences in safety, cost, operational availability, and performance likely exist between the two (“Appendix G – Notes on Fissile Implementation”). Furthermore, like RIPTPs, fissile thermal penetrators could pose significantly less collateral damage hazard than the existing alternative of penetrating low-yield nuclear bombs while potentially being significantly more lethal to DBHT spaces than RIPTPs.

3. If a potential for thermal subterranean viability as a munition is found to exist, then the physical phenomena associated with a thermal subterranean breaching a cavity in hard rock should be explored for varying Peclet numbers to characterize terminal effects against DBHT spaces.
4. The possibility of cost-effective enrichment of ytterbium-168 to high isotopic abundance should be assessed. The isotope has potential with regard to enabling rapid production of high power density heat sources in final form (without post-irradiation isotope processing/concentration) that are: compactly shieldable so as to emit zero external radiation; pose no potential of long-term radiological hazard; and can be produced using comparatively available commercial or university-type reactor facilities.
5. Other radioisotopes that were eliminated from consideration for RIPTP application only because of insufficient nuclear property data should be further evaluated as they can potentially offer significant advantages in performance, producibility, operational suitability, and safety with respect to short mission duration RHS applications.
6. Dual-use thermal subterranean technology areas such as nuclear waste disposal and deep geological exploration should be assessed. Interest in these applications should be leveraged to facilitate better understanding of material science, close-contact melting, physics of melt-bubbles in geological materials, high-temperature mineralogy, geology, and other important considerations common among thermal penetrator applications. Considering the recent renewed interest in disposal of radioactive waste by

means of melting and deep geological exploration, a subscale thermal subterrene experiment using a short half-life isotope might be of great interest to portions of the scientific and engineering communities as a safe means of experimenting with thermal subterrene concepts using actual geological materials in the field.

APPENDIX A – ISOTOPES EVALUATED

Table 55 below lists all of the isotopes identified from the ENDF database on the basis of radioisotope half-life. For each isotope the atomic mass number A, elemental symbol, decay type, half-life in years, and precursor isotopes for production are listed. B- = beta-decay, IT = Internal Transition, and ν denotes the radioisotope is producible via neutron capture.

Table 55: Isotopes evaluated from ENDF

A	DECAY	HALF-LIFE (YEARS)	PRODUCTION MECHANISM	PRECURSOR
¹³³ XE	B-	0.014364	ν	¹³² Xe
¹²⁹ XE	IT	0.024329	ν	¹²⁸ Xe
¹²⁶ I	EC	0.035425	ν	¹²⁴ Xe
²³⁷ U	B-	0.018493		
²³⁴ TH	B-	0.066027		
²³⁰ PA	A	0.047671		
²³⁰ U	A	0.056986		
²²⁷ TH	A	0.051178		
²²⁵ AC	A	0.027397		
²²⁵ RA	B-	0.040822		
²²³ RA	A	0.031315		
²⁰⁶ BI	EC	0.017104		
²⁰⁶ PO	A	0.02411		
²⁰⁵ BI	EC	0.041945		
²⁰² TL	EC	0.033507		
¹⁹⁶ AU	B-	0.01694		
¹⁹⁰ IR	EC	0.032274		
¹⁸⁹ IR	EC	0.036164		
¹⁸⁸ PT	A	0.027945		
¹⁷⁸ W	EC	0.059178		
¹⁷² LU	EC	0.018356		
¹⁷¹ LU	EC	0.022575		
¹⁶⁷ TM	EC	0.025342		
¹⁵⁶ TB	EC	0.014658		
¹⁵⁵ TB	EC	0.014575		
¹⁴⁹ GD	EC	0.025425		
¹⁴⁷ EU	A	0.066027		

A	DECAY	HALF-LIFE (YEARS)	PRODUCTION MECHANISM	PRECURSOR
¹⁴⁵ EU	EC	0.016247		
¹⁴⁰ BA	B-	0.034937		
¹²⁰ SB	EC	0.015781		
¹¹⁸ TE	EC	0.016438		
¹⁰⁶ AG	EC	0.022685		
⁹⁹ RH	EC	0.04411		
⁹² NB	EC	0.027808		
⁷⁴ AS	B-	0.048685		
⁷² SE	EC	0.023014		
⁵⁶ NI	EC	0.016644		
⁵² MN	EC	0.015318		
⁴⁸ V	EC	0.043763		
¹³¹ I	B-	0.021975	v	¹³⁰ Te
¹²⁵ SN	B-	0.026411	v	¹²⁴ Sn
¹²⁶ SB	B-	0.033836	v	¹²³ Sb, ¹²⁴ Sn
⁸⁶ RB	B-	0.051074	v	⁸⁵ Rb
¹¹⁷ SN(M)	IT	0.037699	v	¹¹⁶ Sn
¹²¹ TE	EC	0.052493	v	¹²⁰ Te
²¹⁰ BI	B-	0.013732	v	²⁰⁹ Bi
¹¹¹ AG	B-	0.020411	v	¹¹⁰ Pd
³² P	B-	0.039074	v	³¹ P
⁷¹ GE	EC	0.031315	v	⁷⁰ Ge
¹³⁶ CS	B-	0.036055	v	¹³³ Cs
⁴⁷ CA	B-	0.012427	v	⁴⁶ Ca
¹³² CS	EC	0.017751	v	¹³⁰ Ba
¹³¹ BA	EC	0.031507	v	¹³⁰ Ba
¹³¹ XE	IT	0.032696	v	¹³⁰ Ba
¹³¹ CS	EC	0.026545	v	¹³⁰ Ba
¹⁵⁶ EU	B-	0.041616	v	¹⁵³ Eu, ¹⁵⁴ Sm
¹⁴⁸ PM	B-	0.014707	v	¹⁴⁶ Nd
¹⁴⁷ ND	B-	0.030082	v	¹⁴⁶ Nd
¹⁴³ PR	B-	0.037178	v	¹⁴² Ce, ¹⁴¹ Pr
¹⁰³ PD	EC	0.046551	v	¹⁰² Pd
¹⁶¹ TB	B-	0.018921	v	¹⁶⁰ Gd, ¹⁵⁹ Tb
¹⁹³ IR(M)	IT	0.028849	v	¹⁹² Ir
¹⁹¹ OS	B-	0.042192	v	¹⁹⁰ Os
¹⁸³ TA	B-	0.013973	v	¹⁸¹ Ta
¹⁷⁷ LU	B-	0.018211	v	¹⁷⁶ Lu, ¹⁷⁶ Yb
¹⁶⁹ ER	B-	0.025753	v	¹⁶⁸ Er
²²⁷ AC	A	21.772	Chemical extraction from uranium, plutonium?	
¹⁰⁵ AG	EC	0.113123		
¹¹⁰ AG(M)	B-	0.684274	v	¹⁰⁹ Ag
³⁷ AR	EC	0.096	v	³⁶ Ar

A	DECAY	HALF-LIFE (YEARS)	PRODUCTION MECHANISM	PRECURSOR
⁴² AR	B-	32.9	v	⁴⁰ Ar
⁷³ AS	EC	0.22		
¹⁹⁵ AU	EC	0.509858		
¹³³ BA	EC	10.54493	v	¹³² Ba
²⁰⁷ BI	EC	32.9		
²⁴⁹ BK	A	0.90411		²⁴⁸ Cm
⁴⁵ CA	B-	0.445507	v	⁴⁴ Ca
¹⁰⁹ CD	EC	1.26411	v	¹⁰⁸ Cd
¹¹³ CD	B-	14.1	v	¹¹² Cd
¹¹⁵ CD	B-	0.122082	v	¹¹⁴ Cd
¹³⁹ CE	EC	0.377099	v	¹³⁸ Ce
¹⁴¹ CE	B-	0.089063	v	¹⁴⁰ Ce
¹⁴⁴ CE	B-	0.780575	v	¹⁴² Ce
²⁴⁸ CF	A	0.913699		
²⁵⁰ CF	A	13.08		
²⁴⁰ CM	A	0.073973		
²⁴¹ CM	A	0.089863		
²⁴² CM	A	0.446027		
²⁴³ CM	A	29.1		
²⁴⁴ CM	A	18.1		
⁵⁶ CO	EC	0.211597		
⁵⁷ CO	EC	0.744493		
⁵⁸ CO	EC	0.194137		
⁶⁰ CO	B-	5.274795	v	⁵⁹ Co
⁵¹ CR	EC	0.075897	v	⁵⁰ Cr
¹³⁴ CS	EC	2.067123	v	¹³³ Cs
¹³⁷ CS	B-	30.07	v	¹³³ Cs
¹⁵⁹ DY	EC	0.395616	v	¹⁵⁸ Dy
¹⁴⁷ EU	A	0.066027		
¹⁴⁸ EU	A	0.149315		
¹⁴⁹ EU	EC	0.255068		
¹⁵⁰ EU	EC	36.9		
¹⁵² EU	EC	13.516	v	¹⁵² Eu
¹⁵⁴ EU	B-	8.593	v	¹⁵³ Eu
¹⁵⁵ EU	B-	4.7611	v	¹⁵³ Eu
⁵⁵ FE	EC	2.737	v	⁵⁴ Fe
⁵⁹ FE	B-	0.121904	v	⁵⁸ Fe
¹⁴⁶ GD	EC	0.132247		
¹⁵¹ GD	A	0.339726		
¹⁵³ GD	EC	0.65863	v	¹⁵² Gd
⁶⁸ GE	EC	0.741918		
³ H	B-	12.32	v	² H
¹⁷² HF	EC	1.87		

A	DECAY	HALF-LIFE (YEARS)	PRODUCTION MECHANISM	PRECURSOR
¹⁷⁵ HF	EC	0.191781	v	¹⁷⁴ Hf
¹⁷⁸ HF(M)	IT	31	v	¹⁷⁷ Hf
¹⁷⁹ HF(M)	IT	0.06863	v	¹⁷⁸ Hf
¹⁸¹ HF	B-	0.116137	v	¹⁸⁰ Hf
²⁰³ HG	B-	0.127704	v	²⁰² Hg
¹²⁵ I	EC	0.16274		
¹¹⁴ IN(M)	EC	0.135644	v	¹¹³ In
¹⁹² IR	B-	0.202266	v	¹⁹¹ Ir
¹⁹⁴ IR(M)	B-	0.468493	v	¹⁹³ Ir
⁸⁵ KR	B-	10.77918	v	⁸⁴ Kr
¹⁷³ LU	EC	1.37		
¹⁷⁴ LU	IT	0.389041		
¹⁷⁴ LU	EC	3.31		
¹⁷⁷ LU	B-	0.439562	v	¹⁷⁶ Lu
⁵⁴ MN	B-	0.855123		
²² NA	EC	2.6019		
⁹¹ NB	IT	0.16674		
⁹³ NB	IT	16.13		⁹² Nb
⁹⁵ NB	B-	0.095866	v	⁹³ Nb
²³⁵ NP	A	1.085205		
¹⁸⁵ OS	EC	0.256438	v	¹⁸⁴ Os
¹⁹⁴ OS	B-	6	v	¹⁹² Os
³³ P	B-	0.069425	v	³¹ P
²³³ PA	B-	0.073882	N	²³² Th
²¹⁰ PB	A	22.3	N	²⁰⁸ Pb
¹⁴³ PM	EC	0.726027		
¹⁴⁴ PM	EC	0.994521		
¹⁴⁵ PM	A	17.7	v	¹⁴⁴ Sm, ¹⁴⁵ Sm
¹⁴⁶ PM	B-	5.53		
¹⁴⁷ PM	B-	2.6234	v	¹⁴⁶ Nd
¹⁴⁸ PM	B-	0.113123	v	¹⁴⁴ Pm
²⁰⁸ PO	A	2.898		
²¹⁰ PO	A	0.379112	v	²⁰⁹ Bi
¹⁹³ PT	EC	50	v	¹⁰² Pt
²³⁶ PU	A	2.858		
²³⁷ PU	A	0.123836		
²³⁸ PU	A	87.7	v	²³⁷ Np
²⁴¹ PU	A	14.29	v	²³⁹ Pu
²²⁸ RA	B-	5.75		
⁸³ RB	EC	0.236164		
⁸⁴ RB	B-	0.089781		
¹⁸³ RE	EC	0.191781		
¹⁸⁴ RE	EC	0.10411		

A	DECAY	HALF-LIFE (YEARS)	PRODUCTION MECHANISM	PRECURSOR
¹⁸⁴ RE	EC	0.463014		
¹⁰¹ RH	EC	3.3		
¹⁰² RH	B-	0.567123		
¹⁰² RH	IT	2.9		
¹⁰³ RU	B-	0.107562		¹⁰² Ru
¹⁰⁶ RU	B-	1.023534	v	¹⁰⁴ Ru
³⁵ S	B-	0.239753	v	³⁴ S
¹²⁴ SB	B-	0.164932	v	¹²³ Sb
¹²⁵ SB	B-	2.75856	v	¹²⁴ Sb
⁴⁶ SC	B-	0.229562	v	⁴⁵ Sc
⁷⁵ SE	EC	0.328162	v	⁷⁴ Se
¹⁴⁵ SM	EC	0.931507	v	¹⁴⁴ Sm
¹⁵¹ SM	B-	90	v	¹⁵⁰ Sm
¹¹³ SN	EC	0.315315	v	¹¹² Sn
¹¹⁹ SN	IT	0.803014	v	¹¹⁸ Sn
¹²¹ SN	B-	55	v	¹²⁰ Sn
¹²³ SN	B-	0.353973	v	¹²² Sn
⁸² SR	EC	0.07		
⁸⁵ SR	EC	0.177644	v	⁸⁴ Sr
⁸⁹ SR	B-	0.138438	v	⁸⁸ Sr
⁹⁰ SR	B-	28.79	v	
¹⁷⁹ TA	EC	1.82		
¹⁸² TA	B-	0.313507	v	¹⁸¹ Ta
¹⁵⁷ TB	EC	71		
¹⁶⁰ TB	B-	0.198082	v	¹⁵⁹ Tb
⁹⁵ TC	EC	0.167123		
⁹⁷ TC	IT	0.250411		
¹²¹ TE	IT	0.421918	v	¹²⁰ Te
¹²³ TE	IT	0.327397	v	¹²² Te
¹²⁵ TE	IT	0.15726	v	¹²⁴ Te
¹²⁷ TE	B-	0.29863	v	¹²⁶ Te
¹²⁹ TE	B-	0.092055	v	¹²⁸ Te
²²⁸ TH	A	1.9116	v	²³¹ Pa
²³⁴ TH	B-	0.066027	v	²³² Th
⁴⁴ TI	EC	60		
²⁰⁴ TL	B-	3.78	v	²⁰³ Tl
¹⁶⁸ TM	B-	0.255068		
¹⁷⁰ TM	B-	0.352329	v	¹⁶⁹ Tm
¹⁷¹ TM	B-	1.92	v	
²³⁰ U	A	0.056986		
²³² U	A	68.9	v	²³¹ Pa
⁴⁹ V	EC	0.90411		
¹⁷⁸ W	EC	0.059178		

A	DECAY	HALF-LIFE (YEARS)	PRODUCTION MECHANISM	PRECURSOR
¹⁸¹ W	EC	0.332055	v	¹⁸⁰ W
¹⁸⁵ W	B-	0.205753	v	¹⁸⁴ W
¹⁸⁸ W	B-	0.191178	v	¹⁸⁶ W
¹²⁷ XE	EC	0.099726	v	¹²⁶ Xe
⁸⁸ Y	EC	0.292192		
⁹¹ Y	B-	0.160301	v	⁸⁹ Y, ⁹⁰ Y
¹⁶⁹ YB	EC	0.087742	v	¹⁶⁸ Yb
⁶⁵ ZN	EC	0.668658	v	⁶⁴ Zn
⁸⁸ ZR	EC	0.228493		
⁹⁵ ZR	B-	0.17543	v	⁹⁴ Zr

Table 56, below, contains the screening results of the radioisotopes identified to be producible through neutron transmutation. Rows corresponding to potentially satisfactory radioisotopes are in bold, rows corresponding to unsatisfactory radioisotopes are in italic.

Content of each column is as follows: the “RI OK?” column contains the determination, if any, as to suitability of the specified radioisotope for a RIPTP RHS; “Reason for Rejection?” lists the reason the author chose to discard or were inclined to discard the corresponding radioisotope; radioisotope half-life is listed in years; density ρ is for the elemental form at STP; energy per decay and maximum gamma photon energies are in MeV and were obtained from the MIRD database²⁵⁸; power is for isotopically pure radioisotope in elemental form after the elapse of one-third of a half-life; “PI” is the Precursor Isotope identified by the author for radioisotope production through transmutation; “% NA” is the percent natural abundance of the precursor isotope; and σ is the thermal neutron capture cross section for transmutation of the precursor isotope.

Table 56: Screening of neutron producible radioisotopes

RI	RI OK?	Reason for Rejection?	Half-Life Yr	ρ g/cm ³	E _{Decay} MeV	Max γ MeV	Power watt/cm ₃	PI	% NA	σ barn
¹⁹¹OS	Yes		0.042	22.60	0.21	0.13	985.9	¹⁹⁰ Os	26.26	13.1
¹⁷⁰TM	Yes		0.352	9.32	0.33		86.9	¹⁶⁹ Tm	100	105
¹⁶⁹YB	Yes		0.088	6.90	0.43	0.31	334.2	¹⁶⁸ Yb	0.13	2300
¹⁴¹CE	Maybe		0.089	6.77	0.25		224.0	¹⁴⁰ Ce	88.45	0.57
⁵¹CR	Maybe		0.076	7.19	0.04	0.32	114.0	⁵⁰ Cr	4.345	15.9
¹⁶⁹ER	Maybe		0.026	9.07	0.10	0.12	361.0	¹⁶⁸ Er	26.8	11
¹⁷⁵HF	Maybe		0.192	13.31	0.39	0.43	262.8	¹⁷⁴ Hf	0.16	561
¹⁷⁹HF(M)	Maybe		0.069	13.31	1.10	0.45	2004.7	¹⁷⁸ Hf	27.28	53
²⁰³HG	Maybe		0.128	13.55	0.34	0.28	295.4	²⁰² Hg	29.86	4.89
¹⁷⁷LU	Maybe		0.018	9.84	0.18	0.32	929.4	¹⁷⁶ Lu, ¹⁷⁶ Yb	2.59	2090

RI	RI OK?	Reason for Rejection?	Half-Life Yr	ρ g/cm ³	E _{Decay} MeV	Max γ MeV	Power watt/cm ₃	PI	% NA	σ barn
¹⁰³ PD	Maybe	Low γ yield, low max power density...	0.047	12.00	0.06	0.50	237.9	¹⁰² Pd	1.02	
¹⁴³ PR	Maybe	Low γ yield...	0.037	6.77	0.32	0.74	674.7	¹⁴² Ce, ¹⁴¹ Pr		
⁷⁵ SE	Maybe		0.328	4.79	0.40	0.40	131.9	⁷⁴ Se	0.89	51.8
¹¹¹ AG	No	γ , low power density	0.020	10.50	0.38	0.87	2938.9	¹¹⁰ Pd		
¹¹⁰ AG(M)	No	γ	0.684	10.50	2.82	1.56	661.7	¹⁰⁹ Ag	48.16	4.7
³⁷ AR	No	Noble Gas	0.096	1.78	0.00		1.8	³⁶ Ar	0.337	
⁴² AR	No	Noble Gas, short half-life precursor	32.90	1.78	1.94	2.42	4.2	⁴⁰ Ar	99	
¹³¹ BA	No	γ	0.032	3.59	0.52	1.05	753.5	¹³⁰ Ba		
¹³³ BA	No	Power density too low	10.54	3.59	0.45	0.38	1.9	¹³² Ba	0.1	
²¹⁰ BI	No	Poor production	0.014					²⁰⁹ Bi		
⁴⁵ CA	No	Power density too low	0.446	1.55	0.08		10.0	⁴⁴ Ca	2.09	
¹⁰⁹ CD	No	Power density too low	1.264	8.65	0.11		11.2	¹⁰⁸ Cd	0.89	
¹¹³ CD	No	Power density too low	14.10	8.65	0.19		1.7	¹¹² Cd	24.1	
¹¹⁵ CD	No	γ	0.122	8.65	0.83	0.53	862.2	¹¹⁴ Cd	28.73	0.036
¹³⁹ CE	No	Power density too low	0.377	6.77	0.19		41.7	¹³⁸ Ce	0.25	1.1
¹⁴⁴ CE	No	Power density too low	0.781	6.77	0.11		11.1	¹⁴² Ce	11.1	
⁶⁰ CO	No	γ	5.275	8.90	2.60	2.51	123.0	⁵⁹ Co	100	20.4
¹³¹ CS	No	Power density too low	0.027	1.87	0.03	0.00	25.2	¹³⁰ Ba		
¹³² CS	No	γ	0.018	1.87	0.72	1.03	967.9	¹³⁰ Ba		
¹³⁴ CS	No	γ	2.067	1.87	1.56	1.37	17.7	¹³³ Cs	100	
¹³⁶ CS	No	γ	0.036	1.87	2.26	1.24	1449.7	¹³³ Cs		
¹³⁷ CS	No	γ	30.07	1.87	0.81	0.66	0.6	¹³³ Cs	100	
¹⁵⁹ DY	No	Power	0.396	8.55	0.06		12.6	¹⁵⁸ Dy	0.1	43.6

RI	RI OK?	Reason for Rejection?	Half-Life Yr	ρ g/cm ³	E _{Decay} MeV	Max γ MeV	Power watt/cm ₃	PI	% NA	σ barn
		<i>density too low</i>								
¹⁵² EU	No	γ	13.52	5.24	1.20	1.30	5.1	¹⁵² Eu	47.8	6.3
¹⁵⁴ EU	No	γ	8.593	5.24	1.28	1.60	8.5	¹⁵³ Eu	52.2	312
¹⁵⁵ EU	No	<i>Power density too low</i>	4.761	5.24	0.12	0.15	1.5	¹⁵³ Eu	52.2	312, 1340
¹⁵⁶ EU	No	γ	0.042	5.24	1.67	2.27	2267.2	¹⁵³ Eu, ¹⁵⁴ Sm		
⁵⁵ FE	No	<i>Power density too low</i>	2.737	7.87	0.06		5.0	⁵⁴ Fe	5.8	2.25
⁵⁹ FE	No	γ	0.122	7.87	1.31	1.48	2411.1	⁵⁸ Fe	0.282	1.28
¹⁵³ GD	No	<i>Power density too low</i>	0.659	7.90	0.15	0.10	19.1	¹⁵² Gd	0.2	735
⁷¹ GE	No	<i>Power too low</i>	0.031	5.32	0.01	0.00	36.3	⁷⁰ Ge		
³ H	No	gas	12.32	0.09				² H	0.015	0.000 519
¹⁸¹ HF	No	γ	0.116	13.31	0.73	0.62	778.5	¹⁸⁰ Hf	35.08	13.04
¹⁷⁸ HF(M)	No	γ	31.00	13.31	2.44	0.57	9.9	¹⁷⁷ Hf	18.6	
¹²⁶ I	No	γ	0.035	4.93	0.45	0.88	826.7	¹²⁴ Xe		
¹³¹ I	No	γ	0.022	4.93	0.57	0.72	1650.6	¹³⁰ Te		
¹¹⁴ IN(M)	No	γ	0.136	7.31	0.78	1.30	617.0	¹¹³ In	4.29	8.1
¹⁹² IR	No	γ	0.202	22.40	0.85	0.88	828.6	¹⁹¹ Ir	37.3	309
¹⁹³ IR(M)	No	<i>Production Impractical (precursor)</i>	0.029	22.50	0.08	0.08	513.9	¹⁹² Ir		
¹⁹⁴ IR(M)	No	γ	0.468	22.40	0.90	2.04	372.3	¹⁹³ Ir	62.7	5.8
⁸⁵ KR	No	<i>Noble gas, γ</i>	10.78	3.75	0.25	0.51	1.7	⁸⁴ Kr	57	
¹⁷⁷ LU(M)	No	<i>Power density too low</i>	0.440	9.84	0.18	0.32	38.5	¹⁷⁶ Lu	2.59	3.2
⁹⁵ NB	No	γ	0.096	8.57	0.81	0.77	1280.5	⁹³ Nb	100	1.15, 14.9
¹⁴⁷ ND	No	γ	0.030	7.01	0.41	0.69	1085.2	¹⁴⁶ Nd		
¹⁸⁵ OS	No	γ	0.256	22.60	0.70	0.88	562.5	¹⁸⁴ Os	0.02	3000
¹⁹⁴ OS	No	γ	6.000	22.60	0.92	2.04	29.9	¹⁹² Os	41.08	2, 38
³² P	No	<i>Power too low</i>	0.039	1.82	0.69	0.00	1701.4	³¹ P		
³³ P	No	<i>Power too low</i>	0.069	1.82	0.08		102.1	³¹ P		.172

RI	RI OK?	Reason for Rejection?	Half-Life Yr	ρ g/cm ³	E _{Decay} MeV	Max γ MeV	Power watt/cm ₃	PI	% NA	σ barn
²³³ PA	No	Impractical production	0.074	15.40	0.42	0.42	630.5	²³² Th		7.37
²¹⁰ PB	No	Power too low	22.30	11.35	0.43		1.7	²⁰⁸ Pb	51.4	0.00049
¹⁴⁵ PM	No	Power too low	17.70	7.30	0.04		0.2	¹⁴⁴ Sm, ¹⁴⁵ Sm	3.1	
¹⁴⁷ PM	No	Power too low	2.623	7.30	0.06	0.20	2.0	¹⁴⁶ Nd	17.19	1.4
¹⁴⁸ PM	No	γ	0.015	7.30	1.30	2.28	7333.7	¹⁴⁶ Nd		
¹⁴⁸ PM	No	γ	0.113	7.30	1.30	2.28	953.4	¹⁴⁴ Pm		
¹⁴⁸ PM(M)	No	γ	0.113	7.30	2.15	1.01	1576.8	¹⁴⁶ Nd		
²¹⁰ PO	No	γ	0.379	9.30	5.41	0.80	1063.0	²⁰⁹ Bi	0.0242	
¹⁹³ PT	No	Power too low	50.00	21.45	0.01		0.0	¹⁰² Pt	0.8	10
²³⁸ PU	No	Power too low	87.70	19.84	5.50	0.10	8.8	²³⁷ Np	0	176
²⁴¹ PU	No	Power too low	14.29	19.84	0.01		0.1	²³⁹ Pu		
⁸⁶ RB	No	γ	0.051	1.53	0.76	1.08	445.9	⁸⁵ Rb		
¹⁰³ RU	No	γ	0.108	12.37	0.60	0.61	1125.0	¹⁰² Ru	31.55	1.21
¹⁰⁶ RU	No	γ	1.024	12.37	1.62	2.41	310.7	¹⁰⁴ Ru	18.62	0.32
³⁵ S	No	Power too low	0.240	2.07	0.05		20.2	³⁴ S	4.22	0.227
¹²⁴ SB	No	γ	0.165	6.68	2.21	2.09	1214.2	¹²³ Sb	42.79	4.2
¹²⁵ SB	No	γ	2.759	6.68	0.54	0.67	17.4	¹²⁴ Sb		17.4
¹²⁶ SB	No	γ	0.034	6.68	3.11	1.48	8196.5	¹²³ Sb, ¹²⁴ Sn		
⁴⁶ SC	No	γ	0.230	2.99	2.12	2.01	1009.7	⁴⁵ Sc	100	17.4
¹⁴⁵ SM	No	Power too low	0.932	7.52	0.09	0.49	8.4	¹⁴⁴ Sm	3.1	0.73
¹⁵¹ SM	No	Power too low	90.00	7.52	0.02		0.0	¹⁵⁰ Sm	7.4	104
¹¹³ SN	No	Γ	0.315	7.31	0.42	0.65	145.3	¹¹² Sn	0.97	0.71
¹¹⁷ SN(M)	No	Production C-Section too low	0.038	7.31	0.31	0.31	872.5	¹¹⁶ Sn		
¹¹⁹ SN	No	Power too low	0.803	7.31	0.09		11.1	¹¹⁸ Sn	24.23	0.225
¹²¹ SN	No	Power too low	55.00	7.31	0.13		0.2	¹²⁰ Sn	32.59	5.17
¹²³ SN	No	γ	0.354	7.31	0.53	1.34	149.7	¹²² Sn	4.63	0.001
¹²⁵ SN	No	γ	0.026	7.31	1.13	2.28	4208.6	¹²⁴ Sn		
⁸⁵ SR	No	γ	0.178	2.54	0.51	0.95	144.0	⁸⁴ Sr	0.56	0.35
⁸⁹ SR	No	γ	0.138	2.54	0.59	0.91	202.9	⁸⁸ Sr	82.58	5.8e-3

RI	RI OK?	Reason for Rejection?	Half-Life Yr	ρ g/cm ³	E _{Decay} MeV	Max γ MeV	Power watt/cm ₃	PI	% NA	σ barn
⁹⁰ SR	No	γ	28.79	2.54	1.13	2.19	1.9			
¹⁸² TA	No	γ	0.314	16.65	1.50	1.37	736.3	¹⁸¹ Ta	99.98	20.5
¹⁸³ TA	No	Ta182 γ	0.014	16.65	0.63	0.41	6889.3	¹⁸¹ Ta		
¹⁶⁰ TB	No	γ	0.198	8.23	1.38	1.31	602.8	¹⁵⁹ Tb	100	23.4
¹⁶¹ TB	No	Tb160 γ too high, Gd pathway power too low	0.019	8.23	0.23	0.55	1054.3	¹⁶⁰ Gd, ¹⁵⁹ Tb		
¹²¹ TE	No	γ	0.052	6.24	0.59	0.57	968.4	¹²⁰ Te	.09	
¹²¹ TE	No	γ	0.422	6.24	0.81	0.57	167.4	¹²⁰ Te	0.096	
¹²⁷ TE	No	γ	0.299	6.24	0.31	0.66	86.3	¹²⁶ Te	18.95	
¹²⁹ TE	No	γ	0.092	6.24	1.03	1.40	909.1	¹²⁸ Te	31.69	
¹²³ TE(M)	No	Power too low	0.327	6.24	0.25	0.25	64.1	¹²² Te	2.603	
¹²⁵ TE(M)	No	Power too low	0.157	6.24	0.14	0.14	74.2	¹²⁴ Te	4.816	3.8
²²⁸ TH	No	γ	1.912	11.72	34.65	2.59	1567.3	²³¹ Pa		
²³⁴ TH	No	γ	0.066	11.72	1.70	1.93	2169.5	²³² Th		
²⁰⁴ TL	No	γ	3.780	11.85	2.39	1.27	61.7	²⁰³ Tl	29.52	11.4
¹⁷¹ TM	No	Power density too low	1.920	9.32	0.03		1.2	¹⁶⁹ Tm	100	92
²³² U	No	Production not very practical (precursor)	68.90	18.95	39.88		79.5	²³¹ Pa		
¹⁸¹ W	No	Power density too low	0.332	19.35	0.05	0.15	24.6	¹⁸⁰ W	0.13	
¹⁸⁵ W	No	Power density too low	0.206	19.35	0.13	0.13	108.6	¹⁸⁴ W	30.67	1.7
¹⁸⁸ W	No	γ	0.191	19.35	0.94	1.96	848.5	¹⁸⁶ W	28.6	
¹²⁷ XE	No	γ	0.100	5.90	0.31	0.62	243.7	¹²⁶ Xe	0.09	3.5
¹²⁹ XE	No	Noble Gas	0.024					¹²⁸ Xe		
¹³¹ XE	No	Noble Gas	0.033	5.90	0.16	0.16	375.4	¹³⁰ Ba		
¹³³ XE	No	Noble Gas	0.014					¹³² Xe		
⁹¹ Y	No	γ	0.160	4.47	0.61	1.21	312.3	⁸⁹ Y, ⁹⁰ Y		1.28, 6.5
⁶⁵ ZN	No	γ	0.669	7.13	0.59	1.12	162.5	⁶⁴ Zn	48.63	0.76
⁹⁵ ZR	No	γ	0.175	6.51	0.85	0.77	560.5	⁹⁴ Zr	17.38	.050

APPENDIX B – PROPERTIES OF GRANITE VS. TEMPERATURE

Information for Figure 78 derives in part from a Sandia National Laboratory (SNL) report and in part from a United Aircraft Research Laboratories (UARL) report.^{130,}

270****

Information for Figure 79 through Figure 81 derives from the above mentioned SNL report.

**** Note that information in the UARL report regarding thermal conductivities of rock should not be used as the UARL report's authors have applied a relation derived for thermal conductivity of metals to ionic solids. This is invalid as electrons constitute a significant heat transfer mechanism in metals as compared to ionic solids.

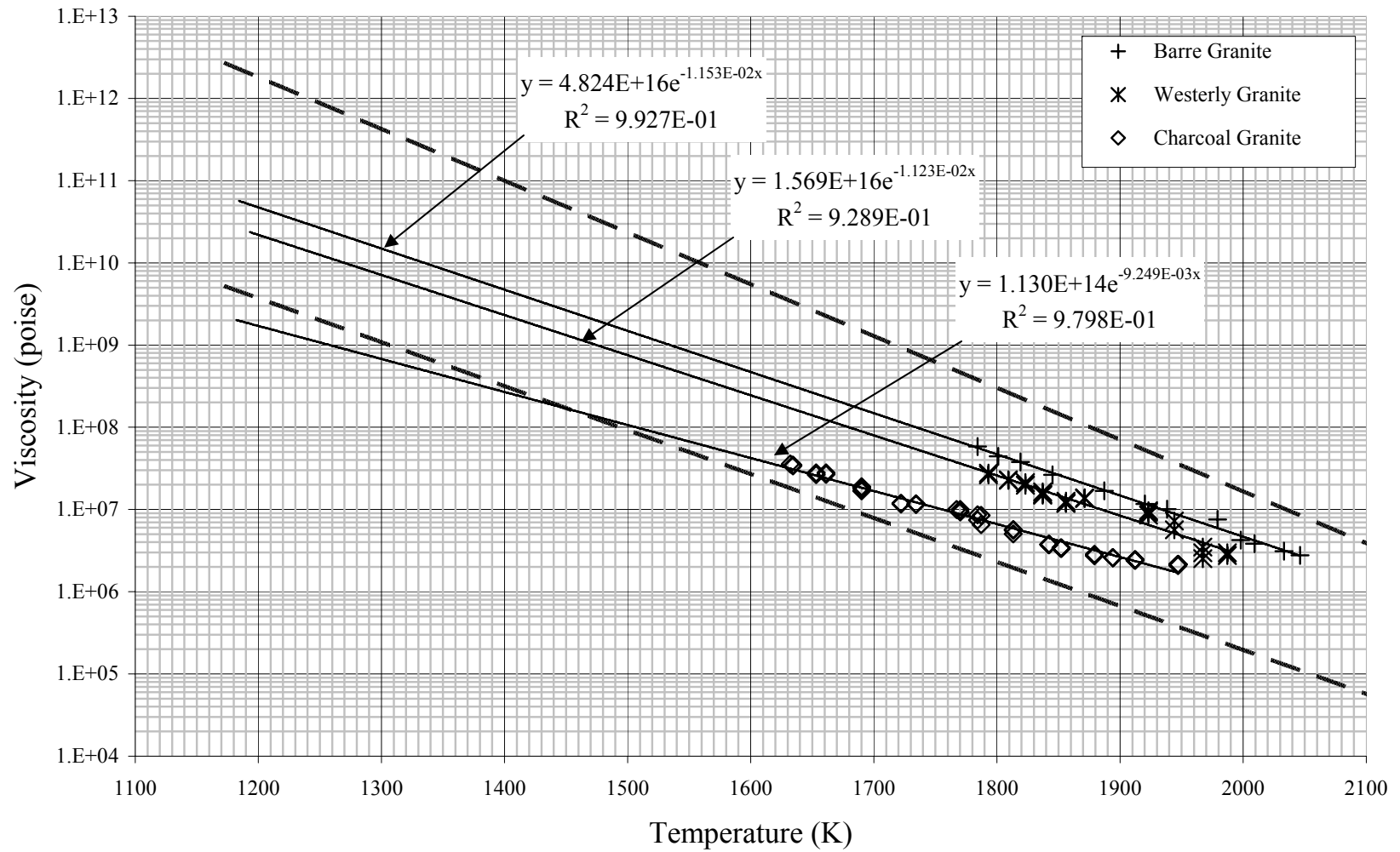


Figure 78: Viscosity of granite melts

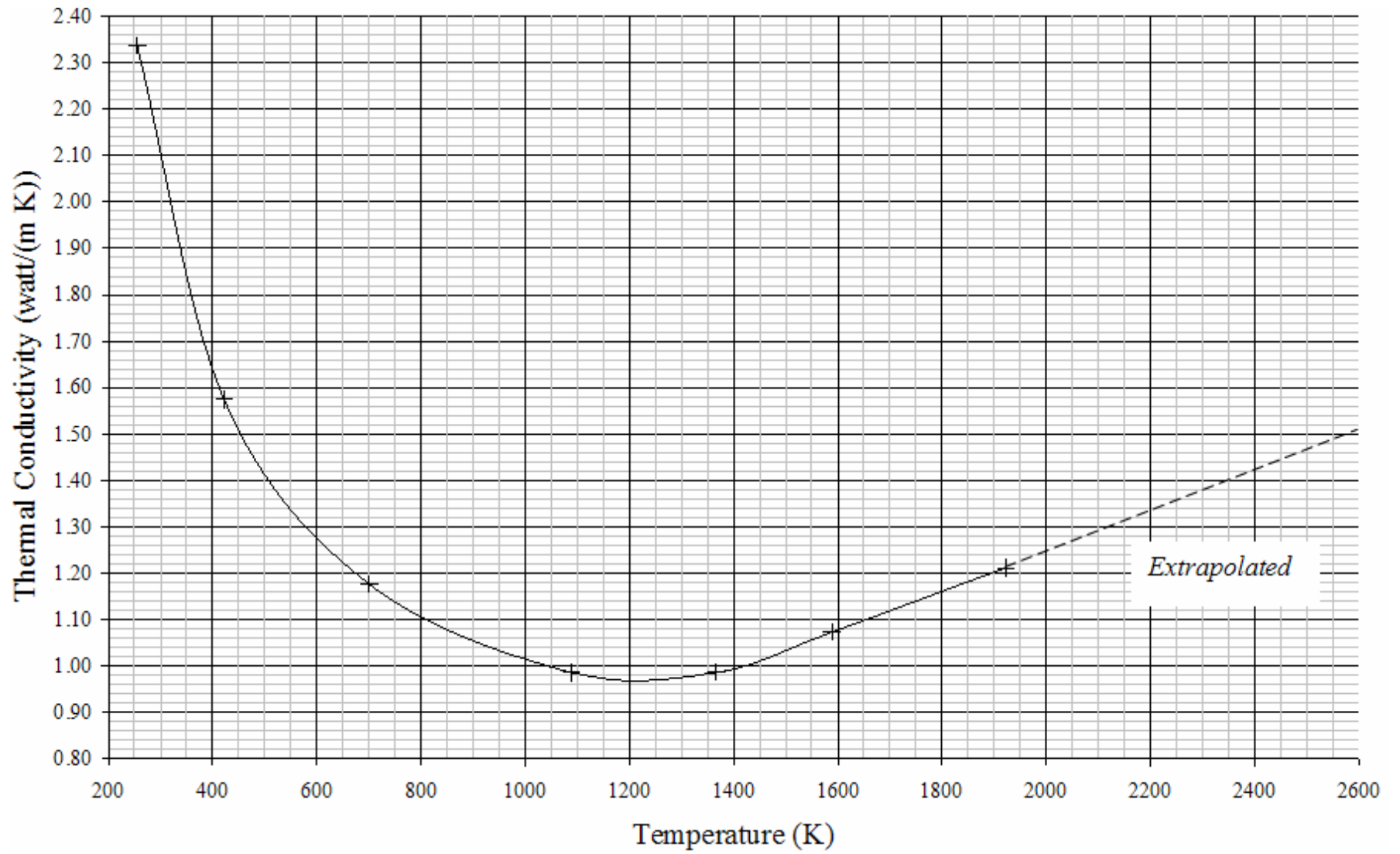


Figure 79: Thermal conductivity of granite

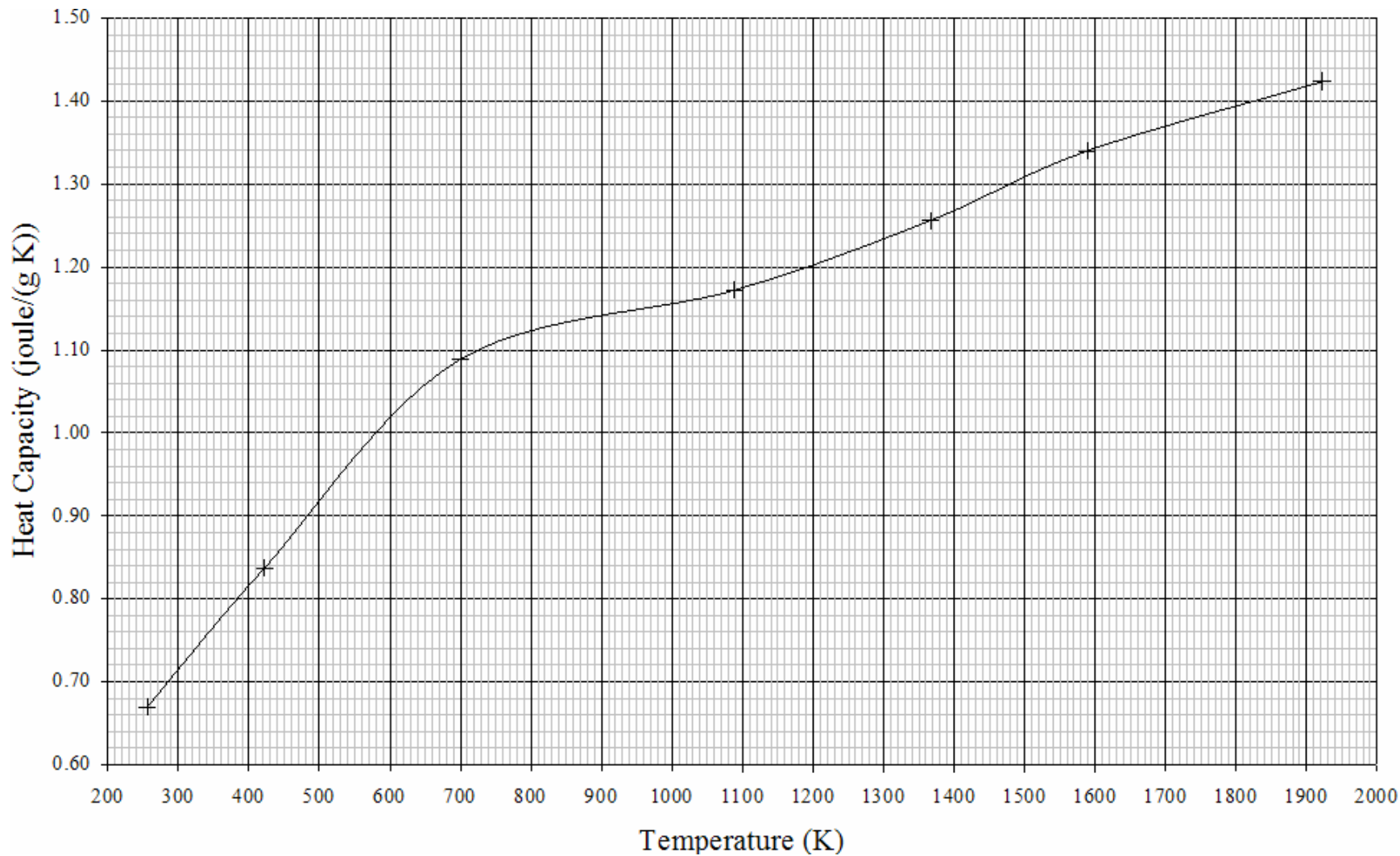


Figure 80: Heat capacity of granite

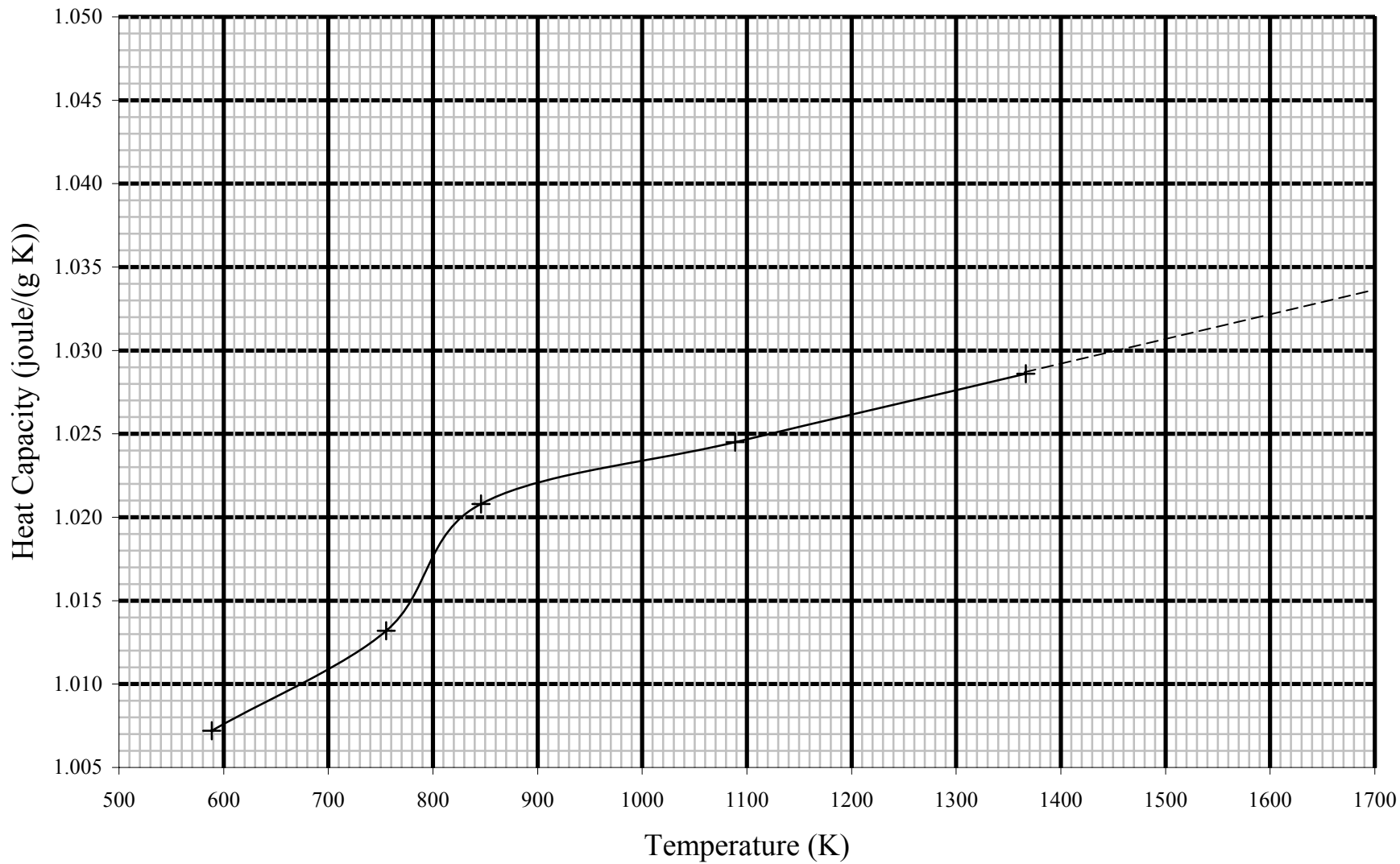


Figure 81: Thermal expansion of “Salisbury Pink” Granite

APPENDIX C – THERMAL CONDUCTIVITY OF REPRESENTATIVE PENETRATOR MATERIALS

Figure 82 gives thermal conductivity for an assortment of rare earth oxides. Of particular interest is thulium-oxide. Also of potential interest are ytterbium-oxide and lutetium-oxide.

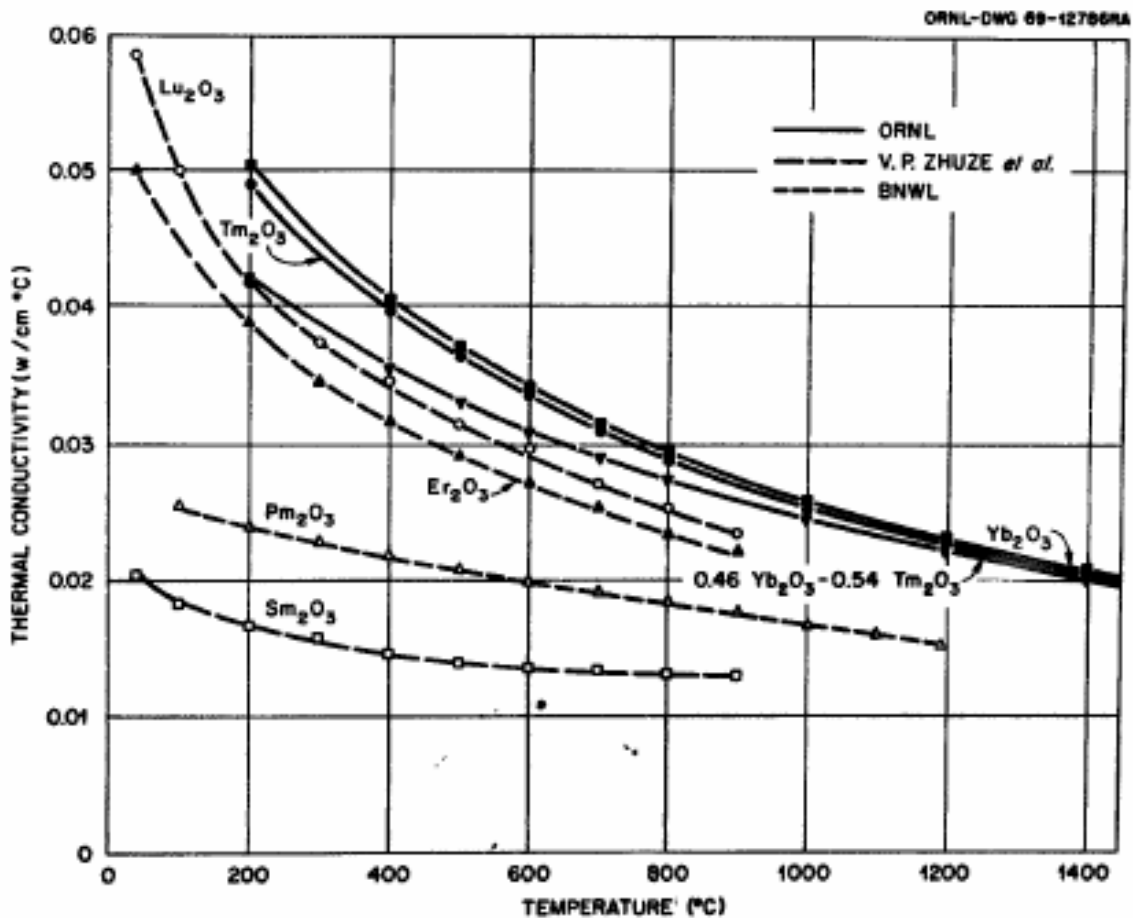


Figure 82: Rare earth oxide thermal conductivity vs. temperature

Figure 83 gives thermal conductivities of tungsten as a function of temperature as a representative refractory case material.^{266, 293} Note that thermal conductivities were extrapolated linearly past 1950 K when necessary for thermal calculations, with any

phase changes not represented in the available data ignored (maximum predicted temperatures were checked against melting temperatures to identify whether melting would occur). This is a conservative approach as the interplay of various contributors to thermal conductivity such as mean free path of thermal energy carriers, number of thermal energy carriers (electrons, phonons, photons), and mean velocity of the carriers generally result in one of two types of behavior – either continually increasing thermal conductivity or a minimum thermal conductivity value at some intermediate temperature.^{294, 295} One might expect something like a $1/T$ variation in thermal conductivity or less while thermal conductivity is decreasing. A linear extrapolation should therefore be conservative.

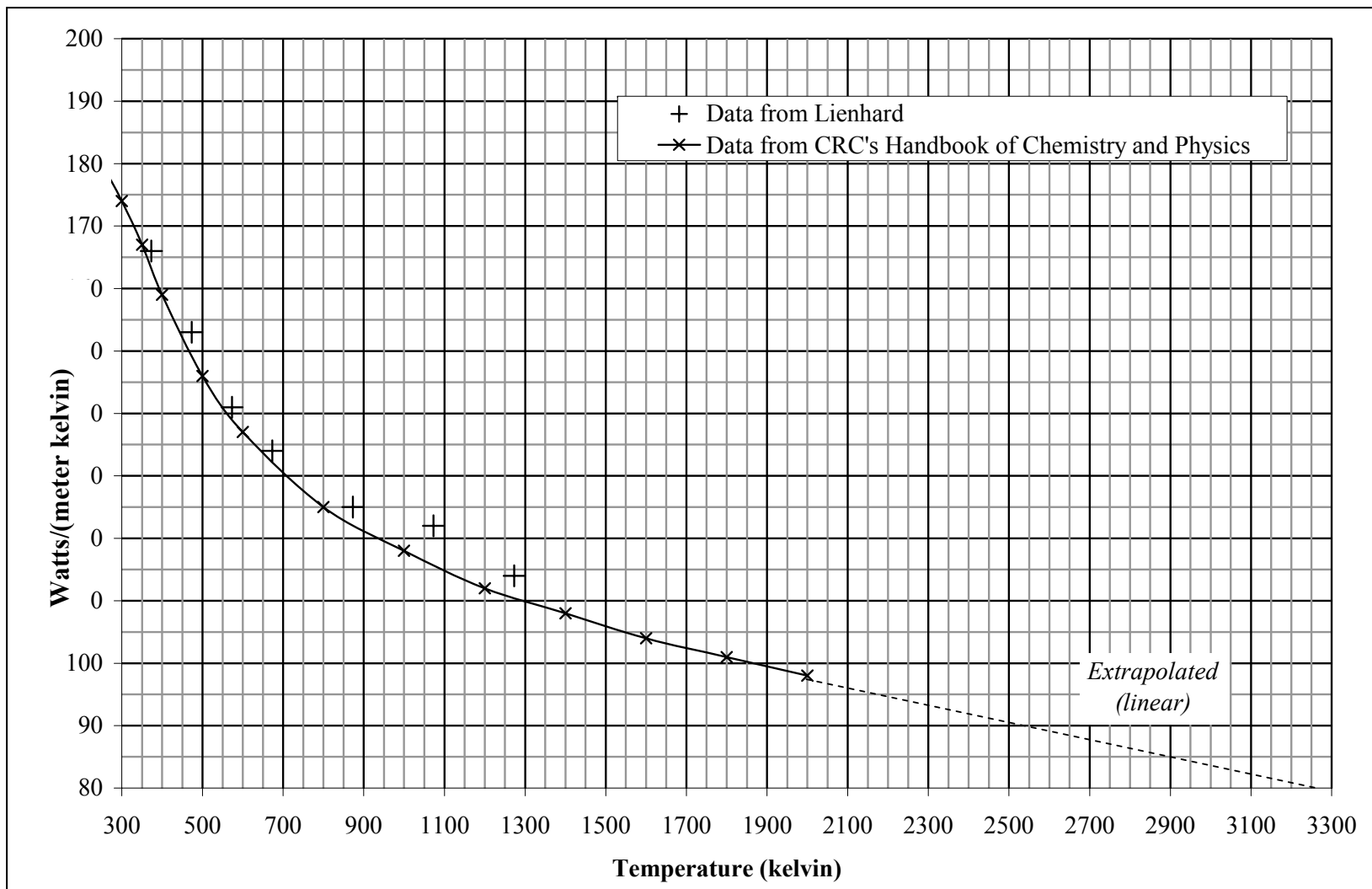


Figure 83: Tungsten thermal conductivity vs. temperature

APPENDIX D – RADIOISOTOPE PRODUCTION

BACKGROUND

Short half-life radioisotopes can only be produced in the quantities required for a RIPTP RHS in nuclear reactors. In a nuclear reactor, two principle mechanisms of radioisotope production exist. First, radioisotope fission products are produced by fission of heavy nuclei (principally ^{235}U , Figure 84). The isotopes produced have an atomic mass distribution sharply peaked in the range of 90 to 100 Atomic Mass Units (AMUs) and 135 to 145 AMUs, and are typically neutron-rich and successively decay to other more stable isotopes called “daughter products.” These radioisotopes are the natural by-product of commercial nuclear power generation. Second, radioisotopes are produced through transmutation of isotope nuclei through neutron capture (Figure 85). If a particular radioisotope is desired, a target of the precursor isotope that will lead to its production can be placed in a reactor. Both production mechanisms have historically been used to produce radioisotope materials for RHS applications. For example, strontium-90 is a daughter product produced through fission, and plutonium-238 is principally produced by a transmutation/decay chain starting with uranium-235.

Radioisotopes are typically not produced in a reactor in the purity and/or concentration required for the final application. Concentration of isotopes is possible through two fundamentally different approaches. First of all, an isotope may be separated chemically along with all other isotopes of the same element that are present. This is generally a comparatively inexpensive process. Secondly, a specific isotope of an element may be enriched. The largest application for isotope enrichment is the isotopic

enrichment of fissile elements such as uranium-235 and plutonium-239 for nuclear power and weapon applications. Enrichment is an expensive process, with the cost strongly dependent on the degree of isotopic enrichment required and the level of radioactivity present in the raw material being enriched.

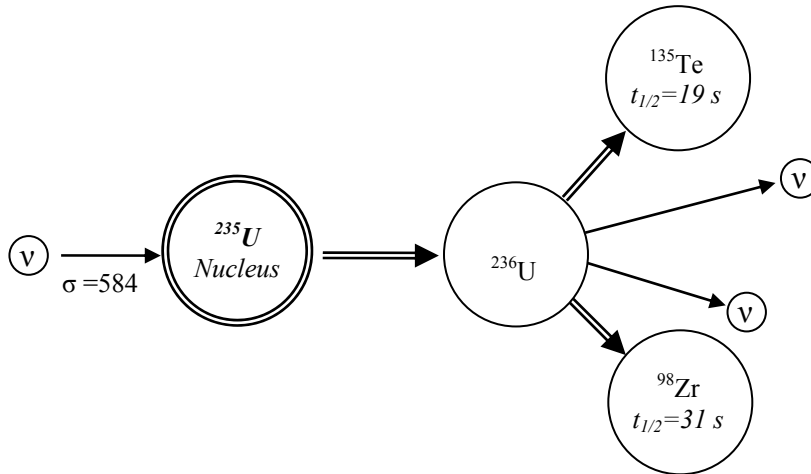


Figure 84: One of the many uranium-236 fission reactions

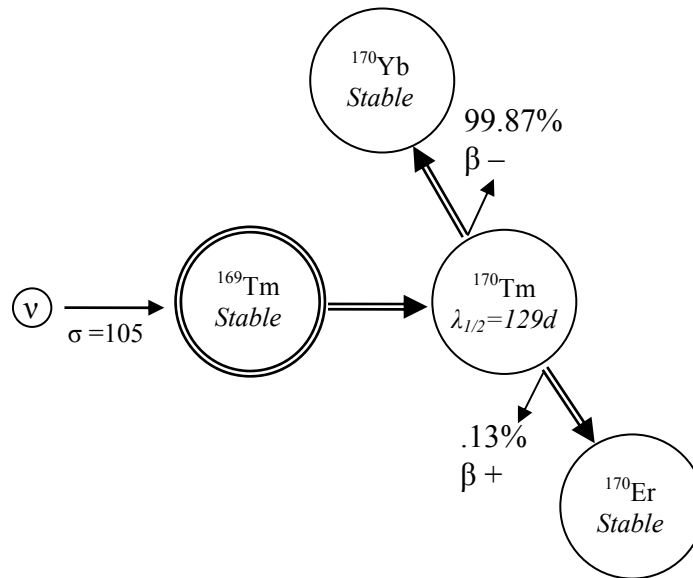


Figure 85: Radioisotope production through neutron capture by a target isotope

For production of an RHS using strontium-90, spent reactor fuel rods would be placed in a fuel storage pool and allowed to go through a “cool-down period” of a few years. During this period, short-lived radioisotopes are allowed to decay and the overall level of radioactivity of the fuel greatly decreases, making the eventual processing of the spent fuel less hazardous. After the cool-down period, all isotopes of the element strontium would be chemically separated from the fuel and the resulting radioactive strontium metal would typically be about ~55% strontium-90. This material is then chemically processed into the preferred compound, SrTiO₃, and then mechanically processed into its preferred final physical form for the intended application.

APPENDIX E – ISOTOPE ENRICHMENT TECHNOLOGIES

The various enrichment technologies that might be used for enriching/depleting candidate radioisotopes surveyed are outlined below in Table 57. One conclusion from this survey was that technologies with the highest known TRL for enrichment of the interesting precursor isotopes are the Plasma Separation Process (PSP), and Calutron enrichment. Of these PSP is significantly less expensive, but still on the order of \$10M per kilogram for enrichment of an isotope (ytterbium-168 or hafnium-174) from the order of .1% natural abundance to 10% abundance. Both of these enrichment technologies are considered infeasible for RIPTP RHS production.

Table 57: Isotope separation technologies in rough order of technical maturity

CALUTRON

Original enrichment technology (Manhattan Project)
Single-pass isotope enrichment
No isotope-specific technology
Extremely costly

GAS DIFFUSION

Current method used in the US for reactor & weapon materials
Hundreds to thousands of passes required
Capital cost high
Some isotope-specific technology
Energy cost per SWU very high – 2,200 to 2,500 kilowatt-hours per Separative Work Unit (kWh/SWU)

GAS CENTRIFUGE

Dozens to hundreds of passes required
Well developed off-the-shelf technology
Some isotope-specific technology involved
Lowest energy cost of proven technologies – 50-250 kWh/SWU
Capital costs high
Existing infrastructure may be usable

PLASMA SEPARATION PROCESS

Only 1 to 4 passes required for enrichment
Minimal isotope specific technology
Only 1 to 4 passes required for enrichment
Yb168/Hf174 single-pass enrichment costs to ~10% approximately 50k\$/gram – not a viable technology for isotope enrichment for a RIPTP

AVLIS

Laser separation process employing selective ionization of isotope atoms in an atomic vapor
Some isotope-specific technology involved
Technology at the transition-to-production developmental level
AVLIS demonstrated on a large scale by LLNL
Funding discontinued both in the US and internationally
Claims lower infrastructure cost than centrifuges
Claims very high per-pass enrichment
Low energy cost – 40 kWh per SWU

SILEX AND MLIS

Laser separation processes employing selective ionization of molecules containing isotope
Isotope-specific technology involved
SILEX development continuing to be pursued by the Silex company of Australia and the United States Enrichment Corporation (USEC)
MLIS potentially not as energy efficient as modern gas centrifuge at 150 kWh/SWU
Technologies claim lower infrastructure cost than centrifuges

AVLIS, SILEX, and MLIS type enrichment processes might provide means of relatively inexpensive isotope enrichment, but could require major technology investment at significant risk. Although funding for AVLIS technology development was recently discontinued both domestically and abroad after over two decades of technology development, a pilot facility did demonstrate tons of uranium throughput in the enrichment process. Mention of efforts to investigate/develop AVLIS for medical isotope separation/development of a prototype facility for this purpose was encountered by the author, but current status of such work could not be determined. Available facilities, if any, for AVLIS separation and their potential suitability for enrichment of candidate isotopes should be further investigated. Progress of the SILEX and MLIS separation technologies' development should also be monitored.

One of the most interesting enrichment technologies identified with the greatest potential for near-term production of large quantities of low cost highly enriched isotopes is gas centrifuge isotope separation. Gas centrifuge technology has advanced enormously in the last two decades with the latest generation centrifuge cascades approaching the efficiencies touted by the AVLIS process. *If* it is possible to run a suitable gaseous compound of the element of interest through existing cascades without major modification to the cascade or facilities and achieve comparable performance as with uranium separation, *then* it could be possible to manufacture very large quantities of highly enriched isotopes without the cost or delay of technology development or investment in new enrichment infrastructure.^{††††} The author has not investigated the feasibility of this option with respect to centrifuge technology, but there are certainly

^{††††} Note that the US does not have a current centrifuge capability as the decision was made to stay with the gaseous diffusion technology until AVLIS came on line. With the cancellation of AVLIS it is probable that the US will invest in modern centrifuge capabilities in the near future.

many at the United States Enrichment Corporation (USEC) and the national labs who could give a ready answer as to whether centrifuge separation of a compound other than uranium hexafluoride would necessarily require major facility modifications. Considering the probable ease of evaluating this option (identifying and speaking with subject experts) and the high potential payoff, it should be a priority for further investigation.

In an attempt to ascertain whether gaseous compounds existed for the elements of precursor isotopes interesting to the author for RIPTP RHS radioisotope production, lists of chemical compounds of these elements were screened.²⁹³ The author compiled those compounds that were gaseous below 400°C.

Table 58: Gaseous compounds of elements of possible interest for short half-life RHS

	VAPORIZATION TEMPERATURE (Celsius)	DECOMPOSITION TEMPERATURE (Celsius)
ISOTOPE: ²³⁵U		
UF ₆	57° (s)	233°
ISOTOPE: ⁵⁰CR		
Cr ₂ O ₂ Cl ₂	117°	
ISOTOPE: ¹⁷⁴HF		
HfI ₄	121° (s)	
HfBr ₄	323° (s)	
HfCl ₄	317° (s)	
ISOTOPE: ¹⁹⁰OS		
OsF ₆	47.5°	
OsO ₄	135°	
ISOTOPE: ⁷⁴SE		
SeH ₂	-5°	138°
SeCl ₂ O	177°	
SeF ₆	-46°	72°
SeO ₂	315° (s)	
COSe	-21.5°	
CSe ₂	125°	

(s) denotes that the vaporization temperature is a sublimation point

APPENDIX F – SOME NOTES ON THE FEASIBLE DESIGN SPACE ASSESSMENT PROPOSED IN TIF

There are some mathematical (and practical) flaws in the approach used by Kirby and others in a number of published works (see those cited re TIF^{10, 11, 22} and cross-referenced TIF and TIES-related work), particularly with the method used for determination of existence of a feasible design space. It is stated in a number of these papers that a Monte-Carlo Simulation (MCS) is performed to determine if feasible design space exists, and what its extent is in relation to the entire design space (see step six of the TIF methodology previously described in the “Approach” section).

One potentially critical problem with this approach is related to the well known fact that the tails of a probability distribution require significantly larger numbers of samples to resolve in an MCS than the parts of the distribution which occur with greatest frequency. It is entirely possible (and in some cases mathematically probable) to perform an MCS with a very large number of points (10^4 is a number often cited in the previously referenced works) and find a resultant probability distribution function whose minimum and maximum is very much less than the true range which exists in the space. If one directly follows the method outlined by Kirby the design space for such a system would be considered infeasible.

The potential significance of this error in approach is exacerbated by dimensionality. To illustrate this assume that the desirable minimum (or maximum) of a metric’s response is unique and exists at a corner of the design space. Further, let’s suppose that instead of random sampling, we are exhaustively sampling corner points so

if we sample all we are guaranteed of finding the desired extremum of the metric. The number of k dimensional entities in an n dimensional side constrained space is given by E , the equation for which is listed below.

$$E = 2^{n-k} \frac{n!}{k!(n-k)!}$$

In the present situation we are considering points, zero-dimensional entities, so $k=0$, and E is just equal to 2^n . If sample size for our extremum sampling “Monte-Carlo Simulation” is 10^4 points, then we are guaranteed of finding our extremum until we reach fourteen variables, at which point we have only a 61% chance of finding the extremum. With each additional independent variable we halve the probability – adding just three additional variables results in less than an 8% chance of finding the extremum.

In reality the problem with the MCS approach to assessing existence and extent of feasible design space can be far worse, as design points in the MCS proposed are being sampled randomly from uniform distributions on continuous variables (and thus are not space filling sets), and no knowledge of the curvature of the function or its dimensionality is considered in determining an appropriate sample size.

Another difficulty with the TIF approach to assessing feasibility of a design space is that the proportion of the sampled points from an MCS which meet or exceed a specified requirement for viability has nothing inherently to do with suitability of the design space with respect to the potential for identifying either feasible or robust designs. If a fixed MCS sample size is specified, then the proportion of the sample exhibiting “feasibility” as described by Kirby has a natural inclination to decrease with increasing dimensionality. This can potentially reach the point where “large” feasible plenums of a design space exist (“large” with respect to the designer’s freedom to specify the design

variables and the uncertainty in responses due to noise), but an MCS with a “large” number of samples interpreted following TIF indicates *no* proportion of the space *approaching* feasibility.

Consider a side-constrained space in which the fraction p of the normalized range for each dimension results in a response satisfying some feasibility criteria. For one dimension, the fraction of the overall space which is viable is p . For two dimensions, p^2 . For n dimensions, p^n . So if half the normalized range of each dimension resulted in a feasible design space ($p=.5$), then a monte-carlo would correctly indicate that half the n -dimensional measure polytope design space were feasible for a single dimension design space, but only $1/1000^{\text{th}}$ the measure polytope design space of a ten dimensional space were viable. With sufficient dimensionality an MCS might indicate no feasible design space when in fact a quite large feasible design space might exist with respect to the reasonable ranges design variables could take.

As a practical example of this, consider the resulting Probability and Cumulative Distribution Functions (PDF & CDF) in Figure 86 below that were produced by uniform random sampling of the baseline penetrator design space using 50,000 sampled points. Figure 87 shows the results using uniformly distributed latin-hypercube sampling (a space-filling sampling approach) with essentially equivalent results. From either figure it would be concluded following Kirby’s TIF Methodology that feasible design space does not exist as a minimum penetration rate of 80 meters/day is required and the results of neither MCS simulation indicate design points meeting this requirement.

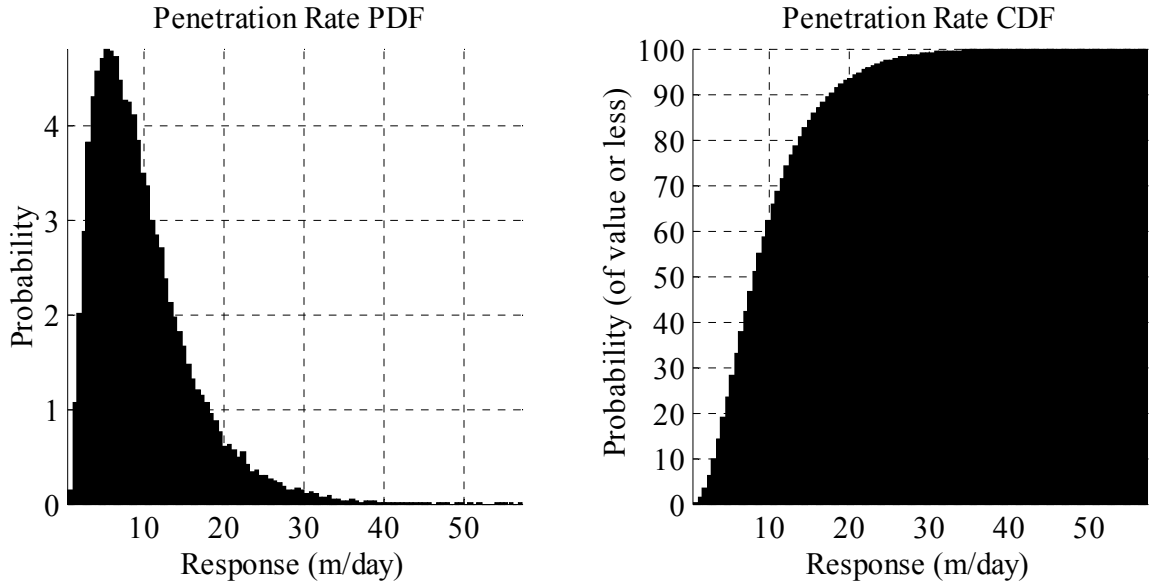


Figure 86: Penetration rate distribution functions for 5E+04 uniform random samples of the design space

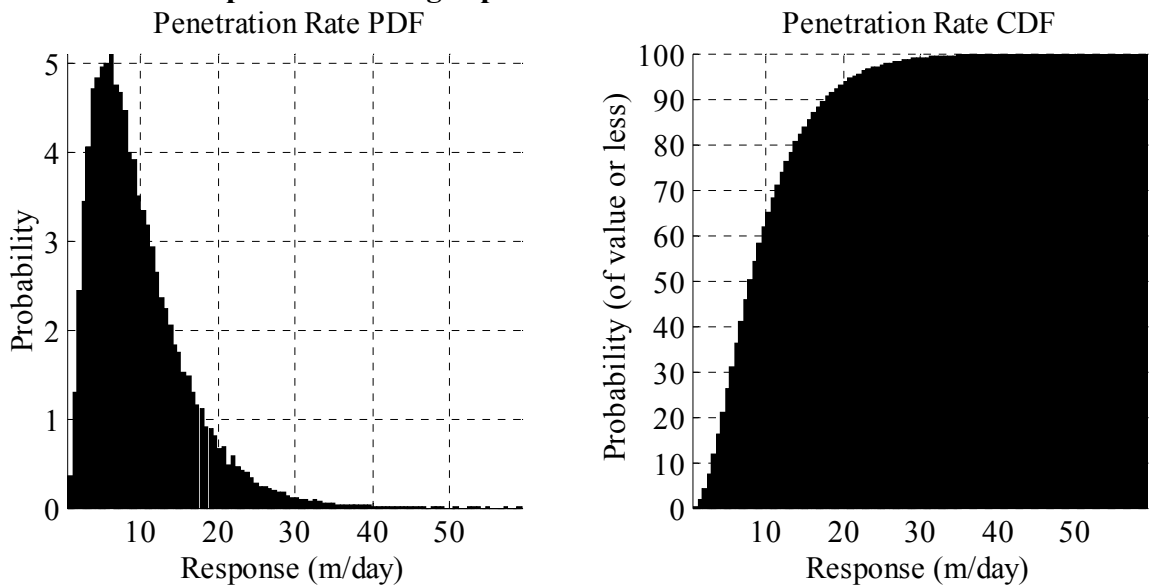


Figure 87: Penetration rate distribution functions for 5E+04 uniform latin-hypercube samples of the design space

This is an incorrect conclusion. Specification of a few of the more important design variables (that were previously assigned random settings) to slightly less than their most advantageous settings and re-execution of the MCS with uniformly random sampling on the non-fixed variables yields the results illustrated in Figure 88. All that has

changed is that: the dimensionality of the space sampled has been reduced by eight (effectively increasing the point sampling density); and the sampled sub-space of the original design space has been selected as one for which the metric function (penetration rate) has better values. Specification of the eight excluded variables at close to their best settings concentrates the new denser sampling of points in an advantageous part of the design space. Nothing about the existence or extent of the feasible design space has changed.

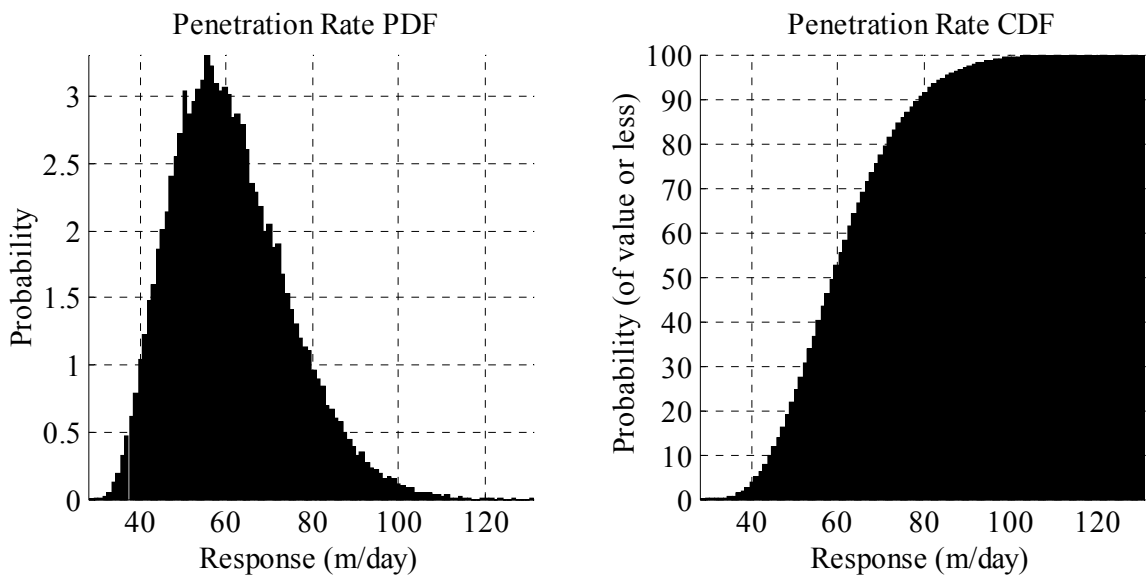


Figure 88: Penetration rate distribution functions for 5E+04 uniform latin-hypercube samples of a design sub-space

A more appropriate method of assessing *existence* of feasible design space as compared to an MCS is through analytical solution, numerical optimization, or graphical exploration of the RSE's or design space. Assessing *extent* of feasible design space inasmuch as it is of importance to the design process *must* take into account the impact of uncertainty on feasibility. If the effects of uncertainty are quite small, a feasible design

space closely bounded by constraints can be robust. Greater effects of uncertainty imply greater required relief from constraints for a robust design.

MCSs for “evaluating” feasible design space are at best useless, and at worst misleading. Better, more rational approaches exist to accomplish this purpose.

APPENDIX G – NOTES ON FISSILE IMPLEMENTATION

The principle reason for not pursuing a fissile implementation in a non-strategic (or even strategic) context is that, irrespective of its potential advantages as compared to the existing alternative for DBHT defeat of a nuclear bomb, development of such a device would be “politically incorrect.”

In a nuclear reactor implementation additional lethality would be present due to neutron diffusion through the walls of the DBHT. This could be a potent lethality mechanism even in the event of a clean miss of the DBHT spaces. During its descent past the DBHT it would be continually irradiating any proximate DBHT spaces. If penetration into a DBHT space occurred by a fissile implementation, intense direct irradiation of the space would result along with release of neutron activated radionuclides from the melt bubble. This radioactive molten rock from the melt bubble could render the DBHT facility uninhabitable for prolonged periods.

Despite the stigma against nuclear related lethality mechanisms, in terms of collateral damage a fissile kinetic/thermal penetrator should be enormously superior to even the low yield nuclear bombs which are the only existing alternative available for robust DBHT defeat. This relative superiority of the kinetic/thermal penetrator approach should hold whether judged by probable collateral damage or environmental dispersal of radioactive materials. Where nuclear radiation based modes of lethality are undesirable, radioisotope implementations offer radiation free lethality through conventional-only kill mechanisms.

FISSILE POWERED THERMAL PENETRATOR – MOTIVATION

Radioisotope powered thermal penetrators inherently have issues with thermal management as they constantly generate large amounts of heat – in quantities sufficient to melt granite – from the time they are assembled to the time the radioisotope they contain decays. This makes RIPTP safe storage, handling, transport, and aircraft/weapon guidance package integration potentially challenging. RIPTPs possess no temperature-related feedback control on power generation rate, and hence are absolutely dependent on sustained cooling (passive or active) to prevent overheating and thermal failure of the case. Another concern from a safety standpoint is that they pose a significant radiotoxicity hazard in the event of rupture of the penetrator case. While they may reduce potential hazard to enemy combatants, they increase potential radiological hazard to friendly forces and non-combatants.

In contrast, a fissile source might be designed so as to produce power only upon activation and passive feedback mechanisms might be designed to maintain a fairly constant temperature level irrespective of cooling load, enabling more robust operation through more diverse strata than granite. Development of a fissile thermal penetrator munition would be a zero-yield device and so would not violate the terms of the comprehensive test ban treaty. Also, fissile materials are already available in large stockpiles and might be more cost and logistics effective. Further, the nominal historical fissile power densities are an order of magnitude (or more) greater than the highest historically achieved RI power densities. Finally, fissile penetrators could be stored in inventory for decades with minimal change in performance characteristics, as contrasted to the maximum potential shelf-life of months for RIPTPs.

A final consideration is that while intensive unshielded radiation is in some ways a disadvantage of fissile implementations, it can also be an advantage. The high levels of radiation produced by fissile devices once they activated below the surface could provide an additional means of attacking deeply-buried Nuclear, Biological, and Chemical (NBC) production and storage bunkers. Such an attack might degrade to some degree stores of biological and chemical agents or nuclear weapons while rendering the bunker uninhabitable for a period of several months to several years. Incorporation of incendiary payloads such as reactive metals might enhance NBC material neutralization.

As compared to a nuclear bomb that might otherwise be required to defeat the specified DBHT, the anticipated hazard to the general population might be substantially less. Such an option could plausibly comprise a more credible deterrent to rogue regimes against first use of NBC weapons as compared to holding at threat (of nuclear counterstrike) a dictator's captive population.

CHALLENGES WITH IMPLEMENTATION

Design of a fissile powered thermal penetrator is a more complex problem as compared to a radioisotope (RI) implementation. Fundamentally, all that's required for an RI implementation is a refractory case and/or alloying refractory material to contain the RI. This case prevents escape of the RI into the surrounding environment and shields any nearby personnel from the radiation emitted by the RI decay. Alloying materials can serve to provide additional protection against release of the RI, shield its emissions, as well as conduct the thermal power produced.

For a fissile implementation, more considerations become important. A fissile implementation would essentially be a specialized, dense, highly compact nuclear reactor with few (if any) moving parts.

The single most important concern pertaining to the feasibility of such a reactor is that it must possess some means of regulating the power produced; otherwise it will either: not produce the power required; suffer melt-down; or explosively disassemble. Design options for controlling the criticality of a fissile reactor in this application are different from many used historically, as no sizeable void spaces or moving mechanisms are likely to be permissible during operation. This is because any void space can lead to pressure induced structural failures at the high pressures likely to be encountered in a melt bubble, while moving mechanisms tend to be impractical or prone to failure at extreme temperatures, pressures, and radiation fluxes. Sensor dependent feedback mechanisms or computer controls are also infeasible for the same reasons. Thus the greatest challenge in implementing such a system is likely to be designing a robust, passive means for power regulation at high temperatures, pressures, and radiation fluxes.

FUNCTIONAL REQUIREMENTS

The author proposes the following broad functional requirements for a thermal penetrator reactor:

1. one time activation
2. low probability of inadvertent criticality prior to activation, particularly with respect to immersion in various environments such as water, sand, etc.

3. passive, temperature dependent reactivity control
4. minimal void space
5. no moving parts critical to operation at high temperatures and pressures at depth (allowed for initial activation)
6. sustained operation at temperature $1200\text{K} > T > 2500\text{K}$
7. weight less than 5000 kg
8. shelf life at least 5 years
9. no significant pre-activation emitted radiation
10. no requirement for limited post-activation emitted radiation
11. no shutdown capability required

ACHIEVEMENT OF COMPACT SIZE REQUIRED FOR AERIAL DELIVERY

The following characteristics could contribute to achieving the small reactor size desired for a thermal penetrator: employment of highly enriched uranium or plutonium as compared to ordinary reactor grade uranium; no design requirements for active regulation of the reactor after activation; no requirement for shielding of radiation; no provisions for replenishment of depleted fuel; increased maximum allowable design temperatures; and no requirement for experimental access to or observation of the reactor core.

OPTIONS CONSIDERED FOR IMPLEMENTATION

Multiple possible schemes for implementing power regulation systems for a thermal penetrator have been identified, and fall into the two categories of fast-flux

reactors and thermal-flux reactors. Fast and thermal refer to the characteristic energy spectrums of the neutrons used to propagate the nuclear reaction. Criticality in thermal-flux reactors is principally maintained by neutrons having an energy spectrum in thermal equilibrium with a relatively cool moderator (such as liquid water). Thermal neutron reactors require a substantial body of material to moderate (e.g., thermalize) the high energy neutrons produced in fission reactions down to the lower energies where they are most likely to undergo capture by a fissile nuclei and produce additional reactions. Formulating feasible thermal reactor concepts may be challenging because of the constraints imposed by the mass and volume of moderator typically required, particularly if a reactor is going to be operated at much higher temperatures than usually employed. Taking advantage of the surrounding rock material as a moderator/reflector may make design of a compact thermal flux reactor powered penetrator more feasible.

Fast flux reactors principally produce power through fission by essentially unmoderated neutrons.

Possible mechanisms that have been identified for regulating power in a compact fast and/or thermal flux reactor include: decrease in fissile material density due to thermal expansion; expansion due to increase in internal pressure in cavities; density based concentration of fissile materials in fluid column as counteracted by heat driven convection; concentration of fissile materials by precipitation; contained periodic explosive disassembly; prompt negative coefficient of reactivity through moderation in a hydride or other light moderator element containing fuel (analogous to TRIGA); thermal expansion driven movement of a moderator, neutron source, or neutron reflector; solution/precipitation of one or more components in an alpha-n reaction neutron source;

decrease in moderation of neutrons due to temperature change in surrounding granite; decrease in reflection of neutrons due to phase changes in surrounding granite; etc. Incorporation of a neutron absorbing shell (such as one incorporating boron) outside of the fissile components might provide a means to achieve greater decoupling of the reactor from its environment but would make minimization of reactor size more challenging. Such a shell might also provide a chemical advantage with respect to penetration of silicate rocks.

Multiple design options are available for activation of such a device and are similar in nature to those available for reactivity regulation, although movement of parts would be allowable for activation. Some possibilities include: introduction of a neutron source; removal of a neutron absorber such as boron or cadmium; introduction of reactor into moderator; introduction of moderator into reactor; assembly of fissile components to create initially super-critical mass; and removal or introduction of a neutron reflector.

These and other options for design of passively regulated fissile power system for penetration of rock are available in the existing reactor design literature.

FISSILE VS. RADIOISOTOPE IMPLEMENTATIONS

Ideal thermal penetrator

The hypothetical ideal thermal penetrator would involve a refractory casing enclosing a power source capable of developing a sufficiently high temperature to melt through granite or most other rock types. The refractory casing would contain the power source even in corrosive environments at extreme temperatures, as well as withstand high pressures and impact loads. The power source could be regulated and would provide

thermal power to maintain the refractory case at temperatures sufficient to melt granite. This ideal system would be in all ways non-hazardous before activation, and non-hazardous after activation other than its steady production of heat. Such a hypothetical penetrator would thus virtually eliminate all hazard of collateral damage while providing a possible means of robust DBHT defeat independent of depth.

This ideal of course can only be approached. Principally this is because only two types of nuclear power sources, radioisotope decay or fission, can provide the required sustained volume-specific power. Both potentially possess adequate power densities to thermally penetrate most rock types while developing a sufficiently large melt bubble to ensure robust terminal defeat of the target.

Radioisotope powered penetrator

In the case of a radioisotope penetrator, safety for surface non-combatants is assured in nominal scenarios because the radioisotope and penetrator case are selected so as to assure safe levels of external nuclear radiation. A radioisotope thermal penetrator would only be hazardous due to the accumulated storage of penetrator thermal energy in the melt bubble. Much as for a concrete bomb, only phenomenal bad luck – as in standing at or very near a penetrator’s point of impact – would cause harm.

Another advantage of a radioisotope powered penetrator as compared to a nuclear bomb (or fissile powered penetrator) is that due to the short half-lived isotopes employed, residual hazard posed by the encapsulated radioactivity would exponentially decay. This would make it unlikely that any significant amounts of radioisotope which might escape the penetrator case could ever migrate through ground water or rock strata to affect the health of those on the surface. Further, the nominal final penetration depth would be in

excess of 1500 meters into the Earth's crust, well isolated from the surface for the time scales of concern.

Fission powered penetrator

In contrast to a radioisotope thermal penetrator, a fissile thermal penetrator would potentially produce lethal levels of irradiation to individuals directly exposed to the device after activation, but would pose enormously smaller worst case radiological hazards prior to activation. However, the hazard would be minimized for non-combatants due to the initial kinetic penetration of the device. Interposed earth and rock should at least partially shield individuals close to the point of impact, thus greatly reducing their potential exposure.

No fallout would be produced by a fissile penetrator and only limited levels of neutron-activated isotopes would exist outside the penetrator's case. Thus there would be relatively small quantities of uncontained radioactive isotopes to contribute to a persistent or dispersed external radiation hazard as compared to a nuclear bomb. Of the external radioactive isotopes produced by neutron activation of the surrounding melt and rock, a significant portion would be sealed contained in the vitrified glass column left by the penetrator's passage.

Of particular note are the advantages of fissile penetrator implementations for strategic military missions requiring defeat of a target in which more radiotoxic lethality is allowed or desired with less potential harm to civilian populations than nuclear bombs. Potential examples of such missions include defeat of deeply buried WMD facilities, as well as super-hard targets. For such missions the potential for high levels of killing radiation production by fissile devices once they activate below the surface might provide

an enhanced capability for attacking NBC production and storage bunkers, neutralizing stored weapons and rendering the bunker uninhabitable for a period of several months to decades, without exposing the general populace to disproportionate hazard or creating a highly visible event (all effects being contained below ground).

Against such targets, fissile powered thermal penetrators offer the potential of robust, prolonged functional defeat. Irradiation/neutron activation of the interior of a DBHT could greatly increase the difficulty of reconstituting the facility, and might render the reactivation of the facility impractical.

Some of the concerns vs. benefits for FIPTPs as compared to RIPTPs for scientific and military applications are listed in Table 59, below. To summarize, the principal advantages of radioisotope decay are that some forms of decay may be easily shielded so as to approach the ideal of pure thermal power production, and a simple physical implementation, whereas the principal disadvantages that go along with radioisotopes are constant, unregulated production of power at an ever decaying level, as well as low isotope availability. The principal advantage of fissile implementations are the much lower radiological hazard prior to activation, the ability to turn the device on and regulate the level of power produced to match desired operating temperature, as well as good availability of the required materials, whereas the principal disadvantage is an inability to compactly shield the high-levels of emitted radiation.

Table 59: Qualitative comparison of radioisotope and fissile power sources for military and scientific applications

<i>PERFORMANCE CONCERN</i>	<i>MILITARY APPLICATION</i>		<i>SCIENTIFIC APPLICATION</i>	
	<i>Radioisotope Powered</i>	<i>Fissile Powered</i>	<i>Radioisotope Powered</i>	<i>Fissile Powered</i>
<i>Temperature Management: logistics</i>	Must be continually cooled. Poss. incompatibilities w/ other systems. Risk of radioisotope release in event of cooling failure	No thermal management hazard as activated only upon trigger – should be more robust to fire than existing nuclear explosive devices.	Similar but reduced hazards as compared to military application. May be immediately used and/or transported in more robust, safer ground transport.	Little difference as compared to military application.
<i>Temperature Management: employment</i>	Dependent upon equilibrium conditions as determined by unique target environs.	Inherent temperature feedback control of power generation can be incorporated in design. Results in more robust operation with potential for higher performance.	Concerns reduced as employment environment may be better characterized.	Concerns reduced as employment environment may be better characterized.
<i>External Radiation: pre-employment</i>	Possible design, safety issue – particularly for isotopes such as Cm242, Cm244, etc.	Negligible if high purity fissile isotopes (U235 or Pu239) are employed because of extremely long half-lives. Can be designed to emit below background dose prior to activation.	Some reduction in hazards due to lower probable inventory, more robust safety systems viable.	Negligible.
<i>External Radiation: employment</i>	Low radiation, insignificant when penetrator established in sealed melt shaft. Radiation hazard greatly lower than hazard posed by conventional kill mechanisms.	High/probably lethal levels of radiation. Failure to thermally penetrate material could lead to lack of containment and direct irradiation/neutron activated isotope release. Radiation beneficial as means to neutralize Nuclear / Biological / Chemical agents and render facility inoperable for extended period.	Benign.	Significantly greater risk than radioisotope device.
<i>Diversion of hazardous materials for enemy use.</i>	Significant risk in some scenarios. Short half-life radioisotopes would rapidly decay to a fraction of a percent in a period of several	Greater risk pre-activation as nuclear material easier to handle and convert to use in alternate weapon systems.	Risk low as fewer devices would be used in controlled, secured environment instead of hostile territory.	Risk low as fewer devices used in controlled, secured environment instead of hostile territory.

<i>PERFORMANCE CONCERN</i>	<i>MILITARY APPLICATION</i>		<i>SCIENTIFIC APPLICATION</i>	
	<i>Radioisotope Powered</i>	<i>Fissile Powered</i>	<i>Radioisotope Powered</i>	<i>Fissile Powered</i>
	years, reducing exposure to risk.	Greatly reduced risk post-activation as high radioactivity makes difficult to divert materials post-application.		Melt shaft might pose prolonged radiological hazard if individuals actively removed material.
<i>Power source isotope production</i>	Challenging due to short half-life necessary to get required power. Difficult to accumulate much due to rate of decay, high power makes difficult to handle	Abundant suitable material available at relatively low cost. Excess of material in national inventory.	Less of a concern due to the probably smaller numbers of devices desired.	Little issue with materials availability – possibly some concern regarding control of weapons grade materials in a non-military endeavor.
<i>Power source cost</i>	Significant – difficult to produce and handle material, produced in small amounts.	Low – material supply significant.	Moderate	Low
<i>Lethality (conventional)</i>	May not be possible to accumulate sufficient isotope to build large devices to get desired effects.	Likely to be fabricated in larger diameters which would be associated with larger melt bubbles and significantly greater lethality.	N/A	N/A
<i>Lethality (radiation)</i>	Very little effect.	Large, possibly dominant lethality mechanism	N/A	N/A
<i>Production lead-time</i>	Lead time required may be up to a year or so due to necessity to produce short-lived isotopes.	Unimportant as fissile isotopes have extremely long lives and could be produced and stockpiled.	Little concern as utility of device not time of use dependent.	Unimportant... could be stockpiled and used as desired.
<i>Shelf life</i>	Shelf life ~ 3-4 months.	Shelf-life > 10 years.	See above.	See above.

REFERENCES

- 1 Younger, S. M., "Nuclear Weapons in the Twenty-First Century," Los Alamos National Laboratory, LAUR-00-2850, New Mexico, June 27, 2000.
- 2 Ahearne, J. F. and et al, "Effects of Nuclear Earth Penetrators and Other Weapons," National Research Council, www.nap.edu/catalog/11282.html, 2005.
- 3 "Report to Congress on the Defeat of Hard and Deeply Buried Targets," Required by Section 1044 of the Floyd D. Spence National Defense Authorization Act for Fiscal Year 2001, PL 106-398, Washington, DC, July, 2001.
- 4 Bulletin of the Atomic Scientist, "NRDC: Nuclear Notebook -- US Nuclear Stockpile, July 1996."
http://www.thebulletin.org/article_nn.php?art_ofn=ja96norris. Downloaded from internet: Jan. 23, 2006.
- 5 Gibson, J. N., "U.S. Nuclear Weapon Enduring Stockpile."
<http://nuclearweaponarchive.org/Usa/Weapons/Wpngall.html>. Downloaded from internet: Jan. 23, 2006.
- 6 Nelson, R. W., "Low Yield Earth-Penetrating Nuclear Weapons," *Science and Global Security*, No. 10, Feb. 20, 2002, pp. 1-20.
- 7 Mazur, G., "TRIZ -- Theory of Inventive Problem Solving."
<http://www.mazur.net/triz/>. Downloaded from internet: Feb. 12, 2006.
- 8 "DoD Guide to Integrated Product and Process Development," Office of the Under Secretary of Defence, Department of Defence, Feb. 5, 1996.
- 9 Schrage, D. P. and Mavris, D. N., "Integrated Product/Process Design/Development (IPPD) Through Robust Design Simulation," AIAA, Los Angeles, California, Sept., 1995.
- 10 Kirby, M. R. and Mavris, D. N., "Forecasting the Impact of Technology Infusion on Subsonic Transport Affordability," Society of Automotive Engineers, SAE Paper No. 985576, 1998.

- 11 Kirby, M. R. and Mavris, D. N., "An Approach for the Intelligent Assessment of Future Technology Portfolios," AIAA, Reno, NV, 2002.
- 12 Eastler, T. E., Percious, D. J., and Fisher, P. R.. Role of Geology in Assessing Vulnerability of Underground Fortifications to Conventional Weapons Attack. Reviews in Engineering Geology XIII, 173-187. 1998.
- 13 Hickerson, James P. Jr., Zanner, Frank J., Baldwin, Michael D., and Maguire, Michael C., *Monolithic Ballasted Penetrator*, Patent US 6,186,072, issued Feb. 13, 2001.
- 14 Peurifoy, R., Jeanloz, R., Goodby, J., and Drell, S.. A Strategic Choice: New Bunker Buster vs. Non-proliferation. Arms Control Today [March]. 2003. http://www.armscontrol.org/act/2003_03/drelletal_mar03.asp, Arms Control Association.
- 15 Guirguis, Raafat H., *Super-cavitating penetrator warhead*, Patent US 6,601,517 , issued Aug. 5, 2003.
- 16 Levi, M. A., "Fire in the Hole," Carnegie Endowment for International Peace, 31, Washington, DC, Nov., 2002.
- 17 Nelson, R. W.. Nuclear "Bunker Busters" Would More Likely Disperse than Destroy Buried Stockpiles of Biological and Chemical Agents. 2003.
- 18 MNK-BAA-02-0002, AFRL/MN Armament Technology Research. Commerce Business Daily . 2002.
- 19 Selinger, M.. Boeing Tapped To Develop Massive Penetrator Bomb. Aerospace Daily & Defense Report . 11-3-2004. http://www.aviationnow.com/avnow/news/channel_aerospacedaily_story.jsp?id=news/BOEBOMB11034.xml, Aviation Week.
- 20 Brubaker, D.. Full Dimensional Defeat, powerpoint presentation. 6-6-2002. 6-6-2002.
- 21 Saxelby, R.. Conversations with Mr. Robert Saxelby, Senior Combustion Devices Design Engineer of Rocketdyne. 1998.

- 22 Mavris, D. N., Mantis, G., and Kirby, M. R., "Demonstration of a Probabilistic Technique for the Determination of Economic Viability," American Institute of Aeronautics and Astronautics, AIAA-97-5585, 1997.
- 23 Box, G. E. P. and Draper, N. R., *Empirical Model Building and Response Surfaces*, John Wiley & Sons, New York, NY, 1987.
- 24 Mavris, D. N., Bandte, O., and Shrage, D. P., "Effect of Mission Requirements on the Economic Robustness of an HSCT Concept," ISPA, Cannes, France, June, 1996.
- 25 Mavris, D. N. and Roth, B. A., "A Methodology for Robust Design of Impingement-cooled HSCT Combustion Liners," American Institute of Aeronautics and Astronautics, AIAA 97-0288, 1997.
- 26 "Memorandum for the President: National Deep Underground Command Center as a Key FY 1965 Budget Consideration," The LBJ Library and Museum; Austin, TX, National Security File, Subject File, Box 8, folder titled "Deep Underground Command Center", Nov. 7, 1963.
- 27 Adriaans, M. J., "Superconducting Gravity Gradiometers for Underground Target Recognition," Sandia National Laboratories, SAND98-0465, Albuquerque, NM, Jan., 1998.
- 28 Godun, R. M., D'Arcy, M. B., Summy, G. S., and Burnett, K., "Prospects for atom interferometry," *Contemporary Physics*, Vol. 42, No. 2, 2001, pp. 77-95.
- 29 Godwin, J., "The Man-Made Earthquake: A Short History of Very Heavy Conventional Aerial Bombs."
<http://home.aol.com/nukeinfo2/#A.%20Project%20Ruby>. Downloaded from internet: Jan. 1, 2006.
- 30 Hansen, C., "A Hindenburg in the Bomb Bay: The Transition from Liquid to Solid Fueled Thermonuclear Weapons, 1951 - 1954," Los Alamos, NM, Aug. 9, 1998.
- 31 Woods, R., Scott, W., and et al, "B-1B Fact Book," North American Aircraft, Rockwell International, NA 95-1210, July 20, 1995.

- 32 Federation of American Scientists, "B-52 History."
http://www.fas.org/nuke/guide/usa/bomber/b-52_hist.htm. Downloaded from internet: Jan. 5, 2006.
- 33 Jenkins, D. R. and Landis, T.. North American XB-70A Valkyrie. 1st[34]. 2002. North Branch, MN, Specialty Press Publishers and Wholesalers. Warbird Tech Series.
- 34 Savage, D., "All About Guppys." <http://www.allaboutguppys.com/>. Downloaded from internet: Jan. 6, 2006.
- 35 Spick, M., *The Great Book of Modern Warplanes*, 1st ed., Salamander Books Ltd., London, UK, 2003.
- 36 Kandebo, S. and et al. 2004 Aerospace Sourcebook. Aviation Week & Space Technology 160[3], 36-37. 1-19-2004. New York, NY, McGraw Hill.
- 37 Ari, G.. Cargo Aircraft Bombing System. 2003. Air Force Institute of Technology.
- 38 Kandebo, S. and et al. 2004 Aerospace Sourcebook. Aviation Week & Space Technology 160[3], 38-39. 1-19-2004. New York, NY, McGraw Hill.
- 39 Wikipedia Contributors, "C-5 Galaxy."
http://en.wikipedia.org/w/index.php?title=C-5_Galaxy&oldid=33247386.
Downloaded from internet: Jan. 6, 2006.
- 40 Wikipedia Contributors, "C-17 Globemaster III."
http://en.wikipedia.org/w/index.php?title=C-17_Globemaster_III&oldid=33960231. Downloaded from internet: Jan. 6, 2006.
- 41 Donald, D., *The Encyclopedia of Civil Aircraft*, 1st ed., Thunder Bay Press, Cremona, Italy, 1999.
- 42 Antonov Airlines, "Antonov Airlines Homepage."
<http://www.heavylift.co.uk/services/an124.asp?tab=aircraft>,
<http://www.heavylift.co.uk/services/an225.asp?tab=aircraft>. Downloaded from internet: Jan. 6, 2006.

- 43 Boeing Corporation, "Technical Specifications -- 747 Classics." http://www.boeing.com/commercial/747family/pf/pf_classics.html. Downloaded from internet: Jan. 5, 2006.
- 44 Boeing Corporation, "Document D6-58326 -- 747 Airplane Characteristics for Airport Planning." <http://www.boeing.com/assocproducts/aircompat/747.htm>. Downloaded from internet: Jan. 5, 2006.
- 45 Boeing Corporation. Lockheed L-1011-200 'TriStar' Freighter -- Performance Summary. 2003. http://www.tiaca.org/content/Boeing_2003_2.pdf, Boeing.
- 46 Kandebo, S. and et al. 2002 Aerospace Sourcebook. Aviation Week & Space Technology 156[2], 70-71. 1-14-2002. New York, NY, McGraw Hill.
- 47 Wikipedia Contributors, "Aero Spacelines Super Guppy." http://en.wikipedia.org/w/index.php?title=Aero_Spacelines_Super_Guppy&oldid=30746592. Downloaded from internet: Jan. 6, 2006.
- 48 Langevin, G. S., "Crashworthiness." <http://oea.larc.nasa.gov/PAIS/Concept2Reality/crashworthiness.html>. Downloaded from internet: Jan. 9, 2006.
- 49 Kennedy, D. R., "History of the Shaped Charge Effect: The First 100 Years," LANL, AD-A220095, Los Alamos, NM, Mar. 30, 1990.
- 50 Jenkins, D. R., *Hypersonic: The Story of the North American X-15*, 1st ed., Specialty Press, North Branch, MN, 2003, pp. 131-147.
- 51 Sublette, C., "The Tsar Bomba ("King of Bombs"): The World's Largest Nuclear Weapon." <http://nuclearweaponarchive.org/Russia/TsarBomba.html>. Downloaded from internet: June 21, 2002.
- 52 Wade, M., "Encyclopedia Astronautica: Pegasus XL." <http://www.astronautix.com/lvs/pegsusxl.htm>. Downloaded from internet: Jan. 4, 2006.
- 53 WaffenHQ, "Messerschmitt Me 321 Gigant." <http://www.waffenhq.de/flugzeuge/me321.html>. Downloaded from internet: Jan. 4, 2006.

- 54 Jenkins, D. R., *Space Shuttle: The History of the National Space Transportation System*, 3rd ed., Dennis R. Jenkins, Cape Canaveral, FL, 2001, pp. 211.
- 55 Wade, M., "Encyclopedia Astronautica: Minuteman 1." <http://www.astronautix.com/lvs/mineman1.htm>. Downloaded from internet: Jan. 2, 2006.
- 56 GlobalSecurity.org, "GBU-43/B "Mother Of All Bombs"." <http://www.globalsecurity.org/military/systems/munitions/moab.htm>. Downloaded from internet: Jan. 2, 2006.
- 57 Barton, R., "Minuteman ICBM History Website." http://www.geocities.com/minuteman_missile/diagrams.htm. Downloaded from internet: Jan. 2, 2006.
- 58 Wade, M., "Encyclopedia Astronautica: X-15A-2." <http://www.astronautix.com/lvs/x15a2.htm>. Downloaded from internet: Jan. 4, 2006.
- 59 Adamsky, V. and Smirnov, Y.. Moscow's Biggest Bomb: The 50-Megaton Test of October 1961. Coldwar International History Project Bulletin Fall[4], 3-21. 1994. Online at http://wilsoncenter.org/index.cfm?fuseaction=topics.home&topic_id=1409.
- 60 Wade, M., "Encyclopedia Astronautica: Burlak." <http://www.astronautix.com/lvs/burlak.htm>. Downloaded from internet: Jan. 4, 2006.
- 61 Torrasi, S. A., "Cargo Gliders for Complex Emergencies and Operations Other Than War: New Uses for an Old Neglected Warhorse," *Journal of Humanitarian Assistance*, 1999.
- 62 Kevin, R., "Italeri 1/72 Messerschmitt Me 323 "Gigant": "Inbox Review"." <http://www.fortunecity.com/meltingpot/portland/971/Inbox/k-m/me-323-i.htm>. Downloaded from internet: Jan. 4, 2006.
- 63 SiloMan, "Air Mobile Feasibility Demonstration." <http://www.siloworld.com/MINUTEMAN/Airmobile/airmobile.htm>. Downloaded from internet: Jan. 4, 2006.

- 64 Neely, M., "Lockheed C-5 Galaxy."
<http://www.theaviationzone.com/factsheets/c5.asp>. Downloaded from internet:
Jan. 6, 2006.
- 65 Wade, M., "Encyclopedia Astronautica: LRALT."
<http://www.astronautix.com/lvs/lralt.htm>. Downloaded from internet: Jan. 4, 2006.
- 66 Drab, J. and Patterson, B. C.. Massive Ordnance Air Blast Weapon Development:
Development to flight test of a 21,700 lb weapon took less than 10 months. 2004.
Eglin Air Force Base, Air Force Research Lab Munitions Directorate.
- 67 Dornheim, M. A.. Air Drops Dummy Rocket for Darpa's Falcon. Aviation Week &
Space Technology . 10-23-2005. Online at
http://www.aviationnow.com/avnow/news/channel_awst_story.jsp?id=news/102405p1.xml.
- 68 Couffer, J., *Bat Bomb: World War II's Other Secret Weapon*, University of Texas
Press 1992.
- 69 The History Net.com, "Top Secret Bat and Bird Bomber Program."
<http://historynet.com/ahi/blbatnirdbomber/index.html>. Downloaded from internet:
Feb. 9, 2006.
- 70 DePriest, P. and Ward, A.. Conversations regarding information security of
hypothetical hardened facilities. 2006. 2006.
- 71 Cole, E., *Hackers Beware: The Ultimate Guide to Network Security*, 1st ed., Sans
2001.
- 72 Internet Security Systems, "Internet Security Website." www.iss.net.
Downloaded from internet: July 20, 2006.
- 73 Security Focus, "Internet Security Website." www.securityfocus.com.
Downloaded from internet: July 20, 2006.
- 74 SANS Institute Inc., "SysAdmin, Audit, Network, Security Institute."
www.sans.org. Downloaded from internet: July 20, 2006.

- 75 Insecure.org, "Internet and network exploits, security, and software." www.insecure.org. Downloaded from internet: July 20, 2006.
- 76 Metasploit, "Metasploit Framework: Hack the Planet." www.metasploit.com. Downloaded from internet: July 20, 2006.
- 77 Nessus, "Nessus: Network Exploitation/Security Test Toolsets." www.nessus.org. Downloaded from internet: July 20, 2006.
- 78 Core Security, "Core Impact: An automated, comprehensive testing product." www.coresecurity.com. Downloaded from internet: July 20, 2006.
- 79 Immunity Security, "Canvas: A comprehensive exploitation framework." www.immunitysecurity.com. Downloaded from internet: July 20, 2006.
- 80 Banks, E. E., "Fracture and Fragmentation in Shock Loading of Metals," *The Journal of the Australian Institute of Metals*, Vol. 13, No. 1, June 21, 1968, pp. 39-47.
- 81 Wilkins, M. L., "Calculation of Spall Based on a One-Dimensional Model," Lawrence Livermore National Labs, UCRL-6356, Livermore, California, Mar. 30, 1961.
- 82 Davison, L. and Graham, R. A., "Shock Compression of Solids," *Physics Reports*, Vol. 55, No. 4, 1979, pp. 255-379.
- 83 Carleone, J., Kennedy, D. R., and et al, *Tactical Missile Warheads*, 1st ed., Vol. 155, American Institute of Aeronautics and Astronautics, Washington DC, 1993, pp. 1-745.
- 84 Heuze, F. E., "An overview of projectile penetration into geological materials, with emphasis on rock.," *Int.J.Rock Mech.Min.Sci.& Geomech.Abst.*, Vol. 27, No. 1, 1990, pp. 1-14.
- 85 GlobalSecurity.org, "Small Diameter Bomb / Small Smart Bomb." <http://www.globalsecurity.org/military/systems/munitions/sdb.htm>. Downloaded from internet: Jan. 20, 2006.

- 86 Federation of American Scientists, "Guided Bomb Unit-28 (GBU-28) -- BLU-113 Penetrator." <http://www.fas.org/man/dod-101/sys/smart/gbu-28.htm>. Downloaded from internet: Jan. 20, 2006.
- 87 Federation of American Scientists, "M829 120mm, APFSDS-T." <http://www.fas.org/man/dod-101/sys/land/m829a1.htm>. Downloaded from internet: Jan. 20, 2006.
- 88 Rosset, W. S., "An Overview of Novel Penetrator Technology," Army Research Laboratory, ARL-TR-2395, Aberdeen Proving Ground, MD, Feb., 2001.
- 89 Hopson, J. W., Hantel, L. W., and Sandstrom, D. J., "Evaluation of Depleted Uranium Alloys for Use in Armor Penetrating Projectiles," Los Alamos Scientific Laboratory, LA-5238; Los Alamos, NM, June, 1973.
- 90 Hodge, J. L., Littlefield, D. L., Bless, S., Short, A., and Pedersen, B., "Novel Kinetic Energy Penetrators for Electromagnetic Guns," DTIC, Dec., 2004.
- 91 Engineering Fundamentals, "Tool Steel AISI S5." http://www.efunda.com/materials/alloys/tool_steels/show_tool.cfm?ID=AISI_S5&prop=uts&Page_Title=Tool%20Steel%20AISI%20S5. Downloaded from internet: May, 2006.
- 92 Japan Nuclear Cycle Development Institute, "H12: Project to Establish the Scientific and Technical Basis for High Level Waste Disposal in Japan," Supporting Report 2, <http://www.jaea.go.jp/04/tisou/zh12/h12/>, Nov., 1999.
- 93 Young, C. W., "Penetration Equations," Sandia National Laboratories, SAND97-2426, Albuquerque, New Mexico, Nov., 1997.
- 94 O'Dwyer, J. M., *Directional Control of Missiles*, Patent Queensland, AU 6,889,935, issued May 10, 2005.
- 95 O'Dwyer, J. M., *Barrel Assembly with Axially Stacked Projectiles*, Patent Brisbane, AU 6,510,643, issued Jan. 28, 2003.
- 96 Metal Storm, "Metal Storm." <http://www.metalstorm.com/index.php?src=news&category=Latest%20Video%20>

[%26%20Live%20Firings&srctype=list&page=2&spp=8](#). Downloaded from internet: Nov., 2005.

- 97 Swinford, N. F. and Kudlick, D. A., "A Hard and Deeply Buried Target Defeat Concept," DTIC, M97-03-2054, 1996.
- 98 Eather, R. F. and Griffiths, N., "Some Historical Aspects of the Development of Shaped Charges," RARDE/DTIC, 2/84, AD-A144098, London, UK, 1984.
- 99 Walters, W. P., "The Shaped Concept, Part III: Application of Shaped Charges," Ballistic Research Laboratory, BRL-TR-3168, AD-A228492, Aberdeen Proving Ground, MD, Oct., 1990.
- 100 Walters, W. P., "The Shaped Concept, Part II: The History of Shaped Charges," Ballistic Research Laboratory, BRL-TR-3158, AD-A226772, Aberdeen Proving Ground, MD, Sept., 1990.
- 101 Walters, W. P., "The Shaped Concept, Part I: Introduction," Ballistic Research Laboratory, BRL-TR-3142, AD-A226401, Aberdeen Proving Ground, MD, Aug., 1990.
- 102 Walters, W. P. and Golaskey, S. K., "Hemispherical and Conical Shaped-Charge Liner Collapse and Jet Formation," US Army Ballistic Research Laboratory, BRL-TR-2781, AD-A179735, Aberdeen Proving Ground, MD, Feb., 1987.
- 103 Chi, D., "Fundamentals of Penetration Mechanics -- Jets and Rods," *Tactical Missile Warheads*, edited by Joseph Carleone Progress in Astronautics and Aeronautics, American Institute of Aeronautics and Astronautics, Washington DC, 1993, pp. 467.
- 104 Vigil, M. G., "Design of Largest Shaped Charge: Generation of very large diameter, deep holes in rock and concrete structures," Sandia National Laboratories, SAND2003-1160, Albuquerque, NM, Apr., 2003.
- 105 Birkhoff, G., MacDougal, D. P., Pugh, E. M., and Taylor, G., "Explosives with Lined Cavities," *Journal of Applied Physics*, Vol. 19, 1948, pp. 563-582.
- 106 Hill, R., Mott, H. F., and Pack, D. C., "Penetration by Munroe Jets," HMSO, A.C. Number 5756, London, UK, Jan., 1944.

- 107 Pack, D. C. and Evans, W. M., "Penetration by High Velocity Munroe Jets-1," *Proceedings of the Physical Society of London*, Vol. 64, No. Section B, 1951, pp. 298.
- 108 Pack, D. C. and Evans, W. M., "Penetration by High Velocity Munroe Jets-2," *Proceedings of the Physical Society of London*, Vol. 64, No. Section B, 1951, pp. 303.
- 109 Rollins, R. R., Clark, G. B., and Kalia, H. N., "Penetration in Granite by Shaped Charge Liners of Various Metals," Rock Mechanics & Explosives Research Center, RMERC-TR-70-13, University of Missouri -- Rolla, Apr., 1971.
- 110 Vigil, M. G., "Shaped Charge Penetration Velocities, Depths, and Times for Various Continuous Jet and Target Materials," Sandia National Laboratories, SAND91-2281, Albuquerque, NM, Dec., 1991.
- 111 Lewis, N., Garwin, R., Hammer, D., and et al, "High Energy Density Explosives," The MITRE Corporation, JASON Program Office, JSR-97-110, McLean, VA, Oct., 1997.
- 112 Collins, C. B., "Essential Fundamentals of Quantum Nucleonics." <http://www.utdallas.edu/research/quantum/Tutorial.htm>. Downloaded from internet: May, 2006.
- 113 Zoita, N. C.. Experimental study of photon induced gamma emission of Hafnium-178(m2) by nuclear spectroscopy methods. 2005. The University of Texas at Dallas.
- 114 Kennedy, D. R., "Warheads: An Historical Perspective," *Tactical Missile Warheads*, edited by Joseph Carleone Progress in Astronautics and Aeronautics, American Institute of Aeronautics and Astronautics, Washington DC, 1993, pp. 25.
- 115 Fong, Richard, *Segmented kinetic energy explosively formed penetrator assembly*, Patent US 6,510,797 , issued Jan. 28, 2003.
- 116 Peterson, P. F., "Issues for Detecting Undeclared Post-Closure Excavation at Geologic Repositories," *Preprint for Science and Global Security*, Apr. 3, 2004.

- 117 Moallemi, M. K. and Viskanta, R., "Melting Around A Migrating Heat-Source," *Journal of Heat Transfer-Transactions of the Asme*, Vol. 107, No. 2, 1985, pp. 451-458.
- 118 Graduate Studies Office of the Georgia Institute of Technology, "Guidelines for PhD Dissertation Research." <http://www.grad.gatech.edu/thesis/index.html>. Downloaded from internet: Jan. 15, 2006.
- 119 Adams, W. M., *Nuclear Reactor Apparatus for Earth Penetration*, Patent US 3,115,194, issued Dec. 24, 1963.
- 120 Eninger, James E., Miller, Joseph, Murch, Charles K., and Ginbey, Leland A., *Ice Penetrating Method and Apparatus*, Patent US 4,651,834, issued Mar. 24, 1987.
- 121 Armstrong, Dale E., McInteer, Berthus B., Mills, Robert L., Potter, Robert M., Robinson, Eugene S., Rowley, John C., and Smith, Morton C., *Method and Apparatus for Tunneling by Melting*, Patent US 3,693,731, issued Sept. 26, 1972.
- 122 Greenlaw, Robert T. and Kornblith, Jeffrey S., *Ice Penetrating Hot Point*, Patent US 5,484,027, issued Jan. 16, 1996.
- 123 Bussod, Gilles Y., Dick, Aaron J., and Cort, George E., *Rock Melting Tool with Anneal Section*, Patent US 5,735,355, issued Apr. 7, 1998.
- 124 Reilly, Hugh T., *Penetrating assault weapons*, Patent US 5,129,305, issued July 14, 1992.
- 125 Aamot, Harold W. C., *Pendulum Steered Thermal Probe*, Patent US 3,390,729, issued July 2, 1968.
- 126 Gibb, F. G. F., "High-temperature, very-deep, geological disposal: a safer alternative for high-level radioactive waste.," *Waste Management*, Vol. 19, 1999, pp. 207-211.
- 127 Gibb, F. G. F., "A new scheme for the very deep geological disposal of high-level nuclear waste," *Journal of the Geological Society*, Vol. 157, 2000, pp. 27-36.
- 128 Donea, J., "Operation Hot Mole," *Euro Spectra*, Vol. 2, No. 18, Dec., 1972.

- 129 Logan, S. E., "Deep self-burial of radioactive wastes by rock-melting capsules," June 10, 1973.
- 130 Klett, R. D., "Deep Rock Nuclear Waste Disposal Test: Design and Operation," Sandia Laboratories, SAND74-0042, Albuquerque, NM, Sept., 1974.
- 131 Gibb, F. G. F. and Attrill, P. G., "Granite recrystallization: The key to the nuclear waste problem?," *Geology*, Vol. 31, No. 8, 2003, pp. 657-660.
- 132 Gibb, F. G. F., "A new scheme for the very deep geological disposal of high-level radioactive waste," *Journal of the Geological Society*, Vol. 157, 2000, pp. 27-36.
- 133 Gibb, F. G. F., "High-temperature, very deep, geological disposal: a safer alternative for high-level radioactive waste?," *Waste Management*, Vol. 19, No. 3, 1999, pp. 207-211.
- 134 Logan, S. E., "Deep Self-Burial of Radioactive Wastes by Rock Melting Capsules," *Transactions of the American Nuclear Society*, Vol. 16, No. JUN, 1973, pp. 177-178.
- 135 Donea, J., "Operation Hot Mole," *Euro-Spectra*, Vol. 11, No. 4, 1972, pp. 102-109.
- 136 Distefan, J. R., "Compatibility of Strontium Compounds with Superalloys at 900 and 1100 Degrees C," *Nuclear Technology*, Vol. 17, No. 2, 1973, pp. 127-142.
- 137 Bottinga, Y. and Weill, D. F., "Viscosity of Magmatic Silicate Liquids - Model for Calculation," *American Journal of Science*, Vol. 272, No. 5, 1972, pp. 438-&.
- 138 Cohen, J. J., Braun, R. L., and Lewis, A. E., "In-Situ Incorporation of Nuclear Waste in Deep Molten Silicate Rock," *Nuclear Technology*, Vol. 14, No. 1, 1972, pp. 76-&.
- 139 Shaw, H. R., Wright, T. L., Peck, D. L., and Okamura, R., "Viscosity of Basaltic Magma - An Analysis of Field Measurements in Makaopuhi Lava Lake Hawaii," *American Journal of Science*, Vol. 266, No. 4, 1968, pp. 225-&.

- 140 Krupka, M. C., "Internal Reaction Phenomena in Prototype Subterrene Radiant Heater Penetrators," Los Alamos Scientific Lab., LA5094, N, 1972.
- 141 Krupka, M. C., "Thermodynamic Stability Considerations in the Mo-Bn-C System. Application to Prototype Subterrene Penetrators," Los Alamos Scientific Lab., LA4959, N, 1972.
- 142 Robinson, E. S., Potter, R. M., Mcinteer, B. B., Rowley, J. C., and Armstrong, D. E., "Preliminary Study of the Nuclear Subterrene," Los Alamos Scientific Lab., LA4547, N, 1971.
- 143 Gido, R. G., "Subterrene Penetration Rate: Melting Power Relationship," Los Alamos Scientific Lab., LA5204MS, N, 1973.
- 144 Neudecker, J. W., Giger, A. J., and Armstrong, P. E., "Design and Development of Prototype Universal Extruding Subterrene Penetrators," Los Alamos Scientific Lab., LA5205MS, N, 1973.
- 145 Williams, R. E., "Development and Construction of a Modularized Mobile Rock-Melting Subterrene Demonstration Unit," Los Alamos Scientific Lab., LA5209MS, N, 1973.
- 146 Neudecker, J. W., "Design Description of Melting-Consolidating Prototype Subterrene Penetrators," Los Alamos Scientific Lab., LA5212MS, N, 1973.
- 147 Murphy, D. J. and Gido, R. G., "Heat Loss Calculations for Small Diameter Subterrene Penetrators," Los Alamos Scientific Lab., LA5207MS, N, 1973.
- 148 Hanold, R. J., "Large Subterrene Rock-Melting Tunnel Excavation Systems. A Preliminary Study," Los Alamos Scientific Lab., LA5210MS, N, 1973.
- 149 Krupka, M. C., "Phenomena Associated with the Process of Rock Melting. Application to the Subterrene System," Los Alamos Scientific Lab., LA5208MS, N, 1973.
- 150 Gido, R., "Internal Temperature Distribution of a Subterrene Rock-Melting Penetrator," Los Alamos Scientific Lab., LA5135, N, 1973.

- 151 Neudecker, J. W., "Subterrene Instrumentation Requirements," Los Alamos Scientific Lab., CONF7305101; LAUR73459, N, 1973.
- 152 Hanold, R. J., "Subterrene Rock-Melting Excavation Program," Los Alamos Scientific Lab., CONF73091081; LAUR74801, N.Mex, 1973.
- 153 Neudecker, J. W., "Conceptual Design of a Coring Subterrene Geoprospector," Los Alamos Scientific Lab., LA5517MS, N, 1974.
- 154 Stark, W. A., Wallace, T. C., Witteman, W., Krupka, M. C., and David, W. R., "Application of Thick Film and Bulk Coating Technology to the Subterrene Program," Los Alamos Scientific Lab., CONF7401032; LAUR7420, N.Mex, 1974.
- 155 Hanold, R. J., "Rapid Excavation by Rock Melting -- LASL Subterrene Program -- December 31, 1972 to September 1, 1973," Los Alamos Scientific Lab., LA5459, N, 1973.
- 156 Cort, G. E., "Rock Heat-Loss Shape Factors for Subterrene Penetrators," Los Alamos Scientific Lab., LA5435, N, 1973.
- 157 Stark, W. A., "Carbon Receptor Reactions in Subterrene Penetrators," Los Alamos Scientific Lab., LA5423MS, N.Mex, 1973.
- 158 Altseimer, J. H., "Systems and Cost Analysis for a Nuclear Subterrene Tunneling Machine. A Preliminary Study," Los Alamos Scientific Lab., LA5354, N, 1973.
- 159 Altseimer, J. H., "Systems and Cost Analysis for a Nuclear Subterrene Tunneling Machine. A Preliminary Study," Los Alamos Scientific Lab., LA5354MS, N, 1973.
- 160 Williams, R. E. and Griggs, J. E., "Use of the Rock-Melting Subterrene for Formation of Drainage Holes in Archaeological Sites," Los Alamos Scientific Lab., LA5370MS, N, 1973.
- 161 Stark, W. A. and Krupka, M. C., "Chemical Corrosion of Molybdenum and Tungsten in Liquid Basalt, Tuff, and Granite with Application to Subterrene Penetrators," Los Alamos Scientific Lab., LA5857MS, N, 1975.

- 162 Altseimer, J. H., "Geothermal Well Technology and Potential Applications of Subterrene Devices: A Status Review," Los Alamos Scientific Lab., CONF7505255; LAUR75971, N.Mex, 1975.
- 163 Fisher, H. N., "Thermal Analysis of Some Subterrene Penetrators," Los Alamos Scientific Lab., CONF75110617; LAUR75877, N.Mex, 1975.
- 164 Webster, L. C., "Use of the Subterrene for Military Drilling Applications," Army Engineer Waterways Experiment Station Livermore Calif Explosive Excavation Research Lab. Sponsor: Office of the Chief of Engineers (Army) Washington, EERLMPE745; ADA0015222, D.C, 1974.
- 165 Altseimer, J. H., "Geothermal Well Technology and Potential Applications of Subterrene Devices. A Status Review," Los Alamos Scientific Lab., LA5689MS, N, 1974.
- 166 Altseimer, J. H., "Geothermal Well Technology and Potential Applications of Subterrene Devices: A Status Review," Los Alamos Scientific Lab., LA5689MS, N.Mex, 1974.
- 167 Griggs, J. E., "Development of a Mobile Rock-Melting Subterrene Field Unit for Universal Extruding Penetrators," Los Alamos Scientific Lab., LA5573MS, N, 1974.
- 168 Armstrong, P. E., "Subterrene Electrical Heater Design and Morphology," Los Alamos Scientific Lab., LA5211MS, N, 1974.
- 169 Stanton, A. E., "Heat Transfer and Thermal Treatment Processes in Subterrene-Produced Glass Hole Linings," Los Alamos Scientific Lab., LA5502MS, N, 1974.
- 170 Hanold, R. J., "Rapid Excavation by Rock Melting (LASL Subterrene Program). Status Report, September 1973--June 1976," Los Alamos Scientific Lab., LA5979SR, N.Mex, 1977.
- 171 Murphy, H. D., Neudecker, J. W., Cort, G. E., Turner, W. C., and McFarland, R. D., "Development of Coring, Consolidating, Subterrene Penetrators," Los Alamos Scientific Lab., LA6265MS, N.Mex, 1976.

- 172 Altseimer, J. H., "Subterrene Rock-Melting Concept Applied to the Production of Deep Geothermal Wells," Los Alamos Scientific Lab., CONF7609066; LAUR761302, N.Mex, 1976.
- 173 Nielsen, R. R., bou-Sayed, A., and Jones, A. H., "Characterization of Rock-Glass Formed by the LASL Subterrene in Bandelier Tuff," Terra Tek, TR7561, Inc., Salt Lake City, UT, 1975.
- 174 Pharr, G. M., "Rock Property Measurements Pertinent to the Construction of Drainage Systems at Archaeological Sites in Arizona by Subterrene Penetrators," Los Alamos Scientific Lab., LA6135MS, N.Mex, 1975.
- 175 Turner, W. C., "Unique Refractory Techniques for Fabricating Subterrene Penetrators," Los Alamos Scientific Lab., LA6038MS, N, 1975.
- 176 "Cost Comparison Between Subterrene and Current Tunneling Methods," Mathews (A. A.), PB244480SET, Inc., Rockville, Md, 1975.
- 177 Bledsoe, J. D., Hill, J. E., and Coon, R. F., "Cost Comparison Between Subterrene and Current Tunneling Methods," Mathews (A. A.), 9013; NSFRAT75001; PB2444818, Inc., Rockville, Md, 1975.
- 178 Bledsoe, J. D., Hill, J. E., and Coon, R. F., "Cost Comparison Between Subterrene and Current Tunneling Methods. Appendix A. Baseline Cost Analyses," Mathews (A. A.), 9013A; NSFRAT75001A; PB2444826, Inc., Rockville, Md, 1975.
- 179 Bledsoe, J. D., Hill, J. E., and Coon, R. F., "Cost Comparison Between Subterrene and Current Tunneling Methods. Appendix B. Subterrene Cost Analyses," Mathews (A. A.), 9013B; NSFRAT75001B; PB2444834, Inc., Rockville, Md, 1975.
- 180 Neudecker, J. W., "Application of rock melting to construction of storage holes for nuclear waste," Los Alamos National Laboratory, LA-UR-88-3961, Los Alamos, NM, 1988.
- 181 Altseimer, J. H., "Technical and cost analysis of rock-melting systems for producing geothermal wells. [GEOWELL]," 1976.

- 182 Burnham, J. B., Bloomster, C. H., Cohn, P. D., Eliason, J. R., Peterson, P. L., Rohrman, C. A., Sandness, G. A., Stewart, D. H., and Wallace, R. W., "Recommendations for a US geothermal research plan. Volume 1," 1975.
- 183 Colp, J. L., *Magma-Tap: the ultimate geothermal energy program* 1974.
- 184 Demuth, R. B. and Harlow, F. H., "Thermal fracture effects in geothermal energy extraction," 1979.
- 185 Goff, F. and Nielson, D. L., "Caldera processes and magma-hydrothermal systems continental scientific drilling program: thermal regimes, Valles caldera research, scientific and management plan," 1986.
- 186 Hammel, E. F., "Los Alamos Scientific Laboratory energy-related history, research, managerial reorganization proposals, actions taken, and results. History report, 1945--1979," 1997.
- 187 Harris, R. L., Olson, G. K., Mah, C. S., and Bujalski, J. H., "Geothermal absorption refrigeration for food processing industries. Final report, December 13, 1976--November 13, 1977," 1977.
- 188 Heiken, G. H., Ander, M. E., and Shankland, T. J., *Workshop on exploration for hot dry rock geothermal systems* 1983.
- 189 Hill, T. R. and Sepehrnoori, K., "Geopressured geothermal bibliography (Geopressure Thesaurus)," 1981.
- 190 Howard, J. H., "Present status and future prospects for nonelectrical uses of geothermal resources," 1975.
- 191 J.D, B., D.S, D., and T.T, M., *The 3rd Dimension of Planetary Exploration - Deep Subsurface Sampling* 2000.
- 192 Kalyoncu, R. S. and Snyder, M. J., "High-temperature cementing materials for completion of geothermal wells. Final report," 1981.
- 193 Kestin, J., DiPippo, R., Khalifa, H. E., and Ryley, D. J., "Sourcebook on the production of electricity from geothermal energy," 1980.

- 194 Knutson, C. K. and Boardman, C. R., "Assessment of non-destructive testing of well casing,, cement and cement bond in high temperature wells,".
- 195 Malone, R. D., *Proceedings of the natural gas RD&D contractors review meeting, Volume II* 1995.
- 196 *Proceedings of the second United Nations symposium on the development and use of geothermal resources held at San Francisco, California, May 20--29, 1975. Volume I* 1976.
- 197 "Geothermal project summaries. Geothermal energy research, development, and demonstration program," 1976.
- 198 "Hot dry rock geothermal energy: status of exploration and assessment. Report No. 1 of the hot dry rock assessment panel," 1977.
- 199 "Geothermal Energy Research, Development and Demonstration Program. First annual report," 1977.
- 200 "Compilation of geothermal information: exploration," 1978.
- 201 "Rock physics at Los Alamos Scientific Laboratory," 1980.
- 202 "International Energy: Subject Thesaurus. Revision 1," 1993.
- 203 "Acronym master list," 1995.
- 204 O'Rourke, J. E. and Ranson, B. B., "Instruments for subsurface monitoring of geothermal subsidence," 1979.
- 205 Rowley, J. C., Hanold, R. J., Bankston, C. A., and Neudecker, J. W., "Rock melting Subterrenes: their role in future excavation technology," 1974.
- 206 Sanyal, S. K., Wells, L. E., and Bickham, R. E., "Geothermal well log interpretation midterm report," 1979.

- 207 Sepehrnoori, K., Carter, F., Schneider, R., Street, S., and McGill, K., "Geopressured geothermal bibliography. Volume II (geopressure thesaurus). Second Edition," 1983.
- 208 Sepehrnoori, K., Carter, F., Schneider, R., Street, S., and McGill, K., "Geopressured geothermal bibliography. Volume I. Citation extracts. Second edition," 1983.
- 209 Sherwood, A. E., "Explosive stimulation of a geothermal steam reservoir," 1972.
- 210 Smith, M. C., *Future of hot dry rock geothermal energy systems* 1979.
- 211 Smith, M. C., *Progress of the US Hot-Dry-Rock Program* 1982.
- 212 Smith, M. C., "The furnace in the basement: Part 1, The early days of the Hot Dry Rock Geothermal Energy Program, 1970--1973," 1995.
- 213 Walter, R. A., "Modeling and optimization of geothermal power plants using the binary fluid cycle," 1976.
- 214 Cort, G. E., Goff, S. J., Rowley, J. C., Neudecker, J. W., and Dreesen, D. S., "Rock melting approach to drilling," Los Alamos National Lab., LAUR933191; CONF9401262; DE93040162, NM, 1993.
- 215 Neudecker, J. W., Blacic, J. D., and Rowley, J. C., "SUBSELENE: A Nuclear Powered Melt Tunneling Concept for High-Speed Lunar Subsurface Transportation Tunnels," Los Alamos National Lab., LAUR862897; CONF86091411; DE86015305, NM, 1986.
- 216 Rowley, J. C., "Potential for Tunneling Based on Rock and Soil Melting. Abstracts," Los Alamos National Lab., LAUR861832; CONF8504240ABSTS; DE86011237, NM, 1985.
- 217 Rowley, J. C. and Neudecker, J. W., "In-Situ Rock Melting Applied to Lunar Base Construction and for Exploration Drilling and Coring on the Moon," Los Alamos National Lab., LAUR85384; CONF84102307; DE85006716, NM, 1984.

- 218 Heuze, F. E., "Modeling of Nuclear Waste Disposal by Rock Melting," Lawrence Livermore National Lab., UCRL87510; CONF8208033; DE82012798, CA, 1982.
- 219 Heuze, F. E., "Geotechnical Modeling of High-Level Nuclear Waste Disposal by Rock Melting," Lawrence Livermore National Lab., UCRL53183; DE82007913, CA, 1981.
- 220 Unruh, C. M., "Environmental Effects of Reactor Waste Disposal Alternatives," Battelle Pacific Northwest Labs., PNLSA8604; CONF80062141; DE82005911, Richland, WA, 1980.
- 221 Shupe, M. W. and Kreiter, M. R., "Environmental Impact Statement on Management of Commercially Generated Radioactive Wastes," Department of Energy, PNLSA7945; CONF79110828; DE82010668, Richland, WA, 1979.
- 222 Benson, G. M., "Thermocorer for Rapid Drilling Tunneling and Excavating," Energy Research and Generation, NSFRA760483; PB2669224, Inc., Oakland, Calif, 1976.
- 223 "Excavation Technology: Publications from the RANN Program, Bibliography," Capital Systems Group, NSFRA760079; PB2604973, Inc., Rockville, Md, 1976.
- 224 Ehrenberg, S. N., Perkins, P. C., and Krupka, M. C., "Petrography and Chemistry of Minerals and Glass in Rocks Partially Fused by Rock-Melting Drills," Los Alamos Scientific Lab., LA5838, N.Mex, 1975.
- 225 Sims, D. L., "A Versatile Rock-Melting System for the Formation of Small-Diameter Horizontal Glass-Lined Holes," Los Alamos Scientific Lab., LA5422, N, 1973.
- 226 Crough, S. L., "Proceedings of Conference on Research in Tunneling and Excavation Technology, Held at Spring Hill Conference Center, Wayzata, Minnesota on September 14-15, 1973," Minnesota Univ., NSFRAT73097; PB2466803, Minneapolis, 1973.
- 227 Gido, R. G., "Description of Field Tests for Rock-Melting Penetration," Los Alamos Scientific Lab., LA5213MS, N, 1973.

- 228 Adams, W. M., "A Direct Method for Investigating the Interior of the Earth," Lawrence Radiation Laboratory Report, UCRL-6306, Livermore, CA, Feb., 1961.
- 229 Armstrong, D. E., Coleman, J. S., McInteer, B. B., Potter, R. M., and Robinson, E. S., "Rock Melting as a Drilling Technique," Los Alamos Scientific Laboratory Report, LA-3243, Los Alamos, NM, Mar., 1965.
- 230 Armstrong, Dale E., McInteer, Berthus B., Mills, Robert L., Potter, Robert M., Robinson, Eugene S., Rowley, John C., and Smith, Morton C., *Method and Apparatus for Tunneling by Melting*, Patent US 3,693,731, issued Sept. 26, 1972.
- 231 Adams, W. M., *Nuclear Reactor Apparatus for Earth Penetration*, Patent US 3,115,194, issued Dec. 24, 1963.
- 232 Bussod, Gilles Y., Dick, Aaron J., and Cort, George E., *Rock Melting Tool with Anneal Section*, Patent US 5,735,355, issued Apr. 7, 1998.
- 233 Attrill, P. G. and Gibb, F. G. F., "Partial melting and recrystallization of granite and their application to deep disposal of radioactive waste Part 1 - Rationale and partial melting," *Lithos*, Vol. 67, No. 1-2, 2003, pp. 103-117.
- 234 Fomin, S. A., Saitoh, T. S., and Chugunov, V. A., "Contact melting materials with non-linear properties," *Heat and Mass Transfer*, Vol. 33, No. 3, 1997, pp. 185-192.
- 235 Vertman, A. A., Polyakov, A. S., and Poluektov, P. P., "Metallurgical technologies and problems related to self-disposal of radioactive waste by deep rock melting," *Advanced Performance Materials*, Vol. 4, No. 2, 1997, pp. 239-245.
- 236 Kashcheev, V. A., Nikiforov, A. S., Poluektov, P. P., and Polyakov, A. S., "Toward A Theory of Self-Disposal of High-Level Waste," *Atomic Energy*, Vol. 73, No. 3, 1992, pp. 735-739.
- 237 Moallemi, M. K. and Viskanta, R., "Experiments on Fluid-Flow Induced by Melting Around A Migrating Heat-Source," *Journal of Fluid Mechanics*, Vol. 157, No. AUG, 1985, pp. 35-51.

- 238 Moallemi, M. K. and Viskanta, R., "Melting Around A Migrating Heat-Source," *Journal of Heat Transfer-Transactions of the Asme*, Vol. 107, No. 2, 1985, pp. 451-458.
- 239 Peterson, P. F., "Issues for Detecting Undeclared Post-Closure Excavation at Geologic Repositories," *Preprint for Science and Global Security*, Apr. 3, 2004.
- 240 Klett, R. D., "Deep Rock Nuclear Waste Disposal Test: Design and Operation," Sandia Laboratories, SAND74-0042, Albuquerque, NM, Sept., 1974.
- 241 Bacon, J. F., Russel, S., and Carstens, J. P., "Determination of Rock Thermal Properties," United Aircraft Research Laboratories, UARL-L911397-4, AD-755 218, East Hartford, CT, Jan., 1973.
- 242 Traeger, R. K., Colp, J. L., and Neel, R. R., "Magma Energy Research, 79-1. Semiannual Report, October 1, 1978-March 31, 1979," Sandia Laboratories, SAND-79-1344, Albuquerque, NM, July, 1979.
- 243 Gibb, F. G. F., "High-temperature, very-deep, geological disposal: a safer alternative for high-level radioactive waste.," *Waste Management*, Vol. 19, 1999, pp. 207-211.
- 244 Keddy, E. S., "High Temperature Evaluation of Mo-Tm₂O₃ Cermet," Los Alamos National Laboratory, LA-4856-MS, Los Alamos, NM, Jan., 1972.
- 245 Yaojiang, H. and Suyi, H., "A generalized analysis of close-contact melting processes in two-dimensional axisymmetric geometries," *Int. Comm. Heat and Mass Transfer*, Vol. 26, No. 3, 1999, pp. 339-347.
- 246 Fukusako, S. and Yamada, M., "Melting heat transfer inside ducts and over external bodies," *Experimental Thermal and Fluid Science*, No. 19, 1999, pp. 93-117.
- 247 Emerman, S. H. and Turcotte, D. L., "Stoke's Problem with Melting," *International Journal of Heat and Mass Transfer*, Vol. 26, No. 11, 1983, pp. 1625-1630.

- 248 Heuze, F. E., "High-temperature Mechanical, Physical, and Thermal Properties of Granitic Rocks: A Review," *Int.J.Rock Mech.Min.Sci.& Geomech.Abst.*, Vol. 20, No. 1, 1983, pp. 3-10.
- 249 Black, D. L., "Basic Understanding of Earth Tunneling By Melting -- Volume I, Earth Structure and Design Solutions," National Technical Information Service, PB-235085, Springfield, VA, July, 1974.
- 250 Black, D. L., "Basic Understanding of Earth Tunneling By Melting -- Volume I, Basic Physical Principles," National Technical Information Service, PB-235084, Springfield, VA, July, 1974.
- 251 Stevenson, D.. A Modest Proposal: Mission to Earth's Core. *Nature* [423], 239-240. 5-15-2003.
- 252 Nuclear Data File -- "NuDat on the web". 2003. <http://www-original.nndc.bnl.gov/nndc/nudat/xriform.html>, National Nuclear Data Center, Brookhaven National Laboratory.
- 253 Case, K. M., Hoffmann, F., and Placzek, G., *Introduction to the Theory of Neutron Diffusion*, Vol. 1, Los Alamos Scientific Laboratory, Los Alamos, NM, 1953.
- 254 Alexander, C.. Conversation by phone with Dr. Alexander of HFIR Facility, ORNL, Department of Energy, regarding HFIR capabilities and characteristics. Branscome, E. C. 2003.
- 255 "HFIR Facility Description." www.ornl.gov/hfir. Downloaded from internet: 2003.
- 256 Schnitzler, B.. Conversation by phone with Dr. Schnitzler of ATR Facility, INL, Department of Energy, regarding ATR capabilities and operational characteristics. Branscome, E. C. 2003.
- 257 Walter, C. E., "Infrastructure for Thulium-170 Isotope Power Systems for Autonomous Underwater Vehicle Fleets," Lawrence Livermore National Laboratory, DE91 017464, UCRL-JC-107583, Livermore, California, Sept. 23, 1991.

- 258 Evaluated Nuclear Data File. 2003. <http://www.nndc.bnl.gov/>, National Nuclear Data Center, Brookhaven National Laboratory.
- 259 Medical Internal Radiation Dosimetry. 2003. <http://www.nndc.bnl.gov/>, National Nuclear Data Center, Brookhaven National Laboratory.
- 260 Bureau of Labor Statistics, "Producer Price Index." www.data.bls.gov. Downloaded from internet: 2004.
- 261 "Isotope Development Program Quarterly Report," 1973.
- 262 Pacific Northwest Laboratory, "Estimate of Future Radioisotope Costs," 1973.
- 263 Walter, C. E., Kammeraad, J. E., Newman, J. G., Konynenbug, R. V., and VanSant, J. H., "Thulium Heat Source IR&D Project: Second Trimester Status Report," Lawrence Livermore National Laboratory, UCRL-ID--106866, DE91 012138, Livermore, CA, May 10, 1991.
- 264 Fukusako, S. and Yamada, M., "Melting heat transfer inside ducts and over external bodies," *Experimental Thermal and Fluid Science*, No. 19, 1999, pp. 93-117.
- 265 Moallemi, M. K. and Viskanta, R., "Experiments on Fluid-Flow Induced by Melting Around A Migrating Heat-Source," *Journal of Fluid Mechanics*, Vol. 157, No. AUG, 1985, pp. 35-51.
- 266 Lienhard, J. H. I. and Lienhard, J. H. V., *A Heat Transfer Textbook*, 3rd edition ed., Phlogiston Press, Cambridge, MA, 2003, pp. 245.
- 267 Fomin, S. A., Saitoh, T. S., and Chugunov, V. A., "Contact melting materials with non-linear properties," *Heat and Mass Transfer*, Vol. 33, No. 3, 1997, pp. 185-192.
- 268 Kashcheev, V. A., Nikiforov, A. S., Poluektov, P. P., and Polyakov, A. S., "Toward A Theory of Self-Disposal of High-Level Waste," *Atomic Energy*, Vol. 73, No. 3, 1992, pp. 735-739.

- 269 Yaojiang, H. and Suyi, H., "A generalized analysis of close-contact melting processes in two-dimensional axisymmetric geometries," *Int. Comm. Heat and Mass Transfer*, Vol. 26, No. 3, 1999, pp. 339-347.
- 270 Bacon, J. F., Russel, S., and Carstens, J. P., "Determination of Rock Thermal Properties," United Aircraft Research Laboratories, UARL-L911397-4, AD-755 218, East Hartford, CT, Jan., 1973.
- 271 Krupka, M. C., "Phenomena Associated with the Process of Rock Melting. Application to the Subterrene System," Los Alamos Scientific Lab., LA5208MS, N, 1973.
- 272 Briesmeister, J. F.. MCNP: Monte Carlo N-Particle Transport Code System. [4B]. 1997. Oak Ridge, TN, Radiation Safety Information Computational Center.
- 273 Hotspot: Health Physics Codes for the PC. [2.05]. 2004. Livermore, CA, Lawrence Livermore National Laboratory.
- 274 Baum, E. M., Knox, H. D., and Miller, T. R., *Chart of the Nuclides -- Wall Chart Information Booklet*, 16th ed., Knolls Atomic Power Laboratory, Schenectady, NY, 2002, pp. 36-37.
- 275 Kulcinski, G. L., "Lecture 5: Basic Elemts of Static RTG's," Fusion Technology Institute, University of Wisconsin-Madison, Madison, WI -- available at <http://fti.neep.wisc.edu/neep602/SPRING00/neep602.html>, 2000.
- 276 Chmielewski, A. B. and Borshchevsky, A., "A Survey of Russian RTG Capabilities," Jet Propulsion Laboratory, 94-0898, 1994.
- 277 Chu, S. Y., Nordberg, H., and Firestone, R. B.. Isotope Explorer. [2.23]. 1-28-1999. ie.lbl.gov/isoexpl/isoexpl.htm, Nuclera Physics Division of the U.S. Department of Energy.
- 278 Kubose, D., Lai, M., and Goya, H., "Radioactivity Release from Radionuclide Power Sources, IX. Release from Thulium-170/171 Oxide and Promethium-147 Oxide to Seawater," Naval Ordnance Laboratory, White Oak, NOLTR 71-206, AD736603, Silver Spring, MD, Dec. 8, 1971.

- 279 Nelson, C. A., "Thulium Oxide for Thermal Source Applications," Sanders Nuclear Corporation, SNC3693-2; Nashua, N.H., 1970.
- 280 Keddy, E. S., "High Temperature Evaluation of Mo-Tm₂O₃ Cermet," Los Alamos National Laboratory, LA-4856-MS, Los Alamos, NM, Jan., 1972.
- 281 Traeger, R. K., Colp, J. L., and Neel, R. R., "Magma Energy Research, 79-1. Semiannual Report, October 1, 1978-March 31, 1979," Sandia Laboratories, SAND-79-1344, Albuquerque, NM, July, 1979.
- 282 Cornman, W. R., "Production of Thulium-170," Savannah River Laboratory, DP 1052, DE94 006719, Aiken, SC, Feb., 1967.
- 283 Walter, C. E., Kammeraad, J. E., Konynenbug, R. V., and VanSant, J. H., "Thulium Heat Source for High Endurance and High Energy-Density Power Systems," Lawrence Livermore National Laboratory, UCRL-JC-105761, CONF-910801-23, Livermore, CA, May, 1991.
- 284 Schnitzler, B.. Conversation by phone with Dr. Schnitzler of ATR Facility, INL, Department of Energy, regarding ATR production capability for Plutonium-238 from Neptunium targets. Branscome, E. C. 2004.
- 285 Zaitseva, L. and Hand, K., "Nuclear Smuggling Chains -- Suppliers, End-users, and Intermediaries," *American Behavioral Scientist*, Vol. 46, No. 6, Feb., 2003, pp. 822-844.
- 286 Wald, P. H. and Mode, V. A., "A Review of the Literature on the Toxicity of Rare-Earth Metals as it Pertains to the Engineering Demonstration System Surrogate Testing," Lawrence Livermore National Laboratory, UCID--21823, DE90 008049, Livermore, CA, Oct., 1989.
- 287 Mills, W. A., "Estimates of Human Cancer Risks Associated with Internally Deposited Radionuclides," *Internal Radiation Dosimetry*, edited by O. G. Raabe Medical Physics Publishing, Madison, WI, 1994, pp. 609-632.
- 288 Raabe, O. G., "Three-Dimensional Models of Risk from Internally Deposited Radionuclides," *Internal Radiation Dosimetry*, edited by O. G. Raabe Medical Physics Publishing, Madison, WI, 1994, pp. 633-656.

- 289 Stacey, W. M., "Reactor Safety," *Nuclear Reactor Physics* John Wiley & Sons, New York, 2001, pp. 269-291.
- 290 Lilley, J. S., "Biological Effects of Radiation," *Nuclear Physics -- Principles and Applications* John Wiley & Sons, New York, 2001, pp. 181-204.
- 291 Raabe, O. G., "Characterization of Radioactive Airborne Particles," *Internal Radiation Dosimetry*, edited by O. G. Raabe Medical Physics Publishing, Madison, WI, 1994, pp. 111-142.
- 292 SAS Institute Inc.. JMP: The Statistical Discovery Software. [5.1.2]. 2004. www.jmp.com. 2004.
- 293 Ambrose, D. and et al, "Handbook of Chemistry and Physics," , edited by D. R. Lide CRC Press, Washington, D.C., 2000, pp. 200.
- 294 Schaffer, J. P., Sashena, A., Antolovich, S. D., Sanders, T. H. Jr., and Warner, S. B., "Thermal Properties," *The Science and Design of Engineering Materials* Irwin, Chicago, 1995, pp. 576-578.
- 295 Olander, D. R., *Fundamental Aspects of Nuclear Reactor Fuel Elements*, National Technical Information Service, TID-26711-P1, 1976, pp. 121-122.

VITA

Caleb Branscome was born in Decatur, Georgia, on November 15th, 1974. In 1992 after his junior year of High School he enrolled at the Georgia Institute of Technology, graduating with a Bachelor's of Aerospace Engineering in April of 1997. Post-graduation he was employed by Rocketdyne as a Combustion Devices Design Engineer on the Space Shuttle Main Engine Product Team. During the Summer of 1999, Mr. Branscome was granted an educational leave of absence to undertake graduate studies at the Georgia Institute of Technology. After his first year at Georgia Tech he joined the Aerospace Systems Design Lab where he has been pursuing his doctoral studies in advanced design methodologies. Some of his research interests have included sequential metamodeling based regression and optimization, historical propulsion system reliability regression analysis, robust design analysis of launch vehicles, and alternative approaches to hard target defeat.